

KATHOLIEKE UNIVERSITEIT
LEUVEN

Arenberg Doctoral School of Science, Engineering & Technology
Faculty of Engineering
Department of Electrical Engineering

DIGITAL COMPENSATION OF FRONT-END NON-IDEALITIES IN BROADBAND COMMUNICATION SYSTEMS

Deepaknath TANDUR

Dissertation presented in partial
fulfillment of the requirements
for the degree of
Doctor in Engineering

March 2010



KATHOLIEKE UNIVERSITEIT LEUVEN
FACULTY OF ENGINEERING
DEPARTMENT OF ELECTRICAL ENGINEERING
RESEARCH GROUP:ESAT-SISTA/COSIC/DOCARCH
Kasteelpark Arenberg 10, B-3001 Leuven, Belgium

DIGITAL COMPENSATION OF FRONT-END NON-IDEALITIES IN BROADBAND COMMUNICATION SYSTEMS

Deepaknath TANDUR

Jury:
Prof. em.dr.ir. Y. Willems, president
Prof. dr.ir. M. Moonen, promotor
Prof. dr.ir. J. Vandewalle
Prof. dr.ir. G. Gielen
Prof. dr.ir. G. Leus (T.U.Delft)
Prof. dr.ir. F. Horlin (U.L.B.)
Prof. dr.ir. D. Slock (EURECOM)

Dissertation presented in partial fulfillment of the requirements for the degree of Doctor in Engineering

March 2010

©2010 Katholieke Universiteit Leuven – Faculty of Engineering
Kasteelpark Arenberg 1/2200, B-3001 Leuven, Belgium

Alle rechten voorbehouden. Niets uit deze uitgave mag worden vermenigvuldigd en/of openbaar gemaakt worden door middel van druk, fotocopie, microfilm, elektronisch of op welke andere wijze ook zonder voorafgaande schriftelijke toestemming van de uitgever.

All rights reserved. No part of the publication may be reproduced in any form by print, photoprint, microfilm or any other means without written permission from the publisher.

D/2010/7515/23
ISBN 978-94-6018-184-9

Dedicated to Pati and Appa

Foreword

What a journey this has been! I would like to express my sincere gratitude to all of those who have helped me during my PhD. Your help has made this work possible.

Firstly, I would like to thank Prof. Marc Moonen for giving me the opportunity to join his group, for his continuous encouragement, guidance, enthusiasm, and most importantly for believing in me. I have learned a lot and my experience here has been a very rewarding one. Thanks for always pointing me the right direction. For patiently reading and improving so many of my draft papers. You have been a great supervisor.

I would also like to thank the jury members: Prof. Joos Vandewalle, Prof. Georges Geilen, for their time, effort and continued support throughout my doctorate. Prof. Dirk Slock, Prof. Gert Leus, Prof. Francois Horlin and the chairman Prof. Yves Willems for agreeing to be on the board of examiners. Thanks for your critical reading of the thesis. I am grateful for all your valuable feedback in improving the final version of the text.

Many thanks to the group at the Katholieke Universtiet Leuven: Simon, Imad, Geert V.M., T.J., Gert C., Matteo, Ann, Geert R., Hilde, Toon, Vincent, Paschal, Jan, Sam, Guang, Romain, Sylvester, Alexander, Pepe, Beier, Amir, Bruno, Rodrigo. Thank you for all the nice and wonderful moments we have had during my PhD period. Your ideas, thoughts and energy have been inspiring. Special thanks to Prabin for all the discussions. Thank you for your company and good humor. Bram for being my Dutch translator from time to time. Kim for helping me in so many other things.

To all the other Indian and Belgian friends I have made here. Special thanks to Anil, Jibi, Maya, Ravi, Hannelore, Stephanie, Ronan, Nalini, Marijn, Nandini, J.E., Sampath, Swathi, Suresh, Bela, Bina. Thank you for your hospitality and friendship, for all the dinners together. Your company has made living here not only a rewarding experience, but an enjoyable one as well. Your friendship has made life abroad a lot easier.

I would like to thank my family for always believing in me and taught me to believe in myself. To my mother for all her support, patience and unconditional love. To my brother and sister-in-law for coming to Belgium especially for my defence to support me. To Reshma's family in Bangalore, Cologne and to my aunts for giving me all the encouragement and love that made this journey a pleasant one. I love you all very much.

Last but not least, I would like to thank my dear wife for all her patience, support and enthusiasm. For making umpteen trips back and forth between the two countries. I guess its time to make use of the mileage awards.

Abstract

The wireless communication industry has seen a tremendous growth in the last few decades. The ever increasing demand to stay connected at home, work, and on the move, with voice and data applications, has continued the need for more sophisticated end-user devices. A typical smart communication device these days consists of a radio system that can access a mixture of mobile cellular services (GSM, UMTS, etc), indoor wireless broadband services (WLAN-802.11b/g/n), short range and low energy personal communications (Bluetooth), positioning and navigation systems (GPS), etc. A smart device capable of meeting all these requirements has to be highly flexible and should be able to reconfigure radio transmitters and receivers as and when required. Further, the radio modules used in these devices should be extremely small so that the device itself is portable. In addition, the device should also be economical in terms of costs and energy requirements. In short, building a compact, low cost, flexible and reconfigurable radio for present and future wireless systems is an extremely challenging task.

An attractive hardware solution to limit the size and the cost of the radio is to use only small and necessary analog electronic components in the front-end. This means that most of the processing that was traditionally performed in the analog domain is now pushed into the digital domain. A direct conversion architecture is a suitable radio front-end for such systems. However, a direct conversion radio module may be very sensitive to various mismatches and imperfections of its analog components. These imperfections are due to manufacturing defects, varying operating temperatures etc, and may result in front-end non-idealities such as in-phase/quadrature-phase (IQ) imbalance, phase noise, carrier frequency offset (CFO), etc. If these front-end non-idealities are not properly understood and compensated, they can easily become a limiting factor to the quality and performance of the radio device and the entire communication link. Multicarrier systems such as OFDM, one of today's dominant transmission scheme is considered to be particularly more sensitive to these non-idealities. Rather than reducing the effects of these non-idealities by using expensive analog electronic components, it is easier and more flexible to tolerate these effects in the analog domain and then compensate them digitally.

In this dissertation, the effects and the compensation solutions of two of the most essential front-end non-idealities encountered in direct conversion radio transceiver design and implementation are investigated, namely mirror frequency interference due to IQ imbalance and the CFO. Various training based digital compensation solutions for these front-end non-idealities are proposed. The proposed algorithms are assessed based on an OFDM system similar to the WLAN IEEE 802.11a standard. However, the proposed techniques are equally applicable to other systems operating in a similar environment.

The most challenging architectural case of a wideband multicarrier transceiver scenario in which a wide collection of carriers are subjected to different amounts of IQ imbalance is analyzed. Thus IQ imbalance is considered to be frequency selective in nature with variation over different carriers. The IQ imbalance is also considered to be present at both transmitter and receiver front-end. The dissertation also considers the case of OFDM transmission with an insufficient cyclic prefix length, i.e., the case where the cyclic prefix is unable to completely accommodate the combined transmitter/receiver filters and the channel impulse response. In addition, the dissertation also considers different multiple antenna scenarios, from single-user multiple-input multiple-output (MIMO) systems and space time coded systems to multiple-user MIMO systems.

The proposed solutions allow for low complexity implementations and can adequately compensate for non-ideality levels much higher than those observed in today's transceiver designs. This guarantees robustness/effectiveness of the proposed schemes also for next generation systems where the effects of front-end non-idealities are expected to be much more severe. The presented compensation solutions allow to relax the analog requirements for low cost, small, flexible and highly reconfigurable radios in broadband communication systems.

Korte Inhoud

De draadloze communicatie industrie heeft een enorme groei gekend in de afgelopen decennia. De steeds toenemende vraag om verbonden te blijven thuis, op het werk, en op verplaatsing, met spraak en data applicaties, heeft de behoefte aan meer geavanceerde end-user apparaten versterkt. Een typisch hedendaags smart communicatie apparaat bestaat uit een radiosysteem dat toegang heeft tot een mix van cellulaire mobiele diensten (GSM, UMTS, enz.), indoor draadloze breedbanddiensten (WLAN-802.11b/g/n), lage energie persoonlijke communicatie met een kort bereik (Bluetooth), positionerings-en navigatiesystemen (GPS), enz. Een slim apparaat dat aan al deze eisen voldoet, moet zeer flexibel zijn en zou in staat moeten zijn om radio-zenders en-ontvangers te herconfigureren indien nodig. De radiomodules in deze apparaten moeten daarenboven uiterst klein zijn, zodat het apparaat zelf draagbaar is. Daarnaast moet het apparaat ook zuinig zijn wat betreft kosten en energie vereisten. Kortom, het bouwen van een compacte, goedkope, flexibele en herconfigureerbare radio voor de huidige en toekomstige draadloze systemen is een uiterst moeilijke opgave.

Een aantrekkelijke hardware oplossing om de omvang en de kosten van de radio te beperken is om alleen kleine en noodzakelijke analoge elektronische componenten te gebruiken in de front-end. Dit betekent dat de meeste van de verwerking, die traditioneel werd uitgevoerd in het analoge domein, nu in het digitale domein wordt uitgevoerd. Een directe conversie architectuur is een geschikte radio front-end voor dergelijke systemen. Een dergelijke directe conversie module kan echter zeer gevoelig zijn aan verschillende mismatches en imperfecties van de analoge componenten. Deze niet-idealiteiten zijn te wijten aan fabricagefouten, variarende werkingstemperaturen etc, en kan resulteren in front-end imperfecties zoals in-phase/quadrature-phase (IQ) onevenwicht, fase-ruis, carrier frequency offset (CFO), enz. Als deze front-end niet-idealiteiten niet ingeschat en gecompenseerd worden, kunnen ze gemakkelijk een beperkende factor worden voor de kwaliteit en prestaties van het radio-apparaat en de gehele communicatie link. Meerdere-draaggolf systemen zoals OFDM, een van de hedendaagse dominante transmissie schema's, wordt als bijzonder gevoelig aan deze niet-idealiteiten aanzien. In plaats van het verminderen van de effecten van deze niet-idealiteiten met behulp van

dure analoge elektronische componenten, is het makkelijker en flexibeler om deze effecten te tolereren in het analoge domein en vervolgens digitaal te compenseren.

In dit proefschrift worden de effecten en de compenseringsoplossingen van twee van de meest essentiale front-end niet-idealiteiten, ondervonden bij directe conversie radio transceiver ontwerp en implementatie, onderzocht, namelijk de spiegelfrequentie interferentie te wijten aan IQ onevenwicht, en CFO. Diverse trainingsgebaseerde digitale compenseringsoplossingen voor deze front-end niet-idealiteiten worden voorgesteld. De voorgestelde algoritmes worden beoordeeld op basis van een OFDM systeem vergelijkbaar met de WLAN standaard IEEE 802.11a. De voorgestelde technieken zijn echter eveneens van toepassing op andere systemen, die in een soortgelijke omgeving werken.

Het meest uitdagende geval van een breedband meerdere-draaggolf transceiver scenario, waarin een ruime collectie van draaggolven onderworpen zijn aan verschillende hoeveelheden van IQ onevenwicht, wordt geanalyseerd. IQ onevenwicht wordt zo beschouwd als een frequentie selectief probleem met een variatie over verschillende draaggolven. Het IQ onevenwicht wordt ook geacht aanwezig te zijn bij zowel de zender als de ontvanger front-end. Het proefschrift beschouwt ook het geval van OFDM transmissie met een te korte cyclische prefix, dat wil zeggen het geval waarbij de cyclische prefix niet in staat is om de gecombineerde zender/ontvanger filters en de kanaal impulsresponsie te accommoderen. Bovendien behandelt het proefschrift ook verschillende meerdere-antenne scenario's, van enkelvoudige-gebruiker multiple-input multiple-output (MIMO) systemen en ruimte-tijd gecodeerde systemen naar meerdere-gebruikers MIMO systemen.

De voorgestelde oplossingen laten implementaties met een lage complexiteit toe en kunnen een niet-idealiteitsniveau, dat veel hoger is dan wat wordt waargenomen bij hedendaagse transceiver designs, voldoende compenseren. Dit garandeert ook robuustheid/effectiviteit van de voorgestelde schema's voor de volgende generatie systemen, waarbij wordt verwacht dat de effecten van de front-end niet-idealiteiten veel ernstiger zijn. De voorgestelde compenseringsoplossingen laten toe om de analoge eisen voor goedkope, kleine, flexibele en herconfigureerbare radio's in breedband communicatiesystemen, te relaxeren.

Nomenclature

Mathematical Notation

x	scalar term
$\mathbf{x}$	time domain vector or matrix
$\mathbf{x}(t)$	continuous time baseband signal
$\mathbf{x}[n]$	discrete time baseband signal
$\mathbf{X}$	frequency domain vector or matrix
$\mathbf{X}[l]$	l^{th} subcarrier (element) of the frequency domain vector or matrix $\mathbf{X}$
$\mathbf{x} \star \mathbf{y}$	linear convolution between $\mathbf{x}$ and $\mathbf{y}$
$\mathbf{X}.\mathbf{Y}$	component-wise vector multiplication between $\mathbf{X}$ and $\mathbf{Y}$
$\mathbf{X} \div \mathbf{Y}$	component-wise vector division between $\mathbf{X}$ and $\mathbf{Y}$
$\mathbf{X} \otimes \mathbf{Y}$	Kronecker product of matrix $\mathbf{X}$ and $\mathbf{Y}$
$x!$	factorial of x
$\mathbf{x}^*$	complex conjugate of vector $\mathbf{x}$
$\mathbf{X}^{-1}$	inverse of matrix $\mathbf{X}$
$\mathbf{X}^{\dagger}$	pseudo-inverse of matrix $\mathbf{X}$
$\mathbf{X}^T$	transpose of matrix $\mathbf{X}$
$\mathbf{X}^H$	Hermitian transpose of matrix $\mathbf{X}$
$\mathbf{F}_N$	$N \times N$ discrete Fourier transform
$\mathbf{F}_N^{-1}$	$N \times N$ inverse discrete Fourier transform
$\mathbf{I}_N$	$N \times N$ Identity matrix
$\mathbf{0}_{M \times N}$	$M \times N$ all zero matrix
$\Xi\{.\}$	expectation operator
$\widetilde{\mathbf{x}}$	estimate of $\mathbf{x}$
$\Re\{x\}$	Real part of x
$\Im\{x\}$	Imaginary part of x
$\lceil x \rceil$	smallest integer larger or equal to x
$\lfloor x \rfloor$	largest integer smaller or equal to x
$x \approx y$	x is approximately equal to y
$\lvert . \rvert$	absolute value

$\| \mathbf{X} \|$	Frobenius norm of matrix $\mathbf{x}$
$x >> y$	x is much larger than y
$x << y$	x is much smaller than y

Acronyms and Abbreviations

1G	First Generation Mobile Wireless Systems
2G	Second Generation Mobile Wireless Systems
3G	Third Generation Mobile Wireless Systems
3GPP	Third Generation Partnership Project
4G	Fourth Generation Mobile Wireless Systems
ADC	Analog to Digital Converters
AMPS	Advanced Mobile Phone Service
AWGN	Additive White Gaussian Noise
BEM	Basis Expansion Model
BER	Bit Error Rate
BPF	Bandpass Filter
BPSK	Binary Phase Shift Keying
BS	Base Station
CDMA	Code Division Multiple Access
CFO	Carrier Frequency Offset
CP	Cyclic Prefix
DAB	Digital Audio Broadcasting
DAC	Digital to Analog Converters
DAMPS	Digital AMPS
dB	Decibels
D-FEQ	Decoupled FEQ
DFT	Discrete Fourier Transform
DSP	Digital Signal Processing
DVB	Digital Video Broadcasting
DVB-H	Digital Video Broadcasting-Handheld
DVB-S	Digital Video Broadcasting-Satellite
ECMA	Standardization of Information and Communication Technology & Consumer Electronics
EDGE	Enhanced Data Rates for GSM Evolution
e.g.	exempli gratia : for example
EM	Expectation Maximization
ETSI	European Telecommunications Standard Institute
E-UTRA	Evolved Universal Terrestrial Radio Access
FDM	Frequency Division Multiplexing
FEQ	Frequency Domain Equalizer
FI	Frequency Independent

FIR	Finite Impulse Response
FM	Frequency Modulation
FS	Frequency Selective
GPRS	General Packet Radio Service
GPS	Global Positioning System
GSM	Global System for Mobile Communications
HSDPA	High Speed Downlink Packet Access
HSUPA	High Speed Uplink Packet Access
Hz	Hertz
ICI	Inter-Carrier-Interference
IDFT	Inverse Discrete Fourier Transform
i.e.	id est : that is
IEEE	Institute of Electrical and Electronics Engineers
IF	Intermediate Frequency
IIR	Infinite Impulse Response
IQ	In-Phase Quadrature-Phase
IRR	Image Rejection Ratio
ISI	Inter-Symbol-Interference
ITU	International Telecommunication Union
LAN	Local Area Network
LNA	Low Noise Amplifier
LO	Local Oscillator
LPF	Low Pass Filter
LS	Least Squares
LT	Long Training
LTE	Long Term Evolution
MAC	Medium Access Control
MC	Multicarrier
MC-CDMA	Multicarrier Code Division Multiple Access
MIMO	Multiple-Input Multiple-Output
MISO	Multiple-Input Single-Output
ML	Maximum Likelihood
MMSE	Minimum Mean Square Error
MSE	Mean Square Error
MU	Multi-User
NLS	Non-Linear Least Squares
NMT	Nordic Mobile Telephone
OFDM	Orthogonal Frequency Division Multiplexing
PAPR	Peak to Average Power Ratio
PDP	Power Delay Profile
PR-FEQ	Phase Rotated FEQ
PR-PTEQ/FEQ	Phase Rotated PTEQ/FEQ

P/S	Parallel-to-Serial
PTEQ	Per-Tone Equalizer
QAM	Quadrature Amplitude Modulation
QOSTBC	Quasi Orthogonal STBC
QPSK	Quadrature Phase Shift Keying
RF	Radio Frequency
RLS	Recursive Least Squares
rms	Root Mean Square
SC FDMA	Single Carrier Frequency Division Multiple Access
SDR	Software Defined Radio
SISO	Single-Input Single-Output
SMS	Short Message Service
SNR	Signal to Noise Ratio
S/P	Serial-to-Parallel
ST	Short Training
STBC	Space Time Block Code
SU	Single-User
TACS	Total Access Communication System
T-DMB	Terrestrial Digital Multimedia Broadcasting
TEQ	Time Domain Equalizer
UMTS	Universal Mobile Telecommunications Systems
UWB	Ultra Wideband
VGA	Variable Gain Amplifier
vs.	versus
WiMax	Worldwide Interoperability for Microwave Access
WLAN	Wireless LAN
WPAN	Wireless Personal Area Network
ZF	Zero Forcing

Parameter Naming Conventions

T	symbol period
B_c	coherence bandwidth
f_c	carrier frequency
N	number of subcarriers in an OFDM symbol
ν	cyclic prefix length
L	length of channel impulse response
L_t	length of impulse response of the transmitter filter
L_r	length of impulse response of the receiver filter
Δf	carrier frequency offset
M_s	sequence length of short training symbols
M_l	sequence length of long training symbols
N_t	number of transmit antennas
N_r	number of receive antennas
N_u	number of users
N_b	number of base station antennas
N_y	number of antennas supported by user's individual local oscillator

Contents

Contents xv

1 Introduction 1

1.1 Problem Statement 4

1.2 Objectives and Solution Approach 6

1.3 Outline of the Thesis and Contributions 7

2 End-to-End System Model 13

2.1 Introduction 13

2.2 Front-End Architecture 15

2.3 Channel Characteristics 18

2.3.1 Discrete Time Channel Model 21

2.4 OFDM Background 23

2.4.1 WLAN IEEE 802.11a Case Study 26

2.5 Summary 28

I Single Antenna OFDM Systems 29

3 IQ Imbalance 31

3.1 Introduction 31

3.2 Joint IQ Imbalance and Channel Compensation 33

3.2.1 System Model with IQ Imbalance 33
3.2.2 Influence of IQ Imbalance 37
3.2.3 IQ Imbalance Compensation 39
3.2.4 Initialization Algorithms 40
3.3 Joint IQ Imbalance and Channel Compensation under Insufficient CP Length 43
3.3.1 System Model with IQ Imbalance and Insufficient CP Length 43
3.3.2 IQ Imbalance Compensation 44
3.4 Simulation Results 49
3.5 Conclusion 54

4 IQ Imbalance and CFO **57**
4.1 Introduction 57
4.2 System Model with CFO and IQ Imbalance 59
4.3 CFO Estimation 62
4.4 Joint FI IQ imbalance, CFO and Channel Compensation 64
4.5 Joint FS IQ imbalance, CFO and Channel Compensation under Insufficient CP length 70
4.5.1 TEQ + FEQ based Compensation 71
4.5.2 PTEQ based Compensation 73
4.6 Simulation Results 79
4.7 Conclusion 84

5 Decoupled Compensation Schemes **85**
5.1 Introduction 85
5.2 Decoupled FEQ Schemes 86
5.2.1 Decoupled Transmitter IQ Imbalance Compensation 87
5.2.2 Decoupled Receiver IQ Imbalance Compensation 90

5.2.3 Decoupled Transmitter and Receiver IQ Imbalance Compensation . . . 91
5.3 Phase Rotation Schemes . . . 97
5.3.1 Decoupled Receiver IQ Imbalance Compensation . . . 97
5.3.2 Decoupled Receiver IQ Imbalance and CFO Compensation 100
5.4 Simulation Results . . . 106
5.5 Conclusion . . . 115

II Multiple Antenna OFDM Systems 117

6 Joint Compensation Schemes 119
6.1 Introduction . . . 119
6.2 System Model . . . 121
6.3 Joint IQ Imbalance and Channel Compensation . . . 123
6.4 Joint IQ Imbalance, CFO and Channel Compensation . . . 126
6.5 Space-Time Block Codes . . . 132
6.5.1 Joint IQ Imbalance and Channel Compensation . . . 133
6.5.2 Joint IQ Imbalance, CFO and Channel Compensation . . . 135
6.6 Multi-User MIMO . . . 138
6.6.1 Down-Link Scenario . . . 139
6.6.2 Up-Link Scenario . . . 140
6.7 Simulations . . . 145
6.8 Conclusion . . . 148

7 Decoupled Compensation Schemes 149
7.1 Introduction . . . 149
7.2 Decoupled FEQ Schemes . . . 150
7.2.1 Compensation Entirely at the Receiver . . . 152
7.2.2 Compensation with Pre-Distortion of Transmitted Symbols 154

7.2.3 Estimation of Transmitter and Receiver IQ Imbalance Gain Parameters 156
7.3 Phase Rotation Based Schemes 163
7.4 Simulation Results 167
7.5 Conclusion 171

8 Conclusions and Future Work **173**
8.1 Conclusions 173
8.2 Further Research 178

Bibliography **181**

Publication List **193**

Curriculum Vitae **197**

Chapter 1

Introduction

The wireless communication industry has seen a tremendous growth in the last few decades. In 2008, there were 4.1 billion mobile cellular subscriptions in the world, this accounts for an average 61% penetration rate worldwide [47]. In contrast to this, fixed line telephony has experienced nearly no growth and its global penetration has been stagnating at just under 20% in the last years.

The reason behind this sudden spurt in wireless devices can be attributed to a variety of reasons. In most of the world, the increase in demand to stay connected at home, work, and on the move, with voice and data applications, has continued the need for more sophisticated end-user devices. The demand for higher data rates at the user's device is expected to continue as more and more data based applications become available. In many developing countries, wireless communication has finally allowed for basic accessibility to remote areas that were once nearly impossible to be reached with fixed line telephony. Also wireless systems are much easier to implement in scantily populated regions, where the costs of laying down the fixed lines can be prohibitively expensive.

Mobile wireless communications have taken several generations to evolve depending on the technology used and the services provided. Here is a snap shot of different generations of mobile telecommunications:

First generation (1G): The first generation of mobile devices appeared in 1970s and were mainly used for voice services, for example AMPS in North America, NMT in parts of Europe and TACS in Europe, Middle east and Asia. These systems were based on analog frequency modulation (FM) schemes.

Second generation (2G): In the beginning of the 1980's, the second generation network, commonly known as GSM, started its operation in Europe [72]. The 2G networks were based on digital transmission schemes and for the first time the

phone conversations were digitally encrypted and data services such as SMS were available. Later on the 2G technology evolved to accommodate higher speed of data reaching up to 384 Kbit/s with the introduction of EDGE (2.5G) technology. This development was also achieved by other technologies in other parts of the world, for e.g. CDMA, DAMPS, etc.

Third generation (3G): The need for multimedia services and internet access has resulted in the introduction of third generation systems such as UMTS [59]. Further improvement in the 3G technology based on high speed packet access (HSDPA/HSUPA) schemes, allow the mobile user to access data services up to 14.4 Mbit/s on the down-link and 5.8 Mbit/s on the up-link. The mobile user can continue to stay connected to the internet while on the move.

Fourth generation (4G): The 4G systems are currently under development and are expected to be released soon. These systems are based on LTE and WiMax technologies [50] that are promising an internet speed that reaches 233 Mbit/s for mobile users [49], [104].

Similarly there has been progress in wireless communication standards for a variety of other applications. The broadcasting standard includes digital audio broadcasting (DAB) [79], and digital video broadcasting (DVB) [27], [74] transmission schemes. The DVB standard is now capable of distributing data using a variety of approaches, including satellite (DVB-S, DVB-S2), terrestrial television (T-DMB) and terrestrial television via handhelds (DVB-H,DVB-SH).

A variety of standards also exist for indoor networks [24]. Bluetooth technology offers cheap, short range communications and its low data rate (under 2-3 Mbps) targets applications such as cable replacement to create wireless personal area networks (WPAN) [33]. Zigbee, as standardized in IEEE 802.15.4 targets even lower data rates (20-250 kbps), and very low power applications [28]. On the other hand, the high speed ultra wideband (UWB) PAN also known as WiMedia UWB, aims at data rates up to 480 Mbps [25]. It has been certified as the next generation wireless USB standard.

The Wi-Fi Alliance, an industry association of more than 300 member companies devoted to the growth of wireless local area networks (WLANs), has ratified as recently as Oct. 2009, the next generation WLAN standard called IEEE 802.11n [45]. The IEEE 802.11n standard is an amendment to the IEEE 802.11-2007 wireless networking standard to improve network throughput over previous standards, such as 802.11b and 802.11g [43], with a significant increase in the maximum raw data rate from 54 Mbit/s to a maximum of 600 Mbit/s. IEEE 802.11 networks are short range, high bandwidth networks primarily developed for data. As WLANs offer attractive throughputs over indoor wireless channels, they are considered to be a major stepping stone towards the development of future broadband wireless communications.

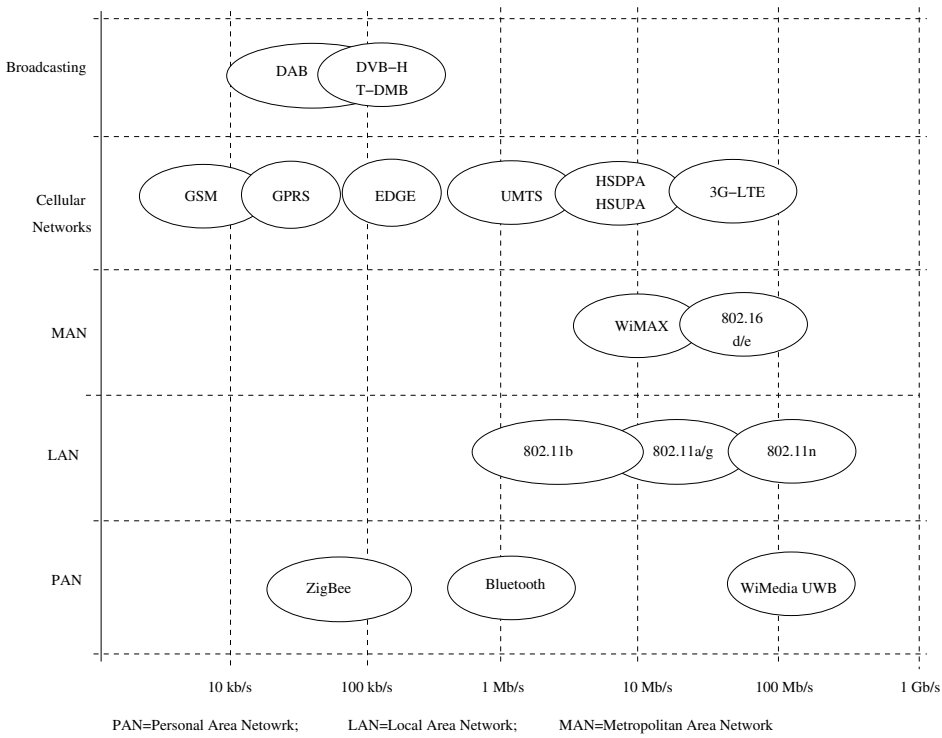

Figure 1.1: The diverse wireless communication landscape [42],[46],[26], [25]

The reader is referred to an excellent overview presented in [34], [38] for detailed information about various wireless standards of the past and present. For later generations the reader is referred to [83], [82], and [117]. The diverse wireless communication landscape of the present and the near future is shown in **Figure 1.1**. These standards have been or are currently being defined by standardization bodies, such as the Institute of Electrical and Electronics Engineers (IEEE) [42], the International Telecommunication Union (ITU) [46], European Telecommunications Standards Institute (ETSI) [26] or the Standardization of Information and Communication Technology and Consumer Electronics (ECMA) [25].

Many of the present and the upcoming wireless standards, namely, DAB, DVB-H, T-DMB, 3G-LTE, WiMAX, WiMedia UWB, 802.11a/g/n, etc are based on multicarrier transmission techniques such as orthogonal frequency division multiplexing (OFDM) [10]. The OFDM transmission scheme is increasingly being employed due to its ability to efficiently use the available spectrum and its robustness towards multipath environment. The new generation of wireless

standards implement OFDM in multiple antenna (MIMO) scenarios, to take advantage of spatial multiplexing and antenna diversity. Systems based on MIMO OFDM are considered to be a dominant technology for future high data rate applications [11]. The focus of this dissertation, therefore, is to investigate front-end non-idealities in systems relying on OFDM as their transmission technique. Throughout this dissertation, the performance of the proposed algorithms is assessed based on an OFDM system similar to the WLAN IEEE 802.11a standard. However, the proposed techniques are equally applicable to other systems, operating in a similar environment. The proposed algorithms have also been extended to various multiple antenna scenarios.

1.1 Problem Statement

Wireless communication devices are becoming smaller, smarter and more sophisticated [83]. The ability to stay connected to the internet whether at home, work or on the move has generated a tremendous demand for these smart communication devices. A typical smart communication device consists of a radio system that can access a mixture of mobile cellular services (GSM, EDGE, UMTS, LTS, etc), indoor wireless broadband services (WLAN-802.11b/g/n), short range and low energy personal communications (Bluetooth), positioning and navigation systems (GPS), and broadcasting systems (DVB-H), etc. In many cases, these devices have to operate under multiple frequencies for the same wireless standard globally (GSM).

A smart device capable of meeting all these requirements has to be highly flexible and should be able to reconfigure radio transmitters and receivers as and when required [13], [21]. The need for flexibility and reconfigurability prevents using dedicated hardware designed and optimized for only a single application or part of the radio spectrum. Further, the radio modules used in these devices should be extremely small so that the device itself is portable. In addition, the device should also be economical in terms of costs and energy requirements. All these problems are more prominent when a device has to support multiple antennas at the transmitter and receiver front-ends, because in this case multiple parallel radios have to be implemented in a single device [57]. In short, building a compact, low cost, flexible and reconfigurable radio for present-day and future wireless systems is an extremely challenging task. As the demand for such devices increases, manufacturers have to cope with multiple new challenges both in the analog and digital domain.

An attractive hardware solution to limit the size and the cost of the radio is to use only small and necessary analog electronics in the front-end. This means that most of the processing that was traditionally performed by analog domain, such as frequency translations and selectivity, are now pushed into the digital

domain. Thus most of the processing takes place in the software while the hardware performs minimal functions. A direct conversion architecture is a suitable radio front-end for such systems as it requires minimal analog electronics for its operation. The direct conversion front-end can be made highly reconfigurable so that the communication device can access any radio standard whenever the need arises, giving rise to the concept of so-called software defined radio (SDR). A SDR requires very sophisticated software modules for its control and operation. As an extension to reconfigurability, a communication device can also be used to access any available sub-part or chunk of the overall radio spectrum, making the radio cognitive in nature [58].

As the front-end of a reconfigurable radio uses minimal analog electronic components, a simple radio module will have to process wideband high dynamic range signals. A typical direct conversion radio implementation of this kind may be very sensitive to various mismatches and imperfections in the front-end. These imperfections are due to manufacturing defects, varying operating temperatures etc, and may result in front-end non-idealities such as in-phase/quadrature-phase (IQ) imbalance; non-linearities in analog to digital converters (ADC), digital to analog converters (DAC) and amplifiers; phase noise and carrier frequency offset (CFO) due to local oscillator (LO) defects, etc. The front-end non-idealities are also commonly called radio frequency (RF) impairments [15], [30]. If front-end non-idealities are not properly understood and compensated, they can easily become a limiting factor to the quality and performance of the radio device and the entire communication link. In particular, the OFDM based communication systems are considered to be very sensitive to such non-idealities. As next generation wireless systems, many of them based on OFDM, will require more simplified, low cost, flexible and reconfigurable radio front-ends, the use of cheaper components will increase, and as a result the effect of front-end non-idealities will become even more severe. To summarize, many of the advantages for which smart communication devices have been designed, may be rendered ineffective due to the presence of front-end non-idealities in communication systems.

Rather than reducing the effects of these non-idealities by using expensive analog electronic components, it is easier and more flexible to tolerate these effects in the analog domain and then compensate them digitally. It then becomes imperative to study the effects of these non-idealities in both transmitter and receiver front-ends. A communication system of this kind requires various digital signal processing (DSP) techniques for an adequate operation of the entire communication link. This dissertation looks into problems associated with such low cost radios designed for OFDM systems used in present-day and future wireless devices.

1.2 Objectives and Solution Approach

The overall objective of this dissertation is to provide digital solutions that can enable low cost, small and highly reconfigurable radios in broadband communication systems. More specifically, we investigate the effects of two of the most essential front-end non-idealities encountered in radio transceiver design and implementation, and their impact in the modern radio system context. In particular, we investigate mirror frequency interference due to IQ imbalance and CFO. We have developed various training based compensation solutions for these front-end non-idealities. The solutions proposed meet the following requirements:

- The solutions take into account the practical problems inherent to real-life communication systems. The IQ imbalance is considered to be present at the transmitter as well as the receiver front-end. We consider the most challenging architectural case of a wideband multicarrier or multichannel transceiver scenario in which a wide collection of carriers are subjected to different amounts of IQ imbalance. Thus IQ imbalance is considered to be frequency selective in nature with variation over different carriers. The multicarrier system considered here is based on OFDM transmission.

  Throughout this dissertation, the channel is considered to be unknown at the transmitter and it is characterized as a quasi static frequency selective multipath fading channel. The time variation in the channel results from the CFO due to the mismatch between the transmitter and receiver local oscillators.

  The dissertation also considers the case of insufficient cyclic prefix (CP) length, i.e., the case where the CP used in the OFDM transmission is unable to completely accommodate the combined transmitter/receiver IQ imbalance and channel impulse response.

  In addition, the dissertation also considers different multiple antenna scenarios: from single-user MIMO systems and space time coded systems to multi-user MIMO systems.

- The solutions allow for low complexity implementation. The proposed solutions should not degrade the radio's integration possibilities, because the integration leads to a small form factor, an attractive feature for wireless mobile radios. To this end, we have proposed various decoupled compensation solutions, where the compensation of IQ imbalance and CFO is performed independently of the channel equalization. Such decoupled solutions result in an overall lower computational cost and lower training overhead.

  Furthermore, it is shown that the most general form of the equalization structure that considers transmitter/receiver IQ imbalance, CFO, multipath

channel distortion and insufficient CP length in a multiple antenna scenario, can be simplified to a reduced structure for specific sub-problems when only some of the distortion parameters are considered in the system model.

- The solutions can adequately compensate for non-ideality levels much higher than those observed in today's transceiver designs. This is to guarantee the robustness/effectiveness of the proposed schemes for next generation systems where the effects of non-idealities are expected to be much more severe. The proposed solutions perform equally well for higher order modulated wideband communication waveforms that are particularly more sensitive to front-end non-idealities. The various compensation schemes are demonstrated to provide a performance that is close to the ideal case without any front-end non-idealities.

- The solutions require minor adjustments so as to be accommodated in the existing standards. Throughout this dissertation, the performance of the proposed algorithms is assessed based on an OFDM system similar to the WLAN IEEE 802.11a standard. However, the proposed solutions are generic enough to be extended in a straightforward manner to other systems operating under similar conditions.

In the long term, SDRs are expected to become the dominant technology in radio communications. While the concept of SDR is not new, the rapidly evolving capabilities of digital electronics are making processes that were once only theoretically possible, a practical reality [58]. The digital compensation techniques that are proposed in this dissertation allow to relax the analog requirements for such communication systems.

1.3 Outline of the Thesis and Contributions

A general overview of the thesis and its major contributions are now given:

In chapter 2, we provide a general overview of an end-to-end system model in a modern wireless communication scenario. The system model comprises all important building blocks in a broadband wireless communication link: the most important digital, analog blocks, together with the OFDM transmission system and the multipath channel model are introduced. A brief overview of different front-end radio architectures along with some of the most common non-idealities are also discussed. The channel parameters of the underlying wireless channel are presented in detail. Finally the basic building blocks and the parameters associated with the OFDM transmission scheme along with the WLAN IEEE 802.11a case study are presented. In subsequent chapters, various training based digital solutions are developed based on an end-to-end system model presented in

this chapter. It is shown that this model allows for a complete realistic performance analysis and solution.

The rest of the dissertation focuses on the study and development of digital compensation algorithms for non-idealities such as IQ imbalance and CFO in an OFDM system. The dissertation consists of two parts. The first part discusses compensation solutions in a single-antenna OFDM scenario and the second part discusses the compensation solutions in various multiple antenna scenarios.

In **Part I** we investigate the effects and the compensation schemes of non-idealities for single-antenna OFDM systems. The derivation and analysis of the single-antenna systems is essential in order to extend the compensation solutions later for the multiple antenna systems.

In **Chapter 3**, the presence of only IQ imbalance in an OFDM system is considered. An input-output system model considering both frequency independent and frequency selective IQ imbalance at transmitter and receiver analog front-ends is derived. It is shown that IQ imbalance can severely limit the performance of an OFDM system. A joint transmitter/receiver IQ imbalance compensation and channel equalization scheme based on a two-tap frequency domain equalizer (FEQ) per subcarrier is realized. In this chapter we also consider the case of an insufficiently long CP length that cannot completely accommodate the combined channel and transmitter/receiver IQ imbalance impulse response. The short CP length results in inter-symbol-interference (ISI) between adjacent OFDM symbols. A two-branch per-tone equalizer (PTEQ) solution is proposed to compensate for the joint effects of ISI, IQ imbalance and channel distortion. The publications that are related to this chapter are:

- **D.Tandur** and M.Moonen, "Joint compensation of OFDM frequency selective transmitter and receiver IQ imbalance", Eurasip Journal on Wireless Communications and Networking (JWCN), Volume 2007 (2007), Article ID 68563, 10 pages.
- **D.Tandur** and M.Moonen, "Adaptive compensation of OFDM frequency selective transmitter and receiver IQ imbalance", Poster at IAP-motion 2nd workshop on Mobile Multimedia Communication Systems and Networks (IAP), Liege, Belgium, Nov. 2006.
- **D.Tandur** and M.Moonen, "Joint compensation of OFDM frequency selective transmitter and receiver IQ imbalance", in Proc. of IEEE International Conference on Acoustics, Speech and Signal Processing (ICASSP), Honolulu, Hi, April 2007, pp. III-81.

In **Chapter 4**, we investigate the case of joint IQ imbalance and CFO in an OFDM system. We first study the impact of CFO with and without IQ

imbalance in a typical OFDM system. We then consider some of the suitable CFO estimation schemes available in the literature that can be used in the presence of IQ imbalance. A joint transmitter/receiver IQ imbalance, CFO and channel compensation solution is then derived. The compensation solution first considers the case of only frequency independent transmitter/receiver IQ imbalance and CFO. It is shown that in the presence of only frequency independent IQ imbalance, the joint compensation scheme can straightforwardly be obtained in the frequency domain by a four-tap FEQ. However, in the case of frequency selective IQ imbalance and CFO, the compensation has to be performed in multiple stages consisting of time domain and frequency domain operations. A four-branch PTEQ is then derived that provides a unified compensation solution for frequency selective IQ imbalance, CFO and insufficient CP length. The PTEQ solution can be considered as the most generalized form of compensation structure, as the equalizer can compensate for different combination of non-idealities and also for ISI distortion. The publications that are related to this chapter are:

- **D.Tandur** and M.Moonen, "Joint adaptive compensation of transmitter and receiver IQ imbalance under carrier frequency offset in OFDM based systems", IEEE Transactions on Signal Processing (IEEE TSP), vol. 55, no. 11, pp. 5246-5252, Nov. 2007.
- **D.Tandur** and M.Moonen, "Digital compensation of RF impairments for Broadband wireless systems", in Proc. of 14th IEEE Symposium on Communications and Vehicular Technology (SCVT), Delft, The Netherlands, Nov 2007.
- **D.Tandur** and M.Moonen, "Adaptive compensation of frequency selective IQ imbalance and carrier frequency offset for OFDM based receivers", in Proc. of 8th IEEE workshop on Signal Processing Advances in Wireless Communications (SPAWC), Helsinki, Finland, June 2007.
- **D.Tandur** and M.Moonen, "Joint compensation of carrier frequency offset and frequency selective IQ imbalance for OFDM based receivers", in Proc. of 3rd IEEE BENELUX/DSP Valley Signal Processing Symposium (SPS-DARTS), Antwerp, Belgium, March 2007, pp. 13-16.
- **D.Tandur** and M.Moonen, "Joint compensation of OFDM transmitter and receiver IQ imbalance in the presence of carrier frequency offset", in Proc. of 14th European Signal Processing Conference (EUSIPCO), Florence, Italy, Sept. 2006.

In **Chapter 5**, we derive so-called decoupled solutions for single-antenna systems. We have proposed training based compensation schemes that can decouple the compensation of transmitter and receiver IQ imbalance from the compensation

of the channel distortion. We have proposed two decoupled solutions: the D-FEQ decoupled solution, where the transmitter/receiver IQ imbalance and channel distortion parameters are estimated based on compensation coefficients obtained from the joint estimation/compensation solution, and the PR-(PTEQ)/FEQ decoupled solution, where the receiver IQ imbalance parameters are estimated based on a specific sequence of specially induced phase rotated long training symbols. The PR-(PTEQ)/FEQ scheme can estimate receiver IQ imbalance parameters irrespective of the amount of CFO. It is shown that under certain conditions (for large CFOs), the PR-(PTEQ)/FEQ scheme can also be applied in the presence of transmitter IQ imbalance. The publications that are related to this chapter are:

- **D.Tandur** and M.Moonen, "Efficient compensation of transmitter and receiver IQ imbalance in OFDM systems", Eurasip Journal on Advances in Signal Processing (JASP), submitted in Dec. 2009.
- **D.Tandur** and M.Moonen, "Efficient compensation of frequency selective Tx and Rx IQ imbalances in OFDM systems", Springer Lecture Notes on Electrical Engineering, Multi-Carrier Systems & Solutions, 2009.
- **D.Tandur** and M.Moonen, "Efficient compensation of frequency selective Tx and Rx IQ imbalances in OFDM systems", in Proc. of IEEE 7th International Workshop on Multi-Carrier Systems & Solutions (MC-SS), Herrsching, Germany, May 2009.
- **D.Tandur**, Chong-you Lee and M.Moonen, "Efficient compensation of RF impairments for OFDM systems", in Proc. of IEEE Wireless Communications and Networking Conference (WCNC), Budapest, Hungary, April 2009.

In **Part II**, we investigate the effects and the compensation schemes for front-end non-idealities in various multiple antenna scenarios. The problem of front-end non-idealities is even more prominent when a device has to support multiple antenna transmitter and receiver radio front-ends, as in this case multiple parallel radios have to be implemented in a single device. Thus it becomes extremely important to keep these RF front-ends simple with minimal analog electronics so as to maintain the cost, size and power consumption within an acceptable limit.

In **Chapter 6**, we derive a PTEQ based joint compensation solution for transmitter/receiver IQ imbalance and CFO. It is shown that for the case of single-user MIMO systems, the joint compensation scheme can be easily scaled for any number of transmitter and receiver antennas. In the case of space time coded systems, we exploit the inherent structure of the orthogonal codes to obtain an efficient and optimal receiver architectures that are robust to front-end non-idealities. The PTEQ scheme has also been extended for multi-user scenarios, where individual users may experience a different CFO. It is shown

that in the down-link communication scenario, the single-user PTEQ solution can straightforwardly be implemented. However, the solution for the up-link communication scenario is more complex and the PTEQ solution is limited to lower order systems. The compensation scheme for higher order systems leads to high implementation costs. The publications that are related to this chapter are:

- **D.Tandur** and M.Moonen, "MIMO OFDM systems with digital RF impairment compensation", Signal Processing, accepted with minor revision, Jan. 2010.
- **D.Tandur** and M.Moonen, "STBC MIMO OFDM systems with implementation impairments", in Proc. of IEEE Vehicular Technology Conference (VTC2008-fall), Calgary, Canada, Sept. 2008, pp. 1-5.
- **D.Tandur** and M.Moonen, "Compensation of RF impairments in MIMO OFDM systems", in Proc. of IEEE International Conference on Acoustics, Speech and Signal Processing (ICASSP), Las Vegas, Nevada, April 2008, pp. 3097-3100.

In **Chapter 7**, we derive decoupled solutions for multiple antenna systems. It is shown that in the presence of transmitter/receiver IQ imbalance, the D-FEQ decoupled scheme requires only two independent channel realizations between any one transmit/receive antenna pair, to estimate the IQ imbalance parameters for the remaining transmit and receive antenna branches. In the case of PR-(PTEQ)/FEQ scheme, the extension from single-antenna to multiple antennas is rather straightforward, as the estimation of receiver IQ imbalance parameter takes place separately for every individual receive antenna branch. The publications that are related to this chapter are:

- **D.Tandur** and M.Moonen, "Decoupled compensation of IQ imbalance in MIMO OFDM systems", Signal Processing, submitted in Feb. 2010.

In **Chapter 8**, conclusions are drawn and directions for further research are explored.

Chapter 2

End-to-End System Model

2.1 Introduction

The objective of this dissertation is to provide digital solutions that can enable low cost, small and highly reconfigurable radios in broadband communication systems. In this chapter, a general overview of some of the essential digital and analog building blocks in an end-to-end system model is presented. We identify the most common non-idealities associated with the analog blocks. Later we also provide a brief description of the channel characteristics, the OFDM transmission scheme and the WLAN case study considered in this work.

Many studies investigate the performance of communication systems based on only the digital building blocks, ignoring the impact of the analog front-end. This is equivalent to assuming that the analog front-end is near perfect and introduces negligible distortion. One of the reasons is that the exact modeling and simulation of the front-end is extremely involved and time consuming. However, as the aim of this dissertation is to develop algorithms to enable low cost, low power radio design, we consider the most important analog building blocks and the non-idealities associated with them in our performance study.

We evaluate the system performance based on a communication over a noisy multipath channel between the two terminals, one of them can be a base station and the other a mobile device. **Figure 2.1** shows an end-to-end system model for this system setup. The figure shows that each terminal consists of a physical layer that is made up of a baseband section and a front-end section with an antenna connected to it. Since the baseband processing is digital and the front-end processing is analog, the two sections are connected through digital to analog and analog to digital converters (ADC/DAC) at the transmitter and the receiver

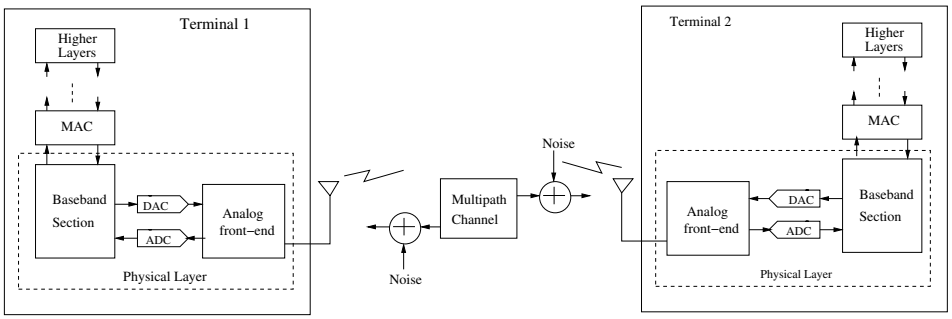

Figure 2.1: End-to-end system model

respectively. The baseband section is also connected to the higher medium access control (MAC) layer. The MAC layer in turn is connected to other higher layers such as the network layer, etc that are required for further digital processing.

During the *transmission* process, the network layer invokes service requests to the MAC layer which in turn initiates a corresponding service request to the physical layer. The baseband section then processes the data burst obtained from the MAC layer into a format that can be up-converted by the transmitter front-end. The baseband processing at the transmitter typically involves channel coding, signal modulation, and the burst formation. The signal from the baseband section is then forwarded to the front-end where the principal processing involves the conversion of the digital signal to the analog format, frequency translation of the baseband signal to various intermediate frequency (IF) stages, frequency translation to the desired RF carrier and then the power amplification. During the front-end processing, we also assume that the signal suffers from non-idealities associated with the mismatched and imperfect analog electronics. Finally the antenna at the transmitter sends the information over the wireless channel consisting of a rich multipath environment, which is then picked up by the antenna at the receiver terminal. The received signal is then also distorted by additive white Gaussian noise (AWGN).

The corresponding principal processing at the *receiver* side includes the initial band limitation to control the incoming signal dynamics, amplification to compensate for the transmission losses, frequency translation to IF/baseband stages, selectivity filtering combined with conversion to the digital domain. The received signal is once again assumed to suffer from various front-end non-idealities before the signal is forwarded to the baseband section. The baseband section involves the exact reverse operation to that of the transmitter baseband in addition to the channel equalization and the compensation of non-idealities. The equalized and decoded signal is then finally sent to the MAC and other higher layers for further processing.

The MAC layer and other higher layers further up are beyond the scope of this dissertation. We will therefore focus in the remaining of this chapter on the physical layer and the shared wireless media between the two terminals. This chapter is organized as follows: **Section 2.2** discusses the front-end architectures and the essential non-idealities associated with them. **Section 2.3** explains the channel characteristics as encountered in a targeted broadband wireless application. **Section 2.4** gives an overview of the OFDM transmission scheme and introduces the WLAN IEEE 802.11a case study. Finally, we summarize the chapter in **section 2.5**.

2.2 Front-End Architecture

The impact of different front-end non-idealities is heavily dependent on the type of radio architecture implemented. This applies both to the transmitter and receiver implementations. However, the receiver side is conceptually more sensitive to non-idealities, as the received signal is typically very weak and needs to be processed and detected in the presence of other strong out of band signals, channel distortion and noise. Also the desired signal may already have suffered from non-idealities at the transmitter front-end. Thus the received signal has to be detected in the presence of both transmitter and receiver non-idealities.

Figure 2.2 shows a block diagram of a classical *superheterodyne receiver architecture* [73]. It converts the RF signal down to digital baseband in several steps, passing via number of IF stages each with its own local oscillator (LO). At each analog IF stage (IF1, IF2 and so on), the filtering is performed by means of band pass filters (BPF), low pass filters (LPF) and amplification by means of low noise amplifiers (LNA) and variable gain amplifiers (VGA). The superheterodyne architecture can generally maintain a very good selectivity and sensitivity if good components are used in the front-end. The in-phase/quadrature-phase (IQ) modulation and demodulation may be performed in the digital domain resulting in perfect IQ separation. The drawback of this architecture, however, is that it requires a lot of components to reach this good signal quality. At each analog IF, the filters and the amplifier all add to the component cost. Not only are they quite expensive components, but as they are external, they also add to the assembling cost.

Currently, most radio devices are based on the so-called *direct conversion (zero IF) radio architecture* or some of its variants like the low IF architecture [22], [1], [51]. As the name suggests, the direct conversion architecture converts the RF signal directly to baseband or vice-versa without any IFs. **Figure 2.3** illustrates a typical direct conversion receiver architecture [51]. The figure shows that a direct conversion architecture has a lower component count and consequently a lower cost. The direct conversion architecture also enables an easier integration and

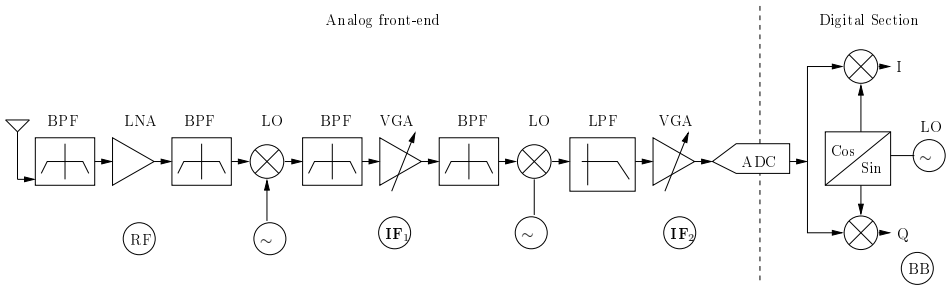

Figure 2.2: Superheterodyne receiver architecture

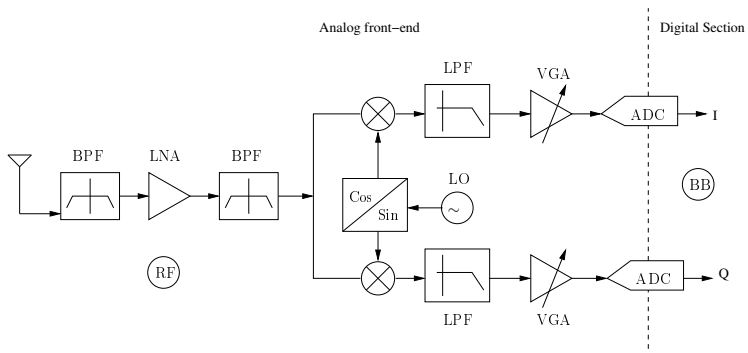

Figure 2.3: Direct conversion receiver architecture

leads to a smaller form factor. In a typical implementation of WLAN radio, it is shown that a direct conversion architecture can save up to 15-20% on total radio cost compared to a superheterodyne architecture [23], [103].

However, there are also drawbacks in using a direct conversion architecture. As the front-end now uses minimal analog electronic components, a simple radio module will have to process wideband high dynamic range signals, resulting in poor selectivity and sensitivity. A typical radio implementation will be very sensitive to any mismatches and imperfections in the front-end resulting in non-idealities. Also note that the direct conversion architecture performs IQ modulation and demodulation in the analog domain. The mismatch between the analog I and Q paths may then result in severe IQ imbalance distortion.

While any front-end radio architecture can exhibit non-idealities, it is usually more severe in a direct conversion architecture. Depending on the design choices and design tradeoffs, the effects of some of the non-idealities can be more severe compared to others, resulting in a significant performance deterioration of the

system. Below are some of the non-idealities typically associated with the front-end components:

- **DAC, ADC and Samplers**: Common non-idealities are non-ideal passband response i.e. unintentional filtering, aliasing, quantization noise, jitter noise due to instabilities of the sampling clock, non linear distortion due to clipping in ADC, deviation in the representation of quantization levels in DAC and DC offsets. The differences in ADCs and DACs in the I and Q branch leads to IQ imbalance.
- **Mixers**: Common non-idealities are non-linear distortions such as out of band harmonics, in-band inter-modulation products. Mixers also result in finite isolation between the input, local oscillator and output ports, and DC offsets. The relative difference between the I and Q branch mixers also contribute to IQ imbalance.
- **Local oscillator**: Common non-idealities are phase noise due to random fluctuation of the oscillator phase, carrier frequency offset (CFO) and phase offsets due to differences between the local oscillators at transmitter and receiver. Also the deviation in amplitude and phase shift from the ideal 90° for the I and the Q branch result in IQ imbalance.
- **Amplification stages (LNAs, VGAs, power amplifier at transmitter)**: Common non-idealities are various non-linear distortion effects such as in-band interference, harmonic distortion and inter modulation distortion. The difference in I and Q branch amplifiers also result in IQ imbalance.
- **Filters (LPF, BPF)**: Typically result in insufficient stop band attenuation and non-ideal passband response. The relative difference between the I and Q branch filters contribute to IQ imbalance which can vary as a function of frequency also within the interesting signal band.

In this dissertation, we investigate the effects and propose compensation algorithms for non-idealities such as CFO and IQ imbalance. The influence of other front-end non-idealities are modeled as an AWGN source at the receiver. For further details about various other front-end non-idealities and their compensation schemes, the reader is referred to [39]. In order to understand the system behavior we always consider the baseband equivalent impairment models of IQ imbalance and CFO. This baseband behavioral model allows us to easily implement the influence of these non-idealities in the baseband end-to-end system simulation setup. The behavioral model is independent of a particular front-end architecture and considers only the impact of these non-idealities on the received baseband signal.

2.3 Channel Characteristics

The study of the statistical models of the wireless channel is essential to analyze and design appropriate signal processing algorithms for reliable communication. This section elaborates on the channel model used in this dissertation. We first introduce different channel parameters in a multipath channel, from which, subsequently a discrete time channel model is derived.

In wireless communications, the transmitted signal arrives at the receiver from a number of different paths, referred to as multipaths as shown in **Figure 2.4**. Multipath propagation arises due to reflection, refraction, and scattering of the electromagnetic wave on objects that lie in the vicinity of the transmitter and/or receiver. The waves either propagate through the objects, diffract, scatter or reflect off them. The signals propagating via these indirect paths will be delayed, attenuated and phase shifted relatively to the signal received via the direct path. It can be shown that the equivalent baseband channel impulse response at time t, and propagation delay τ can be modelled as [70], [35]:

$$\mathbf{h}(t,\tau) = \sum_{p=1}^{N_p(t)} \alpha_p(t) e^{\jmath\phi_p(t)} \delta(\tau - \tau_p(t)) \tag{2.1}$$

where $\delta(t)$ is the Dirac impulse, $N_p(t)$ is the number of multipath components, $\alpha_p(t)$ is the attenuation, τ_p is the time delay and $\phi_p(t) = 2\pi f_c \tau_p(t) + \theta_p(t)$ is the phase shift that consists of a component due to free space propagation plus a component $\theta_p(t)$ due to other phase shifts experienced in the channel. Here f_c is the carrier frequency. Thus the wireless channel may generally be characterized as linear, time varying multipath in nature.

In equation (2.1), all parameters in the channel model $N_p(t), \alpha_p(t), \phi_p(t), \theta_p(t)$ are a function of time t and can therefore be time varying. This is a valid assumption for a fast varying channel. However, in this dissertation we consider the channel to be quasi static, i.e. the channel is assumed to be static (invariant) over a burst of symbols, such that the initial channel estimate can be used for the complete burst. The channel is assumed to characterize slow fading where the channel impulse response changes at a rate much slower than the symbol period T of the transmitted signal. As the channel parameters are constant, the explicit function of time t is omitted, thus the quasi static channel can be re-written as:

$$\mathbf{h}(\tau) = \sum_{p=1}^{N_p} \alpha_p e^{\jmath\phi_p} \delta(\tau - \tau_p) \tag{2.2}$$

Based on equation (2.2), we can now define a number of relevant channel parameters, that allow us to further characterize the channel. These are defined below:

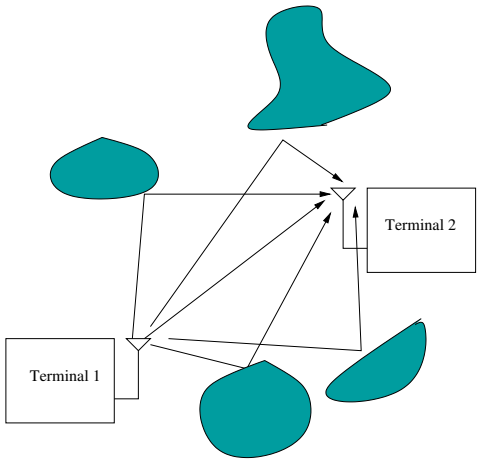

Figure 2.4: Multipath propagation between two wireless terminals

- **Delay domain parameters:** The delay domain parameters are usually described as a function of the excess delay τ , which is defined as the delay relative to the first incoming path. One of the important delay domain parameter is the power delay profile (PDP) which is defined as the power of the channel impulse response, this is given as:

$$\mathbf{p}_D(\tau) = \sum_{p=1}^{N_p} |\alpha|^2 \delta(\tau - \tau_p) = \sum_{p=1}^{N_p} \alpha^2 \delta(\tau - \tau_p) \tag{2.3}$$

A PDP profile of a channel is considered to decay exponentially with the amount of delay in the propagation. This is because the signals that take a longer path typically encounter more obstacles, resulting in larger delays and attenuation.

The first order moment of the PDP results in a mean propagation delay, which is given as [3]:

$$\bar{\tau} = \frac{\int_{-\infty}^{\infty} \mathbf{p}_D(\tau)\tau d\tau}{\int_{-\infty}^{\infty} \mathbf{p}_D(\tau) d\tau} = \frac{\sum_{p=1}^{N_p} \alpha_p^2 \tau_p}{\sum_{p=1}^{N_p} \alpha_p^2} \tag{2.4}$$

The root mean square (rms) delay spread σ_τ is given by the square root of the second order moment of the PDP, given as:

$$\sigma_\tau^2 = \frac{\int_{-\infty}^{\infty} \mathbf{p}_D(\tau)(\tau - \bar{\tau})^2 d\tau}{\int_{-\infty}^{\infty} \mathbf{p}_D(\tau) d\tau} = \frac{\sum_{p=1}^{N_p} \alpha_p^2 (\tau - \bar{\tau})^2}{\sum_{p=1}^{N_p} \alpha_p^2} \tag{2.5}$$

The rms delay spread is often used as a parameter to measure the time dispersion of the channel. If the rms delay spread is small compared to the symbol period T, then all multipath components arrive within the same symbol. Thus, consecutive symbols do not interfere with one another and there is no inter-symbol-interference (ISI). On the other hand, if the rms delay spread is large compared to the symbol period, then consecutive symbols interfere with one another and more complex equalization schemes are needed.

- **Frequency domain parameters:** The frequency domain response of the channel, which is obtained by the Fourier transform of the impulse response and expressed as a function of frequency f is given as:

$$\mathbf{H}(f) = \int_{-\infty}^{\infty} \mathbf{h}(\tau) e^{-\jmath 2\pi f \tau} d\tau \tag{2.6}$$

The channel response is generally considered to be frequency dependent because of the inherent multipath characteristic.

We can now define the correlation between the channel responses at different frequencies as:

$$\mathbf{r}_h(\Delta f) = \frac{1}{f_{high} - f_{low}} \int_{f_{low}}^{f_{high}} \mathbf{H}(f)\mathbf{H}^*(f + \Delta f) df \tag{2.7}$$

where f_{low} and f_{high} indicate the minimum and maximum frequency of the channel band under consideration. It is observed that as the frequency separation Δf increases, the correlation decreases.

Another important frequency domain parameter is the channel coherence bandwidth B_c, which is defined as a measure of the channel frequency selectivity, i.e. the width of the band of the frequencies which are similarly affected by the channel. The channel coherence bandwidth is inversely proportional to the channel maximum delay spread, $B_c = \frac{1}{\tau_{N_p}}$.

2.3.1 Discrete Time Channel Model

In digital communication systems, the transmitted signal consists of discrete symbols $\mathbf{x}[n]$ that are sampled at the symbol rate $1/T$ and pulse shaped with the transmit filter $\mathbf{g}_t(t)$. This pulse shaping operation is usually performed by the DAC at the transmitter. A similar pulse shaping operation is also performed with the receive filter $\mathbf{g}_r(t)$ by the ADC at the receiver. Subsequently, the signal is sampled at the symbol rate $1/T$ resulting in the discretization of the received signal $\mathbf{r}[n]$. The equivalent discrete time input-output relationship can be modeled as [7],[66]:

$$\mathbf{r}[n] = \mathbf{r}(nT) = \sum_{k=-\infty}^{\infty} \mathbf{d}[k]\mathbf{x}[n-k] + \mathbf{n}[n] \tag{2.8}$$

where $\mathbf{n}[n]$ is the AWGN noise and $\mathbf{d}[k]$ is the equivalent channel denoting the combined impulse response of the channel and transmit/receive filters. Now the kth tap of the equivalent channel can be given as:

$$\begin{aligned} \mathbf{d}[k] &= \int_0^{\tau_p} \mathbf{g}(kT-\tau)\mathbf{h}(\tau)d\tau \\ &= \sum_{p=1}^{N_p} \alpha_p e^{\jmath\phi_p} \mathbf{g}(kT-\tau_p) \end{aligned} \tag{2.9}$$

where $\mathbf{g}(t) = \mathbf{g}_t(t) \star \mathbf{g}_r(t)$ denotes the combined impulse response of the transmit/receive filters. Assuming an ideal pulse shaping filter $\mathbf{g}(t)$ =sinc$(\pi t/T)$, then the equivalent channel can be written as:

$$\mathbf{d}[k] = \sum_{p=1}^{N_p} \alpha_p e^{\jmath\phi_p} \text{sinc}\left(\tfrac{\pi(kT-\tau_p)}{T}\right) \tag{2.10}$$

Equation (2.9)-(2.10) shows that the effective channel consists of a concatenation of the multipath channel and the transmit/receive filters.

For causal frequency selective channel with finite maximum delay spread τ_{N_p} and number of resolvable multipath components $L = \lceil \tau_{N_p}/T \rceil$, the input-output relationship (2.8) can be written as:

$$\mathbf{r}[n] = \sum_{l=0}^{L-1} \mathbf{d}[l]\mathbf{x}[n-l] + \mathbf{n}[n] \tag{2.11}$$

Equation (2.11) assumes that the delay of the first arriving path is zero and the delay of the last arriving path is $L-1$. Equation (2.11) represents the tapped

delay line model with L uniformly spaced taps. The tap spacing between adjacent taps is T, and each tap is characterized by a complex valued gain parameter $\mathbf{d}[l]$. We consider the time delay τ_p of the arriving paths to be an integer multiple of T, thus the entire energy from the arriving paths can be mapped on L taps of the tapped delay line model, and as a result there are no leakages or sidelobes [114]. The finite length tapped delay line is a realistic model for a multipath channel [35], [48] and [56]. **Figure 2.5** illustrates the tapped delay line model in a noiseless case.

In order to determine the channel coefficients $\mathbf{d}[l]$ for the tapped delay line channel model, a wide range of realizations has to be generated, i.e. resorting to measurements and converting them into discrete time models. This process can be quite cumbersome and time consuming as it requires the full knowledge of all parameters of different propagation paths and the characteristics of transmit/receive filters. Alternatively more convenient stochastic models can be used to derive channel coefficients. This approach allows the generation of channel realizations on the basis of only a few essential parameters of the multipath environment. We will regard the PDP, rms delay spread, fading distribution as sufficient parameters to accurately model the channel. We will use this assumption throughout the thesis.

If we regard (2.11) as the basis of the channel model, then the channel coefficient can be obtained as:

$$\mathbf{d}[l] = \sqrt{\mathbf{p}_{D_N}[l]}\beta[l] \tag{2.12}$$

where $\mathbf{p}_{D_N}[l]$ is the normalized PDP, and $\beta[l]$ models the fading of the channel taps.

The fading term $\beta[l]$ is modeled as a standard complex normal distribution with zero mean and a unit variance. This results in a uniform and Rayleigh distributed amplitude and phase of the fading parameter. This model is commonly used for indoor and non line of sight outdoor environments [61], [67] . This shows that each channel tap consists of a sum of N_p paths. For large N_p, the central limit theorem holds and the summation results in complex Gaussian taps. Measurements reveal that the correlation between channel taps is rather small [70]. Therefore, statistically independent channel taps are assumed.

The normalized PDP is modeled as a exponentially decaying function of the excess delay [52]. The time discrete version of the normalized PDP is given as:

$$\mathbf{p}_{D_N}[l] = \begin{cases} \frac{e^{-lT/\sigma_\tau}}{\sum_{l=0}^{L-1} e^{-lT/\sigma_\tau}} & \text{for } \sigma_\tau > 0, \\ 1 & \text{for } \sigma_\tau = 0 \end{cases} \tag{2.13}$$

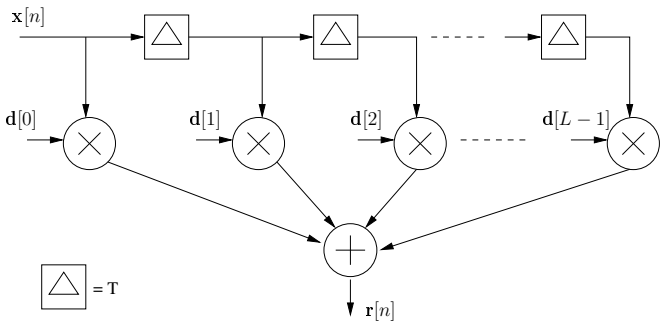

Figure 2.5: Tapped delay line model of frequency selective channel

The stochastic channel model, as proposed in this section, will be applied for evaluation purpose throughout this dissertation.

2.4 OFDM Background

In chapter 1, it was shown that OFDM is a popular transmission scheme for a number of broadband wireless systems, e.g., WLAN, WiMAX, DVB, etc. OFDM is increasingly being employed because of its efficient utilization of the available spectrum and its robustness against multipath fading. This dissertation therefore focuses its investigation of front-end non-idealities in systems relying on OFDM as their transmission technique. In this section an overview of the OFDM transmission scheme is given, followed by a brief introduction of the WLAN case study.

OFDM is a multicarrier transmission technique, where the information symbols are transmitted on multiple subcarriers [20], [118]. It is a special case of the frequency division multiplexing (FDM) transmission scheme [76]. In the classical FDM scheme, multiple baseband signals are multiplexed onto multiple subcarriers to create a composite transmission signal [119]. The front-end then requires multiple RF carriers for up-conversion and similarly multiple carriers and filters are needed for down-conversion of the received RF signal. The transmission scheme is not bandwidth efficient as every signal band is appropriately separated from its neighboring bands to allow for adequate filtering of the desired signal at the receiver.

On the other hand, the OFDM scheme generates different subcarrier signals in an orthogonal fashion, as a result of which the total signal bandwidth is much smaller compared to the classical FDM scheme. **Figure 2.6** illustrates the spectra of three subcarriers in classical FDM and OFDM. The figure shows that the OFDM

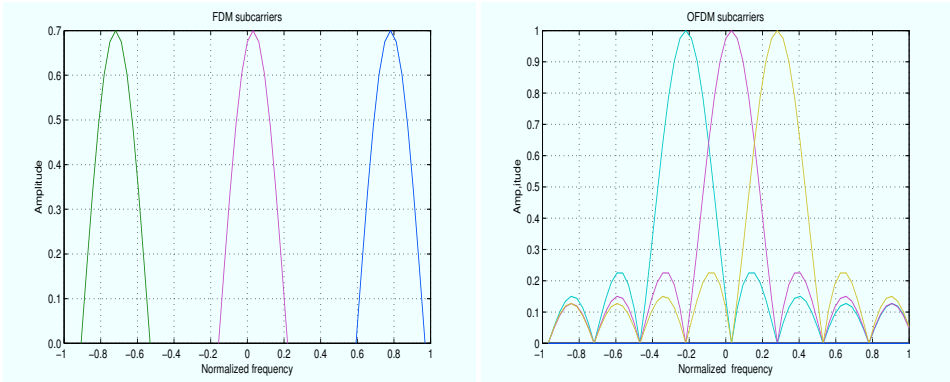

(a) Classical FDM (b) OFDM

Figure 2.6: Spectrum associated with classical FDM and OFDM scheme

subcarriers have overlapping spectra and are orthogonal. The arrangement is such that the peak amplitude of one subcarrier corresponds to the zero amplitude of the other subcarriers. This orthogonality allows for an efficient utilization of the spectrum as more data can now be transmitted in the available bandwidth. The subcarriers are modulated and demodulated in the baseband section by means of an inverse discrete Fourier transform (IDFT) and discrete Fourier transform (DFT) operation at the transmitter and receiver respectively. The DFT/IDFT operation allows for a cheap and spectrally efficient method of modulating the subcarriers. The front-end now requires only one RF carrier signal for up-conversion and also only one carrier and filter for down-conversion at the receiver.

The basic idea behind OFDM is to divide the available system bandwidth B into N parallel, overlapping, orthogonal and multiple frequency subcarriers. If the number of subcarriers N is sufficiently large, then the resulting subcarrier spacing is narrow compared to the coherence bandwidth B_c of the channel. As a result, each subcarrier experiences approximately frequency flat fading. In order to preserve the orthogonality, a cyclic prefix (CP), which is a copy of the last ν time domain samples of an OFDM symbol, is added at the head of every OFDM symbol. If the CP length ν is longer than the channel impulse response of length L, then the linear convolution operation with the channel appears as a cyclic convolution operation at the receiver. The convolution theorem states that a cyclic convolution in the time domain corresponds to an element wise multiplication in the frequency domain. Thus a simple one-tap frequency domain equalizer (FEQ) per subcarrier is sufficient to preserve the orthogonality and there is no inter-carrier-interference (ICI).

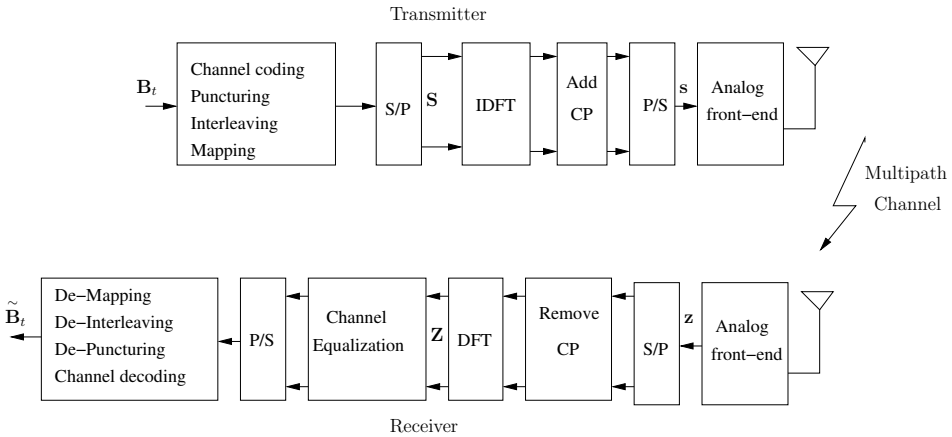

Figure 2.7: OFDM system model

Besides ICI, a CP also provides an elegant way to cope with the problem of inter-symbol-interference (ISI). The CP prevents an OFDM symbol from interfering with the adjacent symbols, thus limiting the influence of ISI within its own length. This allows for independent detection of all symbols. Since the CP contains only redundant information, it is removed before the demodulation (DFT) operation at the receiver. The addition of CP reduces the overall effective data rate of the system, thus it is important to consider the right CP length ν and the OFDM symbol length N as a tradeoff between the robustness and the effective data rate.

Figure 2.7 depicts the block diagram of an OFDM communication scheme. The figure shows that the input bitstream $\mathbf{B}_t$ is first processed through the baseband processing that typically consists of channel coding, puncturing, interleaving and mapping into the complex constellation space. The complex signal is then serial-to-parallel (S/P) converted resulting in OFDM symbol $\mathbf{S}$ of length N. The symbols are then transformed to the time domain by an IDFT operation. A CP of length ν is added at the head of the symbol, resulting in a time domain symbol $\mathbf{s}$ of length $N+\nu$. The symbol $\mathbf{s}$ is then parallel-to-serial (P/S) converted before being fed to the transmitter front-end. The baseband signal is then converted to the analog domain, up-converted to RF and finally transmitted through the multipath channel.

Similarly the received signal is down-converted by the receiver front-end to baseband, resulting in a time domain symbol $\mathbf{z}$. The symbol $\mathbf{z}$ is serial-to-parallel converted and the part corresponding to the CP is removed. The resulting vector is then transformed to the frequency domain by the DFT operation, yielding the symbol $\mathbf{Z}$. The remaining baseband processing involves channel equalization, parallel-to-serial conversion, de-mapping, de-interleaving, de-puncturing, channel

System Parameter	Parameter Value
Constellation	BPSK, QPSK, 16QAM, 64QAM
Coding	Convolution
Coding Rate	1/2, 2/3, 3/4
Number of OFDM subcarriers N	64
Number of data subcarriers	48
Number of pilot subcarriers	4
Number of CP Subcarriers ν	16
Bandwidth B	20 Mhz
Total symbol duration (OFDM+CP)	4 μs
CP duration	800 ns
Subcarrier Spacing B_s	312.5 kHz

Table 2.1: Parameters of IEEE 802.11a standard

decoding, etc. The subsequent decisions represent the estimate of the transmitted bitstream given as $\widetilde{\mathbf{B}}_t$.

2.4.1 WLAN IEEE 802.11a Case Study

Throughout this dissertation, the performance of the proposed algorithms is assessed based on an OFDM system similar to the WLAN IEEE 802.11a standard. However, the proposed techniques are equally applicable to other systems, operating in a similar environment. This section briefly introduces the IEEE 802.11a standard. For a more in depth study of the standard, the reader is referred to [43], [37], [115] and [116].

In the IEEE 802.11a standard, the receive part of the physical layer specifies only the quality requirements, thus the implementation may vary between different manufacturers. The focus of this section is only on the transmit specification. The main parameters of the standard are summarized in **Table 2.1**. The table shows that there is a wide choice between various constellation schemes and the coding rate. The transmitter can select any suitable data format based on the channel and noise condition. Typically a 1/2 coded BPSK mode is used in the lowest signal to noise ratio (SNR) scenario, while the 3/4 coded 64QAM mode is used in the best SNR scenario. The OFDM symbol consists of $N = 64$ subcarriers, of which only 52 subcarriers are modulated. Of these 52 non-zero subcarriers, 48 subcarriers are modulated by data symbols and 4 subcarriers are modulated with known BPSK pilot symbols. The DC subcarrier and the subcarriers at the edges of the spectrum are not used so as to meet the spectral mask requirements and not to cause interference to the neighbouring channels. The OFDM symbol is sampled at 20 MHz, resulting in a inter carrier spacing $B_s = 312.5$ kHz. The length of the

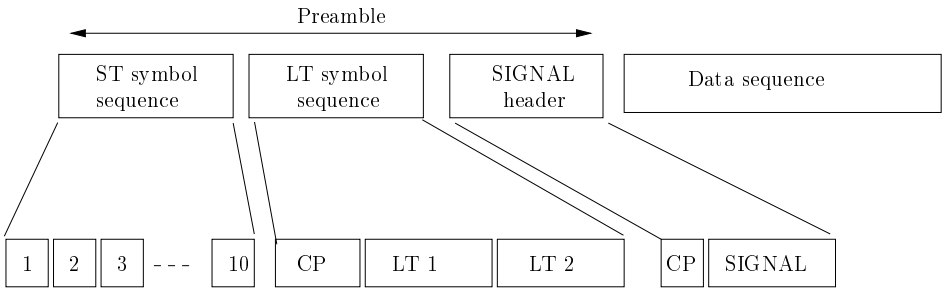

Figure 2.8: IEEE 802.11a packet structure

CP is $\nu = 16$ samples, resulting in an overhead of 20%. This leads to a total OFDM symbol duration of $4\mu s$.

IEEE 802.11a is a packet transmission scheme, consisting of a known part called the preamble followed by the data sequence. The receiver uses the preamble portion of the packet for synchronization, channel estimation and to identify the length, format of the data sequence, etc. This packet structure is illustrated in **Figure 2.8**. The figure shows that the preamble consists of three parts: the first part consists of a 10 times repeated, short training (ST) symbol of 16 samples in length. The second part consists of twice repeated, long training (LT) symbol of 64 samples in length. The third part consists of a preamble header called SIGNAL symbol of 64 samples in length. The ST sequence can be used for packet detection, automatic gain control, coarse estimation of CFO and also receiver IQ imbalance estimation. The figure shows that the LT sequence is preceded by an extended CP length, i.e. a copy of the final 32 samples of the LT symbol. The LT sequence can be used for channel estimation, noise estimation, fine CFO estimation, timing synchronization and IQ imbalance estimation. The preamble header, contains information such as the packet length, data rate and applied constellation scheme in the data part. As this information is crucial, it is always transmitted in the most robust mode (1/2 coded BPSK). The subsequent data part consists of the OFDM data sequence, which forms the substantial part of the packet with varying length. The data sequence is transmitted in the data rate mode indicated in the SIGNAL symbol.

Throughout this dissertation, we will adhere to a similar packet structure consisting of a ST symbol sequence, followed by a LT symbol sequence and then finally the data sequence.

2.5 Summary

In this chapter, we have provided an end-to-end system model of a modern OFDM based wireless communication scenario. The system model comprises of all important building blocks in a broadband wireless communication link: the most important digital, analog blocks, together with the OFDM system and multipath channel model have been introduced. A brief overview is given of different front-end radio architectures and some of the most common non-idealities are also discussed. The parameters of the underlying wireless channel have been presented in detail. We have considered a stochastic channel model to derive the channel coefficients. The stochastic approach allows the generation of channel realizations on the basis of only a few essential parameters of the multipath environment. Finally the basic building blocks and the parameters associated with the OFDM transmission scheme and with the WLAN IEEE 802.11a case study have been presented.

In the following chapters, we develop various training based digital solutions to compensate for some of the essential analog front-end non-idealities, such as IQ imbalance and CFO, based on the end-to-end system model presented in this chapter. It is shown that this model allows for a complete realistic performance analysis.

Part I

Single Antenna OFDM Systems

Chapter 3

IQ Imbalance

3.1 Introduction

An OFDM system based on a direct conversion architecture is very sensitive to front-end non-idealities such as IQ imbalance. Though OFDM is robust against the interference caused by the multipath propagation, its orthogonality may be destroyed due to the presence of IQ imbalance.

In the last decade, several articles have been published that address the problem of IQ imbalance. An extensive study of the performance degradation due to IQ imbalance has been presented in [54]. In [100] and [78], compensation solutions for receiver IQ imbalance based on an adaptive training scheme have been proposed. In [17] the estimation of receiver IQ imbalance based on minimizing the residual channel energy in the time domain is discussed. These proposed solutions have been extended to also consider transmitter IQ imbalance together with receiver IQ imbalance in [102] and [18]. In [106] and [108], the authors separately propose the estimation of receiver IQ imbalance and transmitter IQ imbalance based on minimizing the notch response of the channel due to IQ imbalance. In [12] calibration schemes have been developed to directly estimate receiver IQ imbalance at the analog front-end. The estimates are then fed back to digital baseband where the compensation of IQ imbalance is implemented. This front-end calibration scheme requires extra analog hardware to estimate the IQ imbalance. The hardware needs to be carefully designed in order not to introduce any additional IQ imbalance, which may in turn bias the IQ imbalance measurement. All these solutions consider the influence of only frequency independent IQ imbalance. For a wideband communication system it is important to also consider frequency selective distortions introduced by IQ imbalances. These frequency selective

distortions arise mainly due to mismatched filters in the I and Q branch of the front-end.

In [111], [110], [4] compensation solutions for frequency selective receiver IQ imbalance based on statistical signal properties have been developed. In [53], adaptive training based and, in [55], maximum likelihood based compensation solutions for frequency selective transmitter and receiver IQ imbalance are proposed. In [64] the authors address the problem of joint transmitter and receiver IQ imbalance under high mobility. Thus several solutions that consider different combinations of frequency selective/frequency independent transmitter/receiver IQ imbalance have been developed. However, in the above mentioned works, the cyclic prefix (CP) is consistently assumed to be longer than or equal to the the combined transmitter/receiver IQ imbalance and channel impulse response length. In this chapter we consider the case where the CP is short, and furthermore frequency selective transmitter and receiver IQ imbalance is present, leading to severe inter-symbol-interference and inter-carrier-interference within an OFDM symbol. To the best of our knowledge, no general solution has been proposed so far for the problem combining insufficient CP length and frequency selective transmitter/receiver IQ imbalance. The material related to this chapter has been published in [84], [89], and [90].

The chapter is organized as follows: In **section 3.2**, we consider the case of a sufficiently long CP length, thus there is no ISI between adjacent OFDM symbols. We first derive an input-output system model considering both frequency independent and frequency selective IQ imbalance in the transmitter and receiver analog front-ends. The influence of the joint transmitter and receiver IQ imbalance in an OFDM system is discussed. We then derive a joint transmitter/receiver IQ imbalance and channel compensation scheme based on a two-tap frequency domain equalizer (FEQ) per subcarrier. Finally, the training based least squares (LS) and recursive least squares (RLS) algorithms for the initialization of FEQ coefficients are derived.

In **section 3.3**, the case of a short CP length is considered. In this case a simple two-tap adaptive equalizer is not sufficient to preserve the carrier orthogonality and so more complex joint compensation schemes are needed. We propose a frequency domain two-branch per-tone equalizer (PTEQ) [113], which shortens the combined channel and transmitter/receiver IQ imbalance impulse response to fit within the CP length and at the same time compensate for the imperfection of the analog front-end. The PTEQ can also be initialized by any suitable training based algorithm. Simulation results are shown in **section 3.4** and finally conclusions are drawn in **section 3.5**

3.2 Joint IQ Imbalance and Channel Compensation

In this section we investigate the effects and compensation schemes of transmitter and receiver IQ imbalance when the CP length is sufficiently long.

3.2.1 System Model with IQ Imbalance

Let $\mathbf{S}$ be an uncoded frequency domain OFDM symbol of size $(N \times 1)$ where N is the number of subcarriers. This symbol is transformed to the time domain by an inverse discrete Fourier transform (IDFT). A cyclic prefix (CP) of length ν is added to the head of each symbol. The resulting time domain baseband symbol $\mathbf{s}$ is then given as:

$$\mathbf{s} = \mathbf{P_{CI}}\mathbf{F}_N^{-1}\mathbf{S} \tag{3.1}$$

where $\mathbf{F}_N^{-1}$ represents the $N \times N$ inverse discrete Fourier transform matrix and $\mathbf{P_{CI}}$ is the CP insertion matrix given by:

$$\mathbf{P_{CI}} = \left[\begin{array}{c|c} \mathbf{0}_{(\nu \times N-\nu)} & \mathbf{I}_\nu \\ \hline \multicolumn{2}{c}{\mathbf{I}_N} \end{array}\right]$$

Here $\mathbf{0}_{x\times y}$ represents the $x \times y$ all zero matrix and $\mathbf{I}_x$ represents the $x \times x$ Identity matrix.

The symbol $\mathbf{s}$ is parallel-to-serial converted before being fed as an input to the direct conversion transmitter front-end. In general, all analog components at the direct-conversion front-end, such as the local oscillator (LO), mixers, amplifiers, low pass filters (LPF) and digital to analog (DAC) converters contribute to the effective IQ imbalance [22], [105], [111], [123]. We categorize the IQ imbalance resulting from the front-end as frequency selective (FS) and frequency independent (FI) in nature. The imbalance caused by the LO is generally considered FI over the entire symbol bandwidth. This is because the LO produces only a single tone, resulting in a transmitter amplitude and phase mismatch g_t and ϕ_t between the two branches (ideally $g_t = 1$ and $\phi_t = 0$).

The imbalances caused by the DAC, amplifiers, LPFs and mixers generally result in an overall FS IQ imbalance. We represent this imbalance at the transmitter by two mismatched filters with frequency responses given as $\mathbf{H}_{ti} = \mathbf{F}_N\mathbf{h}_{ti}$ and $\mathbf{H}_{tq} = \mathbf{F}_N\mathbf{h}_{tq}$ where $\mathbf{h}_{ti}$ and $\mathbf{h}_{tq}$ are the impulse response of the respective I and Q branch mismatched filters, and $\mathbf{F}_N$ represents the $N\times N$ discrete Fourier transform matrix. Following the derivation in [112], the equivalent baseband symbol $\mathbf{p}$ after front-end distortions can be given as:

$$\mathbf{p} = \mathbf{g}_{ta} \star \mathbf{s} + \mathbf{g}_{tb} \star \mathbf{s}^* \tag{3.2}$$

where $\star$ is the linear convolution operator and $\mathbf{s}^*$ denotes the complex conjugate of vector $\mathbf{s}$. The terms

$$\mathbf{g}_{ta} = \mathbf{F}_N^{-1}\mathbf{G}_{ta} = \mathbf{F}_N^{-1}\left(\frac{\mathbf{H}_{ti} + g_t e^{-\jmath\phi_t}\mathbf{H}_{tq}}{2}\right),$$

$$\mathbf{g}_{tb} = \mathbf{F}_N^{-1}\mathbf{G}_{tb} = \mathbf{F}_N^{-1}\left(\frac{\mathbf{H}_{ti} - g_t e^{\jmath\phi_t}\mathbf{H}_{tq}}{2}\right)$$

Here $\mathbf{g}_{ta}$ and $\mathbf{g}_{tb}$ are mostly truncated to length L_t (and then possibly padded with $N - L_t$ zero elements). They represent the combined FI and FS IQ imbalance at the transmitter. $\mathbf{G}_{ta}$ and $\mathbf{G}_{tb}$ are the frequency domain representations of $\mathbf{g}_{ta}$ and $\mathbf{g}_{tb}$ respectively. Note that $\mathbf{g}_{tb}$ vanishes if $g_t = 1$, $\phi_t = 0$ and $\mathbf{H}_{ti} = \mathbf{H}_{tq}$. From now on we will refer to the combined FI and FS IQ imbalance as the IQ imbalance for conciseness. The transmitted RF symbol $\overset{\hookrightarrow}{\mathbf{p}}$ is then writen as:

$$\overset{\hookrightarrow}{\mathbf{p}} = \Re\left\{\mathbf{p}.e^{\jmath 2\pi f_c \mathbf{t}}\right\} \tag{3.3}$$

where $\mathbf{p} = \mathbf{p}_i + \jmath\mathbf{p}_q$ is the baseband equivalent representation of $\overset{\hookrightarrow}{\mathbf{p}}$, f_c is the carrier frequency, $\Re\{\mathbf{x}\}$ denotes the real part of vector $\mathbf{x}$ and $\mathbf{t}$ is the time vector. Note that we apply a vector function notation, where the (exponential) function is applied to each component of the vector $\mathbf{t}$.

When the symbol $\overset{\hookrightarrow}{\mathbf{p}}$ is transmitted through a quasi static frequency selective channel of length L, then the received baseband symbol $\mathbf{r}$ is given as:

$$\begin{aligned}\mathbf{r} &= \mathbf{c} \star \mathbf{p} + \mathbf{n} \\ &= \mathbf{c} \star \mathbf{g}_{ta} \star \mathbf{s} + \mathbf{c} \star \mathbf{g}_{tb} \star \mathbf{s}^* + \mathbf{n} \\ &= \mathbf{c}_a \star \mathbf{s} + \mathbf{c}_b \star \mathbf{s}^* + \mathbf{n}\end{aligned} \tag{3.4}$$

where $\mathbf{c}$ is the baseband representation of the channel, $\mathbf{c}_a$ and $\mathbf{c}_b$ are the combined transmitter IQ imbalance and channel impulse responses of length $L + L_t - 1$ and $\mathbf{n}$ is proper complex additive white Gaussian noise (AWGN). The channel is considered to be static for the duration of one entire packet which consists of a training sequence followed by a data sequence.

An expression similar to equation (3.2) can be used to model IQ imbalance at the receiver. Let $\mathbf{z}$ represent the down-converted baseband complex symbol after being distorted by receiver IQ imbalance. The IQ imbalance is modeled by filters $\mathbf{g}_{ra}$ and $\mathbf{g}_{rb}$ of length L_r, where $\mathbf{g}_{ra}$ and $\mathbf{g}_{rb}$ are defined similar to $\mathbf{g}_{ta}$ and $\mathbf{g}_{tb}$ in equation (3.2). The received symbol $\mathbf{z}$ is then written as:

$$\mathbf{z} = \mathbf{g}_{ra} \star \mathbf{r} + \mathbf{g}_{rb} \star \mathbf{r}^* \tag{3.5}$$

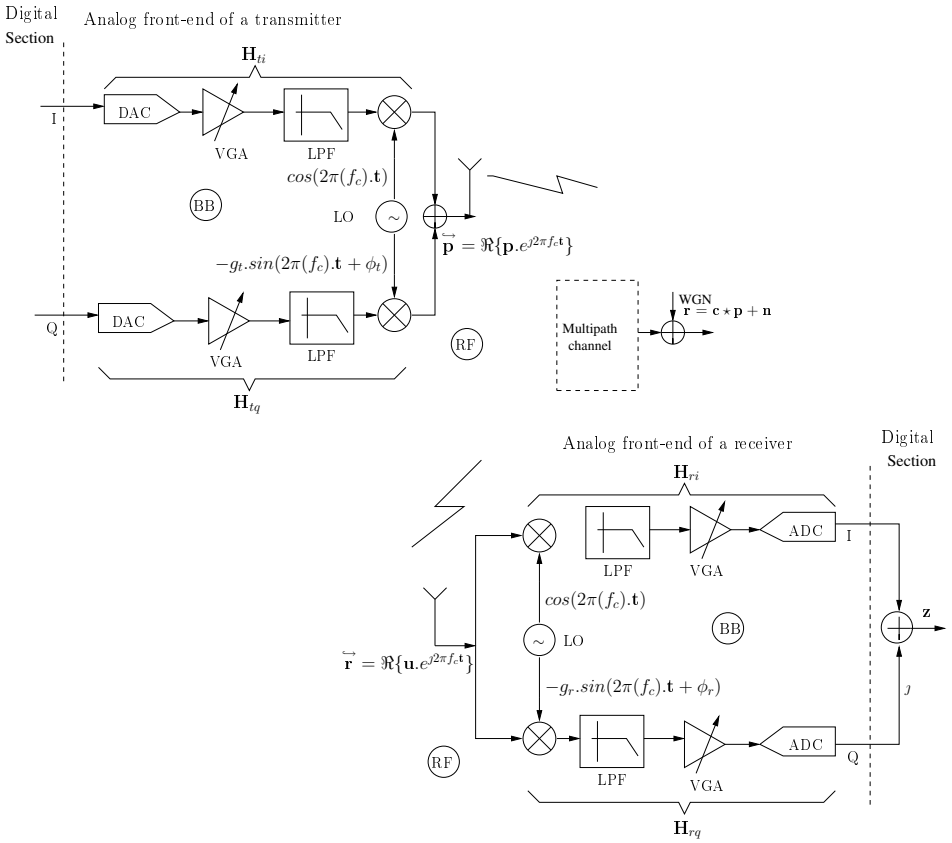

Figure 3.1: Mathematical model of a direct conversion transmitter and receiver front-end

Equation (3.4) can be substituted in equation (3.5) leading to

$$\begin{aligned}\mathbf{z} =&(\mathbf{g}_{ra} \star \mathbf{c}_a + \mathbf{g}_{rb} \star \mathbf{c}_b^*) \star \mathbf{s} + (\mathbf{g}_{ra} \star \mathbf{c}_b + \mathbf{g}_{rb} \star \mathbf{c}_a^*) \star \mathbf{s}^* \\ &+ \mathbf{g}_{ra} \star \mathbf{n} + \mathbf{g}_{rb} \star \mathbf{n}^* \\ =&\mathbf{d}_a \star \mathbf{s} + \mathbf{d}_b \star \mathbf{s}^* + \mathbf{n}_c\end{aligned} \tag{3.6}$$

where $\mathbf{d}_a$ and $\mathbf{d}_b$ are the combined transmitter/receiver IQ imbalance and channel impulse responses of length $L_t + L + L_r - 2$ and $\mathbf{n}_c$ is now a zero mean improper complex noise vector due to the presence of receiver IQ imbalance [65].

The down-converted received symbol $\mathbf{z}$ is serial-to-parallel converted and the part corresponding to the CP is removed. The received symbol is then transformed to

the frequency domain by a discrete Fourier transform (DFT). We consider the CP length ν to be larger than the length of both $\mathbf{d}_a$ and $\mathbf{d}_b$, thus leading to no ISI between adjacent OFDM symbols. The frequency domain received symbol $\mathbf{Z}$ can then be written as:

$$\begin{aligned}\mathbf{Z} =&\mathbf{F}_N\mathbf{P}_{\mathbf{CR}}\{\mathbf{z}\} = \mathbf{D}_a.\mathbf{S} + \mathbf{D}_b.\mathbf{S}^*_m + \mathbf{N}_c \\ =&(\mathbf{G}_{ra}.\mathbf{G}_{ta}.\mathbf{C} + \mathbf{G}_{rb}.\mathbf{G}^*_{tb_m}.\mathbf{C}^*_m).\mathbf{S} + \mathbf{G}_{ra}.\mathbf{N} \\ &+ (\mathbf{G}_{ra}.\mathbf{G}_{tb}.\mathbf{C} + \mathbf{G}_{rb}.\mathbf{G}^*_{ta_m}.\mathbf{C}^*_m).\mathbf{S}^*_m + \mathbf{G}_{rb}.\mathbf{N}^*_m\end{aligned} \tag{3.7}$$

where $\mathbf{G}_{ra}, \mathbf{G}_{rb}, \mathbf{C}, \mathbf{D}_a, \mathbf{D}_b, \mathbf{N}_c, \mathbf{N}$ are the frequency domain representations of $\mathbf{g}_{ra}, \mathbf{g}_{rb}, \mathbf{c}, \mathbf{d}_a, \mathbf{d}_b, \mathbf{n}_c, \mathbf{n}$. $\mathbf{F}_N$ is the $N \times N$ discrete Fourier transform matrix and $\mathbf{P}_{\mathbf{CR}}$ is the CP removal matrix given as:

$$\mathbf{P}_{\mathbf{CR}} = \begin{bmatrix} 0_{(N\times\nu)} & | & \mathbf{I}_N \end{bmatrix}$$

In equation (3.7), $\mathbf{X}.\mathbf{Y}$ denotes the component-wise vector multiplication between $\mathbf{X}$,$\mathbf{Y}$ and $()_m$ denotes the mirroring operation in which the vector indices are reversed, such that $\mathbf{S}_m[l] = \mathbf{S}[l_m]$

$$\text{where} \begin{cases} [l_m] = [2 + N - l] & \text{for } [l] = 2 \dots N \\ [l_m] = [l] & \text{for } [l] = 1 \end{cases}$$

Equation (3.7) shows that due to the presence of transmitter/receiver IQ imbalance, power leaks from the symbol on the mirror subcarrier ($\mathbf{S}^*_m$) to the subcarrier under consideration ($\mathbf{S}$), thus causing inter-carrier-interference (ICI). A generalized mathematical model of a direct conversion transmitter and receiver front-end is shown in **Figure 3.1**.

Note that if no IQ imbalance is present, then $g_t = g_r = 1, \phi_t = \phi_r = 0, \mathbf{H}_{ti} = \mathbf{H}_{tq} = \mathbf{H}_t, \mathbf{H}_{ri} = \mathbf{H}_{rq} = \mathbf{H}_r$. Thus $\mathbf{G}_{ta} = \mathbf{H}_t, \mathbf{G}_{ra} = \mathbf{H}_r$ and $\mathbf{G}_{tb} = 0, \mathbf{G}_{rb} = 0$, leading to the baseband symbol $\mathbf{Z}$ as:

$$\mathbf{Z} = \mathbf{F}_N\mathbf{P}_{\mathbf{CR}}\{\mathbf{h}_r \star \mathbf{r}\} = \mathbf{H}_t.\mathbf{H}_r.\mathbf{C}.\mathbf{S} + \mathbf{H}_r.\mathbf{N} \tag{3.8}$$

where $\mathbf{h}_r$ is the time domain representation of $\mathbf{H}_r$. The terms $\mathbf{H}_t.\mathbf{H}_r$ and $\mathbf{h}_r$ can be treated as part of the frequency domain representation of the channel $\mathbf{C}$ and its time domain representation $\mathbf{c}$, and thus can be ignored for conciseness. The received symbol $\mathbf{Z}$ is now a scaled version of $\mathbf{S}$ with no ICI. A simple one-tap channel equalizer can be used to obtain the estimate of the transmitted symbol $\widetilde{\mathbf{S}}$.

As OFDM is very sensitive to ICI, IQ imbalance may result in a severe performance degradation. The influence of IQ imbalance in an OFDM system is explained in the next section.

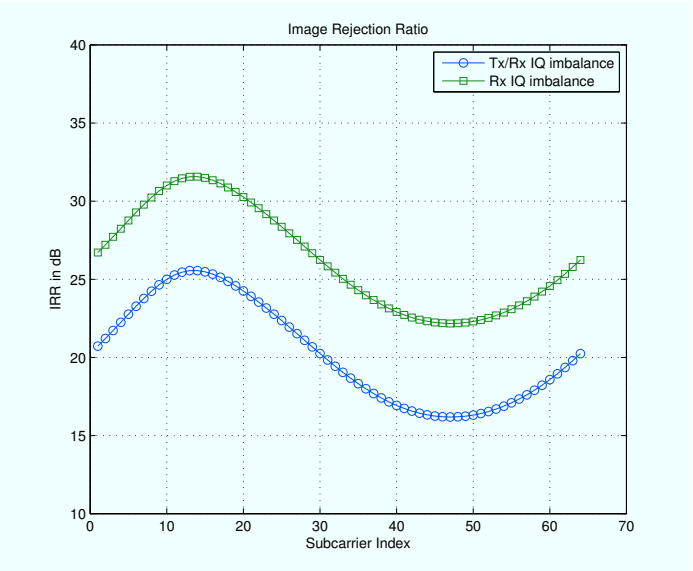

Figure 3.2: IRR for an OFDM system impaired with transmitter and receiver IQ imbalance

3.2.2 Influence of IQ Imbalance

The influence of IQ imbalance in an OFDM system can be measured in terms of image rejection ratio (IRR). In the absence of any compensation scheme, the IRR of the analog front-end processing is defined based on equation (3.7) as:

$$IRR = 10 \times log_{10} \frac{|\mathbf{D}_a[l]|^2}{|\mathbf{D}_b[l]|^2} \tag{3.9}$$

The quality of the IQ imbalance compensation can then be expressed as an improvement in IRR. In practice, the IRR for only receiver IQ imbalance is normally in the order of 20-40 dB [73]. **Figure 3.2** illustrates the IRR observed for an uncoded 64QAM OFDM system impaired with transmitter and receiver IQ imbalance in a noiseless, frequency flat channel scenario. The parameters used in this figure are as follows: We consider OFDM symbol length $N = 64$ with CP length $\nu = 16$. The FI amplitude imbalance of $g_t = g_r = 5\%$ and phase imbalance of $\phi_t = \phi_r = 5^\circ$. The front-end filter mismatched impulse responses are $\mathbf{h}_{ri} = \mathbf{h}_{ti} = [0.03\ 0.5\ 0.01], \mathbf{h}_{tq} = \mathbf{h}_{rq} = [0.01\ 0.5,\ 0.02]$ with filter impulse length $L_t = L_r = 3$. It should be noted that even though a three tap finite impulse response (FIR) filter may not be accurate enough to describe an analog filter, what matters in our discussion is not the absolute I and Q filter responses,

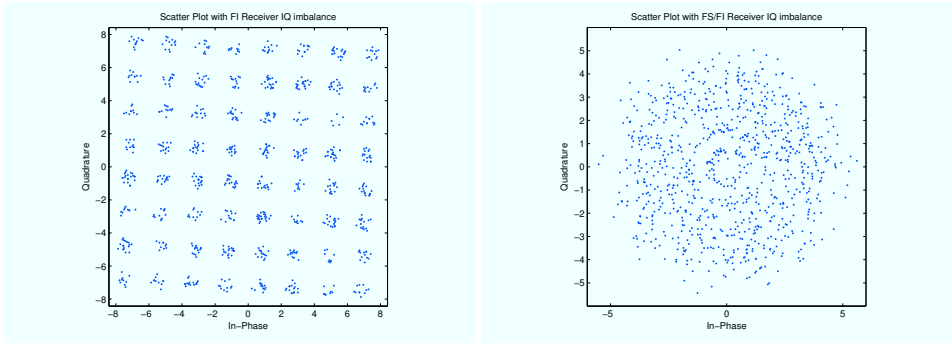

(a) Only FI IQ imbalance (b) Combined FS and FI IQ imbalance

Figure 3.3: Scatter plot observed in the presence of receiver IQ imbalance in a noiseless scenario

but their mismatched responses. We will therefore consider similar mismatched impulse responses for system analysis thoughout this dissertation.

The figure shows that in the presence of both transmitter and receiver IQ imbalance, the IRR is between 16 and 25 dB, which is a severe case of IQ imbalance distortion. With only receiver IQ imbalance and no transmitter IQ imbalance, an improvement of around 7 dB is already obtained. As the amount of IQ imbalance is reduced in the OFDM system, there is a corresponding improvement in the IRR.

The IRR performance measure in equation (3.9), accounts for the IQ imbalance as the only source of distortion. However, as there are many more sources of distortion (channel, CFO, insufficient CP length, etc) that degrade the system's performance, we rely on full system simulations as specified in chapter 2 and quantify the improvement of the IQ imbalance compensation in terms of the improvement in bit error rate (BER). This approach accounts for all sources of distortion and thus gives a realistic performance measure.

Figure 3.3(a)-(b) show the scatter plot obtained following the same simulation setup as in figure 3.2. The scatter plots are observed for the case of only FI receiver IQ imbalance (figure 3.3(a)) and the case of FS/FI receiver IQ imbalance (figure 3.3(b)). We do not consider the presence of transmitter IQ imbalance. Figure 3.3(a) shows a rotation in the scatter plot due to the presence of FI receiver IQ imbalance. As the amount of IQ imbalance increases, a corresponding increase in the scatter plot rotation is observed, resulting in the destruction of the orthogonality of the OFDM symbol. Figure 3.3(b) shows that the addition of FS IQ imbalance, severely distorts the scatter plot. Thus it is important to develop adequate compensation solutions that consider the influence of both FS and FI IQ imbalance. More performance simulation are shown in section 3.2.5.

3.2.3 IQ Imbalance Compensation

We will now derive the joint compensation of transmitter/receiver IQ imbalance and channel distortion. Following the system model from section 3.2.1, equation (3.7) can be rewritten for the received symbol $\mathbf{Z}$ and the complex conjugate of its mirror symbol $\mathbf{Z}^*_m$ as follows:

$$\underbrace{\begin{bmatrix}\mathbf{Z}[l]\\ \mathbf{Z}^*[l_m]\end{bmatrix}}_{\mathbf{Z}_{tot}[l]} = \underbrace{\begin{bmatrix}\mathbf{D}_a[l] & \mathbf{D}_b[l]\\ \mathbf{D}^*_b[l_m] & \mathbf{D}^*_a[l_m]\end{bmatrix}}_{\mathbf{D}_{tot}[l]} \underbrace{\begin{bmatrix}\mathbf{S}[l]\\ \mathbf{S}^*[l_m]\end{bmatrix}}_{\mathbf{S}_{tot}[l]} + \underbrace{\begin{bmatrix}\mathbf{N}_c[l]\\ \mathbf{N}^*_c[l_m]\end{bmatrix}}_{\mathbf{N}_{c_{tot}}[l]} \tag{3.10}$$

The matrix $\mathbf{D}_{tot}[l]$ represents the joint transmitter IQ imbalance, receiver IQ imbalance and channel distortion for the received symbol matrix $\mathbf{Z}_{tot}[l]$.

Assuming $\mathbf{D}_{tot}[l]$ is known, then symbol estimates $\widetilde{\mathbf{S}}[l]$ and $\widetilde{\mathbf{S}}_{tot}[l]$ of $\mathbf{S}[l]$ and $\mathbf{S}_{tot}[l]$ are obtained based on a minimum mean square error (MMSE) criterion as:

$$\widetilde{\mathbf{S}}[l] = \begin{bmatrix}1 & 0\end{bmatrix} \widetilde{\mathbf{S}}_{tot}[l] = \begin{bmatrix}1 & 0\end{bmatrix} \mathbf{D}^H_{tot}[l](\mathbf{D}_{tot}[l]\mathbf{D}^H_{tot}[l] + \mathbf{R}_{Nc}[l])^{-1}\mathbf{Z}_{tot}[l] \tag{3.11}$$

where the noise covariance matrix $\mathbf{R}_{Nc}[l] = \Xi\{\mathbf{N}_{c_{tot}}[l]\mathbf{N}^H_{c_{tot}}[l]\}$. Here Ξ is the expectation operator and $\mathbf{X}^H$ represents the Hermitian transpose of matrix $\mathbf{X}$. In the noiseless case, equation (3.11) reduces to a zero forcing (ZF) solution given as $\widetilde{\mathbf{S}}[l] = \begin{bmatrix}1 & 0\end{bmatrix} \mathbf{D}^{-1}_{tot}[l]\mathbf{Z}_{tot}[l]$.

Based on equation (3.10), we can also directly generate symbol estimates by taking an appropriate linear combination of $\mathbf{Z}[l]$ and $\mathbf{Z}^*[l_m]$ as:

$$\widetilde{\mathbf{S}}[l] = \begin{bmatrix}\mathbf{W}_a[l] & \mathbf{W}_b[l]\end{bmatrix} \begin{bmatrix}\mathbf{Z}[l]\\ \mathbf{Z}^*[l_m]\end{bmatrix} \tag{3.12}$$

where $\mathbf{W}_a[l]$ and $\mathbf{W}_b[l]$ are the coefficients of a **two-tap frequency domain equalizer (FEQ)**. The FEQ coefficients are estimated based on a mean square error (MSE) minimization:

$$\underset{\mathbf{W}_a[l],\mathbf{W}_b[l]}{min}\ \Xi\left\{\left|\widetilde{\mathbf{S}}[l] - \begin{bmatrix}\mathbf{W}_a[l] & \mathbf{W}_b[l]\end{bmatrix} \begin{bmatrix}\mathbf{Z}[l]\\ \mathbf{Z}^*[l_m]\end{bmatrix}\right|^2\right\} \tag{3.13}$$

The basic difference between the compensation in (3.11) and (3.13) is that, (3.11) requires an estimate of the joint channel and transmitter/receiver IQ imbalance matrix $\mathbf{D}_{tot}[l]$, while (3.13) performs a direct equalization under noise.

The OFDM system model with a two-tap FEQ for the compensation of transmitter and receiver IQ imbalance is shown in **Figure 3.4**. Once the FEQ coefficients are accurately known, we can subsequently apply them to data symbols as long as the

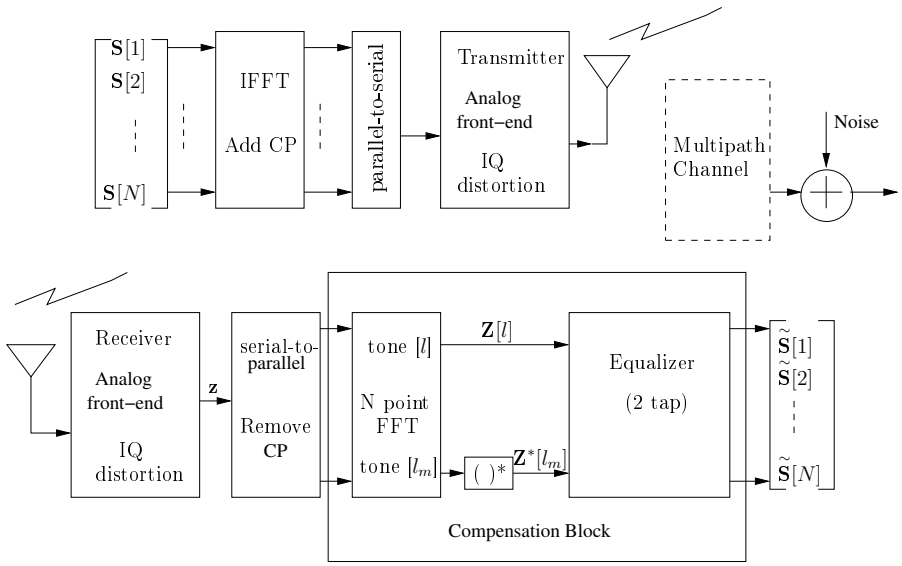

Figure 3.4: OFDM system model with a two-tap FEQ

channel characteristics do not change. It should be noted that equations (3.12) and (3.13) are also valid in the presence of either only transmitter IQ imbalance or only receiver IQ imbalance.

In the following section, we present a training based initialization of the FEQ coefficients.

3.2.4 Initialization Algorithms

The FEQ coefficients can be obtained directly from the LT symbol sequence based on any suitable training algorithm. We consider a least squares (LS) scheme and a recursive least squares (RLS) based adaptive estimation scheme. Both approaches are explained below:

LS Initialization

We consider the availability of an M_l long sequence of LT symbols that are constructed based on equation (3.1). The LS estimate of the FEQ coefficient vector is then computed as [36]:

$$\begin{bmatrix} \mathbf{W}_a[l] \\ \mathbf{W}_b[l] \end{bmatrix} = \mathbf{Z}_{tot}^{Tr^\dagger}[l]\mathbf{S}_{tot-}^{Tr}[l] \tag{3.14}$$

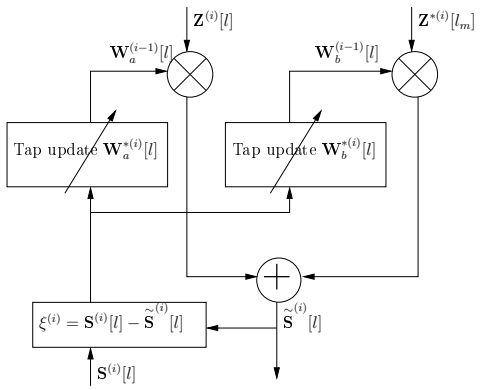

Figure 3.5: Adaptive two-tap FEQ for the compensation of transmitter/receiver IQ imbalance and channel distortion

$$\text{where } \mathbf{S}_{tot-}^{Tr}[l] = \begin{bmatrix} \mathbf{S}^{(1)}[l] \\ \mathbf{S}^{(2)}[l] \\ \hline \vdots \\ \hline \mathbf{S}^{(M_l)}[l] \end{bmatrix} \text{ and } \mathbf{Z}_{tot}^{Tr}[l] = \begin{bmatrix} \mathbf{Z}^{(1)}[l] & \mathbf{Z}^{*(1)}[l_m] \\ \mathbf{Z}^{(2)}[l] & \mathbf{Z}^{*(2)}[l_m] \\ \hline \vdots & \vdots \\ \hline \mathbf{Z}^{(M_l)}[l] & \mathbf{Z}^{*(M_l)}[l_m] \end{bmatrix}$$

Here † is the pseudo-inverse operation and superscript i represents the training symbol number. Equation (3.14) shows that there are M_l equations in 2 unknowns. Hence, we need a LT sequence length $M_l \geq 2$. A longer training sequence will provide improved estimates due to a better noise averaging. If only two LT symbols are available, i.e. $M_l = 2$, we can guarantee the invertibility of $\mathbf{Z}_{tot}^{Tr}[l]$ by generating training symbols such that subcarriers $[l]$ and $[l_m]$ of both LT symbols are linearly independent, e.g., $\mathbf{S}^{*(2)}[l_m] = -\mathbf{S}^{(1)}[l]$.

RLS Adaptive Initialization

We consider a RLS based adaptive initialization of the FEQ coefficients vector as it provides optimal convergence and achieves initialization with an acceptably small number of training symbols. **Figure 3.5** illustrates the adaptive initialization process of a two-tap FEQ based on this algorithm. The two inputs of the FEQ are $\mathbf{Z}[l]$ and $\mathbf{Z}^*[l_m]$ and the taps $\mathbf{W}_a[l], \mathbf{W}_b[l]$ are trained using a sequence of M_l LT symbols. To better illustrate the update equations, we introduce the time (or iteration) index i, i.e. $\mathbf{W}_a^{(i)}$, $\mathbf{W}_b^{(i)}$ represent the equalization coefficients at time instant i. Similarly $\mathbf{Z}^{(i)}[l], \mathbf{Z}^{*(i)}[l_m]$ and $\tilde{\mathbf{S}}^{(i)}$ represent the input and the output of the equalizer at time instant i. **Table 3.1** shows the RLS algorithm for the initialization of the FEQ coefficients based on equation (3.13). In the

- Initialize the algorithm by setting

$$\mathbf{W}_a^{(i=0)} = 0_{N\times 1}; \qquad \mathbf{W}_b^{(i=0)} = 0_{N\times 1}$$

- For all the subcarriers in an OFDM symbol $[l] = 1 \dots N$ compute

$$\mathbf{B}_a^{(i=0)}[l] = \delta^{-1}; \qquad \mathbf{B}_b^{(i=0)}[l] = \delta^{-1}$$

- For each iteration $i = 1 \dots M_l$ compute

$$\overset{\sim}{\mathbf{S}}^{(i)}[l] = \mathbf{W}_a^{(i-1)}[l]\mathbf{Z}^{(i)}[l] + \mathbf{W}_b^{(i-1)}[l]\mathbf{Z}^{*(i)}[l_m]$$

$$\xi^{(i)} = \mathbf{S}^{(i)}[l] - \overset{\sim}{\mathbf{S}}^{(i)}[l]$$

$$\mathbf{B}_{za}^{(i)} = \frac{\mathbf{B}_a^{(i-1)}[l]\mathbf{Z}^{(i)}[l]}{1 + \mathbf{Z}^{*(i)}[l]\mathbf{B}_a^{(i-1)}\mathbf{Z}^{(i)}[l]}$$

$$\mathbf{B}_{zb}^{(i)} = \frac{\mathbf{B}_b^{(i-1)}[l]\mathbf{Z}^{*(i)}[l_m]}{1 + \mathbf{Z}^{(i)}[l_m]\mathbf{B}_b^{(i-1)}\mathbf{Z}^{*(i)}[l_m]}$$

$$\mathbf{W}_a^{*(i)}[l] = \mathbf{W}_a^{*(i-1)}[l] + \mathbf{B}_{za}^{(i)}\xi^{*(i)}$$

$$\mathbf{W}_b^{*(i)}[l] = \mathbf{W}_b^{*(i-1)}[l] + \mathbf{B}_{zb}^{(i)}\xi^{*(i)}$$

$$\mathbf{B}_a^{(i)}[l] = \mathbf{B}_a^{(i-1)}[l] - \mathbf{B}_{za}^{(i)}\mathbf{Z}^{*(i)}[l]\mathbf{B}_a^{(i-1)}[l]$$

$$\mathbf{B}_b^{(i)}[l] = \mathbf{B}_b^{(i-1)}[l] - \mathbf{B}_{zb}^{(i)}\mathbf{Z}^{(i)}[l_m]\mathbf{B}_b^{(i-1)}[l]$$

Table 3.1: RLS algorithm for initialization of two-tap FEQ

algorithm, the regularization factor δ is a small positive constant. Once the equalizer coefficients are trained with a suitable number of training symbols, the final coefficient values are then used to equalize the received symbols according to equation (3.12).

We once again need a LT sequence length $M_l \geq 2$ in order to estimate the FEQ coefficients. The transmission packet for the joint compensation scheme (LS and adaptive RLS) consists of a linearly independent LT symbol sequence for the estimation of FEQ coefficients, followed by the data sequence. The LT symbols can be taken from any suitable alphabet.

3.3 Joint IQ Imbalance and Channel Compensation under Insufficient CP Length

So far we have considered the CP to be sufficiently long to accommodate the combined transmitter/receiver IQ imbalance and the channel impulse response. In this section, we extend the estimation and compensation scheme to also consider the case of an insufficiently long CP. Thus in addition to ICI within an OFDM symbol, there is also inter-symbol-interference (ISI) between adjacent OFDM symbols. In the presence of ISI, a simple two-tap FEQ is not sufficient to preserve the carrier orthogonality. We propose a frequency domain two-branch per-tone equalizer (PTEQ) [113] which shortens the combined transmitter/receiver IQ imbalance and channel impulse response to fit within the CP and at the same time compensate for the IQ imbalance.

3.3.1 System Model with IQ Imbalance and Insufficient CP Length

In order to model the ISI, we now consider two successive OFDM symbols transmitted at time instants $i-1$ and i. The $\mathbf{S}^{(i-1)}$ symbol is the adjacent symbol that causes ISI on the $\mathbf{S}^{(i)}$ symbol, i.e. the symbol of interest. These symbols are transformed to the time domain by an inverse discrete Fourier transform (IDFT). A CP of length ν is then added to the head of each symbol. In the case of no IQ imbalance in the front-end of the transmitter, the resulting time domain baseband symbol is given as:

$$\begin{aligned}\mathbf{s} &= \begin{bmatrix}\mathbf{P_{CI}} & 0\\ 0 & \mathbf{P_{CI}}\end{bmatrix}\begin{bmatrix}\mathbf{F}_N^{-1} & 0\\ 0 & \mathbf{F}_N^{-1}\end{bmatrix}\begin{bmatrix}\mathbf{S}^{(i-1)}\\ \mathbf{S}^{(i)}\end{bmatrix}\\ &= (\mathbf{I}_2 \otimes \mathbf{P_{CI}})(\mathbf{I}_2 \otimes \mathbf{F}_N^{-1})\begin{bmatrix}\mathbf{S}^{(i-1)}\\ \mathbf{S}^{(i)}\end{bmatrix}\end{aligned} \tag{3.15}$$

where $\otimes$ represents the Kronecker product.

Substituting equation (3.15) in equation (3.6) the received symbol can now be written as:

$$\mathbf{z} = [\mathbf{O}_1|\mathbf{T}_{da}](\mathbf{I}_2\otimes\mathbf{P_{CI}})(\mathbf{I}_2\otimes\mathbf{F}_N^{-1})\begin{bmatrix}\mathbf{S}^{(i-1)}\\ \mathbf{S}^{(i)}\end{bmatrix}+[\mathbf{O}_1|\mathbf{T}_{db}](\mathbf{I}_2\otimes\mathbf{P_{CI}})(\mathbf{I}_2\otimes\mathbf{F}_N^{-1})\begin{bmatrix}\mathbf{S}_m^{*(i-1)}\\ \mathbf{S}_m^{*(i)}\end{bmatrix}+\mathbf{n}_c \tag{3.16}$$

where $\mathbf{z}$ is of dimension $(N \times 1)$, $\mathbf{O_1} = 0_{(N\times N+2\nu-L_T-L-L_r+3)}$. $\mathbf{T}_{dk}$ (for $k = a, b$) is an $(N \times N + L_t + L + L_r - 3)$ Toeplitz matrix with first column $[\mathbf{d}_{k(L_t+L+L_r-3)}, 0_{(1\times N-1)}]^T$ and first row $[\mathbf{d}_{k(L_t+L+L_r-3)}, \ldots, \mathbf{d}_{k(0)}, 0_{(1\times N-1)}]$.

As the CP length is considered to be insufficient, i.e. $(\nu < L_t + L + L_r - 2)$, now in addition to ICI from the mirror subcarrier $\mathbf{S}_m^{(i)}$, there is also interference from the adjacent OFDM symbol $\mathbf{S}^{(i-1)}$ leading to ISI. The insufficient CP length together with transmitter/receiver IQ imbalance result in a very poor performance of the OFDM communication system. In the next section, a joint transmitter/receiver IQ imbalance compensation technique under insufficiently long CP is derived.

3.3.2 IQ Imbalance Compensation

In section 3.2.3, all impairments in the communication model, namely, the transmitter IQ imbalance, the channel and the receiver IQ imbalance were estimated and then compensated jointly in the frequency domain. However, in the presence of insufficient CP length, it is not straightforward to jointly compensate all the impairments as shown in equation (3.12). We will first derive a compensation scheme (time domain equalizer (TEQ) + FEQ based compensation), that first compensates the receiver IQ imbalance and then shortens the combined channel and transmitter/receiver IQ imbalance impulse response to fit within the CP length in the time domain by TEQ, and then performs a joint compensation of transmitter IQ imbalance and channel distortion in the frequency domain by a two-tap FEQ. In the second part (per-tone equalizer (PTEQ) based compensation), we merge the entire equalization structure to form one unified equalizer in the frequency domain resulting in a two-branch PTEQ. We show that the two-branch PTEQ reduces to the two-tap FEQ compensation scheme in equation (3.12) when the CP is sufficiently long.

TEQ + FEQ based Compensation

Traditionally, in order to compensate for ISI due to an insufficient CP length, a time domain channel shortening filter is applied to the received symbol such that the filtered channel fits within the CP length [69]. The output of the TEQ is demodulated by the DFT and then a one-tap FEQ is applied to compensate for channel distortion and recover the transmitted symbol. However, due to the presence of transmitter and receiver IQ imbalance, the conventional time domain shortening applied only to the received symbol by a TEQ followed by DFT demodulation and one-tap FEQ is not sufficient to cope with the problem at hand.

We therefore re-model the equalization structure such that the compensation for impairments takes place in the reverse order of their appearance, i.e starting with receiver IQ imbalance by the first stage of TEQ, and then the shortening of the combined transmitter/receiver IQ imbalance and channel impulse response by the second stage of TEQ. This is then followed by a joint compensation of transmitter IQ imbalance and channel distortion in the frequency domain by a FEQ.

In order to compensate for receiver IQ imbalance, we design two TEQ filter branches $\mathbf{v}_c$ and $\mathbf{v}_d$ each of length L_r taps. The first filter branch $\mathbf{v}_c$ is applied to the received symbol $\mathbf{z}$, and the second filter branch $\mathbf{v}_d$ is applied to the complex conjugate version of the received symbol $\mathbf{z}^*$. This leads to:

$$\begin{aligned}\mathbf{z}_q =& \mathbf{v}_c \star \mathbf{z} + \mathbf{v}_d \star \mathbf{z}^* \\ =& \underbrace{(\mathbf{v}_c \star \mathbf{g}_{ra} + \mathbf{v}_d \star \mathbf{g}^*_{rb})}_{\mathbf{f}_1} \star \mathbf{r} + \underbrace{(\mathbf{v}_c \star \mathbf{g}_{rb} + \mathbf{v}_d \star \mathbf{g}^*_{ra})}_{\mathbf{f}_2} \star \mathbf{r}^*\end{aligned} \tag{3.17}$$

The design target for the filters $\mathbf{v}_c$ and $\mathbf{v}_d$ is such that the term $\mathbf{f}_2$ vanishes and the term $\mathbf{f}_1$ can be considered as part of the channel. The solution to this set of equations are $\mathbf{v}_c = \mathbf{g}^*_{ra}.\alpha$ and $\mathbf{v}_d = -\mathbf{g}_{rb}.\alpha$ where α is a non-zero scalar. Thus with appropriate coefficient values for $\mathbf{v}_c$ and $\mathbf{v}_d$, we can have $\mathbf{z}_q$ free of any contributions from $\mathbf{z}^*$, i.e. free from receiver IQ imbalance. It should be noted that the filters $\mathbf{v}_c$ and $\mathbf{v}_d$ only compensate for the mismatch in the receiver IQ imbalance and thus they are not affected by the presence of ISI in the received symbol due to the insufficient CP length.

Once the receiver IQ imbalance has been compensated by the two TEQ branches, we then design a second stage of TEQ that consists of a conventional channel shortening filter branch $\mathbf{v}_a$ of length L' taps [69]. The filter $\mathbf{v}_a$ is applied to the received symbol $\mathbf{z}_q$ such that the filtered channel (now including the absorbed $\mathbf{f}_1$ term) and the transmitter IQ imbalance impulse response fit within the CP length.

In order to accommodate the two stages of the TEQ filters, the dimensions of the received symbol $\mathbf{z}$ has to be re-adjusted. Let $L'' = L_r + L' - 1$ be the combined length of the two stages of cascaded time domain filters of the TEQ, thus the size of the received symbol $\mathbf{z}$ in equation (3.16) is now adjusted to $(N + L'' - 1 \times 1)$. Hence, $\mathbf{O}_1 = 0_{(N+L''-1\times N+2\nu-L-L_T-L_r-L''+4)}, \mathbf{T}_{dk}$ (for $k = a, b$) is of size $(N + L''-1\times N+L_t+L+L_r+L''-4)$ with first column $[\mathbf{d}_{k(L_t+L+L_r-3)}, 0_{(1\times N+L''-1)}]^T$ and first row $[\mathbf{d}_{k(L_t+L+L_r-3)}, \ldots, \mathbf{d}_{k(0)}, 0_{(1\times N+L''-2)}]$.

Now the output of the second stage TEQ filter $\mathbf{z}_{q1} = (\mathbf{v}_a \star \mathbf{z}_q)$ and its complex conjugate output $\mathbf{z}_{q2} = (\mathbf{v}_a \star \mathbf{z}_q)^*$ are stacked into an N vector. The stacked results are then applied to two DFTs. A two-tap FEQ follows the output of the two DFT branches to compensate for the remaining transmitter IQ imbalance and channel

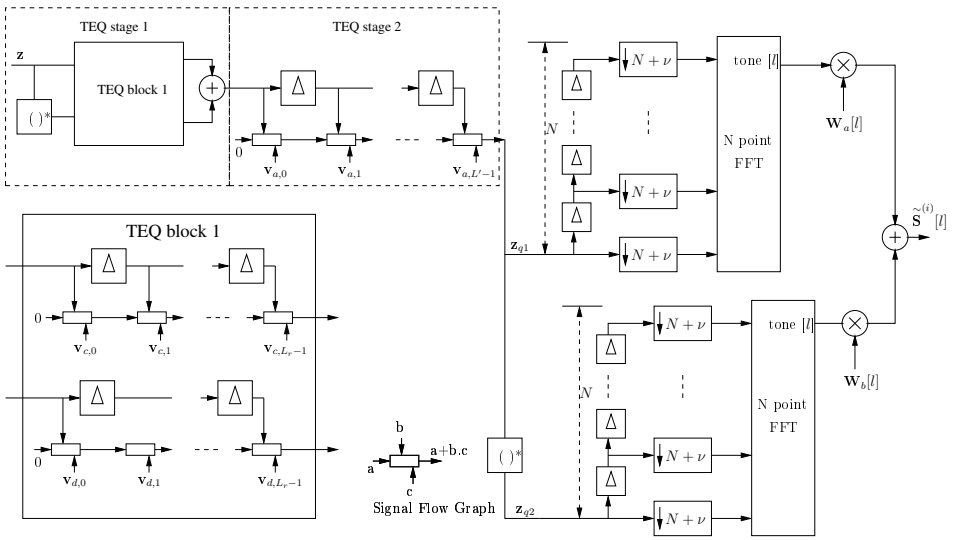

Figure 3.6: TEQ with two-tap FEQ per subcarrier

distortion. The estimate of the transmitted OFDM symbol is obtained as:

$$\begin{aligned}\tilde{\mathbf{S}}^{(i)}[l] &= \begin{bmatrix}\mathbf{W}_a[l] & \mathbf{W}_b[l]\end{bmatrix}\begin{bmatrix}\mathbf{F}_N[l]\mathbf{z}_{q1}\\ \mathbf{F}_N[l]\mathbf{z}_{q2}\end{bmatrix}\\ &= \begin{bmatrix}\mathbf{W}_a[l] & \mathbf{W}_b[l]\end{bmatrix}\begin{bmatrix}\mathbf{F}_N[l](\mathbf{v}_a \star \mathbf{z}_q)\\ \mathbf{F}_N[l](\mathbf{v}_a \star \mathbf{z}_q)^*\end{bmatrix}\end{aligned} \tag{3.18}$$

where $\tilde{\mathbf{S}}^{(i)}[l]$ is the estimate for lth subcarrier of the ith OFDM symbol and $\mathbf{F}_N[l]$ is the lth row of the DFT matrix. The TEQ+FEQ based equalization scheme is shown in **Figure 3.6**. It should be noted that we can alternatively apply the TEQ filter $\mathbf{z}_{q1}$ directly to only one DFT after stacking the results into an N vector. The DFT output is then followed by a two-tap FEQ which is applied to subcarrier $[l]$ and the complex conjugate output of the mirror subcarrier $[l_m]$ (similar to equation (3.12)), to finally obtain an estimate of the transmitted OFDM symbol.

The general disadvantage of the TEQ+FEQ scheme explained above is that it performs the compensation in the time domain and well as in the frequency domain. In practice, it is difficult if not impossible to estimate the receiver IQ imbalance compensation and channel shortening TEQ coefficients and transmitter IQ imbalance and channel distortion compensation FEQ coefficients with sufficient accuracy when the CP is not sufficiently long [113]. In order to simplify the

estimation of the coefficients, we move the TEQ into the frequency domain resulting in a unified compensation structure called per-tone equalizer (PTEQ). This is explained in the next section.

PTEQ based Compensation

A PTEQ is a unified compensation structure where the equalization is performed for each subcarrier separately after the DFT. The PTEQ scheme operates at a lower sampling rate compared to the TEQ+FEQ scheme and may result in an overall lower implementation cost. Also the PTEQ implements a true signal to noise ratio (SNR) optimization per subcarrier. This is because the equalization of one subcarrier is totally independent of the equalization of all other subcarriers, and so the PTEQ can be optimized for every subcarrier separately leading to a much improved performance. We refer to [113] for a detailed description of the PTEQ and its advantages. We will target an MMSE solution where all the impairments can be compensated in a joint fashion.

We first merge the second stage of TEQ filter $\mathbf{v}_a$ with the first stage of TEQ filters $\mathbf{v}_c, \mathbf{v}_d$. This results in two filter branches each of length L''. The resulting inputs to the two DFTs are now given as:

$$\begin{aligned} \mathbf{z}_{q1} &= \mathbf{v}_{ac} \star \mathbf{z} + \mathbf{v}_{ad} \star \mathbf{z}^* \\ \mathbf{z}_{q2} &= \mathbf{v}_{ad}^* \star \mathbf{z} + \mathbf{v}_{ac}^* \star \mathbf{z}^* \end{aligned} \tag{3.19}$$

where the new TEQ filters are obtained as: $\mathbf{v}_{ac} = (\mathbf{v}_a \star \mathbf{v}_c)$ and $\mathbf{v}_{ad} = (\mathbf{v}_a \star \mathbf{v}_d)$.

Following the derivation in [113], the TEQ filtering may then be moved into the frequency domain resulting in a PTEQ employing four DFT operations and $L''-1$ difference terms [113]. Equation (3.19) can then be written as:

$$\begin{aligned} \mathbf{Z}_{q1}[l] &= \begin{bmatrix} \mathbf{V}_{ac}[l] & \mathbf{V}_{ad}[l] \end{bmatrix} \begin{bmatrix} \mathbf{F}_{ext}[l]\mathbf{z} \\ \mathbf{F}_{ext}[l]\mathbf{z}^* \end{bmatrix} \\ \mathbf{Z}_{q2}[l] &= \begin{bmatrix} \mathbf{V}_{ad}^*[l_m] & \mathbf{V}_{ac}^*[l_m] \end{bmatrix} \begin{bmatrix} \mathbf{F}_{ext}[l]\mathbf{z} \\ \mathbf{F}_{ext}[l]\mathbf{z}^* \end{bmatrix} \end{aligned} \tag{3.20}$$

where $\mathbf{F}_{ext}[l]$ is defined as:

$$\mathbf{F}_{ext}[l] = \left[\begin{array}{c|c|c} \mathbf{I}_{L'-1} & 0_{L'-1 \times N-L'+1} & -\mathbf{I}_{L'-1} \\ \hline 0_{1\times L'-1} & \mathbf{F}_N[l] & \end{array}\right]$$

The first block row in $\mathbf{F}_{ext}[l]$ is seen to extract the difference terms, while the last row corresponds to the single DFT. The PTEQ filter coefficients $\mathbf{V}_{ak}[l]$ (for

$k = c, d$) are of size $(L'' \times 1)$ and related to the TEQ coefficients as follows:

$$\begin{bmatrix} \mathbf{V}_{ak,0}[l] \\ \mathbf{V}_{ak,1}[l] \\ \vdots \\ \mathbf{V}_{ak,L''-1}[l] \end{bmatrix} = \begin{bmatrix} (\beta_l)^0 & (\beta_l)^1 & \dots & (\beta_l)^{L''-1} \\ 0 & (\beta_l)^0 & \dots & (\beta_l)^{L''-2} \\ \vdots & \vdots & \ddots & \vdots \\ 0 & 0 & \dots & (\beta_l)^0 \end{bmatrix} \begin{bmatrix} \mathbf{v}_{ak,0} \\ \mathbf{v}_{ak,1} \\ \vdots \\ \mathbf{v}_{ak,L''-1} \end{bmatrix}$$

where $\beta_l = e^{-\jmath 2\pi((l-1)/N)}$ and the subscript x in $\mathbf{V}_{ak,x}[l]$ and $\mathbf{v}_{ak,x}$ (for $k = a, b$) represents the filter tap index.

We finally merge the PTEQ equation (3.20) and the FEQ equation (3.18) into a **two-branch PTEQ**, each branch employing one DFT operation and $L'' - 1$ difference terms. With this transformation the difficult channel shortening problem is avoided and replaced by a simple per-tone optimization problem. The transmitted symbol estimate is then obtained as:

$$\overset{\sim}{\mathbf{S}}^{(i)}[l] = \begin{bmatrix} \mathbf{W}_{va}[l] & \mathbf{W}_{vb}[l] \end{bmatrix} \begin{bmatrix} \mathbf{F}_{ext}[l]\mathbf{z} \\ \mathbf{F}_{ext}[l]\mathbf{z}^* \end{bmatrix} \tag{3.21}$$

where $\mathbf{W}_{va}[l] = (\mathbf{W}_a[l]\mathbf{V}_{ac}[l] + \mathbf{W}_b[l]\mathbf{V}^*_{ad}[l_m])$, and $\mathbf{W}_{vb}[l] = (\mathbf{W}_a[l]\mathbf{V}_{ad}[l] + \mathbf{W}_b[l]\mathbf{V}^*_{ac}[l_m])$. Now the filter vectors $\mathbf{W}_{vk}[l]$ (for $k = a, b$) are of size $(L'' \times 1)$.

The PTEQ structure can be further simplified by taking only one DFT whose conjugated output evaluated on the mirror carrier then provides: $(\mathbf{F}_{ext}[l_m]\mathbf{z})^* = \mathbf{F}_{ext}[l]\mathbf{z}^*$. Thus the estimate of the transmitted OFDM symbol in equation (3.21) can be rewritten as:

$$\overset{\sim}{\mathbf{S}}^{(i)}[l] = \begin{bmatrix} \mathbf{W}_{va}[l] & \mathbf{W}_{vb}[l] \end{bmatrix} \begin{bmatrix} \mathbf{F}_{ext}[l]\mathbf{z} \\ (\mathbf{F}_{ext}[l_m]\mathbf{z})^* \end{bmatrix} \tag{3.22}$$

Equations (3.22) show that the total number of PTEQ coefficients to be estimated is now $2L''$ and in order to estimate these coefficients we need an LT symbol sequence length $M_l \geq 2L''$. A longer training sequence will provide improved estimates due to a better noise averaging. The resulting two-branch PTEQ block scheme is shown in **Figure 3.7**. The PTEQ coefficients for the lth subcarrier can now be obtained based on the following MSE minimization:

$$\underset{\mathbf{W}_{va}[l], \mathbf{W}_{vb}[l]}{min} \mathbb{E}\left\{ \left| \mathbf{S}^{(i)}[l] - \begin{bmatrix} \mathbf{W}_{va}[l] & \mathbf{W}_{vb}[l] \end{bmatrix} \begin{bmatrix} \mathbf{F}_{ext}[l]\mathbf{z} \\ (\mathbf{F}_{ext}[l_m]\mathbf{z})^* \end{bmatrix} \right|^2 \right\} \tag{3.23}$$

It should be noted that the PTEQ equation (3.22) is equally applicable even in the presence of either only transmitter IQ imbalance or receiver IQ imbalance. In the case of sufficiently long CP length, the contribution of the TEQ filter coefficients $\mathbf{v}_a$ in the PTEQ equation (3.22) can be ignored. Also the first stage of TEQ filters $\mathbf{v}_c$ and $\mathbf{v}_d$ are not needed, as the entire compensation can now take place based on

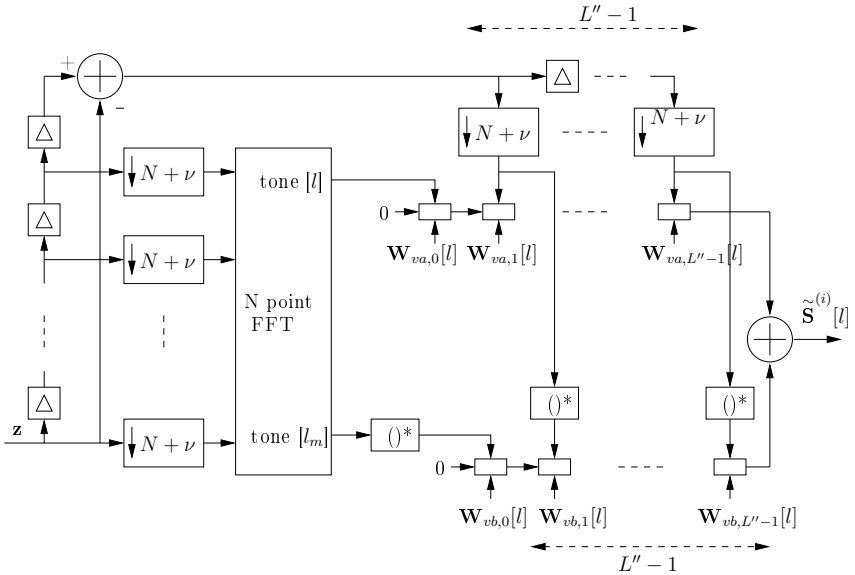

Figure 3.7: Two-branch PTEQ for OFDM with IQ imbalance and insufficient CP length

the suppression of interference from the mirror subcarrier as in equation (3.12). Thus the two-branch PTEQ structure reduces to a two-tap FEQ. We then need an LT symbol sequence length $M_l \geq 2$ to estimate the two coefficients.

Based on equation (3.23), we can once again develop LS and adaptive RLS training based initialization algorithms for the PTEQ coefficients, similar to section 3.2.4.

3.4 Simulation Results

We consider an uncoded 64QAM OFDM transmission with symbol length $N = 64$ and CP length $\nu = 8$. A transmission packet consists of a linearly independent LT symbol sequence followed by a data sequence. We do not consider the ST symbol sequence and the SIGNAL symbol (see section 2.4.1), as they are not needed for the proposed compensation schemes. We consider the LT symbol sequence to be sufficiently long to achieve initialization and adequate noise averaging for the two-tap FEQ (3.13) and the two-branch PTEQ (3.23) coefficients. In general, we have considered the LT symbol sequence to be atleast four to five times longer than the minimal required length for the initialization of equalizer coefficients. However at high signal to noise ratio (SNR), the LT symbol sequence can be further reduced

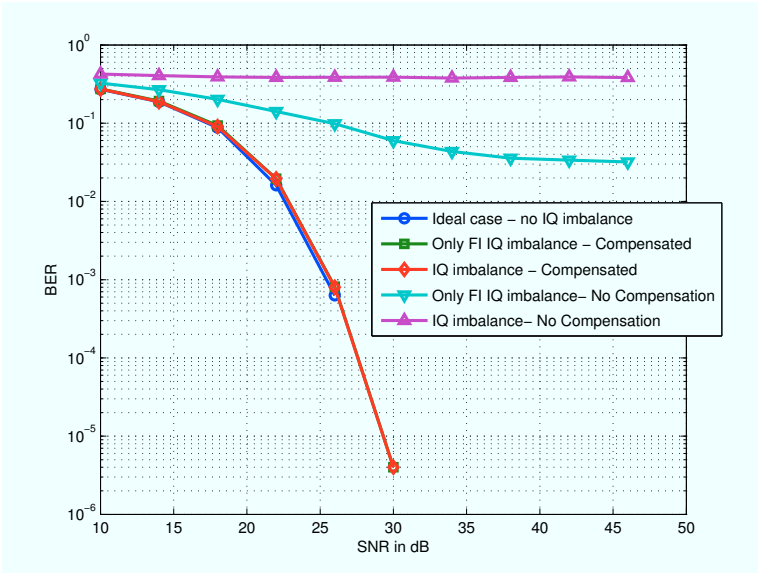

AWGN flat channel

Figure 3.8: BER vs SNR for 64QAM constellation with LS based FEQ initialization. IQ imbalance is considered at both the transmitter and receiver.

to only two to three times the minimal required length for adequate compensation. The initialization of equalizers with the minimal LT sequence length is considered later in chapter 5.

- In the first setup, we compare the bit error rate (BER) versus SNR performance curves for the FEQ scheme. The parameters used in this figure are as follows: We consider FI amplitude imbalance of $g_t, g_r = 5\%$ and phase imbalance of $\phi_t, \phi_r = 5°$. The front-end filter mismatched impulse responses are $\mathbf{h}_{ti} = \mathbf{h}_{ri} = [0.9\ 0.1]$ and $\mathbf{h}_{tq} = \mathbf{h}_{rq} = [0.1\ 0.9]$ with filter impulse length $L_t = L_r = 2$.

  Figure 3.8-3.9 illustrates the performance curves obtained for the setup. There are two different channel profiles considered in the simulation: Figure 3.8 considers an AWGN channel with a single tap unity gain, and figure 3.9 considers a multipath channel with $L = 4$ taps. The channel remains static for the duration of one entire packet and may change independently from one packet to another. The BER results depicted are obtained by averaging the BER curves over 10^4 independent channels. The FEQ is initialized by the LS algorithm as explained in section 3.2.4.

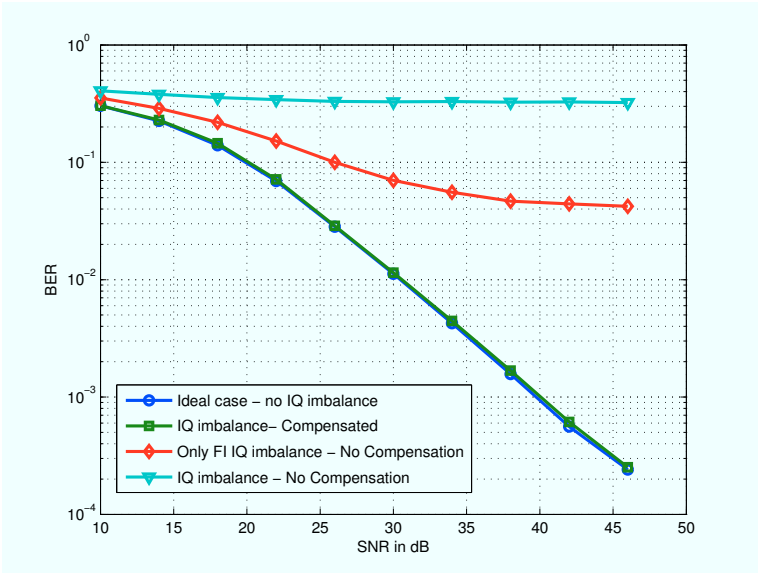

4-tap Rayleigh fading channel

Figure 3.9: BER vs SNR for 64QAM constellation with LS based FEQ initialization. IQ imbalance is considered at both the transmitter and receiver.

The performance comparison is made with an ideal system with no front-end distortion. This ideal case will serve as a benchmark for our equalizer. We also compare the performance with a system with no IQ imbalance compensation scheme in place. Both the ideal system and the system with no IQ imbalance compensation scheme use one-tap FEQ for channel compensation. The figures 3.8-3.9 show that when no compensation scheme is in place, the OFDM system is completely unusable. Even for the case when only FI IQ imbalance is considered, the BER is very high for the system. A close to ideal performance is obtained when a simple two-tap FEQ compensation scheme is considered at the receiver. The FEQ when adequately trained provides a very good performance.

- In the second setup, we evaluate the BER vs SNR performance curves for the PTEQ compensation scheme under insufficient CP length. We consider the same IQ imbalance parameters as explained in setup 1. We now consider a multipath channel of $L = 10$ taps long. The total length of the combined transmitter/receiver IQ imbalance and channel impulse response $L_t + L + L_r - 2 = 12$ is now larger than the CP length. A two-branch PTEQ with $L'' = 10$ and $L'' = 15$ taps is used for compensation.

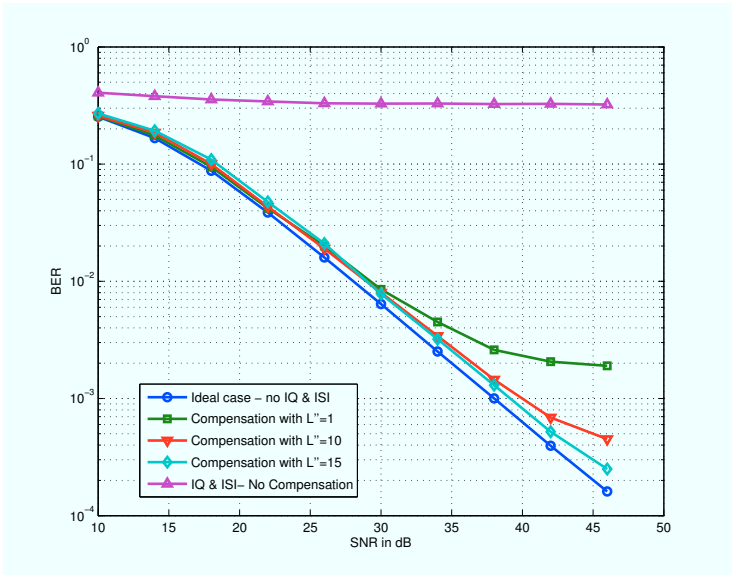

Figure 3.10: BER vs SNR for 64QAM constellation with RLS based PTEQ initialization. IQ imbalance considered only at the receiver

Figure 3.10-3.11 show the BER versus SNR obtained in the presence of only receiver IQ imbalance, and in the presence of both transmitter and receiver IQ imbalance respectively. Once again the performance comparison is made with a system with no compensation scheme in place and an ideal system with no front-end distortion. Only in an ideal system, we consider the channel length $L = 4$ taps long, thus there is no ISI due to insufficient CP length. In addition, the performance comparison is also made with a PTEQ of length $L'' = 1$ which is equivalent to a simple two-tap FEQ compensation scheme. Thus in this case the two-branch PTEQ takes into account only IQ imbalance and not ISI in the received symbol. The PTEQs are initialized by the RLS algorithm.

Figures 3.10-3.11 show that the performance results are nearly identical, a slight performance improvement in PTEQ is observed in the case of only receiver IQ imbalance compared to the case of combined transmitter and receiver IQ imbalance. When no compensation scheme is used, the OFDM system is completely unusable. When a PTEQ of length $L'' = 1$ is used, there is some improvement in the performance but the error floor is still high at 7×10^{-3} and 4×10^{-3} in figures 3.10 and 3.11 respectively. Good performance results close to the ideal case are obtained for a PTEQ of length $L'' = 10$

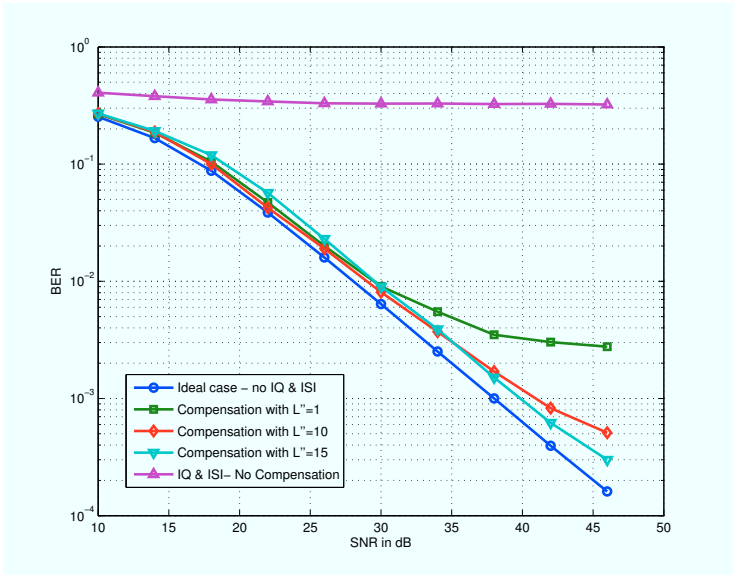

10-tap Rayleigh fading channel

Figure 3.11: BER vs SNR for 64QAM constellation with RLS based PTEQ initialization. IQ imbalance considered at both the transmitter and receiver

and $L'' = 15$. Thus with an increase in PTEQ length, a corresponding improvement in ISI compensation is achievable. It should be noted that there is always an error floor even at $L'' = 10$ and $L'' = 15$, albeit at a very small BER value, due to the fact that a finite length PTEQ is incapable of completely eliminating ISI from a received symbol.

Table 3.2 tabulates the performance (BER loss in dB) of a PTEQ with different lengths L'' when compared to an ideal case at $SNR = 42$ dB. When $L'' = 1$, i.e. ISI not compensated, even with no IQ imbalance at both the transmitter and receiver, the BER is very high and is approximately 2.5 dB higher than for the ideal case. When IQ imbalance is present only at the receiver the loss is about 7 dB and when the IQ imbalance is present at both the transmitter and receiver the BER loss increases to 9 dB. The PTEQ performance improves when the number of taps is increased but this is at the expense of a higher computational complexity. For a PTEQ of tap length $L'' = 15$, the BER loss is 0.45 dB for the case of no IQ imbalance at both transmitter and receiver. When IQ imbalance is present only at the receiver, the BER loss is 1 dB and with IQ imbalance at both the transmitter and receiver, the BER loss increases only marginally to 2 dB. This can also be observed from figure 3.10 and 3.11, where the BER

PTEQ taps L''	g_t, ϕ_t	g_r, ϕ_r	$\mathbf{h}_{ti}$	$\mathbf{h}_{tq}$	$\mathbf{h}_{ri}$	$\mathbf{h}_{rq}$	BER loss in dB
1	$0\%, 0°$	$0\%, 0°$	[1 0]	[1 0]	[1 0]	[1 0]	2.5
	$0\%, 0°$	$5\%, 5°$	[1 0]	[1 0]	[0.9 0.1]	[0.1 0.9]	7
	$5\%, 5°$	$5\%, 5°$	[0.9 0.1]	[0.1 0.9]	[0.9 0.1]	[0.1 0.9]	9
5	$0\%, 0°$	$0\%, 0°$	[1 0]	[1 0]	[1 0]	[1 0]	1.9
	$0\%, 0°$	$5\%, 5°$	[1 0]	[1 0]	[0.9 0.1]	[0.1 0.9]	3.6
	$5\%, 5°$	$5\%, 5°$	[0.9 0.1]	[0.1 0.9]	[0.9 0.1]	[0.1 0.9]	5.2
10	$0\%, 0°$	$0\%, 0°$	[1 0]	[1 0]	[1 0]	[1 0]	1.20
	$0\%, 0°$	$5\%, 5°$	[1 0]	[1 0]	[0.9 0.1]	[0.1 0.9]	1.5
	$5\%, 5°$	$5\%, 5°$	[0.9 0.1]	[0.1 0.9]	[0.9 0.1]	[0.1 0.9]	3
15	$0\%, 0°$	$0\%, 0°$	[1 0]	[1 0]	[1 0]	[1 0]	0.45
	$0\%, 0°$	$5\%, 5°$	[1 0]	[1 0]	[0.9 0.1]	[0.1 0.9]	1
	$5\%, 5°$	$5\%, 5°$	[0.9 0.1]	[0.1 0.9]	[0.9 0.1]	[0.1 0.9]	2

Table 3.2: BER loss in dB for different PTEQ tap lengths L''. The BER loss is compared to the ideal case.

performance curve for $L'' = 15$ is very close to the ideal case. Thus a PTEQ with a sufficient number of taps is essential to shorten the combined channel, transmitter/receiver filter impulse response and also to compensate for the channel and IQ imbalance distortion. The compensation performance depends on how accurately the adaptive equalizer coefficients can converge to the ideal values.

3.5 Conclusion

In this chapter, we have derived the input-output system model and discussed the influence of transmitter and receiver IQ imbalance in an OFDM system. Joint compensation solutions that consider frequency selective transmitter/receiver IQ imbalance and channel distortion were proposed. In the case of a sufficiently long CP length, a simple two-tap FEQ scheme was introduced. In the case of an insufficient CP length, we have proposed a two-branch PTEQ solution which can shorten the combined channel and transmitter/receiver IQ imbalance impulse response to fit within the CP and at the same time compensate for the IQ imbalance. The FEQ and the PTEQ can be initialized by any suitable training based algorithms.

The compensation schemes presented correspond to an efficient, post FFT adaptive equalization which leads to near ideal compensation. The performance curves clearly demonstrate that an OFDM system impaired with IQ imbalance results

in a very poor throughput. The compensation is absolutely necessary to enable a high data rate communication. The presented IQ imbalance compensation schemes therefore allow to greatly relax the front-end design specifications.

Chapter 4

IQ Imbalance and CFO

4.1 Introduction

The OFDM transmission scheme is very sensitive to carrier frequency offset (CFO), therefore this distortion also needs to be taken into account when considering a direct conversion front-end system model. In chapter 3, we proposed a two-tap FEQ and a two-branch PTEQ scheme for the compensation of transmitter and receiver IQ imbalance under sufficient and insufficient CP length, respectively. In this section, we assume that in addition to IQ imbalance, the transmitter and receiver front-ends also suffer from CFO due to a drift in the local oscillators at the transmitter and receiver. In the presence of transmitter/receiver IQ imbalance and CFO, it is not possible to separately compensate for the transmitter/receiver IQ imbalance and for the CFO. This is because the CFO occurs after the transmit IQ imbalance and before the receive IQ imbalance is introduced in the received symbol. Thus any compensation solution must incorporate the joint effect of transmitter/receiver IQ imbalance and CFO.

Different approaches have been proposed to estimate CFO for OFDM transmission. In [60] a training based technique for CFO estimation is proposed assuming no IQ imbalance. A maximum likelihood (ML) CFO estimation is proposed in [123], also assuming no IQ imbalance in the system model. However, these estimation schemes are not accurate when IQ imbalance is also present in the system.

The joint estimation and compensation problem of IQ imbalance and CFO has been addressed extensively in literature. A study on the joint impact of IQ imbalance and CFO in multicarrier systems is provided in [68] and [41]. In [31], nulled subcarriers are used to estimate CFO in the presence of IQ imbalance. The estimation scheme maximizes the energy on the desired subcarrier and its

mirror subcarrier by invoking an exhaustive search algorithm. A time domain CFO estimation scheme based on the phase rotation of received OFDM symbols due to CFO is proposed in [122]. However, the estimate is not accurate for small CFOs under noisy conditions.

In [40], an expectation maximization (EM) approach that approximates the ML based joint estimation of receiver IQ imbalance and CFO is proposed. It is shown that the EM approach results in a very accurate estimation of CFO but the IQ imbalance estimates may suffer at low and high SNR due to the approximated ML approach. In [75] training symbols with artificially superimposed CFO are used to jointly estimate the CFO and receiver IQ imbalance in the time domain. Joint estimation of CFO and receiver IQ imbalance based on minimizing the residual channel energy in the time domain is discussed in [19]. A non-linear least squares (NLS) search algorithm for the estimation of CFO based on a sequence of phase rotated ST symbols is proposed in [121]. In [109] it is assumed that the CFO is estimated based on perfect knowledge of the IQ imbalance parameters, and that the IQ imbalance parameters can be estimated correctly in the presence of CFO. The assumption here is valid for small CFO and small IQ imbalance parameters. A calibration approach to estimate receiver IQ imbalance in the presence of CFO is proposed in [80]. A joint compensation solution for receiver IQ imbalance and CFO over a doubly selective channel has been proposed in [9] and [8]. A PTEQ solution is proposed that compensates for the doubly selective channel based on a basis expansion model (BEM).

Almost all solutions mentioned above consider the presence of either only FI transmitter and receiver IQ imbalance or only receiver IQ imbalance together with CFO in their system model. We have targeted a general case of FS transmitter/receiver IQ imbalance and CFO distortion. In the case of only FI transmitter/receiver IQ imbalance and CFO, a four-tap FEQ solution is proposed. It is shown that this solution can straightforwardly be derived in the frequency domain. The FEQ solution later serves as a basis for analysis of the compensation scheme in the case of FS transmitter and receiver IQ imbalance. For the case of FS transmitter and receiver IQ imbalance, we propose a four-branch PTEQ solution obtained by combining a TEQ and a FEQ. The PTEQ solution can also be extended to consider the case of insufficient CP length. It is shown that the proposed four-branch PTEQ solution provides the most generalized structure that can compensate for all different combination of impairments. The material related to this chapter has been published in [85], [86] [87], [88] and [94].

This chapter is organized as follows: **Section 4.2** introduces the OFDM system model for CFO and transmitter/receiver IQ imbalance. The impact of CFO with and without IQ imbalance is discussed. In **section 4.3**, we derive a strategy to estimate CFO based on some of the existing CFO estimation algorithms available in literature. A joint FI transmitter/receiver IQ imbalance, CFO and channel compensation solution is then derived in **section 4.4**. In **section 4.5**, a PTEQ is

derived that provides a unified compensation solution for FS transmitter/receiver IQ imbalance, CFO and short CP length. The results of the numerical performance evaluation are presented in **section 4.6** and finally conclusions are given in section **section 4.7**.

4.2 System Model with CFO and IQ Imbalance

Ideally during the up and down conversion operation at the transmitter and receiver front-ends, the local oscillator (LO) produces a pure sine wave at the standardized RF carrier frequency to translate the baseband symbol to RF and vice-versa. However, due to component defects and varying operating temperatures, the LO may drift from the generation of the standardized carrier frequency. The carrier frequency may then vary from one realization to another over a long duration of time, resulting in a possible CFO between the transmitter and the receiver.

We now follow the same system of equations as explained in chapter 3. We first consider the influence of CFO in an OFDM system model without any IQ imbalance (see equation (3.8)). In the time domain, the CFO Δf on an incoming symbol $\mathbf{r}$ results in a phase rotation proportional with time, given as [62]:

$$\mathbf{z} = \mathbf{r}.e^{\jmath 2\pi \Delta f.\mathbf{t}} \tag{4.1}$$

where $e^{\jmath \mathbf{x}}$ is the element-wise exponential function on the vector $\mathbf{x}$ and where $\mathbf{t}$ is a time vector.

In the frequency domain the CFO results in energy leakage from the desired subcarrier to all other subcarriers in an OFDM symbol. The energy leakage $\mathbf{P}_\zeta$ from the desired subcarrier $[l]$ to a subcarrier at a distance $[l']$ is given as [68]:

$$\mathbf{P}_\zeta[l'] = e^{\jmath\pi(\zeta - l')\frac{N-1}{N}} \frac{sin\pi(\zeta - l')}{sin\frac{\pi}{N}(\zeta - l')} \tag{4.2}$$

where ζ is the normalized CFO given as the ratio of the actual CFO Δf and the subcarrier spacing $\frac{1}{T.N}$, i.e $\zeta = \Delta f.T.N$.

Figure 4.1(a) illustrates this leakage on an OFDM spectrum for different amounts of normalized CFOs. The figure considers a BPSK data transmission at subcarrier $[l] = 20$. The figure shows that the leakage mainly affects the neighboring subcarriers around the desired subcarrier and also that the energy leakage is proportional to the CFO ζ. For $\zeta = 0.5$, the desired subcarrier $[l] = 20$ and the neighboring subcarrier $[l'] = 21$ share the same amplitude.

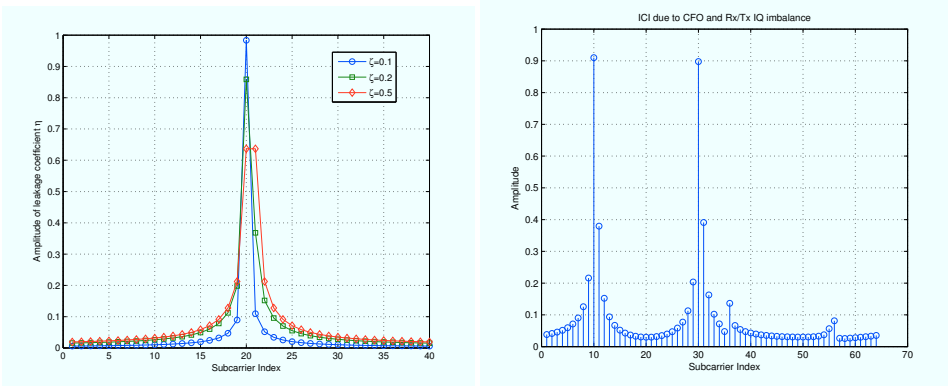

(a) Only CFO (b) CFO and IQ imbalance

Figure 4.1: Energy leakage in an OFDM symbol

Based on equation (4.2), the received OFDM symbol in frequency domain can now be written as:

$$\mathbf{Z}[l] = \sum_{l'=1}^{N} \mathbf{R}[l]\mathbf{P}_{\zeta}[l - l'] \tag{4.3}$$

Equations (4.2) and (4.3) show that due to CFO, the data on the desired subcarrier $[l]$ is rotated and the energy leaking to other subcarriers $[l']$ is no longer zero. In other words, the CFO destroys the orthogonality between subcarriers and hence induces ICI. The ICI results in an error floor limiting the performance of the system even for high signal to noise ratios. The larger the CFO, the wider the ICI span (see Figure 4.2(a)) and higher the BER error floor [14].

It should be noted that the ICI from the CFO is similar to the ICI introduced in a time varying channel resulting from a Doppler spread [6]. In this dissertation, we do not consider the influence of Doppler spread and the channel is always considered static within a transmission packet. Thus the time varying property now attributed to the received symbol, hence the channel, is only due to CFO (4.1).

When CFO is present together with transmitter and receiver IQ imbalance, the resulting baseband symbol can be written as [109]:

$$\begin{aligned}\mathbf{z} =&\mathbf{g}_{ra} \star (\mathbf{r}.e^{\jmath 2\pi \Delta f.\mathbf{t}}) + \mathbf{g}_{rb} \star (\mathbf{r}^*.e^{-\jmath 2\pi \Delta f.\mathbf{t}}) \\ =&\mathbf{g}_{ra} \star ((\mathbf{c} \star \mathbf{g}_{ta} \star \mathbf{s} + \mathbf{c}_b \star \mathbf{g}_{tb} \star \mathbf{s}^*).e^{\jmath 2\pi \Delta f.\mathbf{t}}) \\ &+ \mathbf{g}_{rb} \star ((\mathbf{c} \star \mathbf{g}_{ta} \star \mathbf{s} + \mathbf{c}_b \star \mathbf{g}_{tb} \star \mathbf{s}^*)^*.e^{-\jmath 2\pi \Delta f.\mathbf{t}}) \\ &+ \mathbf{g}_{ra} \star (\mathbf{n}.e^{\jmath 2\pi \Delta f.\mathbf{t}}) + \mathbf{g}_{rb} \star (\mathbf{n}^*.e^{-\jmath 2\pi \Delta f.\mathbf{t}})\end{aligned} \tag{4.4}$$

which effectively means that the received symbol is first distorted by transmitter IQ imbalance and the channel, followed by CFO and finally by receiver IQ imbalance.

The received OFDM symbol in the frequency domain can be written as:

$$\mathbf{Z}[l] = \mathbf{G}_{ra}[l] \sum_{l'=1}^{N} \mathbf{R}[l] \mathbf{P}_{\zeta}[l - l'] + \mathbf{G}_{rb}[l] \sum_{l'_m=1}^{N} \mathbf{R}^*[l_m] \mathbf{P}_{-\zeta}[l_m - l'_m] \tag{4.5}$$

where $\mathbf{P}_{-\zeta}[l_m - l'_m]$ is obtained from equation (4.2) with $\zeta = -\Delta f.T.N$.

The joint effect of transmitter/receiver IQ imbalance and CFO on an OFDM spectrum is illustrated in **Figure 4.1(b)**. The figure considers BPSK data transmission at subcarrier $[l] = [10, 30]$. A noiseless scenario is considered with normalized CFO $\zeta = 0.3$ and FI transmitter/receiver amplitude and phase imbalances $g_t = g_r = 5\%$ and $\phi_t = \phi_r = 5^\circ$. The figure shows the leakage at the neighboring subcarriers of $[l] = [10, 30]$ and also a leakage, albeit small, around the mirror subcarriers of $[l_m] = [56, 36]$ respectively. The leakage to the mirror subcarrier $[l_m] = 36$ is large compared to the mirror subcarrier $[l_m] = 56$, due to the closeness of the subcarrier $[l_m] = 36$ to its corresponding desired subcarrier $[l] = 30$ in the OFDM spectrum. The subcarrier $[l_m] = 36$ is within the significant neighborhood of $[l] = 30$ resulting in large leakage.

The WLAN 802.11a standard [43] specifies a maximum tolerable frequency deviation of 20 ppm. For a transmitter and receiver LO operating between 5 and 6 GHz, this translates to a maximum $\zeta \approx 0.76$. Thus a digital solution at the receiver should be able to compensate for CFO distortion up to $\zeta = 0.76$. A CFO $\zeta = 0.76$ along with transmitter/receiver IQ imbalance can result in a severe performance degradation, as will be shown in section 4.6. A simple two-tap FEQ is not adequate to restore the orthogonality between the subcarriers. More sophisticated and robust equalization techniques are clearly needed to restore the lost orthogonality and so to reduce/eliminate ICI.

Figure 4.2 illustrates an equivalent baseband system model of a direct conversion transmitter and receiver front-ends impaired with transmitter/receiver IQ imbalance, CFO and channel distortion based on equation (4.4). In the following

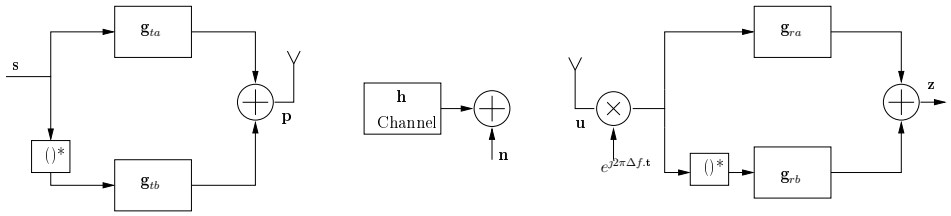

Figure 4.2: Baseband system model of a direct conversion transmitter and receiver front-end

sections, we will develop digital estimation and compensation schemes based on this system model.

4.3 CFO Estimation

In general, any CFO estimation algorithm can be used as long as it is robust in the presence of IQ imbalance. CFO estimation can be carried out in the frequency domain as well as in the time domain. In the frequency domain, however, it is usually very difficult to obtain an exact estimate of the energy leakage to all the neighboring subcarriers caused by the CFO. In [9] an MMSE solution is proposed where the energy leakage can be approximated to few adjacent subcarriers. On the other hand, it is comparatively much easier to estimate and then compensate for the effects of CFO in the time domain by de-rotating the received symbol with the estimated CFO value. In our work we therefore target the estimation of CFO in the time domain so as to obtain an exact solution.

In particular, we consider modified forms of two specific CFO estimation algorithms, presented in [109] and [121], which have very different characteristics. The CFO estimation algorithm in [109] provides a very good estimate in the presence of a small CFO, whereas the non-linear least squares (NLS) based CFO estimation algorithm in [121] is robust in the case of a large CFO. A threshold can be considered for the choice between the two CFO estimation schemes.

In the case of a small CFO, the estimation is based on the auto-correlation between pairs of ST symbols available in a training sequence. We consider an ST sequence consisting of identical symbols with no CP or guard interval inserted between them [43]. Let M_s identical ST symbols of size $(N_s \times 1)$ be available for transmission. Then $\mathbf{z}^{(i_s)}$ represents the baseband ST symbol as defined in equation (4.4) and i_s denotes the training symbol number in the ST symbol sequence. The CFO

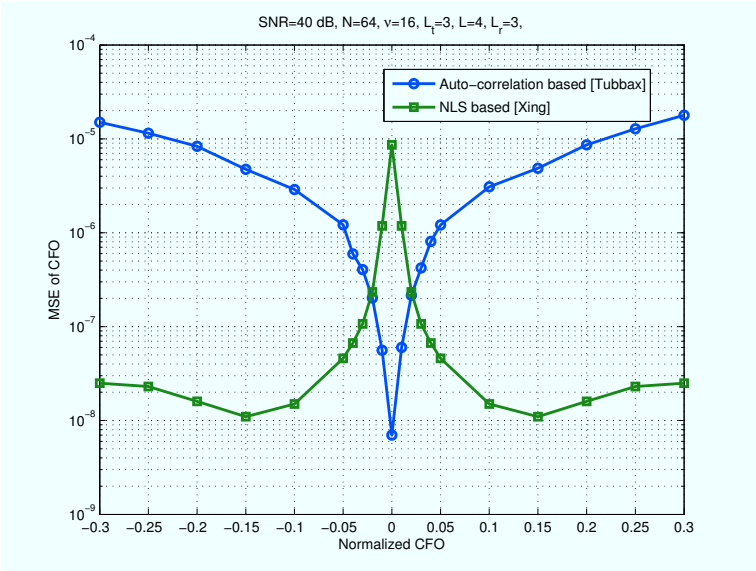

Figure 4.3: MSE in estimation of CFO in the presence of transmitter/receiver IQ imbalance

estimate $\Delta\widetilde{f}$ is then given as:

$$\Delta\widetilde{f} = \Xi\Delta\widetilde{f} = \Xi\left(\frac{arg\{\sum \mathbf{z}^{T(i_s)}\mathbf{z}^{*(j_s)}\}}{2\pi(j_s - i_s)NT}\right) \tag{4.6}$$

where $i_s = 2 \ldots M_s - 1$, $j_s = i_s + 1 \ldots M_s$ and $j_s > i_s$ and Ξ is the expectation operator. It should be noted that we discard the first training symbol in the ST symbol sequence in equation (4.6) as it may be distorted by ISI. Thus the total number of pairs that are considered for the calculation of the CFO is given as: $N_{cfo} = C_2^{M_s-1} = \frac{(M_s-1)!}{2!(M_s-4)!}$.

In the case of a large CFO, the estimation is based on an NLS algorithm. Here also we consider M_s identical ST symbols rather than the specific sequence of phase rotated ST symbols as proposed in [121]. The phase rotated ST symbols can be used in the case of only receiver IQ imbalance, but cannot be used in the presence of transmitter and receiver IQ imbalance. Moreover the choice of identical ST symbols keeps the training requirement simple and uniform for both cases (large and small CFO).

Figure 4.3 compares the two CFO estimation algorithms (Tubbax-[109] and Xing-[121]) for an uncoded 64QAM OFDM system impaired with transmitter and receiver IQ imbalance. The parameters considered in the simulation are as

follows: OFDM symbol length $N = 64$, CP length $\nu = 16$. The multipath channel is $L = 4$ taps long. The transmitter and receiver filter impulse responses are $\mathbf{h}_{ti} = \mathbf{h}_{ri} = [0.01\ 0.5\ 0.06]$ and $\mathbf{h}_{tq} = \mathbf{h}_{rq} = [0.06\ 0.5\ 0.01]$ and the FI amplitude and phase imbalances are $g_t = g_r = 5\%$ and $\phi_t = \phi_r = 5^\circ$ respectively. The performance results are obtained by considering a sequence of 10 identical ST symbols at 40 dB SNR. We obtain the performance curves over normalized CFO ζ. In the case of NLS based CFO estimation scheme we consider a step size of $\Delta\zeta = 0.0005$ for the exhaustive search.

The figure illustrates that the performance of the auto-correlation based CFO estimation scheme [109] deteriorates as the normalized CFO is increased from $\zeta = 0$ to $\zeta = \pm 0.5$. Whereas the NLS scheme [121] shows an inverse characteristic with poorest performance at $\zeta = 0$ and a gradual improvement as the normalized CFO is increased to $\zeta = \pm 0.1$. The mean square error (MSE) for the NLS scheme saturates after $\zeta = \pm 0.1$. It can be seen that for the given IQ imbalance values, a good choice for the threshold between the two CFO estimation schemes will be $\zeta = -0.02$ and $+0.02$. For smaller IQ imbalance values, the performance of both CFO estimation algorithms is expected to provide improved results.

For the time being we assume that the observed CFO estimate is sufficiently accurate i.e. $\Delta\widetilde{f} \simeq \Delta f$. Later on, we will derive an iterative scheme to correct for any residual CFO in the system. The performance of the modified CFO estimation algorithms in the presence of IQ imbalance is further analyzed in the simulation section 4.6.

4.4 Joint FI IQ imbalance, CFO and Channel Compensation

We will first derive a joint compensation solution for FI transmitter and receiver IQ imbalance together with CFO and channel distortion. It is shown that this solution can straightforwardly be derived in the frequency domain and will later serve as a basis for analysis of the compensation scheme in the case of FS transmitter/receiver IQ imbalance.

We will now assume that the I and Q branch filters at the transmitter and receiver front-ends are perfectly matched, i.e, $\mathbf{H}_{ti} = \mathbf{H}_{tq} = \mathbf{H}_t$ and $\mathbf{H}_{ri} = \mathbf{H}_{rq} = \mathbf{H}_r$, thus resulting in only FI transmitter and receiver IQ imbalance. Equations (3.2) and (3.5) are then written as:

$$\begin{aligned} \mathbf{p} &= \mathbf{h}_t \star (g_{ta}\mathbf{s} + g_{tb}\mathbf{s}^*) \\ \mathbf{z} &= \mathbf{h}_r \star (g_{ra}\mathbf{r} + g_{rb}\mathbf{r}^*) \end{aligned} \tag{4.7}$$

where $\mathbf{h}_t$ and $\mathbf{h}_r$ are the time domain representation of $\mathbf{H}_{ti}$ and $\mathbf{H}_{tq}$ respectively. Both $\mathbf{h}_t$ and $\mathbf{h}_r$ are treated as part of the channel $\mathbf{c}$, and thus basically ignored in any further discussion. The remaining parameters in equation (4.7) are given as:

$$g_{ta} = \frac{1 + g_t e^{-\jmath\phi_t}}{2}; \quad g_{tb} = \frac{1 - g_t e^{\jmath\phi_t}}{2}$$

$$g_{ra} = \frac{1 + g_r e^{-\jmath\phi_r}}{2}; \quad g_{rb} = \frac{1 - g_r e^{\jmath\phi_r}}{2}$$

where g_{ta}, g_{tb}, g_{ra} and g_{rb} are scalar IQ imbalance components and are a function of only g_t and ϕ_t.

Following the joint IQ imbalance and CFO system model in section 4.1, the received OFDM symbol in equation (4.4) can now be written as:

$$\mathbf{z} = g_{ra}\mathbf{p}_c.e^{\jmath 2\pi\Delta f.\mathbf{t}} + g_{rb}\mathbf{p}_c^*.e^{-\jmath 2\pi\Delta f.\mathbf{t}} + g_{ra}\mathbf{n}.e^{\jmath 2\pi\Delta f.\mathbf{t}} + g_{rb}\mathbf{n}^*.e^{-\jmath 2\pi\Delta f.\mathbf{t}} \quad (4.8)$$

where $\mathbf{p}_c = \mathbf{c} \star \mathbf{p}$. Equation (4.8) explicitly shows only the CFO, the receiver IQ imbalance and the noise contribution. The channel filtering and the distortion due to transmitter IQ imbalance are hidden in the definition of $\mathbf{p}_c$ and so not considered for the time being.

Given a good estimate $\widetilde{\Delta f}$, obtained by one of the estimation schemes in section 4.3, we first perform an element wise multiplication of the received distorted symbol with the estimated negative frequency offset $e^{-\jmath 2\pi\widetilde{\Delta f}.\mathbf{t}}$. This results in a vector $\mathbf{z}_1$ as follows:

$$\begin{aligned}
\mathbf{z}_1 &= \mathbf{z}.e^{-\jmath 2\pi\widetilde{\Delta f}.\mathbf{t}} \\
&= g_{ra}\mathbf{p}_c + g_{rb}\mathbf{p}_c^*.e^{-2\jmath 2\pi\widetilde{\Delta f}.\mathbf{t}} + g_{ra}\mathbf{n} + g_{rb}\mathbf{n}^*.e^{-2\jmath 2\pi\widetilde{\Delta f}.\mathbf{t}} \\
&= g_{ra}\mathbf{p}_c + g_{rb}\mathbf{p}_{cx} + \mathbf{n}_1
\end{aligned} \quad (4.9)$$

where $\mathbf{p}_{cx} = \mathbf{p}_c^*.e^{-2\jmath 2\pi\widetilde{\Delta f}.\mathbf{t}}$ and $\mathbf{n}_1 = g_{ra}\mathbf{n} + g_{rb}\mathbf{n}^*.e^{-2\jmath 2\pi\widetilde{\Delta f}.\mathbf{t}}$ is now a zero mean improper complex noise vector mainly due to the presence of receiver IQ imbalance.

Similarly, we also perform an element wise multiplication of the complex conjugate of the received symbol with the negative frequency offset $e^{-\jmath 2\pi\widetilde{\Delta f}.\mathbf{t}}$ resulting in a

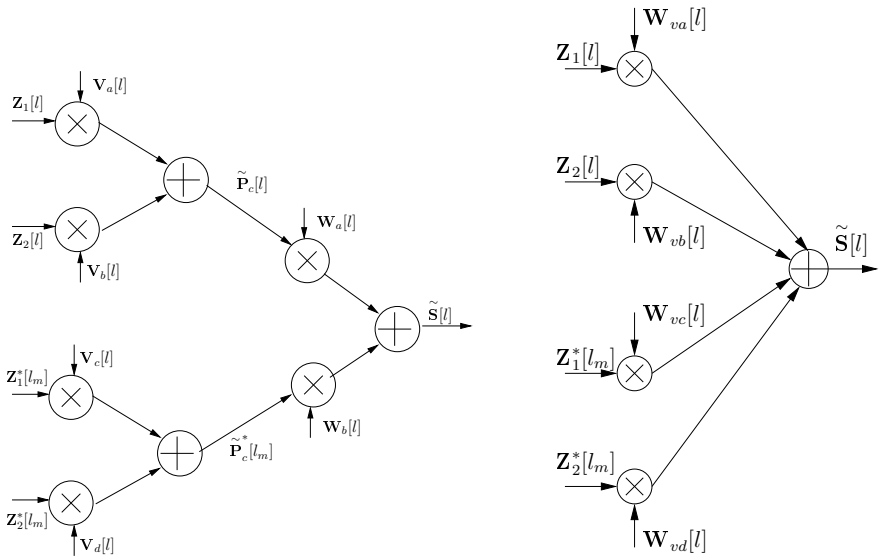

(a) Only FI IQ imbalance (b) Four-tap FEQ

Figure 4.4: Vector graph of compensation scheme for FI transmitter/receiver IQ imbalance together with CFO and channel distortion

vector $\mathbf{z}_2$ as follows:

$$\begin{aligned}\mathbf{z}_2 &= (\mathbf{z})^*.e^{-\jmath 2\pi\Delta\widetilde{f}.\mathbf{t}} \\ &= (g_{ra}^*\mathbf{p}_c^*.e^{-\jmath 2\pi\Delta\widetilde{f}.\mathbf{t}} + g_{rb}^*\mathbf{p}_c.e^{\jmath 2\pi\Delta\widetilde{f}.\mathbf{t}} + g_{ra}^*\mathbf{n}^*.e^{-\jmath 2\pi\Delta\widetilde{f}.\mathbf{t}} + g_{rb}^*\mathbf{n}.e^{\jmath 2\pi\Delta\widetilde{f}.\mathbf{t}}).e^{-\jmath 2\pi\Delta\widetilde{f}.\mathbf{t}} \\ &= g_{rb}^*\mathbf{p}_c + g_{ra}^*\mathbf{p}_c^*.e^{-2\jmath 2\pi\Delta\widetilde{f}.\mathbf{t}} + g_{rb}^*\mathbf{n} + g_{ra}^*\mathbf{n}^*.e^{-2\jmath 2\pi\Delta\widetilde{f}.\mathbf{t}} \\ &= g_{rb}^*\mathbf{p}_c + g_{ra}^*\mathbf{p}_{cx} + \mathbf{n}_2\end{aligned} \tag{4.10}$$

where now $\mathbf{n}_2 = g_{rb}^*\mathbf{n} + g_{ra}^*\mathbf{n}^*.e^{-2\jmath 2\pi\Delta\widetilde{f}.\mathbf{t}}$ is also a zero mean improper complex noise vector.

Both $\mathbf{z}_1$ and $\mathbf{z}_2$ consist of two contributions $\mathbf{p}_c$ and $\mathbf{p}_{cx}$ scaled by different weighing factors plus noise. Here $\mathbf{p}_c$ is called the desired symbol and $\mathbf{p}_{cx}$ the undesired symbol. This is because in the frequency domain, the former gives rise to OFDM symbol of interest, while the latter yields a mirror image and causes ICI (because

of the complex conjugate), subject to leakage caused by the exponential term $(e^{-2\jmath 2\pi\Delta\widetilde{f}.\mathbf{t}})$.

Transforming equations (4.9) and (4.10) to the frequency domain and writing the equations more explicitly for each subcarrier $[l]$, we obtain:

$$\begin{bmatrix}\mathbf{Z}_1[l]\\ \mathbf{Z}_2[l]\end{bmatrix} = \begin{bmatrix}g_{ra} & g_{rb}\\ g^*_{rb} & g^*_{ra}\end{bmatrix}\begin{bmatrix}\mathbf{P}_c[l]\\ \mathbf{P}_{cx}[l]\end{bmatrix} + \begin{bmatrix}\mathbf{N}_1[l]\\ \mathbf{N}_2[l]\end{bmatrix} \tag{4.11}$$

where $\mathbf{Z}_1, \mathbf{Z}_2, \mathbf{P}_c, \mathbf{P}_{cx}, \mathbf{N}_1$ and $\mathbf{N}_2$ are the frequency domain representation of $\mathbf{z}_1, \mathbf{z}_2, \mathbf{p}_c, \mathbf{p}_{cx}, \mathbf{n}_1$ and $\mathbf{n}_2$.

Following the two-tap FEQ scheme in (3.12), we can now obtain the estimate $\widetilde{\mathbf{P}}_c[l]$ of the desired symbol of $\mathbf{P}_c[l] = \begin{bmatrix}g_{ta}\mathbf{C}[l] & g_{tb}\mathbf{C}[l]\end{bmatrix}\begin{bmatrix}\mathbf{S}[l]\\ \mathbf{S}^*[l_m]\end{bmatrix}$ by taking an appropriate linear combination of $\mathbf{Z}_1[l]$ and $\mathbf{Z}_2[l]$, i.e.

$$\widetilde{\mathbf{P}}_c[l] = \begin{bmatrix}\mathbf{V}_a[l] & \mathbf{V}_b[l]\end{bmatrix}\begin{bmatrix}\mathbf{Z}_1[l]\\ \mathbf{Z}_2[l]\end{bmatrix} \tag{4.12}$$

where $\mathbf{V}_a[l]$ and $\mathbf{V}_b[l]$ are the coefficients of the two-tap FEQ filters. $\widetilde{\mathbf{P}}_c[l]$ is now free from both receiver IQ imbalance and the CFO, and it is now only distorted by transmitter IQ imbalance and the channel:

In a similar fashion, an appropriate linear combination of $\mathbf{Z}^*_1[l_m]$ and $\mathbf{Z}^*_2[l_m]$ can be used to obtain the estimate $\widetilde{\mathbf{P}}^*_c[l_m]$ of the desired symbol of $\mathbf{P}^*_c[l_m] = \begin{bmatrix}g^*_{tb}\mathbf{C}^*[l_m] & g^*_{ta}\mathbf{C}^*[l_m]\end{bmatrix}\begin{bmatrix}\mathbf{S}[l]\\ \mathbf{S}^*[l_m]\end{bmatrix}$, i.e

$$\widetilde{\mathbf{P}}^*_c[l_m] = \begin{bmatrix}\mathbf{V}_c[l] & \mathbf{V}_d[l]\end{bmatrix}\begin{bmatrix}\mathbf{Z}^*_1[l_m]\\ \mathbf{Z}^*_2[l_m]\end{bmatrix} \tag{4.13}$$

From (4.12) and (4.13) it follows that an estimate of the transmitted symbol $\widetilde{\mathbf{S}}[l]$ can be obtained by taking an appropriate linear combination of $\widetilde{\mathbf{P}}_c[l]$ and $\widetilde{\mathbf{P}}^*_c[l_m]$:

$$\widetilde{\mathbf{S}}[l] = \begin{bmatrix}\mathbf{W}_a[l] & \mathbf{W}_b[l]\end{bmatrix}\begin{bmatrix}\widetilde{\mathbf{P}}_c[l]\\ \widetilde{\mathbf{P}}^*_c[l_m]\end{bmatrix} \tag{4.14}$$

A vector graph of this compensation scheme is shown in **Figure 4.4(a)**. The compensation scheme consists of three two-tap filters, where the output of the first two filters is used as the input to the third two-tap filter.

Based on this derivation, we can now also derive the transmitted OFDM symbol directly from the received symbols $\mathbf{Z}_1$ and $\mathbf{Z}_2$. For this we merge equation

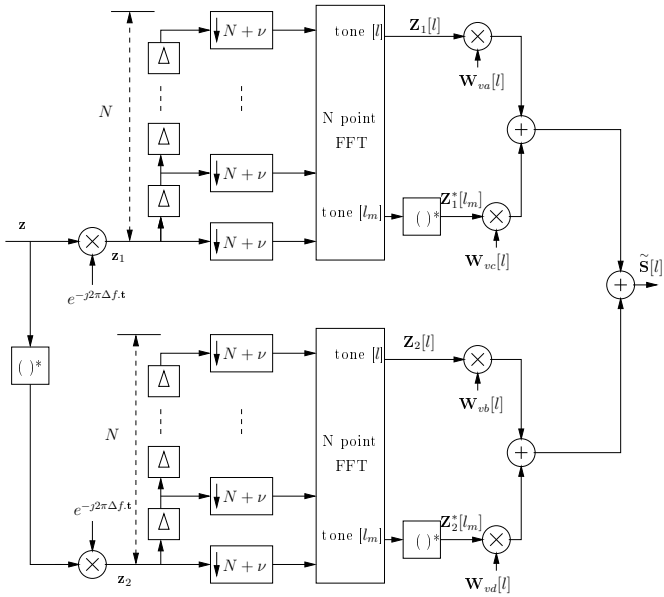

Figure 4.5: Four-tap FEQ scheme for compensation of FI transmitter/receiver IQ imbalance together with CFO and channel distortion

(4.11), the complex conjugate of its mirror, and the definition of $\mathbf{P}_c[l] = \begin{bmatrix} g_{ta}\mathbf{C}[l] & g_{tb}\mathbf{C}[l] \end{bmatrix} \begin{bmatrix} \mathbf{S}[l] \\ \mathbf{S}^*[l_m] \end{bmatrix}$, this results in:

$$\begin{bmatrix} \mathbf{Z}_1[l] \\ \mathbf{Z}_2[l] \\ \mathbf{Z}_1{}^*[l_m] \\ \mathbf{Z}_2{}^*[l_m] \end{bmatrix} = \underbrace{\begin{bmatrix} g_{ra}g_{ta}\mathbf{C}[l] & g_{ra}g_{tb}\mathbf{C}[l] & g_{rb} & 0 \\ g_{rb}^*g_{ta}\mathbf{C}[l] & g_{rb}^*g_{tb}\mathbf{C}[l] & g_{ra}^* & 0 \\ g_{ra}^*g_{tb}^*\mathbf{C}^*[l_m] & g_{ra}^*g_{ta}^*\mathbf{C}^*[l_m] & 0 & g_{rb}^* \\ g_{rb}g_{tb}^*\mathbf{C}^*[l_m] & g_{rb}g_{ta}^*\mathbf{C}^*[l_m] & 0 & g_{ra} \end{bmatrix}}_{\mathbf{D}_{c_{tot}}[l]} \begin{bmatrix} \mathbf{S}[l] \\ \mathbf{S}^*[l_m] \\ \mathbf{P}_{cx}[l] \\ \mathbf{P}_{cx}{}^*[l_m] \end{bmatrix} + \begin{bmatrix} \mathbf{N}_1[l] \\ \mathbf{N}_2[l] \\ \mathbf{N}_1{}^*[l_m] \\ \mathbf{N}_2{}^*[l_m] \end{bmatrix} \tag{4.15}$$

Equation (4.15) shows that the estimate $\widetilde{\mathbf{S}}[l]$ can be obtained by taking an appropriate linear combination of $\mathbf{Z}_1[l], \mathbf{Z}_2[l], \mathbf{Z}_1{}^*[l_m]$ and $\mathbf{Z}_2{}^*[l_m]$, i.e.

$$\widetilde{\mathbf{S}}[l] = \begin{bmatrix} \mathbf{W}_{va}[l] & \mathbf{W}_{vb}[l] & \mathbf{W}_{vc}[l] & \mathbf{W}_{vd}[l] \end{bmatrix} \begin{bmatrix} \mathbf{Z}_1[l] \\ \mathbf{Z}_2[l] \\ \mathbf{Z}_1^*[l_m] \\ \mathbf{Z}_2^*[l_m] \end{bmatrix} \tag{4.16}$$

where the coefficients of the filters $\mathbf{W}_{vk}[l]$ (for $k = a, b, c, d$) are related to the earlier two-tap filter coefficients as follows: $\mathbf{W}_{va}[l] = (\mathbf{W}_a[l]\mathbf{V}_a[l]), \mathbf{W}_{vb}[l] = (\mathbf{W}_a[l]\mathbf{V}_b[l]), \mathbf{W}_{vc}[l] = (\mathbf{W}_b[l]\mathbf{V}_c[l])$ and $\mathbf{W}_{vd}[l] = (\mathbf{W}_b[l]\mathbf{V}_d[l])$.

The formula (4.16) demonstrates that a **four-tap FEQ** receiver structure can be designed that exactly compensates for the transmitter and receiver IQ imbalance, the CFO and the channel effect. The FEQ coefficients are estimated based on a MSE minimization:

$$\underset{\substack{\mathbf{W}_{va}[l], \mathbf{W}_{vb}[l] \\ \mathbf{W}_{vc}[l], \mathbf{W}_{vd}[l]}}{min} \Xi \left\{ \left| \widetilde{\mathbf{S}}[l] - \begin{bmatrix} \mathbf{W}_{va}[l] \\ \mathbf{W}_{vb}[l] \\ \mathbf{W}_{vc}[l] \\ \mathbf{W}_{vd}[l] \end{bmatrix}^T \begin{bmatrix} \mathbf{Z}_1[l] \\ \mathbf{Z}_2[l] \\ \mathbf{Z}_1^*[l_m] \\ \mathbf{Z}_2^*[l_m] \end{bmatrix} \right|^2 \right\} \tag{4.17}$$

The FEQ can be initialized by a LS scheme or an adaptive RLS algorithm based on a LT symbol sequence. We now need a LT symbol sequence length $M_l \geq 4$ to estimate these four coefficients. The transmission packet for the joint compensation scheme now consists of an identical ST symbol sequence for CFO estimation, followed by a linearly independent LT symbol sequence for the estimation of the FEQ coefficients, and finally the data sequence. The ST symbol and LT symbol sequences can be taken from any suitable alphabet.

A vector graph of this compensation scheme is shown in **Figure 4.4(b)** and the detailed illustration of the four-tap FEQ is given in **Figure 4.5**. The final structure consists of two DFT branches each with two outputs. A four-tap FEQ is then applied to the desired subcarrier and the complex conjugate output of the mirror subcarrier obtained from the two DFTs.

Note:

The four-tap FEQ structure discussed so far can be reduced to a two-tap FEQ if any one of the three front-end impairments is not present in the communication model, namely the transmitter IQ imbalance, the receiver IQ imbalance or the CFO. The LT symbol sequence requirement is then reduced to $M_l \geq 2$ to estimate the two coefficients. The following changes are observed in the FEQ structure:

- **Only transmitter IQ imbalance or only receiver IQ imbalance or both transmitter and receiver IQ imbalance but no CFO**: In this case, the received symbols $\mathbf{Z}_1[l] = \mathbf{Z}_2^*[l_m]$ and $\mathbf{Z}_2[l] = \mathbf{Z}_1^*[l_m]$ and the equation (4.16) will reduce to equation (3.12). The output of any one DFT can be taken (instead of both DFT outputs) as the compensation can now be obtained with a two-tap FEQ as explained in section 3.2.3.

- **Only receiver IQ imbalance and CFO**: In this case, the coefficient $\mathbf{W}_b$ will become zero. As a result the compensation structure will now have only two active coefficients $\mathbf{W}_{va}[l]$ and $\mathbf{W}_{vb}[l]$. The FEQ still requires the two DFTs now followed by two-tap FEQ filters applied to only the desired subcarriers ($\mathbf{Z}_1[l]$ and $\mathbf{Z}_2[l]$).

- **Only transmitter IQ imbalance and CFO**: In this case, the coefficient pairs $\mathbf{V}_b$ and $\mathbf{V}_d$ will become zero. As a result the FEQ structure will once again have only two active coefficients $\mathbf{W}_{va}[l]$ and $\mathbf{W}_{vc}[l]$. Both coefficients require the inputs from $\mathbf{Z}_1[l]$ and $\mathbf{Z}_1^*[l_m]$. Only one DFT followed by a two-tap FEQ is applied to the desired subcarrier and the complex conjugate output of the mirror subcarrier. The FEQ structure is similar to the case of only transmitter and receiver IQ imbalance as explained in section 3.2.3.

In the next section we will extend the joint compensation scheme to also consider FS transmitter/receiver IQ imbalance in addition to CFO and channel distortion under insufficient CP length.

4.5 Joint FS IQ imbalance, CFO and Channel Compensation under Insufficient CP length

In this section we derive a joint compensation solution for all the impairments we have discussed so far in the OFDM communication model, namely FS transmitter/receiver IQ imbalance, CFO, the multipath channel and the insufficient CP length. It is shown that this solution provides the most generalized structure that can compensate for all different combinations of impairments. Following the derivation in section 3.3, the compensation scheme in the present case can also be separated into two parts. The first part (TEQ+FEQ based compensation) comprises of a cascade of a time domain and a frequency domain equalizer. In the second part (PTEQ based compensation), we merge the entire equalization structure to form one unified equalizer in the frequency domain.

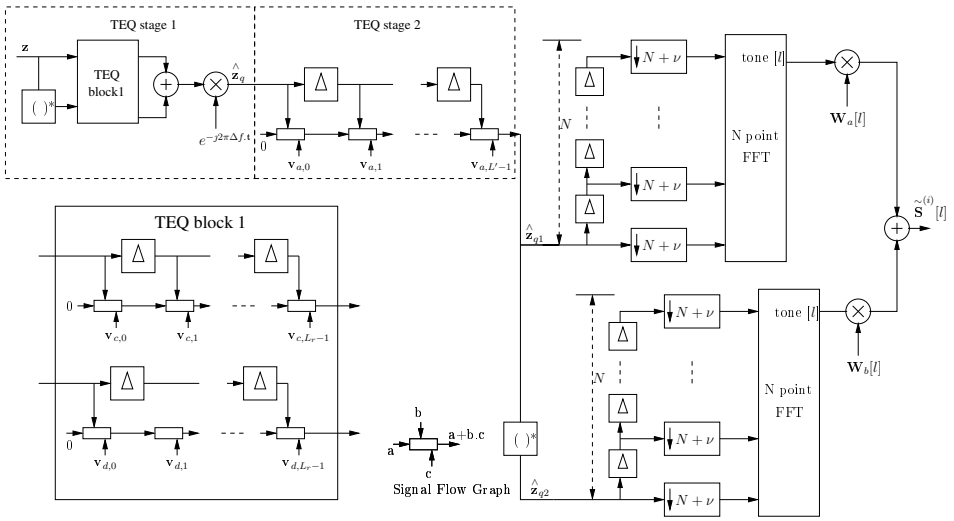

Figure 4.6: TEQ in the presence of FS transmitter/receiver IQ imbalance and CFO under insufficient CP length

4.5.1 TEQ + FEQ based Compensation

Following the section 3.3., we once again develop an equalization structure that can compensate for impairments in the reverse order of their appearance, i.e starting with receiver IQ imbalance and CFO compensation by the first stage of TEQ, and then the shortening of the combined transmitter/receiver IQ imbalance and channel impulse response by the second stage of TEQ. This is then followed by a joint compensation of transmitter IQ imbalance and channel distortion in the frequency domain by a FEQ.

In order to compensate for receiver IQ imbalance, we design two TEQ branches $\mathbf{v}_c$ and $\mathbf{v}_d$ each of length L_r taps. The first filter branch $\mathbf{v}_c$ is applied to the received symbol $\mathbf{z}$, and the second filter branch $\mathbf{v}_d$ is applied to the complex conjugate

version of the received symbol $\mathbf{z}^*$. This leads to:

$$\begin{aligned}\mathbf{z}_q =& \mathbf{v}_c \star \mathbf{z} + \mathbf{v}_d \star \mathbf{z}^* \\ =& \underbrace{(\mathbf{v}_c \star \mathbf{g}_{ra} + \mathbf{v}_d \star \mathbf{g}^*_{rb})}_{\mathbf{f}_1} \star (\mathbf{r}.e^{\jmath 2\pi \Delta f.\mathbf{t}}) \\ &+ \underbrace{(\mathbf{v}_c \star \mathbf{g}_{rb} + \mathbf{v}_d \star \mathbf{g}^*_{ra})}_{\mathbf{f}_2} \star (\mathbf{r}^*.e^{-\jmath 2\pi \Delta f.\mathbf{t}})\end{aligned} \tag{4.18}$$

The design target for the filters $\mathbf{v}_c$ and $\mathbf{v}_d$ is such that the term $\mathbf{f}_2$ vanishes in equation (4.18). The solution to this set of equations are $\mathbf{v}_c = \mathbf{g}^*_{ra}.\alpha$ and $\mathbf{v}_d = -\mathbf{g}_{rb}.\alpha$ where α is a non-zero scalar. Thus with appropriate coefficient values for $\mathbf{v}_c$ and $\mathbf{v}_d$, we can have $\mathbf{z}_q$ free of any contributions from $\mathbf{z}^*$, i.e. free from receiver IQ imbalance.

Once the receiver IQ imbalance has been compensated by the two TEQ branches, we can then de-rotate $\mathbf{z}_q$ by an element wise multiplication with the estimated negative frequency offset $e^{-\jmath 2\pi \Delta \tilde{f}.\mathbf{t}}$. This leads to:

$$\hat{\mathbf{z}}_q = \mathbf{z}_q.e^{-\jmath 2\pi \Delta \tilde{f}.\mathbf{t}} = \hat{\mathbf{f}}_1 \star \mathbf{r} \tag{4.19}$$

where $\hat{\mathbf{f}}_1 = \mathbf{f}_1.(e^{-\jmath 2\pi \Delta \tilde{f}.(0 \ldots (L_r-1))^T})$ is a modulated version of $\mathbf{f}_1$. With this operation the resulting vector $\hat{\mathbf{z}}_q$ is free from CFO and is affected only by the remaining ISI due to the insufficient CP length, and also ICI due to transmitter IQ imbalance along with channel distortion. The filter $\hat{\mathbf{f}}_1$ can be considered to be part of the overall channel filtering.

The rest of the compensation remains exactly the same as the TEQ+FEQ scheme explained in section 3.3.2. The received symbol $\hat{\mathbf{z}}_q$ is then filtered by second stage of TEQ that consists of a conventional channel shortening filter branch $\mathbf{v}_a$ of length L' taps. The output of the second stage TEQ filter $\hat{\mathbf{z}}_{q1} = (\mathbf{v}_a \star \hat{\mathbf{z}}_q)$ and its complex conjugate output $\hat{\mathbf{z}}_{q2} = (\mathbf{v}_a \star \hat{\mathbf{z}}_q)^*$ are then applied to two DFTs after stacking the results into an N vector. A two-tap FEQ is applied to the output of the two DFT branches for the compensation of transmitter IQ imbalance and channel distortion in the frequency domain. The estimate of the transmitted OFDM symbol is thus given as:

$$\begin{aligned}\tilde{\mathbf{S}}^{(i)}[l] &= \begin{bmatrix}\mathbf{W}_a[l] & \mathbf{W}_b[l]\end{bmatrix} \begin{bmatrix}\mathbf{F}_N[l]\hat{\mathbf{z}}_{q1} \\ \mathbf{F}_N[l]\hat{\mathbf{z}}_{q2}\end{bmatrix} \\ &= \begin{bmatrix}\mathbf{W}_a[l] & \mathbf{W}_b[l]\end{bmatrix} \begin{bmatrix}\mathbf{F}_N[l](\mathbf{v}_a \star \hat{\mathbf{z}}_q) \\ \mathbf{F}_N[l](\mathbf{v}_a \star \hat{\mathbf{z}}_q)^*\end{bmatrix}\end{aligned} \tag{4.20}$$

Similar to section 3.3.2, the dimensions of the received symbol $\mathbf{z}$ in equation (3.16) is adjusted to $(N+L''-1\times 1)$. Hence, $\mathbf{O}_1 = 0_{(N+L''-1\times N+2\nu-L-L_T-L_r-L''+4)}$, $\mathbf{T}_{dk}$ (for $k = a, b$) is of size $(N + L'' - 1 \times N + L_t + L + L_r + L'' - 4)$ with first column $[\mathbf{d}_{k(L_t+L+L_r-3)}, 0_{(1\times N+L''-1)}]^T$ and first row $[\mathbf{d}_{k(L_t+L+L_r-3)}, \ldots, \mathbf{d}_{k(0)}, 0_{(1\times N+L''-2)}]$.

The TEQ+FEQ based compensation scheme is shown in **Figure 4.6**. It is usually difficult to estimate the receiver IQ imbalance compensation and channel shortening TEQ coefficients and the transmitter IQ imbalance and channel distortion compensation FEQ coefficients with sufficient accuracy when the CP is not sufficiently long. In order to simplify the estimation of the compensation coefficients, we move the TEQ into the frequency domain resulting in a unified PTEQ compensation structure. This is explained in the next section.

4.5.2 PTEQ based Compensation

To transform the entire TEQ+FEQ scheme into a simpler frequency domain version, we swap the first set of TEQ filters $\mathbf{v}_c$ and $\mathbf{v}_d$ with the multiplication of the de-rotation operation $e^{-\jmath 2\pi \widetilde{\Delta f}.\mathbf{t}}$. This results in a modified form (with modified filter coefficients $\mathbf{v}_c$ and $\mathbf{v}_d$) of equation (4.18) given as:

$$\begin{aligned}
\hat{\mathbf{z}}_q &= \mathbf{v}_c \star (\mathbf{z}.e^{-\jmath 2\pi \widetilde{\Delta f}.\mathbf{t}}) + \mathbf{v}_d \star (\mathbf{z}^*.e^{-\jmath 2\pi \widetilde{\Delta f}.\mathbf{t}}) \\
&= \underbrace{(\mathbf{v}_c \star \hat{\mathbf{g}}_{ra} + \mathbf{v}_d \star \hat{\mathbf{g}}^*_{rb})}_{\mathbf{f}_1} \star \mathbf{r} \\
&\quad + \underbrace{(\mathbf{v}_c \star \hat{\mathbf{g}}_{rb} + \mathbf{v}_d \star \hat{\mathbf{g}}^*_{ra})}_{\mathbf{f}_2} \star (\mathbf{r}^*.e^{-2\jmath 2\pi \widetilde{\Delta f}.\mathbf{t}})
\end{aligned} \tag{4.21}$$

Here $\hat{\mathbf{g}}_{ra} = \mathbf{g}_{ra}.(e^{-\jmath \widetilde{\mathbf{w}}})$, $\hat{\mathbf{g}}_{rb} = \mathbf{g}_{rb}.(e^{\jmath \widetilde{\mathbf{w}}})$ with $\widetilde{\mathbf{w}} = 2\pi \widetilde{\Delta f}.(0 \ldots (L_r - 1))^T$.

To suppress $\mathbf{r}^*$ in equation (4.21), we require $\mathbf{v}_c = \hat{\mathbf{g}}^*_{ra}.\alpha$ and $\mathbf{v}_d = -\hat{\mathbf{g}}_{rb}.\alpha$. The swapping of the de-rotation with the TEQs effectively results in a modulated version of the first set of original filters (so still linear filters but with adjusted filter coefficients).

The TEQ filter of the second stage $\mathbf{v}_a$ is then merged with modified TEQs of the first stage $\mathbf{v}_c, \mathbf{v}_d$. This results in four filter branches each of length L''. The

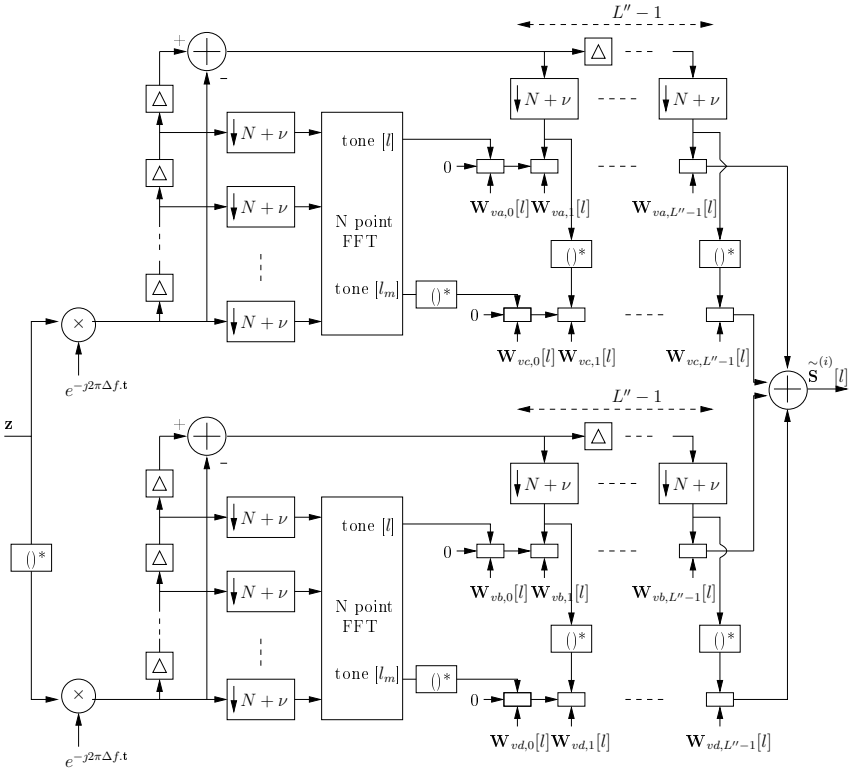

Figure 4.7: Four-branch PTEQ in the presence of FS transmitter/receiver IQ imbalance and CFO under insufficient CP length

resulting inputs to the two DFTs are now given as:

$$\begin{aligned}\hat{\mathbf{z}}_{q1} &= \mathbf{v}_{ac} \star (\mathbf{z}.e^{-\jmath 2\pi\Delta\widetilde{f}.\mathbf{t}}) + \mathbf{v}_{ad} \star (\mathbf{z}^*.e^{-\jmath 2\pi\Delta\widetilde{f}.\mathbf{t}}) \\ \hat{\mathbf{z}}_{q2} &= \mathbf{v}^*_{ac} \star (\mathbf{z}.e^{-\jmath 2\pi\Delta\widetilde{f}.\mathbf{t}})^* + \mathbf{v}^*_{ad} \star (\mathbf{z}^*.e^{-\jmath 2\pi\Delta\widetilde{f}.\mathbf{t}})^*\end{aligned} \tag{4.22}$$

where the new TEQ filters are obtained as: $\mathbf{v}_{ac} = (\mathbf{v}_a \star \mathbf{v}_c)$ and $\mathbf{v}_{ad} = (\mathbf{v}_a \star \mathbf{v}_d)$.

The TEQ filtering may then be moved into the frequency domain resulting in a PTEQ employing four DFT operations and $L''-1$ difference terms [113]. Equation

(4.22) can then be written as:

$$\begin{aligned}
\overset{\wedge}{\mathbf{Z}}_{q1}[l] &= \begin{bmatrix}\mathbf{V}_{ac}[l]\\ \mathbf{V}_{ad}[l]\end{bmatrix}^{T}\begin{bmatrix}\mathbf{F}_{ext}[l]\mathbf{z}.e^{-\jmath 2\pi\Delta\widetilde{f}.\mathbf{t}}\\ \mathbf{F}_{ext}[l]\mathbf{z}^{*}.e^{-\jmath 2\pi\Delta\widetilde{f}.\mathbf{t}}\end{bmatrix}\\
\overset{\wedge}{\mathbf{Z}}_{q2}[l] &= \begin{bmatrix}\mathbf{V}^{*}_{ac}[l_m]\\ \mathbf{V}^{*}_{ad}[l_m]\end{bmatrix}^{T}\begin{bmatrix}\mathbf{F}_{ext}[l](\mathbf{z}.e^{-\jmath 2\pi\Delta\widetilde{f}.\mathbf{t}})^{*}\\ \mathbf{F}_{ext}[l](\mathbf{z}^{*}.e^{-\jmath 2\pi\Delta\widetilde{f}.\mathbf{t}})^{*}\end{bmatrix}
\end{aligned} \tag{4.23}$$

where $\mathbf{F}_{ext}[l], \mathbf{V}_{ac}[l]$ and $\mathbf{V}_{ad}[l]$ are defined as in equation (3.20).

We finally merge the PTEQ equation (4.23) and the FEQ equation (4.20) into a **four-branch PTEQ**. The transmitted symbol estimate is then obtained as:

$$\overset{\sim}{\mathbf{S}}^{(i)}[l] = \begin{bmatrix}\mathbf{W}_{va}[l]\\ \mathbf{W}_{vb}[l]\\ \mathbf{W}_{vc}[l]\\ \mathbf{W}_{vd}[l]\end{bmatrix}^{T}\begin{bmatrix}\mathbf{F}_{ext}[l]\mathbf{z}.e^{-\jmath 2\pi\Delta\widetilde{f}.\mathbf{t}}\\ \mathbf{F}_{ext}[l]\mathbf{z}^{*}.e^{-\jmath 2\pi\Delta\widetilde{f}.\mathbf{t}}\\ \mathbf{F}_{ext}[l](\mathbf{z}.e^{-\jmath 2\pi\Delta\widetilde{f}.\mathbf{t}})^{*}\\ \mathbf{F}_{ext}[l](\mathbf{z}^{*}.e^{-\jmath 2\pi\Delta\widetilde{f}.\mathbf{t}})^{*}\end{bmatrix} \tag{4.24}$$

where $\mathbf{W}_{va}[l] = (\mathbf{W}_a[l]\mathbf{V}_{ac}[l]), \mathbf{W}_{vb}[l] = (\mathbf{W}_a[l]\mathbf{V}_{ad}[l]), \mathbf{W}_{vc}[l] = (\mathbf{W}_b[l]\mathbf{V}^{*}_{ac}[l_m])$ and $\mathbf{W}_{vd}[l] = (\mathbf{W}_b[l]\mathbf{V}^{*}_{ad}[l_m])$. Now the filter vectors $\mathbf{W}_{vk}[l]$ (for $k = a, b, c, d$) are of size $(L'' \times 1)$.

Following the simplification process in equation (3.22), the PTEQ structure can be further simplified by taking the desired subcarrier output and the complex conjugate output of the mirror subcarrier from the first two DFTs. Thus the estimate of the transmitted OFDM symbol is now given as:

$$\overset{\sim}{\mathbf{S}}^{(i)}[l] = \begin{bmatrix}\mathbf{W}_{va}[l]\\ \mathbf{W}_{vb}[l]\\ \mathbf{W}_{vc}[l]\\ \mathbf{W}_{vd}[l]\end{bmatrix}^{T}\underbrace{\begin{bmatrix}\mathbf{F}_{ext}[l]\mathbf{z}.e^{-\jmath 2\pi\Delta\widetilde{f}.\mathbf{t}}\\ \mathbf{F}_{ext}[l]\mathbf{z}^{*}.e^{-\jmath 2\pi\Delta\widetilde{f}.\mathbf{t}}\\ (\mathbf{F}_{ext}[l_m]\mathbf{z}.e^{-\jmath 2\pi\Delta\widetilde{f}.\mathbf{t}})^{*}\\ (\mathbf{F}_{ext}[l_m]\mathbf{z}^{*}.e^{-\jmath 2\pi\Delta\widetilde{f}.\mathbf{t}})^{*}\end{bmatrix}}_{\mathbf{z}_{ext}[l]} \tag{4.25}$$

Equations (4.25) shows that the total number of PTEQ coefficients to be estimated is now $4L''$ and in order to estimate these coefficients we need LT symbol sequence length $M_l \geq 4L''$. The final four-branch PTEQ compensation scheme is shown in **Figure 4.7**. We can now write an MMSE equation for (4.25), similar to equation (4.17), and then the PTEQ can be initialized by a LS scheme or an adaptive RLS algorithm based on a LT symbol sequence.

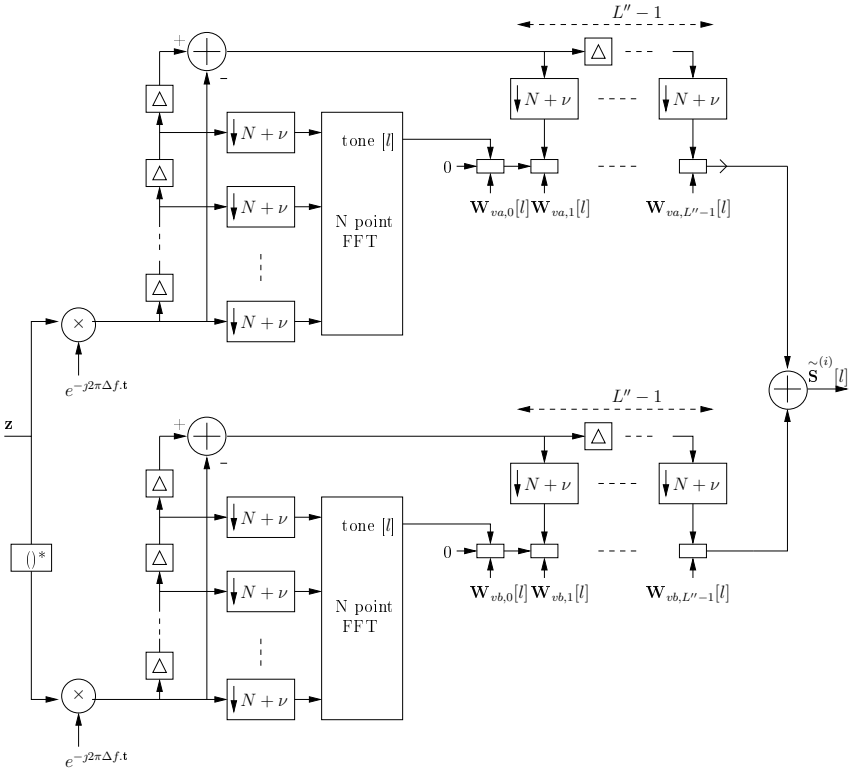

Figure 4.8: Two-branch PTEQ in the presence of only FS receiver IQ imbalance and CFO

Note:

- **Residual CFO error correction:** We have derived equation (4.25) assuming that we accurately know Δf. In practice, the CFO estimation algorithm may not be precise leading to a non-zero residual error $e_{\Delta f} = \Delta f - \Delta\tilde{f}$, and hence a residual CFO effect in $\mathbf{z}_{ext}[l]$ of equation (4.25). This then leads to a poor $\tilde{\mathbf{S}}^{(i)}[l]$ symbol estimate due to residual ICI. The performance of the PTEQ can be further improved by searching amongst various PTEQs and CFO values $\Delta\tilde{f}$ such that the error in $(\mathbf{S}^{(i)}[l] - \tilde{\mathbf{S}}^{(i)}[l])$ is minimized. As we assume to already have a good (initial) CFO estimate, the search amongst CFOs is now restricted to a narrow range of values. In general, this indeed leads to a much more accurate estimation of the CFO (see the simulation results). The PTEQ coefficients for the $[l]^{th}$ sub-carrier

can then be obtained based on the following MSE minimization:

$$\begin{pmatrix} min \\ e_{\Delta f}, \mathbf{W}_{va}[l], \\ \mathbf{W}_{vb}[l], \mathbf{W}_{vc}[l], \\ \mathbf{W}_{vd}[l] \end{pmatrix} \mathbb{E}\left\{ \left| \mathbf{S}^{(i)}[l] - \begin{bmatrix} \mathbf{W}_{va}[l] \\ \mathbf{W}_{vb}[l] \\ \mathbf{W}_{vc}[l] \\ \mathbf{W}_{vd}[l] \end{bmatrix}^T \begin{bmatrix} \mathbf{F}_{ext}[l]\mathbf{z}.e^{-\jmath 2\pi(\Delta\widetilde{f}+e_{\Delta f}).\mathbf{t}} \\ \mathbf{F}_{ext}[l]\mathbf{z}^*.e^{-\jmath 2\pi(\Delta\widetilde{f}+e_{\Delta f}).\mathbf{t}} \\ (\mathbf{F}_{ext}[l_m]\mathbf{z}.e^{-\jmath 2\pi(\Delta\widetilde{f}+e_{\Delta f}).\mathbf{t}})^* \\ (\mathbf{F}_{ext}[l_m]\mathbf{z}^*.e^{-\jmath 2\pi(\Delta\widetilde{f}+e_{\Delta f}).\mathbf{t}})^* \end{bmatrix} \right|^2 \right\} \tag{4.26}$$

A similar residual CFO search can also be performed for the four-tap FEQ scheme explained in section 4.4 to further improve the performance of the compensation scheme.

- **Generalized structure:** The PTEQ structure shown in equation (4.25) is the most generalized form of a joint compensation solution for all the impairments considered so far, namely FS transmitter/receiver IQ imbalance, CFO, the multipath channel and the insufficient CP length. The PTEQ structure can compensate for all different combination of impairments. However, the PTEQ structure may have redundant coefficients if only some of the impairments are present in the OFDM system model. The following changes can be made in the PTEQ structure to reduce its implementation costs:
  - **Transmitter/receiver IQ imbalance and CFO under sufficiently long CP length**: In this case, only the first set of TEQ filters $\mathbf{v}_c$ and $\mathbf{v}_d$ are required to compensate for receiver IQ imbalance. The second stage TEQ filter is set to unit coefficient filter with length $L' = 1$ and tap $\mathbf{v}_{a,0} = 1$. Thus the total length of the TEQ and as a result the length of the PTEQ will be $L'' = L_r$. We now need a LT symbol sequence length $M_l \geq 4L_r$ to estimate the PTEQ coefficients.
  - **FI receiver IQ imbalance and FS transmitter IQ imbalance and CFO under insufficient CP length**: This corresponds to the case of no filter mismatch at the receiver front-end. In this case the impulse response of the perfectly matched receiver front-end filters is considered as part of the channel. Thus the first set of TEQ filters $\mathbf{v}_c$ and $\mathbf{v}_d$ can be set to length $L_r = 1$, where they now compensate only for FI receiver IQ imbalance. The second stage TEQ filter $\mathbf{v}_a$ is still needed to shorten the combined transmitter/receiver IQ imbalance and channel impulse response. Thus the total length of the TEQ and the PTEQ will be $L'' = L'$. It should be noted that the length of the PTEQ is not affected by filter mismatch at the transmitter front-end, as the compensation of transmitter IQ imbalance is always performed

in the frequency domain based on the suppression of interference from the mirror subcarrier. Also note that in the case of sufficiently long CP length, the second stage TEQ filter is set to unit coefficient filter with length $L'' = L' = 1$ and tap $\mathbf{v}_{a,0} = 1$, this reduces the PTEQ to a four-tap FEQ as explained in section 4.4.

- **Transmitter/receiver IQ imbalance under insufficient CP length but no CFO**: This is similar to the case of PTEQ explained in section 3.3. In the four-branch PTEQ scheme, the first and the last PTEQ branch corresponding to the coefficients $\mathbf{W}_{va}[l]$ and $\mathbf{W}_{vd}[l]$ and the second and the third PTEQ branch corresponding to the coefficients $\mathbf{W}_{vb}[l]$ and $\mathbf{W}_{vc}[l]$ will have the same inputs. Thus the output of any one DFT can be taken (instead of both DFT outputs) as the compensation can now be obtained with a two-branch PTEQ as explained in section 3.3. The total number of coefficients to be estimated is $2L''$ per subcarrier and hence the required LT symbol sequence length is $M_l \geq 2L''$. In the case of sufficiently long CP length, the PTEQ structure reduces to the simple case of two-tap FEQ with $L'' = 1$.
- **Only receiver IQ imbalance and CFO under sufficiently long CP length** : In this case, the coefficients $\mathbf{W}_{vc}[l]$ and $\mathbf{W}_{vd}[l]$ will become zero. As a result the PTEQ structure will now have only two active branches corresponding to coefficients $\mathbf{W}_{va}[l]$ and $\mathbf{W}_{vb}[l]$. The equalizer structure still requires the two DFTs but followed by a two-branch PTEQ as shown in **Figure 4.8**. The total number of coefficients to be estimated is $2L''$ per subcarrier and hence the required LT symbol sequence length is $M_l \geq 2L''$.
- **Only transmitter IQ imbalance and CFO under sufficiently long CP length**: The coefficients $\mathbf{W}_{vb}[l]$ and $\mathbf{W}_{vd}[l]$ will now become zero. As a result the PTEQ structure will have only two active branches corresponding to coefficients $\mathbf{W}_{va}[l]$ and $\mathbf{W}_{vc}[l]$. The output of the first DFT can be taken (instead of both DFT outputs) as the compensation can now be obtained by a two-branch PTEQ. The total number of coefficients to be estimated is $2L''$ per subcarrier and hence the required LT symbol sequence length is $M_l \geq 2L''$.

Table 4.1 summarizes the different combination of FI/FS transmitter/receiver IQ imbalance, CFO and sufficient/insufficient CP length and their corresponding joint compensation solutions discussed so far in chapter 3 and 4.

Tx IQ	Rx IQ	CFO	CP length	#taps/ PTEQ branches	branch length	structure
no	no	no	sufficient	1	1	1-tap FEQ
no	no	no	insufficient	1	L'	1-branch PTEQ
FI	FI	no	sufficient	2	1	2-tap FEQ
FS	FS	no	sufficient	2	1	2-tap FEQ
no	FI	yes	sufficient	2	1	2-tap FEQ
FI	FI	no	insufficient	2	L'	2-branch PTEQ
FS	FS	no	insufficient	2	$L' + L_r - 1$	2-branch PTEQ
no	FS	yes	sufficient	2	L_r	2-branch PTEQ
no	FS	yes	insufficient	2	$L' + L_r - 1$	2-branch PTEQ
FI	FI	yes	sufficient	4	1	4-tap FEQ
FS	FI	yes	sufficient	4	1	4-tap FEQ
FI	FI	yes	insufficient	4	L'	4-branch PTEQ
FS	FI	yes	insufficient	4	L'	4-branch PTEQ
FS	FS	yes	sufficient	4	L_r	4-branch PTEQ
FS	FS	yes	insufficient	4	$L' + L_r - 1$	4-branch PTEQ

Table 4.1: Different combination of FI/FS transmitter/receiver IQ imbalance, CFO and sufficient/insufficient CP length and their corresponding joint compensation solutions

4.6 Simulation Results

We consider a transmission packet that consists of a 10 identical ST symbol sequence for CFO estimation, followed by a varying number of linearly independent LT symbol sequence for the estimation of equalizer (FEQ/PTEQ) coefficients, and finally the data sequence for performance evaluation. We consider the LT symbol sequence to be sufficiently long to achieve initialization and adequate noise averaging for the four-tap FEQ (4.17) and the four-branch PTEQ (4.25/4.26) coefficients. In general, we have considered the LT symbol sequence to be atleast four to five times longer than the minimal required length for the initialization of equalizer coefficients. However at high SNR, the LT symbol sequence can be further reduced to only two to three times the minimal required length for adequate compensation. The equalizers are initialized by an adaptive RLS algorithm.

- In the first setup we evaluate the performance of the four-tap FEQ scheme (4.17) for the compensation of FI transmitter/receiver IQ imbalance and CFO. The parameters used in the simulation are as follows: We consider an uncoded OFDM system transmission with symbol length $N = 64$ and CP length $\nu = 16$. The OFDM subcarriers are modulated by a 16QAM

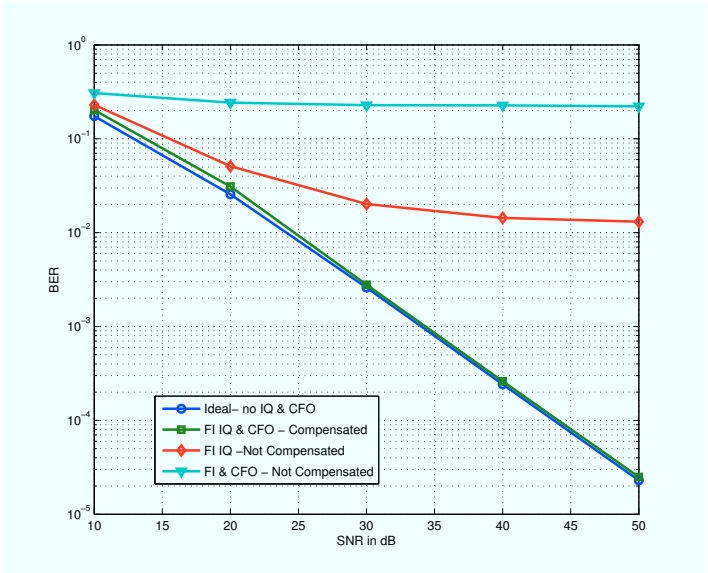

Figure 4.9: BER vs SNR for 16QAM OFDM with FI transmitter/receiver IQ imbalance and CFO under sufficiently long CP length

constellation scheme. We consider FI amplitude imbalance of $g_t = g_r = 5\%$ and phase imbalance of $\phi_t = \phi_r = 5^\circ$ and normalized CFO $\zeta = 0.5$. We assume the receiver has the perfect knowledge of the CFO.

The multipath channel is considered to be $L = 4$ taps long. Thus the CP length is sufficiently longer than the channel impulse response. The taps of the multipath channel are chosen independently with complex Gaussian distribution. **Figure 4.9** shows the BER vs SNR results for this channel profile. BER results depicted are obtained by averaging the BER curves over 10^4 independent channels. The figure shows that with adequate number of LT symbol sequence available for training, even in the presence of large CFO value, the four-tap FEQ provides compensation performance very close to the ideal case. Thus the FEQ performs the compensation as efficiently as expected irrespective of the amount of CFO.

- In the second setup we evaluate the performance of the four-branch PTEQ scheme (4.26) for the compensation of FS transmitter/receiver IQ imbalance, CFO under sufficiently long CP length. The parameters used in the simulation are as follows: We consider an uncoded OFDM system transmission with symbol length $N = 64$ and CP length $\nu = 16$. The OFDM subcarriers are modulated by a 64QAM constellation scheme. The filter impulse responses are $\mathbf{h}_{ti} = \mathbf{h}_{ri} = [0.06\ 0.5\ 0.01]$ and $\mathbf{h}_{tq} = \mathbf{h}_{rq} =$

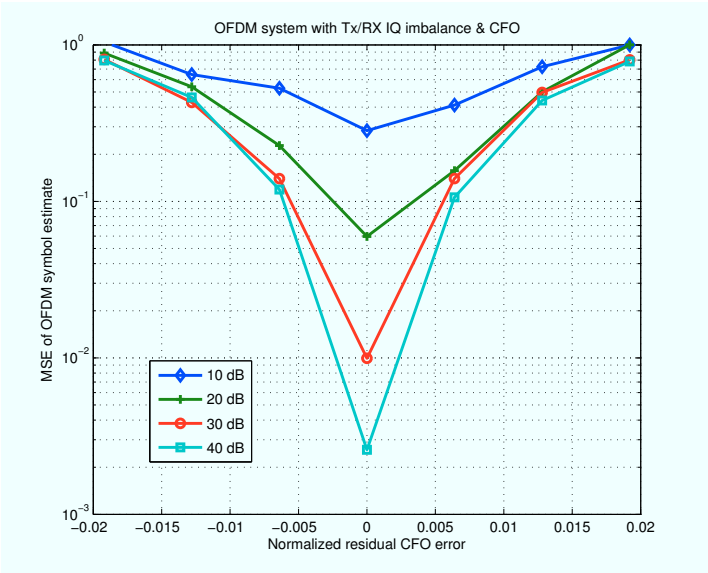

Figure 4.10: MSE in the estimation of CFO in the presence of transmitter/receiver IQ imbalance

[0.01 0.5 0.06] and FI amplitude imbalance of $g_t = g_r = 5\%$ and phase imbalance of $\phi_t = \phi_r = 5°$. The multipath channel length $L = 4$ taps, thus $\nu > L_t + L_r + L - 2$ and there is no ISI distortion between adjacent OFDM symbols. The normalized CFO is now uniformly varied between $\zeta = [-0.4 \longleftrightarrow +0.4]$ and we do not assume the receiver has the knowledge of the CFO in the communication model. Thus we estimate the CFO by selecting one of the schemes shown in section 4.3, where the threshold for selecting the autocorrelation scheme is set at $\zeta = [-0.02 \longleftrightarrow +0.02]$ and the NLS scheme for the remaining CFO values. The iterative scheme (4.26) is also followed to finally obtain an optimal CFO value together with PTEQ coefficients.

In **Figure 4.10**, an iterative search for an optimal CFO value $\widetilde{\zeta} = \Delta\widetilde{f}.T.N$ together with optimal PTEQ coefficients is performed. The PTEQ length is considered fixed at $L'' = 3$. The figure shows that the MSE obtained for various normalized residual CFO estimation errors $e_\zeta = \zeta - \widetilde{\zeta}$. It can be seen that for an accurate estimate of the CFO i.e, $(\widetilde{\zeta} = \zeta)$, the MSE reaches a minimum. There is a big dip in MSE and this becomes even more prominent as the SNR is increased from 10 dB to 40 dB. This shows that a significant improvement in performance can be obtained for a good CFO estimate and that the search for an accurate CFO estimate becomes easier

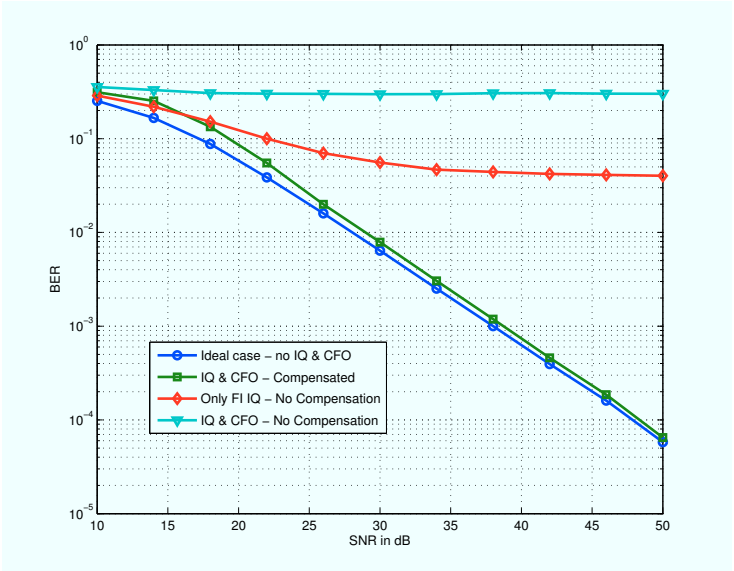

Figure 4.11: BER vs SNR for 64QAM OFDM with FS transmitter/receiver IQ imbalance and CFO under sufficiently long CP length

at higher SNR values. The PTEQ coefficients obtained for this resulting CFO estimate $\widetilde{\zeta}$ are then used for equalization. **Figure 4.11** shows the BER vs SNR results for this simulation setup. As can be observed from the figure, the PTEQ provides a very good compensation performance. For low SNR, it may be difficult to accurately determine the CFO and hence the performance is poor compared to the system with no CFO and also no compensation scheme in place. For high SNR, the PTEQ provides a very good compensation performance even in the presence of large CFO values. The performance depends on how accurately the CFO and PTEQ coefficients can be estimated.

- In the third setup we evaluate the performance of the four-branch PTEQ scheme (4.25) for the compensation of FS transmitter/receiver IQ imbalance, and CFO under insufficient CP length. We assume the perfect knowledge of CFO at the receiver, and thus no iterative residual CFO search is performed. We consider an uncoded OFDM system transmission with symbol length $N = 64$ and CP length $\nu = 8$. We consider FI amplitude imbalance of $g_t, g_r = 3\%$ and phase imbalance of $\phi_t, \phi_r = 3^\circ$. The front-end filter mismatched impulse responses are $\mathbf{h}_{ti} = \mathbf{h}_{ri} = [0.1\ 0.5], \mathbf{h}_{tq} = \mathbf{h}_{rq} = [0.5\ 0.1]$ with filter impulse length $L_t = L_r = 2$. The channel is $L = 10$ taps long, thus

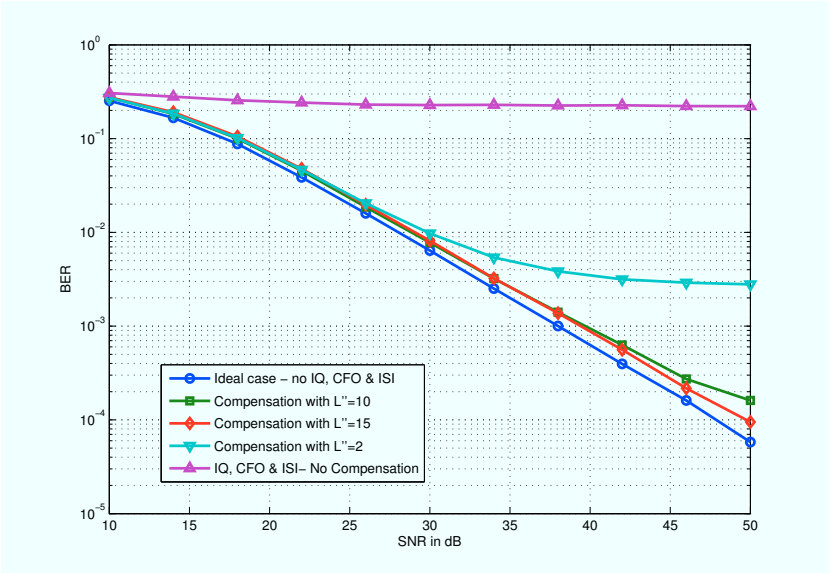

Figure 4.12: BER vs SNR for 64QAM OFDM with FS transmitter/receiver IQ imbalance and CFO under insufficient CP length

$\nu < L_t + L_r + L - 2$. A PTEQ with $L'' = 10$ and $L'' = 15$ taps is used for compensation.

Figure 4.12 shows the BER vs SNR for this simulation setup. The performance comparison is made with a system with no compensation scheme in place and an ideal system with no front-end distortion. Only in an ideal system, we consider the channel length $L = 4$ taps long, thus there is no ISI due to insufficient CP length. In addition, the performance comparison is also made with a PTEQ of length $L'' = 2$. Thus in this case the PTEQ takes into account only transmitter/receiver IQ imbalance and CFO and not ISI in the received symbols. The PTEQs are initialized by the RLS algorithm.

Figure shows that the PTEQ of length $L'' = 2$ shows some improvement in the performance compared to a system with no compensation scheme in place, but the error floor is still high. Good performance results are obtained for a PTEQ of length $L'' = 10$ and $L'' = 15$. Thus as the PTEQ length is increased, the equalizer is increasingly effective against ISI distortion.

4.7 Conclusion

In this chapter the joint effects of transmitter/receiver IQ imbalance and CFO for an OFDM system in a multipath channel environment has been studied. Simulation results show that IQ imbalance together with CFO results in a very severe performance degradation, rendering the system useless, and hence the compensation solutions are essential. We have proposed digital compensation solutions that incorporate CFO compensation in addition to the compensation of transmitter and receiver IQ imbalance.

In the case of FI transmitter and receiver IQ imbalance, a straightforward joint compensation for all the impairments can be obtained by a simple four-tap FEQ. In the case of FS transmitter and receiver IQ imbalance, a four-branch PTEQ solution obtained by combining a TEQ structure with a FEQ structure has been proposed. The PTEQ solution is also applicable in cases where the CP is not sufficiently long to accommodate the combined transmitter/receiver IQ imbalance and channel impulse response. It is shown that the four-branch PTEQ solution is the most generalized form of a joint compensation solution for all the impairments considered so far, namely FS transmitter/receiver IQ imbalance, CFO, the multipath channel and the insufficient CP length. The PTEQ structure is also applicable for all different combinations of impairments. The proposed solution provides a very efficient, post-FFT adaptive equalization with performance very close to the ideal case.

Chapter 5

Decoupled Compensation Schemes

5.1 Introduction

In chapter 3 and 4, we proposed joint estimation and compensation solutions for transmitter/receiver IQ imbalance, CFO and multipath channel distortion under either sufficient or insufficient CP length. It was shown that given adequate training symbols, a joint compensation solution can provide very good performance results that are very close to ideal conditions. As the joint compensation coefficients are estimated directly from the training symbols, the need to estimate each individual distortion parameter (transmitter and receiver IQ imbalance, channel) separately is not required.

However, in a joint compensation solution all compensation coefficients have to be re-estimated for every variation of the channel characteristics even when the IQ imbalance and CFO parameters are constant. As the channel variations are more frequent compared to the front-end impairments, it will be advantageous if we can develop solutions where the estimation of IQ imbalance and CFO is decoupled from the estimation of the channel distortion. This results in a compensation structure where in time varying scenarios only the channel parameters have to be re-estimated while the IQ imbalance and CFO compensation coefficients are indeed kept constant. The decoupled schemes result in an overall lower training overhead and a lower computational requirement, compared to the joint estimation/compensation schemes. Recently in [5], a compensation scheme has been proposed that can decouple the frequency selective receiver IQ imbalance from the channel equalization, resulting in a reliable compensation with a small

training overhead. In this chapter we extend the case to include transmitter IQ imbalance and also the case of CFO together with IQ imbalance. It is shown that the proposed compensation schemes provide very efficient decoupled solutions with a performance close to the ideal case without any IQ imbalance and/or CFO. The publications related to this chapter are: [93], [95], [97] and [98].

This chapter is organized as follows: **Section 5.2** (decoupled FEQ schemes) considers the presence of only transmitter and receiver IQ imbalance in the system model. Here the transmitter/receiver IQ imbalance and the channel parameters are estimated based on coefficients obtained from the joint estimation/compensation solution explained in section 3.2.3. In **section 5.3** (phase rotation schemes), we consider the presence of CFO and receiver IQ imbalance. In this scheme the receiver IQ imbalance parameters can be estimated directly from a sequence of specially induced phase rotated LT symbols. The receiver IQ imbalance parameters are estimated irrespective of the amount of CFO in the system model. It is shown that under certain conditions (for large CFOs), the scheme is also applicable in the presence of transmitter IQ imbalance. Computer simulations are shown in **section 5.4** and finally conclusions are given in **section 5.5**.

5.2 Decoupled FEQ Schemes

In order to derive the decoupled FEQ schemes, the estimates $\widetilde{\mathbf{D}}_a[l], \widetilde{\mathbf{D}}_b[l]$ of the coefficients $\mathbf{D}_a[l], \mathbf{D}_b[l]$ in $\mathbf{D}_{tot}[l]$ are first obtained based on an M_l long sequence of LT symbols, as follows:

$$\underbrace{\begin{bmatrix}\widetilde{\mathbf{D}}_a[l]\\ \widetilde{\mathbf{D}}_b[l]\end{bmatrix}}_{\widetilde{\mathbf{D}}_{tot-}[l]} = \mathbf{S}_{tot}^{Tr^{\dagger}}[l]\mathbf{Z}_{tot-}^{Tr}[l] \tag{5.1}$$

where $\mathbf{Z}_{tot-}^{Tr}[l] = \begin{bmatrix}\mathbf{Z}^{(1)}[l]\\ \mathbf{Z}^{(2)}[l]\\ \hline \vdots \\ \hline \mathbf{Z}^{(M_l)}[l]\end{bmatrix}$ and $\mathbf{S}_{tot}^{Tr}[l] = \begin{bmatrix}\mathbf{S}^{(1)}[l] & \mathbf{S}^{*(1)}[l_m]\\ \mathbf{S}^{(2)}[l] & \mathbf{S}^{*(2)}[l_m]\\ \hline \vdots & \vdots \\ \hline \mathbf{S}^{(M_l)}[l] & \mathbf{S}^{*(M_l)}[l_m]\end{bmatrix}$. Here superscript (i) represents the training symbol number. Equation (5.1) shows that there are M_l equations in 2 unknowns. Hence to estimate $\widetilde{\mathbf{D}}_{tot-}[l]$, we need a LT sequence length $M_l \geq 2$. A longer training sequence will provide improved estimates due to a better noise averaging.

We now develop a decoupled FEQ solution for transmitter and receiver IQ imbalance separately in section 5.2.1-5.2.2. In section 5.2.3, the decoupled FEQ

solution is also extended for a system impaired with both transmitter and receiver IQ imbalance.

5.2.1 Decoupled Transmitter IQ Imbalance Compensation

In the case of only transmitter IQ imbalance ($\mathbf{G}_{ra}[l] = 1, \mathbf{G}_{rb}[l] = 0$), equation (3.10) can be written for the received symbol $\mathbf{Z}[l]$ and the mirror of its complex conjugated symbol $\mathbf{Z}^*[l_m]$ as follows:

$$\underbrace{\begin{bmatrix}\mathbf{Z}[l]\\ \mathbf{Z}^*[l_m]\end{bmatrix}}_{\mathbf{Z}_{tot}[l]} = \underbrace{\begin{bmatrix}\mathbf{B}[l] & \mathbf{B}[l]\mathbf{Q}_t[l]\\ \mathbf{B}^*[l_m]\mathbf{Q}_t^*[l_m] & \mathbf{B}^*[l_m]\end{bmatrix}}_{\mathbf{D}_{tot}[l]}\underbrace{\begin{bmatrix}\mathbf{S}[l]\\ \mathbf{S}^*[l_m]\end{bmatrix}}_{\mathbf{S}_{tot}[l]} + \begin{bmatrix}\mathbf{N}[l]\\ \mathbf{N}^*[l_m]\end{bmatrix} \tag{5.2}$$

where $\mathbf{Q}_t[l] = \frac{\mathbf{G}_{tb}[l]}{\mathbf{G}_{ta}[l]}$ is the transmitter IQ imbalance gain parameter and $\mathbf{B}[l] = \mathbf{G}_{ta}[l]\mathbf{C}[l]$ is the composite channel. The $\mathbf{D}_{tot}[l]$ matrix can now be factorized as follows:

$$\mathbf{D}_{tot}[l] = \begin{bmatrix}\mathbf{D}_a[l] & \mathbf{D}_b[l]\\ \mathbf{D}_b^*[l_m] & \mathbf{D}_a^*[l_m]\end{bmatrix} = \underbrace{\begin{bmatrix}\mathbf{B}[l] & 0\\ 0 & \mathbf{B}^*[l_m]\end{bmatrix}}_{\mathbf{B}_{tot}[l]}\underbrace{\begin{bmatrix}1 & \mathbf{Q}_t[l]\\ \mathbf{Q}_t^*[l_m] & 1\end{bmatrix}}_{\mathbf{Q}_{t_{tot}}[l]} \tag{5.3}$$

Equation (5.3) shows that $\mathbf{Q}_{t_{tot}}[l]$ is independent of the channel distortion and it contains only the transmitter IQ imbalance terms. The channel characteristics are contained entirely in the $\mathbf{B}_{tot}[l]$ matrix. Thus the transmitter IQ imbalance and channel distortion have been decoupled.

The estimates $\widetilde{\mathbf{Q}}_t[l]$ and $\widetilde{\mathbf{B}}[l]$ of $\mathbf{Q}_t[l]$ and $\mathbf{B}[l]$ can be directly obtained from $\widetilde{\mathbf{D}}_{tot-}[l]$ (equation (5.1)) as:

$$\begin{aligned}\widetilde{\mathbf{Q}}_t[l] &= \frac{\widetilde{\mathbf{D}}_b[l]}{\widetilde{\mathbf{D}}_a[l]}\\ \widetilde{\mathbf{B}}[l] &= \widetilde{\mathbf{D}}_a[l]\end{aligned} \tag{5.4}$$

In the case of FI transmitter IQ imbalance, $\widetilde{\mathbf{Q}}_t[l]$ can be averaged over all the subcarriers to obtain an improved estimate $\widetilde{Q}_t = \frac{1}{N}\sum_{l=1}^{N}\widetilde{\mathbf{Q}}_t[l]$. Once $\widetilde{\mathbf{Q}}_t[l]$ is available, variations in channel can be tracked by re-estimating $\widetilde{\mathbf{B}}[l]$ with:

$$\widetilde{\mathbf{B}}[l] = \frac{\mathbf{Z}[l]}{\mathbf{S}[l] + \widetilde{\mathbf{Q}}_t[l]\mathbf{S}^*[l_m]} \tag{5.5}$$

Only one LT symbol is required to re-estimate $\widetilde{\mathbf{B}}[l]$. A longer training sequence will provide improved estimates.

In the compensation phase, the $\widetilde{\mathbf{D}}_{tot}[l]$ can once again be formulated from the new composite channel estimate $\widetilde{\mathbf{B}}[l]$ and the transmitter IQ imbalance gain parameter $\widetilde{\mathbf{Q}}_t[l]$. We can then obtain the estimate of the transmitted OFDM symbol based on equation (3.11). We will refer to the proposed decoupled based frequency domain estimation/compensation scheme as **D-FEQ**.

Compensation of Transmitter IQ Imbalance with Pre-Distortion of Transmitted Symbols

The compensation scheme based on equation (3.11) performs the compensation of transmitter IQ imbalance at the receiver. An alternative solution is to compensate for the transmitter IQ imbalance already at the transmitter. This can be obtained by distorting the transmitted symbol before the IDFT operation such that the resulting transmitted symbol is free of any transmitter IQ imbalance. A pre-distortion system requires a feedback mechanism between the receiver and the transmitter, as will be explained next.

In the pre-distortion scheme, the new OFDM symbol $\mathbf{S_n}$ is defined as $\mathbf{S_n} = \mathbf{S} - \widetilde{\mathbf{Q}}_t.\mathbf{S}^*_m$ where $\widetilde{\mathbf{Q}}_t$ is the $\mathbf{Q}_t$ estimate fed back from the receiver. In matrix form, $\mathbf{S_n}[l]$ and $\mathbf{S^*_n}[l_m]$ can be written as:

$$\begin{bmatrix} \mathbf{S_n}[l] \\ \mathbf{S^*_n}[l_m] \end{bmatrix} = \begin{bmatrix} 1 & -\widetilde{\mathbf{Q}}_t[l] \\ -\widetilde{\mathbf{Q}}^*_t[l_m] & 1 \end{bmatrix} \begin{bmatrix} \mathbf{S}[l] \\ \mathbf{S}^*[l_m] \end{bmatrix} \tag{5.6}$$

Now equation (5.2) is rewritten as:

$$\begin{aligned} \underbrace{\begin{bmatrix} \mathbf{Z}[l] \\ \mathbf{Z}^*[l_m] \end{bmatrix}}_{\mathbf{Z}_{tot}[l]} &= \begin{bmatrix} \mathbf{B}[l] & 0 \\ 0 & \mathbf{B}^*[l_m] \end{bmatrix} \begin{bmatrix} 1 & \mathbf{Q}_t[l] \\ \mathbf{Q}^*_t[l_m] & 1 \end{bmatrix} \begin{bmatrix} \mathbf{S_n}[l] \\ \mathbf{S^*_n}[l_m] \end{bmatrix} + \begin{bmatrix} \mathbf{N}[l] \\ \mathbf{N}^*[l_m] \end{bmatrix} \\ &= \begin{bmatrix} \mathbf{B}[l] & 0 \\ 0 & \mathbf{B}^*[l_m] \end{bmatrix} \underbrace{\begin{bmatrix} (1 - \mathbf{Q}_t[l]\widetilde{\mathbf{Q}}^*_t[l_m]) & (\mathbf{Q}_t[l] - \widetilde{\mathbf{Q}}_t[l]) \\ (\mathbf{Q}^*_t[l_m] - \widetilde{\mathbf{Q}}^*_t[l_m]) & (1 - \mathbf{Q}^*_t[l_m]\widetilde{\mathbf{Q}}_t[l]) \end{bmatrix}}_{\mathbf{Q}_{t_{diff_tot}}[l]} \begin{bmatrix} \mathbf{S}[l] \\ \mathbf{S}^*[l_m] \end{bmatrix} \\ &\quad + \begin{bmatrix} \mathbf{N}[l] \\ \mathbf{N}^*[l_m] \end{bmatrix} \end{aligned}$$

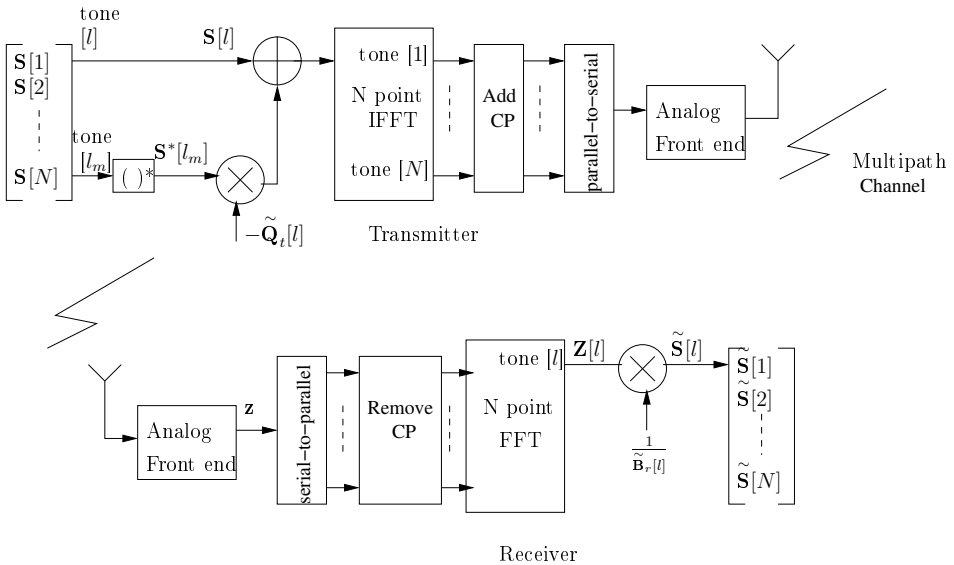

Figure 5.1: Pre-distortion of transmitted symbols with D-FEQ scheme for the compensation of transmitter IQ imbalance and channel distortion

(5.7)

Under ideal conditions $\widetilde{\mathbf{Q}}_t[l] = \mathbf{Q}_t[l]$ and $\widetilde{\mathbf{Q}}_t[l_m] = \mathbf{Q}_t[l_m]$, the matrix $\mathbf{Q}_{t_{diff_tot}}[l]$ is diagonalized and the remaining term $(1-\mathbf{Q}_t[l]\widetilde{\mathbf{Q}}_t^*[l_m])$ can be merged with $\mathbf{B}[l]$. The received symbol $\mathbf{Z}_{tot}[l]$ is then considered to be free of any transmitter IQ imbalance. As the pre-distortion is applied before the noise is added to the symbol, the transmitter IQ imbalance compensation is free from any noise enhancement.

We can now track the variation in channel based on:

$$\widetilde{\mathbf{B}}[l] = \frac{\mathbf{Z}[l]}{(1 - \widetilde{\mathbf{Q}}_t[l]\widetilde{\mathbf{Q}}_t^*[l_m])\mathbf{S}[l]} \tag{5.8}$$

The estimate of OFDM symbols is then obtained as:

$$\widetilde{\mathbf{S}}_{tot}[l] = \widetilde{\mathbf{B}}_{r_tot}[l]\mathbf{B}_{tot}[l]\mathbf{Q}_{t_{tot}}[l]\widetilde{\mathbf{Q}}_{t_{inv_tot}}[l]\mathbf{S}_{tot}[l] \tag{5.9}$$

where $\widetilde{\mathbf{Q}}_{t_{inv_tot}[l]} = \begin{bmatrix} 1 & -\widetilde{\mathbf{Q}}_t[l] \\ -\widetilde{\mathbf{Q}}_t^*[l_m] & 1 \end{bmatrix}$ and $\widetilde{\mathbf{B}}_{r_tot}[l] = \begin{bmatrix} \frac{1}{\widetilde{\mathbf{B}}_r[l]} & 0 \\ 0 & \frac{1}{\widetilde{\mathbf{B}}_r^*[l_m]} \end{bmatrix}$. Here the term $\widetilde{\mathbf{B}}_r[l] = \widetilde{\mathbf{B}}[l](1 - \widetilde{\mathbf{Q}}_t[l]\widetilde{\mathbf{Q}}_t^*[l_m])$. A D-FEQ scheme based on pre-distortion transmitter IQ imbalance compensation is shown in **Figure 5.1**.

5.2.2 Decoupled Receiver IQ Imbalance Compensation

Similarly, in the case of only receiver IQ imbalance ($\mathbf{G}_{ta}[l] = 1, \mathbf{G}_{tb}[l] = 0$), equation (3.10) can be written for the received symbol $\mathbf{Z}[l]$ and the mirror of its complex conjugated symbol $\mathbf{Z}^*[l_m]$ as follows:

$$\begin{bmatrix} \mathbf{Z}[l] \\ \mathbf{Z}^*[l_m] \end{bmatrix} = \underbrace{\begin{bmatrix} \mathbf{B}[l] & \mathbf{Q}_r[l]\mathbf{B}^*[l_m] \\ \mathbf{Q}_r^*[l_m]\mathbf{B}[l] & \mathbf{B}^*[l_m] \end{bmatrix}}_{\mathbf{D}_{tot}[l]} \begin{bmatrix} \mathbf{S}[l] \\ \mathbf{S}^*[l_m] \end{bmatrix} + \begin{bmatrix} \mathbf{N}_c[l] \\ \mathbf{N}_c^*[l_m] \end{bmatrix} \tag{5.10}$$

where $\mathbf{Q}_r[l] = \frac{\mathbf{G}_{rb}[l]}{\mathbf{G}_{ra}^*[l_m]}$ is the receiver IQ imbalance gain parameter and $\mathbf{B}[l] = \mathbf{G}_{ra}[l]\mathbf{C}[l]$ is now the composite channel. $\mathbf{D}_{tot}[l]$ is now factorized as:

$$\mathbf{D}_{tot}[l] = \underbrace{\begin{bmatrix} 1 & \mathbf{Q}_r[l] \\ \mathbf{Q}_r^*[l_m] & 1 \end{bmatrix}}_{\mathbf{Q}_{r_{tot}}[l]} \underbrace{\begin{bmatrix} \mathbf{B}[l] & 0 \\ 0 & \mathbf{B}^*[l_m] \end{bmatrix}}_{\mathbf{B}_{tot}[l]} \tag{5.11}$$

where the estimates $\widetilde{\mathbf{Q}}_r[l]$ and $\widetilde{\mathbf{B}}[l]$ of $\mathbf{Q}_r[l]$ and $\mathbf{B}[l]$ can be obtained from the $\widetilde{\mathbf{D}}_{tot-}[l]$ coefficients (equation (5.1)) as:

$$\begin{aligned} \widetilde{\mathbf{Q}}_r[l] &= \frac{\widetilde{\mathbf{D}}_b[l]}{\widetilde{\mathbf{D}}_a^*[l_m]} \\ \widetilde{\mathbf{B}}[l] &= \widetilde{\mathbf{D}}_a[l] \end{aligned} \tag{5.12}$$

In the case of FI receiver IQ imbalance, $\widetilde{\mathbf{Q}}_r[l]$ can be averaged over all the subcarriers to obtain an improved estimate $\widetilde{Q}_r = \frac{1}{N}\sum_{l=1}^{N} \widetilde{\mathbf{Q}}_r[l]$. The variations in channel can be tracked by re-estimating $\widetilde{\mathbf{B}}[l]$ with only one LT symbol given as:

$$\widetilde{\mathbf{B}}[l] = \frac{(\mathbf{Z}[l] - \widetilde{\mathbf{Q}}_r[l]\mathbf{Z}^*[l_m])}{(1 - \widetilde{\mathbf{Q}}_r[l]\widetilde{\mathbf{Q}}_r^*[l_m])\mathbf{S}[l]} \tag{5.13}$$

We can once again formulate $\widetilde{\mathbf{D}}_{tot}[l]$ from the new composite channel estimate $\widetilde{\mathbf{B}}[l]$, and the receiver IQ imbalance gain parameter $\widetilde{\mathbf{Q}}_r[l]$. The estimate of the transmitted OFDM symbol $\widetilde{\mathbf{S}}[l]$ is then obtained based on equation (3.11).

5.2.3 Decoupled Transmitter and Receiver IQ Imbalance Compensation

The D-FEQ scheme can also be extended for the more general case with both transmitter and receiver IQ imbalance. In this case, the $\mathbf{D}_{tot}[l]$ can be decoupled as follows:

$$\underbrace{\begin{bmatrix}\mathbf{D}_a[l] & \mathbf{D}_b[l]\\ \mathbf{D}_b^*[l_m] & \mathbf{D}_a^*[l_m]\end{bmatrix}}_{\mathbf{D}_{tot}[l]} = \underbrace{\begin{bmatrix}1 & \mathbf{Q}_r[l]\\ \mathbf{Q}_r^*[l_m] & 1\end{bmatrix}}_{\mathbf{Q}_{r_{tot}}[l]}\underbrace{\begin{bmatrix}\mathbf{B}[l] & 0\\ 0 & \mathbf{B}^*[l_m]\end{bmatrix}}_{\mathbf{B}_{tot}[l]}\underbrace{\begin{bmatrix}1 & \mathbf{Q}_t[l]\\ \mathbf{Q}_t^*[l_m] & 1\end{bmatrix}}_{\mathbf{Q}_{t_{tot}}[l]} \quad (5.14)$$

where $\mathbf{B}[l] = \mathbf{G}_{ra}[l]\mathbf{G}_{ta}[l]\mathbf{C}[l]$ is the composite channel, $\mathbf{Q}_t[l] = \frac{\mathbf{G}_{tb}[l]}{\mathbf{G}_{ta}[l]}$ is the transmitter IQ imbalance gain parameter and $\mathbf{Q}_r[l] = \frac{\mathbf{G}_{rb}[l]}{\mathbf{G}^*_{ra}[l_m]}$ is the receiver IQ imbalance gain parameter. The $\mathbf{D}_{tot}[l]$ coefficients $\mathbf{D}_a[l]$ and $\mathbf{D}_b[l]$ can then be re-written as:

$$\begin{aligned}\mathbf{D}_a[l] &= \mathbf{B}[l] + \mathbf{Q}_r[l]\mathbf{Q}_t^*[l_m]\mathbf{B}^*[l_m]\\ \mathbf{D}_b[l] &= \mathbf{Q}_t[l]\mathbf{B}[l] + \mathbf{Q}_r[l]\mathbf{B}^*[l_m]\end{aligned} \quad (5.15)$$

In the presence of both the transmitter and receiver IQ imbalance, it is not possible to obtain $\widetilde{\mathbf{Q}}_t[l], \widetilde{\mathbf{Q}}_r[l]$ and $\widetilde{\mathbf{B}}[l]$ estimates directly from the $\widetilde{\mathbf{D}}_{tot-}[l]$ matrix (equation (5.1)). In order to obtain these estimates we first make an approximation, namely that the second order term $\mathbf{Q}_r[l]\mathbf{Q}_t^*[l_m] = 0$ in $\mathbf{D}_a[l]$. This approximation is based on the fact that $\mathbf{G}_{ta}[l] >> \mathbf{G}_{tb}[l]$ and $\mathbf{G}^*_{ra}[l_m] >> \mathbf{G}_{rb}[l]$ in practice. We can then estimate the channel $\widetilde{\mathbf{B}}[l] \backsimeq \widetilde{\mathbf{D}}_a[l]$ which is in line with (5.4) and (5.12). Equation (5.15) can now be written for $\widetilde{\mathbf{D}}_b[l]$ as follows:

$$\widetilde{\mathbf{D}}_b[l] = \widetilde{\mathbf{Q}}_t[l]\widetilde{\mathbf{D}}_a[l] + \widetilde{\mathbf{Q}}_r[l]\widetilde{\mathbf{D}}_a^*[l_m] \quad (5.16)$$

In the case of FI transmitter and receiver IQ imbalance, the estimates can be straightforwardly obtained from (5.16) as:

$$\begin{bmatrix}\widetilde{Q}_t\\ \widetilde{Q}_r\end{bmatrix} = \begin{bmatrix}\widetilde{\mathbf{D}}_a[2] & \widetilde{\mathbf{D}}_a^*[N]\\ \vdots & \vdots\\ \widetilde{\mathbf{D}}_a[l] & \widetilde{\mathbf{D}}_a^*[l_m]\\ \vdots & \vdots\\ \widetilde{\mathbf{D}}_a[N] & \widetilde{\mathbf{D}}_a^*[2]\end{bmatrix}^{\dagger}\begin{bmatrix}\widetilde{\mathbf{D}}_b[2]\\ \vdots\\ \widetilde{\mathbf{D}}_b[l]\\ \vdots\\ \widetilde{\mathbf{D}}_b[N]\end{bmatrix} \quad (5.17)$$

Here the multipath diversity of the channel $\mathbf{B}[l]$, and hence $\widetilde{\mathbf{D}}_a[l]$, allows us to estimate $\widetilde{Q}_t$ and $\widetilde{Q}_r$ respectively.

In the case of FS transmitter and receiver IQ imbalance, the estimation of the gain parameters is to be performed for each subcarrier individually. In order to obtain these estimates we need at least two independent realizations of the channel i.e. $\mathbf{B}^{(1)}[l]$ and $\mathbf{B}^{(2)}[l]$, and hence $\widetilde{\mathbf{D}}_a^{(1)}[l]$,$\widetilde{\mathbf{D}}_a^{(2)}[l]$ and $\widetilde{\mathbf{D}}_b^{(1)}[l]$ $\widetilde{\mathbf{D}}_b^{(2)}[l]$ respectively. The estimates $\widetilde{\mathbf{Q}}_t[l]$ and $\widetilde{\mathbf{Q}}_r[l]$ can then be obtained from (5.16) as:

$$\begin{bmatrix} \widetilde{\mathbf{Q}}_t[l] \\ \widetilde{\mathbf{Q}}_r[l] \end{bmatrix} = \begin{bmatrix} \widetilde{\mathbf{D}}_a^{(1)}[l] & \widetilde{\mathbf{D}}_a^{*(1)}[l_m] \\ \widetilde{\mathbf{D}}_a^{(2)}[l] & \widetilde{\mathbf{D}}_a^{*(2)}[l_m] \end{bmatrix}^{-1} \begin{bmatrix} \widetilde{\mathbf{D}}_b^{(1)}[l] \\ \widetilde{\mathbf{D}}_b^{(2)}[l] \end{bmatrix} \tag{5.18}$$

For guaranteed invertibility we should have $\widetilde{\mathbf{D}}_a^{(2)}[l] \neq \widetilde{\mathbf{D}}_a^{(1)}[l]$ and/or $\widetilde{\mathbf{D}}_a^{*(2)}[l_m] \neq \widetilde{\mathbf{D}}_a^{*(1)}[l_m]$. If the channel does not vary for a particular subcarrier or its mirror subcarrier, then the joint compensation scheme should be performed on the subcarrier pair as in equation (3.12).

Equation (5.18) provides good estimates as long as $\mathbf{Q}_r[l]\mathbf{Q}_t^*[l_m] \backsimeq 0$, i.e both the transmitter and receiver IQ imbalance gain parameters are relatively small. The results are optimal if either $\mathbf{Q}_r[l] = 0$ (i.e. no receiver IQ imbalance) or $\mathbf{Q}_t[l] = 0$ (i.e. no transmitter IQ imbalance). However, for large transmitter and receiver IQ imbalance values, the estimates obtained from equation (5.18) may not be accurate enough, resulting in only a partial compensation of the transmitter and receiver IQ imbalance. The same holds true for the estimates of the FI transmitter and receiver IQ imbalance gain parameters obtained from equation (5.17). From now on we will not further consider the FI case as the description of the FS case will also apply to the FI case.

If we compensate for the $\mathbf{D}_{tot}[l]$ matrix (removing the superscripts corresponding to different channel realizations), with the raw estimates of the receiver IQ imbalance gain parameter, the resulting matrix $\mathbf{D}_{1_{tot}}[l]$ is given as:

$$\underbrace{\begin{bmatrix} 1 & -\widetilde{\mathbf{Q}}_r[l] \\ -\widetilde{\mathbf{Q}}_r^*[l_m] & 1 \end{bmatrix}}_{\mathbf{D}_{1_{tot}}[l]} \mathbf{D}_{tot}[l] = \begin{bmatrix} 1 - \widetilde{\mathbf{Q}}_r[l]\mathbf{Q}_r^*[l_m] & \mathbf{Q}_r[l] - \widetilde{\mathbf{Q}}_r[l] \\ \mathbf{Q}_r^*[l_m] - \widetilde{\mathbf{Q}}_r^*[l_m] & 1 - \widetilde{\mathbf{Q}}_r^*[l_m]\mathbf{Q}_r[l] \end{bmatrix} \mathbf{B}_{tot}[l]\mathbf{Q}_{t_{tot}}[l] \tag{5.19}$$

Equation (5.19) can be rewritten as:

$$\begin{aligned}\mathbf{D}_{1_{tot}}[l] &= \begin{bmatrix}\mathbf{D}_{a1}[l] & \mathbf{D}_{b1}[l]\\ \mathbf{D}^*_{b1}[l_m] & \mathbf{D}^*_{a1}[l_m]\end{bmatrix}\\ &= \underbrace{\begin{bmatrix}1 & \mathbf{Q}_{r1}[l]\\ \mathbf{Q}^*_{r1}[l_m] & 1\end{bmatrix}}_{\mathbf{Q}_{r1_{tot}}[l]}\underbrace{\begin{bmatrix}\mathbf{B}_1[l] & 0\\ 0 & \mathbf{B}^*_1[l_m]\end{bmatrix}}_{\mathbf{B}_{1_{tot}}[l]}\underbrace{\begin{bmatrix}1 & \mathbf{Q}_{t1}[l]\\ \mathbf{Q}^*_{t1}[l_m] & 1\end{bmatrix}}_{\mathbf{Q}_{t1_{tot}}[l]}\end{aligned} \tag{5.20}$$

which is similar to (5.14), and where $\mathbf{B}_1[l] = \mathbf{B}[l](1 - \widetilde{\mathbf{Q}}_r[l]\mathbf{Q}^*_r[l_m])$, $\mathbf{Q}_{t1}[l] = \mathbf{Q}_t[l]$, $\mathbf{Q}_{r1}[l] = \frac{\mathbf{Q}_r[l]-\widetilde{\mathbf{Q}}_r[l]}{1-\widetilde{\mathbf{Q}}^*_r[l_m]\mathbf{Q}_r[l]}$ and $\mathbf{Q}_{r1}[l] << \mathbf{Q}_r[l]$. The $\mathbf{D}_{1_{tot}}[l]$ coefficients ($\mathbf{D}_{a1}[l]$ and $\mathbf{D}_{b1}[l]$) are now written as:

$$\begin{aligned}\mathbf{D}_{a1}[l] &= \mathbf{B}_1[l] + \mathbf{Q}_{r1}[l]\mathbf{Q}^*_{t1}[l_m]\mathbf{B}^*_1[l_m]\\ \mathbf{D}_{b1}[l] &= \mathbf{Q}_{t1}[l]\mathbf{B}_1[l] + \mathbf{Q}_{r1}[l]\mathbf{B}^*_1[l_m]\end{aligned} \tag{5.21}$$

which is similar to (5.15). Now the estimates $\widetilde{\mathbf{D}}_{a1}[l]$ and $\widetilde{\mathbf{D}}_{b1}[l]$ of $\mathbf{D}_{a1}[l]$ and $\mathbf{D}_{b1}[l]$, can be directly obtained from equation (5.19), with $\mathbf{D}_{tot}[l]$ replaced by the estimate $\widetilde{\mathbf{D}}_{tot}[l]$, as follows:

$$\begin{bmatrix}\widetilde{\mathbf{D}}_{a1}[l] & \widetilde{\mathbf{D}}_{b1}[l]\\ \widetilde{\mathbf{D}}^*_{b1}[l_m] & \widetilde{\mathbf{D}}^*_{a1}[l_m]\end{bmatrix} = \underbrace{\begin{bmatrix}1 & -\widetilde{\mathbf{Q}}_r[l]\\ -\widetilde{\mathbf{Q}}^*_r[l_m] & 1\end{bmatrix}}_{\widetilde{\mathbf{D}}_{1_{tot}}[l]}\widetilde{\mathbf{D}}_{tot}[l] \tag{5.22}$$

Finally $\widetilde{\mathbf{Q}}_{r1}[l]$ and an improved estimate $\widetilde{\mathbf{Q}}_{t1}[l]$ of $\mathbf{Q}_t[l]$ are obtained based on an expression similar to equation (5.18), with $\widetilde{\mathbf{D}}^{(1)}_a[l], \widetilde{\mathbf{D}}^{(2)}_a[l]$ and $\widetilde{\mathbf{D}}^{(1)}_b[l], \widetilde{\mathbf{D}}^{(2)}_b[l]$ replaced by $\widetilde{\mathbf{D}}^{(1)}_{a1}[l], \widetilde{\mathbf{D}}^{(2)}_{a1}[l]$ and $\widetilde{\mathbf{D}}^{(1)}_{b1}[l], \widetilde{\mathbf{D}}^{(2)}_{b1}[l]$.

Equations (5.18)-(5.22) may be repeated a number of times until $\widetilde{\mathbf{Q}}_{ri}[l] \simeq 0$, which corresponds to $\widetilde{\mathbf{D}}_{ai}[l] \simeq \widetilde{\mathbf{B}}_i[l]$, where i represents the iteration number. After performing a sufficient number of iterations, the fine estimate of receiver IQ imbalance $\widetilde{\mathbf{Q}}_{rf}[l]$ can be derived from $\widetilde{\mathbf{Q}}_{ri}[l]$ as:

$$\widetilde{\mathbf{Q}}_{rf}[l] = \frac{\mathbf{Q}_{r1}[l] + \widetilde{\mathbf{Q}}_r[l]}{1 + \mathbf{Q}_{r1}[l]\widetilde{\mathbf{Q}}^*_r[l_m]}$$

where $\mathbf{Q}_{r1}[l] = \frac{\mathbf{Q}_{r2}[l]+\widetilde{\mathbf{Q}}_{r1}[l]}{1+\mathbf{Q}_{r2}[l]\widetilde{\mathbf{Q}}^*_{r1}[l_m]}$ and so on. If only two iterations are considered, for instance, then $\mathbf{Q}_{r2}[l]$ is considered to be zero and therefore $\mathbf{Q}_{r1}[l] = \widetilde{\mathbf{Q}}_{r1}[l]$

and $\widetilde{\mathbf{Q}}_{rf}[l] = \frac{\widetilde{\mathbf{Q}}_{r1}[l]+\widetilde{\mathbf{Q}}_{r}[l]}{1+\widetilde{\mathbf{Q}}_{r1}[l]\widetilde{\mathbf{Q}}_{r}^{*}[l_m]}$. The fine estimate of the transmitter IQ imbalance $\widetilde{\mathbf{Q}}_{tf}[l]$ is the estimate $\widetilde{\mathbf{Q}}_{ti}[l]$ obtained from the last iteration. Finally, the channel estimate $\widetilde{\mathbf{B}}[l]$ is derived based on equation (5.15) as:

$$\widetilde{\mathbf{B}}[l] = \frac{\widetilde{\mathbf{D}}_a[l] - \widetilde{\mathbf{Q}}_{tf}^{*}[l_m]\widetilde{\mathbf{D}}_b[l]}{(1 - \widetilde{\mathbf{Q}}_{tf}^{*}[l_m]\widetilde{\mathbf{Q}}_{tf}[l])} \tag{5.23}$$

A complete D-FEQ algorithm description is provided in **Table 5.1**.

From now, if the channel distortion is time-varying, only one training symbol is needed to re-estimate the composite channel, which can then be tracked based on:

$$\widetilde{\mathbf{B}}[l] = \frac{(\mathbf{Z}[l] - \widetilde{\mathbf{Q}}_{rf}[l]\mathbf{Z}^{*}[l_m])}{(1 - \widetilde{\mathbf{Q}}_{rf}[l]\widetilde{\mathbf{Q}}_{rf}^{*}[l_m])(\mathbf{S}[l] + \widetilde{\mathbf{Q}}_{tf}[l]\mathbf{S}^{*}[l_m])} \tag{5.25}$$

We can once again formulate $\widetilde{\mathbf{D}}_{tot}[l]$ from the new composite channel estimate $\widetilde{\mathbf{B}}[l]$, the transmitter IQ imbalance gain parameter $\widetilde{\mathbf{Q}}_{tf}[l]$ and the receiver IQ imbalance gain parameter $\widetilde{\mathbf{Q}}_{rf}[l]$ for the estimation of the transmitted OFDM symbol $\widetilde{\mathbf{S}}[l]$ based on equation (3.11).

Compensation of Transmitter/Receiver IQ Imbalance with Pre-Distortion of Transmitted Symbols

In the case of pre-distortion, we can track the variation in channel as:

$$\widetilde{\mathbf{B}}[l] = \frac{(\mathbf{Z}[l] - \widetilde{\mathbf{Q}}_{rf}[l]\mathbf{Z}^{*}[l_m])}{(1 - \widetilde{\mathbf{Q}}_{rf}[l]\widetilde{\mathbf{Q}}_{rf}^{*}[l_m])(1 - \widetilde{\mathbf{Q}}_{tf}[l]\widetilde{\mathbf{Q}}_{tf}^{*}[l_m])\mathbf{S}[l]} \tag{5.26}$$

The estimate of the OFDM symbols is then obtained as:

$$\widetilde{\mathbf{S}}_{tot}[l] = \widetilde{\mathbf{B}}_{r_tot}[l]\widetilde{\mathbf{Q}}_{r_{inv_tot}}[l]\mathbf{Q}_{r_{tot}}[l]\mathbf{B}_{tot}[l]\mathbf{Q}_{t_{tot}}[l]\widetilde{\mathbf{Q}}_{t_{inv_tot}}[l]\mathbf{S}_{tot}[l] \tag{5.27}$$

where $\widetilde{\mathbf{Q}}_{t_{inv_tot}[l]} = \begin{bmatrix} 1 & -\widetilde{\mathbf{Q}}_{tf}[l] \\ -\widetilde{\mathbf{Q}}_{tf}^{*}[l_m] & 1 \end{bmatrix}$, $\widetilde{\mathbf{Q}}_{r_{inv_tot}[l]} = \begin{bmatrix} 1 & -\widetilde{\mathbf{Q}}_{rf}[l] \\ -\widetilde{\mathbf{Q}}_{rf}^{*}[l_m] & 1 \end{bmatrix}$ and $\widetilde{\mathbf{B}}_{r_tot}[l] = \begin{bmatrix} \frac{1}{\widetilde{\mathbf{B}}_r[l]} & 0 \\ 0 & \frac{1}{\widetilde{\mathbf{B}}_r^{*}[l_m]} \end{bmatrix}$. Here the term $\widetilde{\mathbf{B}}_r[l] = \widetilde{\mathbf{B}}[l](1-\widetilde{\mathbf{Q}}_{rf}[l]\widetilde{\mathbf{Q}}_{rf}^{*}[l_m])(1-\widetilde{\mathbf{Q}}_{tf}[l]\widetilde{\mathbf{Q}}_{tf}^{*}[l_m])$.

1. Make an approximation, consider the second order term $\mathbf{Q}_r[l]\mathbf{Q}_t^*[l_m] = 0$ in $\mathbf{D}_a[l] = \mathbf{B}[l] + \mathbf{Q}_r[l]\mathbf{Q}_t^*[l_m]\mathbf{B}^*[l_m]$.
2. - In the case of FI transmitter and receiver IQ imbalance, the raw estimates $\widetilde{Q}_r$ and $\widetilde{Q}_t$ are directly derived from $\widetilde{\mathbf{D}}_b[l] = \widetilde{Q}_t[l]\widetilde{\mathbf{D}}_a[l] + \widetilde{Q}_r[l]\widetilde{\mathbf{D}}_a^*[l_m]$.
   - In the case of FS transmitter and receiver IQ imbalance, the raw estimates $\widetilde{\mathbf{Q}}_r[l]$ and $\widetilde{\mathbf{Q}}_t[l]$ are derived from atleast two independent realizations $\widetilde{\mathbf{D}}_a^{(1)}[l]$, $\widetilde{\mathbf{D}}_a^{(2)}[l]$ and $\widetilde{\mathbf{D}}_b^{(1)}[l]$, $\widetilde{\mathbf{D}}_b^{(2)}[l]$ in the equation $\widetilde{\mathbf{D}}_b^{(p)}[l] = \widetilde{\mathbf{Q}}_t[l]\widetilde{\mathbf{D}}_a^{(p)}[l] + \widetilde{\mathbf{Q}}_r[l]\widetilde{\mathbf{D}}_a^{*(p)}[l_m]$, where p denotes a different realization.
3. Compensate $\widetilde{\mathbf{D}}_{tot}[l]$ with the raw estimate of receiver IQ imbalance parameter $\widetilde{\mathbf{Q}}_r[l]$ to obtain the matrix $\widetilde{\mathbf{D}}_{i_{tot}}[l]$ with coefficients $\widetilde{\mathbf{D}}_{ai}[l]$ and $\widetilde{\mathbf{D}}_{bi}[l]$, where i is the iteration number.
4. Obtain $\widetilde{\mathbf{Q}}_{ri}[l]$ and $\widetilde{\mathbf{Q}}_{ti}[l]$ by substituting coefficients $\widetilde{\mathbf{D}}_{ai}[l]$ and $\widetilde{\mathbf{D}}_{bi}[l]$ in step 2.
5. Repeat steps 2-4, until $\widetilde{\mathbf{Q}}_{ri}[l] = 0$.
6. Fine estimate of receiver IQ imbalance is given as:

$$\widetilde{\mathbf{Q}}_{rf}[l] = \frac{\mathbf{Q}_{r1}[l] + \widetilde{\mathbf{Q}}_r[l]}{1 + \mathbf{Q}_{r1}[l]\widetilde{\mathbf{Q}}_r^*[l_m]}$$

   where $\mathbf{Q}_{r1}[l] = \frac{\mathbf{Q}_{r2}[l] + \widetilde{\mathbf{Q}}_{r1}[l]}{1 + \mathbf{Q}_{r2}[l]\widetilde{\mathbf{Q}}_{r1}^*[l_m]}$ and so on.
7. Fine estimate of transmitter IQ imbalance $\widetilde{\mathbf{Q}}_{tf}[l]$ is the estimate $\widetilde{\mathbf{Q}}_{ti}[l]$ obtained from the last iteration.
8. Obtain the channel estimate:

$$\widetilde{\mathbf{B}}[l] = \frac{\widetilde{\mathbf{D}}_a[l] - \widetilde{\mathbf{Q}}_{tf}^*[l_m]\widetilde{\mathbf{D}}_b[l]}{(1 - \widetilde{\mathbf{Q}}_{tf}^*[l_m]\widetilde{\mathbf{Q}}_{tf}[l])} \tag{5.24}$$

Table 5.1: D-FEQ algorithm for the estimation of transmitter and receiver IQ imbalance parameters

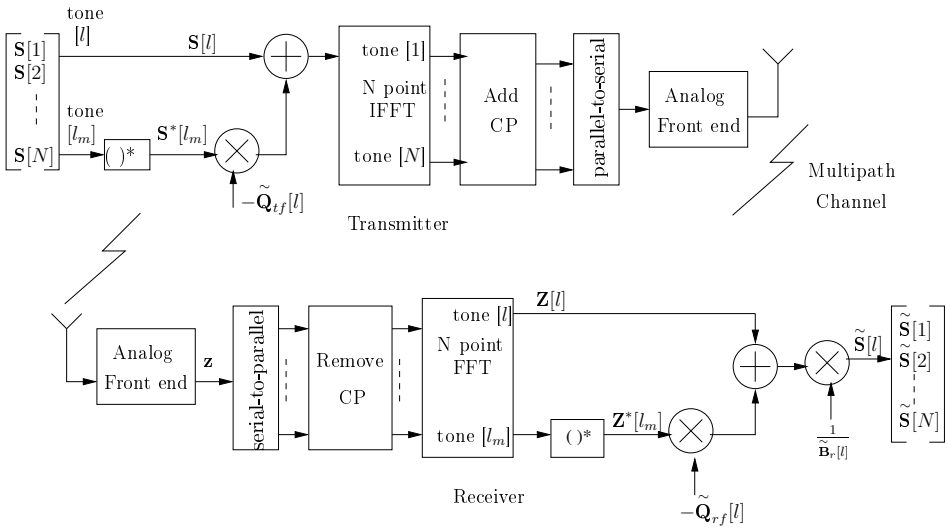

Figure 5.2: Pre-distortion of transmitted symbols with D-FEQ scheme for the compensation of transmitter/receiver IQ imbalance and channel distortion

The D-FEQ scheme with pre-distortion of transmitted symbols for the compensation of transmitter and receiver IQ imbalance is shown in **Figure 5.2**.

Based on equation (5.27), we can also derive the improvement in IRR after the compensation of only transmitter and receiver IQ imbalance, and without the compensation of channel distortion in the received symbol. In this case the received symbol $\mathbf{Z}_{comp}[l]$ is given as:

$$\begin{aligned}\mathbf{Z}_{comp}[l] &= \begin{bmatrix}1 & -\widetilde{\mathbf{Q}}_r[l]\end{bmatrix} \mathbf{Q}_{r_{tot}}[l]\mathbf{B}_{tot}[l]\mathbf{Q}_{t_{tot}}[l]\widetilde{\mathbf{Q}}_{t_{inv_tot}}[l]\mathbf{S}_{tot}[l] \\ &= \begin{bmatrix}\left(\mathbf{B}[l]\mathbf{Q}_{r_{diff1}}[l]\mathbf{Q}_{t_{diff1}}[l] + \mathbf{Q}_{r_{diff2}}[l]\mathbf{B}^*[l_m]\mathbf{Q}^*_{t_{diff2}}[l_m]\right) \\ \left(\mathbf{B}[l]\mathbf{Q}_{r_{diff1}}[l]\mathbf{Q}_{t_{diff2}}[l] + \mathbf{Q}_{r_{diff2}}[l]\mathbf{B}^*[l_m]\mathbf{Q}^*_{t_{diff1}}[l_m]\right)\end{bmatrix}^T \begin{bmatrix}\mathbf{S}[l] \\ \mathbf{S}^*[l_m]\end{bmatrix}\end{aligned} \tag{5.28}$$

where $\mathbf{Q}_{t_{diff1}}[l] = (1 - \mathbf{Q}_t[l]\widetilde{\mathbf{Q}}^*_{tf}[l_m]), \mathbf{Q}_{t_{diff2}}[l] = (\mathbf{Q}_t[l] - \widetilde{\mathbf{Q}}_{tf}[l]), \mathbf{Q}_{r_{diff1}}[l] = (1 - \widetilde{\mathbf{Q}}_{rf}[l]\mathbf{Q}^*_r[l_m])$ and $\mathbf{Q}_{r_{diff2}}[l] = (\mathbf{Q}_r[l] - \widetilde{\mathbf{Q}}_{rf}[l])$.

The IRR improvement is obtained as:

$$IRR_{comp} = 10 \times log_{10} \left(\frac{|\mathbf{B}[l]\mathbf{Q}_{r_{diff1}}[l]\mathbf{Q}_{t_{diff1}}[l] + \mathbf{Q}_{r_{diff2}}[l]\mathbf{B}^*[l_m]\mathbf{Q}^*_{t_{diff2}}[l_m]|^2}{|\mathbf{B}[l]\mathbf{Q}_{r_{diff1}}[l]\mathbf{Q}_{t_{diff2}}[l] + \mathbf{Q}_{r_{diff2}}[l]\mathbf{B}^*[l_m]\mathbf{Q}^*_{t_{diff1}}[l_m]|^2} \right) \tag{5.29}$$

This improvement in IRR performance is later illustrated in section 5.4.

5.3 Phase Rotation Schemes

In this section we propose an alternative scheme to decouple the estimation of the receiver IQ imbalance gain parameter from the channel distortion. We do not consider the presence of transmitter IQ imbalance in the system model. This communication scenario of only receiver IQ imbalance and no transmitter IQ imbalance can be considered as a typical downstream communication between a base station and a mobile device. The mobile device is considered to be low power, inexpensive and so may not have ideal front-end characteristics. As a result the mobile device may be impaired with receiver IQ imbalance. The base station is usually robust and considered to have an ideal front-end.

In section 5.3.1 we consider the presence on only receiver IQ imbalance in the system model. In section 5.3.2, the proposed scheme is also extended to include CFO together with receiver IQ imbalance. The entire compensation is performed in two stages. The first stage compensates for receiver IQ imbalance and CFO, the second stage then compensates for the remaining channel distortion. It is shown that under specific circumstances (large CFOs), the proposed scheme can also be extended to include transmitter IQ imbalance in the system model.

5.3.1 Decoupled Receiver IQ Imbalance Compensation

In section 5.2.2, the proposed D-FEQ scheme first estimates $\mathbf{D}_{tot-}[l]$ based on equation (5.1), and then derives $\widetilde{\mathbf{Q}}_r[l]$ from the $\widetilde{\mathbf{D}}_{tot-}[l]$ coefficients based on (5.12). This implies that to estimate the receiver IQ imbalance gain parameter $\mathbf{Q}_r[l]$, first $\mathbf{D}_a[l], \mathbf{D}_b[l]$ and then $\mathbf{D}_a[l_m], \mathbf{D}_b[l_m]$ have to be estimated. However, estimating the latter coefficient $\mathbf{D}_b[l_m]$ may not be useful per se especially so when the mirror subcarrier for instance is a pilot subcarrier. We therefore propose an alternative scheme where $\widetilde{\mathbf{Q}}_r[l]$ can be estimated directly from the training symbols, thus saving on the computational cost involved in the estimation of the $\mathbf{D}_{tot-}[l]$ coefficients.

We consider a specific sequence of M_l so-called phase rotated LT symbols. All the training symbols are identical up to a different phase rotation $e^{\jmath\Phi^{(i)}}$ where i represents the training symbol number i.e. $\mathbf{S}^{(i)} = \mathbf{S}e^{\jmath\Phi^{(i)}}$. The phase rotations $\Phi^{(i)}$ can be between $0 \dots 2\pi$ radians. At the receiver side, we multiply the complex conjugate of the mirror symbol $\mathbf{Z}^{*(i)}[l_m]$ with a factor $\mathbf{V}_d[l]$ (to be defined) and add the output of this product to the received symbol $\mathbf{Z}^{(i)}[l]$, this results in:

$$\begin{aligned}\mathbf{Z}_q^{(i)}[l] &= \begin{bmatrix}1 & \mathbf{V}_d[l]\end{bmatrix}\begin{bmatrix}\mathbf{Z}^{(i)}[l] \\ \mathbf{Z}^{*(i)}[l_m]\end{bmatrix} \\ &= \begin{bmatrix}1 & \mathbf{V}_d[l]\end{bmatrix}\left(\begin{bmatrix}1 & \mathbf{Q}_r[l] \\ \mathbf{Q}_r^*[l_m] & 1\end{bmatrix}\begin{bmatrix}e^{\jmath\Phi^{(i)}}\mathbf{B}[l]\mathbf{S}[l] \\ e^{-\jmath\Phi^{(i)}}\mathbf{B}^*[l_m]\mathbf{S}^*[l_m]\end{bmatrix}\right. \\ &\quad \left. + \begin{bmatrix}\mathbf{G}_{ra}[l] & \mathbf{G}_{rb}[l] \\ \mathbf{G}_{rb}^*[l_m] & \mathbf{G}_{ra}^*[l_m]\end{bmatrix}\begin{bmatrix}\mathbf{N}^{(i)}[l] \\ \mathbf{N}^{*(i)}[l_m]\end{bmatrix}\right)\end{aligned} \tag{5.30}$$

If $\mathbf{V}_d[l] = -\mathbf{Q}_r[l] = -\frac{\mathbf{G}_{rb}[l]}{\mathbf{G}_{ra}^*[l_m]}$, then the contribution from $\mathbf{S}^*[l_m]$ and $\mathbf{N}^{*(i)}[l_m]$ is eliminated, and so the symbol $\mathbf{Z}_q^{(i)}[l]$ can be considered to be free of receiver IQ imbalance. Finally equation (5.30) can be re-written as:

$$\mathbf{Z}_q^{(i)}[l] = \mathbf{Q}_s[l]e^{\jmath\Phi^{(i)}}\mathbf{B}[l]\mathbf{S}[l] + \mathbf{G}_s[l]\mathbf{N}^{(i)}[l] \tag{5.31}$$

where the scaling term $\mathbf{Q}_s[l] = (1 - \mathbf{Q}_r[l]\mathbf{Q}_r^*[l_m])$ and $\mathbf{G}_s[l] = \left[\mathbf{G}_{ra}[l] - \frac{\mathbf{G}_{rb}[l].\mathbf{G}_{rb_m}^*[l_m]}{\mathbf{G}_{ra_m}^*[l_m]}\right]$. The term $\mathbf{Q}_s[l]$ can be considered as part of the channel.

In the noiseless case, we can relate pairs of received symbols as follows:

$$\begin{aligned}\mathbf{Z}_q^{(j)}[l] &= e^{\jmath\Omega}\mathbf{Z}_q^{(i)}[l] \\ \mathbf{Z}^{(j)}[l] - e^{\jmath\Omega}\mathbf{Z}^{(i)}[l] &= (e^{\jmath\Omega}\mathbf{Z}^{*(i)}[l_m] - \mathbf{Z}^{*(j)}[l_m])\mathbf{V}_d[l]\end{aligned} \tag{5.32}$$

where $\Omega = \Phi^{(j)} - \Phi^{(i)}$, $i = 1 \dots M_l - 1$, $j = i+1 \dots M_l$ and $j > i$. In matrix form, equation (5.32) can be written as:

$$\mathbf{Z}_{A_{tot-}}[l] = \mathbf{Z}_{B_{tot-}}[l_m]\mathbf{V}_d[l] \tag{5.33}$$

$$\text{where } \mathbf{Z}_{A_{tot-}}[l] = \begin{bmatrix} \mathbf{Z}^{(2)}[l] - e^{\jmath(\Phi^{(2)}-\Phi^{(1)})}\mathbf{Z}^{(1)}[l] \\ \hline \vdots \\ \hline \mathbf{Z}^{(M_l)}[l] - e^{\jmath(\Phi^{(M_l)}-\Phi^{(1)})}\mathbf{Z}^{(1)}[l] \\ \mathbf{Z}^{(3)}[l] - e^{\jmath(\Phi^{(3)}-\Phi^{(3)})}\mathbf{Z}^{(2)}[l] \\ \hline \vdots \\ \hline \mathbf{Z}^{(M_l)}[l] - e^{\jmath(\Phi^{(M_l)}-\Phi^{(M_l-1)})}\mathbf{Z}^{(M_l-1)}[l] \end{bmatrix}$$

$$\text{and } \mathbf{Z}_{B_{tot-}}[l_m] = \begin{bmatrix} e^{\jmath(\Phi^{(2)}-\Phi^{(1)})}\mathbf{Z}^{*(1)}[l_m] - \mathbf{Z}^{*(2)}[l_m]) \\ \hline \vdots \\ \hline e^{\jmath(\Phi^{(M_l)}-\Phi^{(1)})}\mathbf{Z}^{*(1)}[l_m] - \mathbf{Z}^{*(M_l)}[l_m]) \\ e^{\jmath(\Phi^{(3)}-\Phi^{(3)})}\mathbf{Z}^{*(2)}[l_m] - \mathbf{Z}^{*(3)}[l_m]) \\ \hline \vdots \\ \hline e^{\jmath(\Phi^{(M_l)}-\Phi^{(M_l-1)})}\mathbf{Z}^{*(M_l-1)}[l_m] - \mathbf{Z}^{*(M_l)}[l_m]) \end{bmatrix}$$

The factor $\mathbf{V}_d[l]$ can then be obtained as:

$$\mathbf{V}_d[l] = \mathbf{Z}^{\dagger}_{B_{tot-}}[l_m]\mathbf{Z}_{A_{tot-}}[l] \tag{5.34}$$

The total number of valid pairs (i, j) that can be considered in equation (5.33) is $N_p = C_2^{M_l} - N_\Omega$ where $C_a^b = \frac{b!}{a!(b-a)!}$ and N_Ω is the total number of pairs with $\Omega = 0, \pi$ and 2π radians. Here $x!$ denotes the factorial of x. We do not consider subcarrier pairs with $\Omega = 0, \pi, 2\pi$ as these lead to ill-conditioning in equation (5.33). The minimal number of phase rotated LT symbols is $M_l > 2$, for equation (5.34) to be valid. N_p shows that as the number of training symbols is increased, we also have additional subcarrier pairs that can be included in equation (5.33), leading to an improved estimation. The coefficient $\mathbf{V}_d[l]$ so obtained provides an estimate of the receiver IQ imbalance gain parameter, i.e. $\mathbf{V}_d[l] = -\widetilde{\mathbf{Q}}_r[l]$, and is independent of the channel characteristic. In the case of FI receiver IQ imbalance, we can average the $\mathbf{V}_d[l]$ over all the subcarriers to obtain an improved estimate $V_d = \frac{1}{N}\sum_{l=1}^{N}\mathbf{V}_d[l]$.

Assuming that the receiver IQ imbalance has been properly compensated, a one-tap FEQ coefficient $\mathbf{W}_a[l]$ is then applied for the estimation of transmitted symbol, given as:

$$\widetilde{\mathbf{S}}[l] = \mathbf{W}_a[l]\begin{bmatrix}1 & \mathbf{V}_d[l]\end{bmatrix}\begin{bmatrix}\mathbf{Z}[l] \\ \mathbf{Z}[l_m]\end{bmatrix} \tag{5.35}$$

The one-tap FEQ in equation (5.35) is a reduced form compared to the two-tap FEQ used in equation (3.12). We now need only one training symbol for the estimation of the FEQ coefficient $\mathbf{W}_a[l]$. The FEQ coefficient can be initialized by

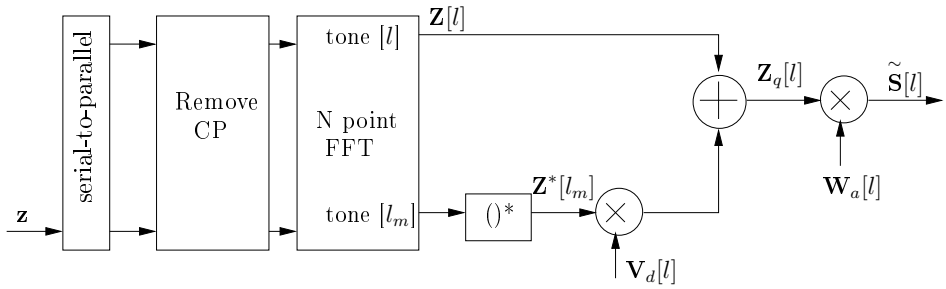

Figure 5.3: PR-FEQ compensation scheme for OFDM system impaired with receiver IQ imbalance

LS or an adaptive RLS training based algorithm. We will refer to this phase rotated LT symbol based estimation scheme as **PR-FEQ**. The PR-FEQ compensation scheme is shown in **Figure 5.3**

5.3.2 Decoupled Receiver IQ Imbalance and CFO Compensation

The phase rotated decoupled scheme can also be extended in the presence of CFO together with receiver IQ imbalance. We follow the compensation structure similar to the TEQ+FEQ scheme in section 4.5, where the impairments are compensated in reverse order of their appearance, i.e starting with receiver IQ imbalance and CFO compensation in the time domain, followed by compensation of the channel distortion in the frequency domain. We assume the CFO estimate $\Delta\widetilde{f}$ has been obtained by one of the estimation schemes discussed in section 4.3. We first do not consider the presence of transmitter IQ imbalance. The CP length is also considered to be longer than the combined receiver IQ imbalance and channel impulse response. This special case of insufficient CP length and the presence of transmitter IQ imbalance is discussed later.

We consider the same TEQ structure as considered in section 4.5, but now with only the first set of TEQs $\mathbf{v}_c$ and $\mathbf{v}_d$ each of length L_r taps. The TEQ filter of the second stage designed to shorten the combined receiver IQ imbalance and channel impulse response is omitted in the present scenario as a sufficient CP length is assumed. This filter is now set to unit coefficient filter with length $L' = 1$ and tap $\mathbf{v}_{a,0} = 1$. The TEQ filters $\mathbf{v}_c$ and $\mathbf{v}_d$ are dependent only on the receiver IQ imbalance parameters, hence once trained, they remain fixed even under variation in channel characteristics. The TEQ structure is again transformed to the frequency domain resulting in a two-branch PTEQ. The output of the PTEQ can then be fed to a one- tap FEQ for channel distortion compensation.

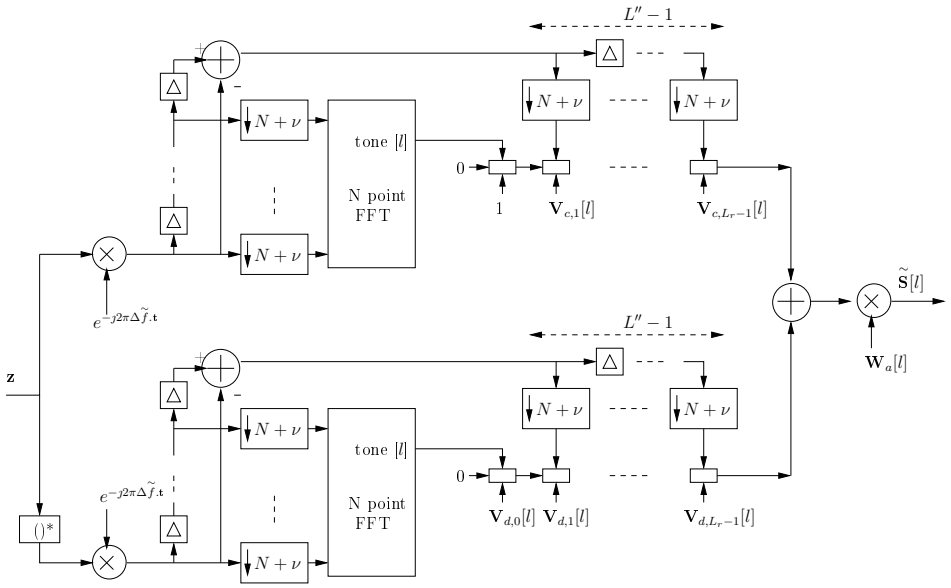

Figure 5.4: PR-PTEQ/FEQ compensation scheme for OFDM system impaired with receiver IQ imbalance and CFO

In order to estimate the two filters $\mathbf{v}_c$ and $\mathbf{v}_d$, we first remove the indeterminacy by setting the first tap of $\mathbf{v}_c$ to 1, thus the coefficients of $\mathbf{v}_c$ are now given as $[1\ \mathbf{v}_{c,1} \dots \mathbf{v}_{c,L_r-1}]$, the coefficients of $\mathbf{v}_d$ remain as $[\mathbf{v}_{d,0}\ \mathbf{v}_{d,1} \dots \mathbf{v}_{d,L_r-1}]$. The design target for the filters in equation (4.18) is then given as: $\mathbf{v}_c = \frac{\mathbf{g}^*_{ra}}{\mathbf{g}^*_{ra,0}}$ and $\mathbf{v}_d = -\frac{\mathbf{g}_{rb}}{\mathbf{g}^*_{ra,0}}$.

We again consider the same sequence of M_l phase rotated LT symbols as explained in section 5.3.1. Now equation (4.18) can be rewritten for the ith training symbol

as follows:

$$\mathbf{z}_q^{(i)} = \mathbf{z}^{(i)} \star \mathbf{v}_c + \mathbf{z}^{*(i)} \star \mathbf{v}_d$$

$$\begin{bmatrix} \mathbf{z}_{q_1}^{(i)} \\ \vdots \\ \mathbf{z}_{q_N}^{(i)} \end{bmatrix} = \left[\begin{array}{ccc|c} \mathbf{z}_1^{(i)} & \mathbf{z}_\nu^{(i)} & \cdots & \mathbf{z}_{\nu-L_r+1}^{(i)} \\ \vdots & & \ddots & \vdots \\ \mathbf{z}_N^{(i)} & \mathbf{z}_{N-1}^{(i)} & \cdots & \mathbf{z}_{N-L_r+1}^{(i)} \end{array}\right] \left[\begin{array}{c} 1 \\ \mathbf{v}_{c,1} \\ \vdots \\ \mathbf{v}_{c,L_r-1} \end{array}\right] \tag{5.36}$$

$$+ \left[\begin{array}{ccc|c} \mathbf{z}_1^{*(i)} & \mathbf{z}_\nu^{*(i)} & \cdots & \mathbf{z}_{\nu-L_r+2}^{*(i)} \\ \vdots & & \ddots & \vdots \\ \mathbf{z}_N^{*(i)} & \mathbf{z}_{N-1}^{*(i)} & \cdots & \mathbf{z}_{N-L_r+1}^{*(i)} \end{array}\right] \left[\begin{array}{c} \mathbf{v}_{d,0} \\ \mathbf{v}_{d,1} \\ \vdots \\ \mathbf{v}_{d,L_r-1} \end{array}\right]$$

where the subscript x in $\mathbf{z}_{q_x}^{(i)}$ and $\mathbf{z}_x^{(i)}$ represents the time index. We can then relate pairs of $\mathbf{z}_q^{(i)}$ vectors as:

$$\mathbf{z}_q^{(j)} = e^{\jmath\Omega}\mathbf{z}_q^{(i)}$$

$$\mathbf{v}_c \star \underbrace{(\mathbf{z}^{(j)} - e^{\jmath\Omega}\mathbf{z}^{(i)})}_{\mathbf{X}^{(j,i)}} = \underbrace{(e^{\jmath\Omega}\mathbf{z}^{*(i)} - \mathbf{z}^{*(j)})}_{\mathbf{Y}^{(j,i)}} \star \mathbf{v}_d \tag{5.37}$$

where $\Omega = 2\pi(j-i)\Delta f NT + \Phi^{(j)} - \Phi^{(i)}$, $i = 1 \ldots M_l - 1$, $j = i+1 \ldots M_l$ and $j > i$. Now equation (5.37) can be written in matrix form as:

$$\left[\begin{array}{ccc|c} \mathbf{X}_1^{(2,1)} & \mathbf{X}_\nu^{(2,1)} & \cdots & \mathbf{X}_{\nu-L_r+2}^{(2,1)} \\ \vdots & \vdots & & \vdots \\ \mathbf{X}_N^{(2,1)} \; \mathbf{X}_1^{(3,1)} & \mathbf{X}_{N-1}^{(2,1)} \; \mathbf{X}_\nu^{(3,1)} & \cdots & \mathbf{X}_{N-L_r+1}^{(2,1)} \; \mathbf{X}_{\nu-L_r+2}^{(3,1)} \\ \vdots & \vdots & & \vdots \\ \underbrace{\mathbf{X}_N^{(M_l,M_l-1)}}_{\mathbf{A}_1} & \underbrace{\mathbf{X}_{N-1}^{(M_l,M_l-1)}}_{\mathbf{A}_2} & \cdots & \mathbf{X}_{N-L_r+1}^{(M_l,M_l-1)} \end{array}\right] \left[\begin{array}{c} 1 \\ \mathbf{v}_{c,1} \\ \vdots \\ \mathbf{v}_{c,L_r-1} \end{array}\right] =$$

$$\left[\begin{array}{ccc|c} \mathbf{Y}_1^{(2,1)} & \mathbf{Y}_\nu^{(2,1)} & \cdots & \mathbf{Y}_{\nu-L_r+2}^{(2,1)} \\ \vdots & & \vdots & \vdots \\ \mathbf{Y}_N^{(2,1)} \; \mathbf{Y}_1^{(3,1)} & \mathbf{Y}_{N-1}^{(2,1)} \; \mathbf{Y}_\nu^{(3,1)} & \cdots & \mathbf{Y}_{N-L_r+1}^{(2,1)} \; \mathbf{Y}_{\nu-L_r+2}^{(3,1)} \\ \vdots & & \vdots & \vdots \\ \underbrace{\mathbf{Y}_N^{(M_l,M_l-1)}}_{\mathbf{B}} & \mathbf{Y}_{N-1}^{(M_l,M_l-1)} & \cdots & \mathbf{Y}_{N-L_r+1}^{(M_l,M_l-1)} \end{array}\right] \left[\begin{array}{c} \mathbf{v}_{d,0} \\ \mathbf{v}_{d,1} \\ \vdots \\ \mathbf{v}_{d,L_r-1} \end{array}\right] \tag{5.38}$$

Based on equation (5.38) the TEQ coefficients can be estimated as:

$$\underbrace{\begin{bmatrix} \mathbf{v}_{d,0} \\ \vdots \\ \mathbf{v}_{d,L_r-1} \\ \mathbf{v}_{c,1} \\ \vdots \\ \mathbf{v}_{c,L_r-1} \end{bmatrix}}_{\mathbf{v}_{cd}} = \left[\mathbf{B}\middle|-\mathbf{A}_2\right]^{\dagger} \mathbf{A}_1 \tag{5.39}$$

For equation (5.39) to be valid, the total number of compensation coefficients to be estimated $(2L_r - 1)$ should always be smaller than the OFDM symbol size N, and the phase rotated LT symbol sequence length $M_l \geq 2$.

Once the TEQ coefficients are known, the resultant symbol $\mathbf{z}_q$ is de-rotated by $e^{-\jmath 2\pi \Delta \widetilde{f}.\mathbf{t}}$ as shown in equation (4.19), and then transformed into a frequency domain symbol $\overset{\wedge}{\mathbf{Z}}_q$. A one-tap FEQ coefficient $\mathbf{W}_a[l]$ is then applied to $\overset{\wedge}{\mathbf{Z}}_q[l]$, to recover the estimate of the transmitted symbol $\widetilde{\mathbf{S}}[l]$. Only one training symbol is needed to estimate $\mathbf{W}_a[l]$.

Finally equations (4.21) and (4.23) are followed to transform the TEQ filters to the frequency domain resulting in a PTEQ employing two DFT operations and $L_r - 1$ difference terms. The output of the two-branch PTEQ are then followed by a one-tap FEQ $\mathbf{W}_a[l]$ to compensate for channel distortion. This finally leads to the estimation of the transmitted symbol, given as:

$$\widetilde{\mathbf{S}}[l] = \mathbf{W}_a[l] \left(\begin{bmatrix} \mathbf{V}_c[l] & \mathbf{V}_d[l] \end{bmatrix} \begin{bmatrix} \mathbf{F}_{ext}[l]\mathbf{z}.e^{-\jmath 2\pi \Delta \widetilde{f}.\mathbf{t}} \\ \mathbf{F}_{ext}[l]\mathbf{z}^*.e^{-\jmath 2\pi \Delta \widetilde{f}.\mathbf{t}} \end{bmatrix} \right) \tag{5.40}$$

where $\mathbf{V}_c[l], \mathbf{V}_d[l]$ are filter vectors of length $L'' = L_r$. From now on only the $\mathbf{W}_a[l]$ coefficient has to be re-estimated for any variation in channel characteristics, the remaining structure continues to be the same. The FEQ coefficient can be initialized by LS or an adaptive RLS training based algorithm. We will refer to the compensation solution obtained in equation (5.40) as the PR-PTEQ/FEQ scheme. **Figure 5.4** illustrates the PR-PTEQ/FEQ scheme for the compensation of receiver IQ imbalance and CFO.

Note:

- **Residual CFO error correction:** In equation (5.40), the TEQ coefficients may not be accurately estimated especially if the auto-correlation based CFO

estimation scheme (4.6) is used in the case of large CFOs. This is because the accuracy of the CFO estimation algorithm in turn depends on the amount of IQ imbalance in the received symbol. Thus in order to further improve the estimate $\widetilde{\Delta f}$, we now replace $\mathbf{z}^{(i_s)}$ and $\mathbf{z}^{(j_s)}$ in equation (4.6) with the symbol $\mathbf{z}_q^{(i_s)}$ and $\mathbf{z}_q^{(j_s)}$ obtained after the receiver IQ imbalance has been partially compensated in the ST symbol sequence. An expression similar to equation (5.36) can now be written for $\mathbf{z}_q^{(i_s)}$ with TEQ estimates obtained from equation (5.39):

$$\mathbf{z}_q^{(i_s)} = \mathbf{z}^{(i_s)} \star \mathbf{v}_c + \mathbf{z}^{*(i_s)} \star \mathbf{v}_d$$

$$\begin{bmatrix} \mathbf{z}_{q_1}^{(i_s)} \\ \hline \vdots \\ \hline \mathbf{z}_{q_{N_s}}^{(i_s)} \end{bmatrix} = \left[\begin{array}{c|ccc|c} \mathbf{z}_1^{(i_s)} & \mathbf{z}_{N_s}^{(i_s-1)} & \cdots & \mathbf{z}_{N_s-L_r+2}^{(i_s-1)} & \begin{bmatrix} 1 \\ \mathbf{v}_{c,1} \\ \hline \vdots \\ \hline \mathbf{v}_{c,L_r-1} \end{bmatrix} \\ \hline \multicolumn{3}{c|}{\vdots \qquad \ddots \qquad \vdots} & \\ \hline \mathbf{z}_{N_s}^{(i_s)} & \mathbf{z}_{N_s-1}^{(i_s)} & \cdots & \mathbf{z}_{N_s-L_r+1}^{(i_s)} & \end{array}\right] \tag{5.41}$$

$$+ \left[\begin{array}{c|ccc|c} \mathbf{z}_1^{*(i_s)} & \mathbf{z}_{N_s}^{*(i_s-1)} & \cdots & \mathbf{z}_{N_s-L_r+2}^{*(i_s-1)} & \begin{bmatrix} \mathbf{v}_{d,0} \\ \mathbf{v}_{d,1} \\ \hline \vdots \\ \hline \mathbf{v}_{d,L_r-1} \end{bmatrix} \\ \hline \multicolumn{3}{c|}{\vdots \qquad \ddots \qquad \vdots} & \\ \hline \mathbf{z}_{N_s}^{*(i_s)} & \mathbf{z}_{N_s-1}^{*(i_s)} & \cdots & \mathbf{z}_{N_s-L_r+1}^{*(i_s)} & \end{array}\right]$$

where $i_s = 2 \ldots M_s$. This time the CFO estimation algorithm (4.6) provides a much finer estimate as the receiver IQ imbalance has been partially compensated. Equations (5.36)-(5.39) are then followed so as to obtain an improved estimate of the filter coefficients. Thus we can repeat the entire set of equations (4.6) and (5.36)-(5.39) a number of times until sufficiently accurate estimates of both $\widetilde{\Delta f}$ and the TEQ coefficients are available.

- **Generalized structure:** The PR-PTEQ/FEQ scheme (5.40) can be considered as a generalized form of the phase rotation compensation scheme, as the proposed scheme can compensate for receiver IQ imbalance irrespective of the amount of CFO in the system model. The following points are to be noted regarding the PR-PTEQ/FEQ scheme:

  - **FI receiver IQ imbalance and zero CFO**: In this case, the length of PTEQ filters in PR-PTEQ/FEQ can be set to $L'' = 1$. This results in PTEQ coefficients $\mathbf{V}_c[l] = 1$ and $\mathbf{V}_d[l] = -\frac{g_{rb}}{g_{ra}^*} = -Q_r$, the latter is the same estimate also obtained with PR-FEQ coefficient $\mathbf{V}_d[l]$ (5.34). Also the PTEQ filters can now be applied to the desired subcarrier and the complex conjugated output of the mirror subcarrier from the same DFT. Thus in the presence of FI receiver IQ imbalance and zero CFO, the PR-PTEQ/FEQ compensation solution reduces to the PR-FEQ solution.

– **FS receiver IQ imbalance and zero CFO**: In the presence of FS receiver IQ imbalance and zero CFO, the PR-PTEQ/FEQ scheme provides a different solution compared to the PR-FEQ scheme. This is because the TEQ filters in PR-PTEQ/FEQ estimate the mismatched impulse responses $\mathbf{v}_c = \frac{\mathbf{g}^*_{ra}}{\mathbf{g}^*_{ra,0}}$ and $\mathbf{v}_d = -\frac{\mathbf{g}_{rb}}{\mathbf{g}^*_{ra,0}}$, whereas the filter coefficient in PR-FEQ estimates the interference from the mirror subcarrier $\mathbf{V}_d[l] = -\mathbf{Q}_r[l] = -\frac{\mathbf{G}_{rb}[l]}{\mathbf{G}^*_{ra}[l_m]}$. Thus the coefficients obtained from the two schemes are different. The PR-FEQ scheme is cheaper to implement as it requires only one coefficient per subcarrier to be estimated whereas the PR-PTEQ/FEQ requires $2L_r - 1$ coefficients to be estimated per subcarrier for the compensation of receiver IQ imbalance.

– **Insufficient CP length**: In the case of insufficient CP length, the TEQ filters $\mathbf{v}_c$ and $\mathbf{v}_d$ can still be initialized as long as there are enough samples in the symbol $\mathbf{z}^{(i)}$ (5.36) that have not been distorted by their adjacent symbol $\mathbf{z}^{(i-1)}$ for $i = 2 \ldots M_l$. Thus, the number of rows has to be longer than or equal to the number of columns in the $[\mathbf{B}| - \mathbf{A}_2]$ matrix in (5.38) to obtain the solution. We also consider a TEQ filter branch $\mathbf{v}_a$ of length L' applied at the output of the first set of TEQs $\mathbf{v}_c$ and $\mathbf{v}_d$, in order to shorten the combined receiver IQ imbalance and the channel impulse response. The TEQ filter branch $\mathbf{v}_a$ is then transformed to a one-branch PTEQ and merged with the FEQ filter. The resulting one-branch PTEQ of length L' is initialized by LS or an adaptive RLS training based algorithm for any variation in the channel characteristics. Finally the first set of TEQ filters, initialized for receiver IQ imbalance compensation, can also be transformed to the frequency domain resulting in a two-branch PTEQ. The coefficients of the two-branch PTEQ always remain constant irrespective of the variation in the channel characteristics. The final compensation structure consists of a two-branch PTEQ for the compensation of receiver IQ imbalance, followed by a one-branch PTEQ for the purpose of channel shortening and its compensation.

  During the estimation phase of the receiver IQ imbalance gain parameters, we consider $M_l \geq 2$ phase rotated LT symbols for the initialization of the two-branch PTEQ, subject to the validity of equation (5.38). Once the estimates of the receiver IQ imbalance parameters are known, we then need $M_l \geq L'$ linearly independent LT symbols for shortening the channel as well as its compensation by the one-branch PTEQ.

– **Transmitter/receiver IQ imbalance and CFO**: In the presence of transmitter/receiver IQ imbalance, the relation between a pair of phase rotated LT symbols will no longer be applicable as shown in equation (5.37). This is because the transmitter IQ imbalance will add both

positive and negative phase rotations to the LT symbols even before these rotations can be introduced by receiver IQ imbalance. Thus in the presence of transmitter IQ imbalance, the two TEQ filter branches can be estimated based on identical symbols without any added phase rotations. In equation (5.37), $\Phi^{(j)} - \Phi^{(i)} = 0$ and $\Omega = 2\pi(j-i)\Delta f N T_s$. Equations (5.37)-(5.39) are then valid as long as Ω is large enough for the estimation of $\mathbf{v}_{cd}$ in (5.39). This is because as Δf becomes close to 0, expressions $\mathbf{X}^{(j,i)}$ and $\mathbf{Y}^{(j,i)}$ will also tend to be 0 and this can result in ill-conditioning in the identification of $\mathbf{v}_{cd}$. The one-tap FEQ filter is now also replaced by a two-tap FEQ filter (3.12) for the joint compensation of transmitter IQ imbalance and channel distortion.

During the estimation phase of the receiver IQ imbalance gain parameters, we consider $M_l \geq 2$ identical LT symbols to initialize the PTEQ structure. The total number of compensation coefficients to be estimated $(2L_r - 1)$ should always be smaller than the OFDM symbol size N for the validity of the equation (5.39). Once the estimates of the receiver IQ imbalance parameters are known, we then need $M_l \geq 2$ linearly independent LT symbols for the compensation of transmitter IQ imbalance and channel distortion by the two-tap FEQ.

One way to improve the robustness of the PTEQ structure is to consider identical symbols with large distance between them in terms of Ω, i.e, symbols that are far apart (large $j - i$) are only considered in equation (5.37). If LT symbol sequence is not sufficient to obtain adequate Ω, then identical data symbols in a data sequence can also be considered. The contents of the data symbols need not be known to the receiver. The receiver only requires to know the location of these symbols. The best location of two identical data symbols will be the first and the last symbol in the data sequence. Even after these measures, if Ω is considered to be insignificantly small, then residual CFO may be ignored, and an approximate but still an acceptable compensation solution of transmitter/receiver IQ imbalance can be obtained. Since the amount of CFO involved is extremely small or non-existing, the performance degradation will be limited. If an exact solution is still desired then a four-branch PTEQ based joint compensation solution as explained in section 4.5 can be implemented.

5.4 Simulation Results

We consider an uncoded OFDM transmission with symbol length $N = 64$ and CP length $\nu = 16$. We consider a quasi static multipath channel of $L = 4$ taps. The taps of the multipath channel are chosen independently with complex Gaussian distribution and their realization may vary from one packet to another. All BER

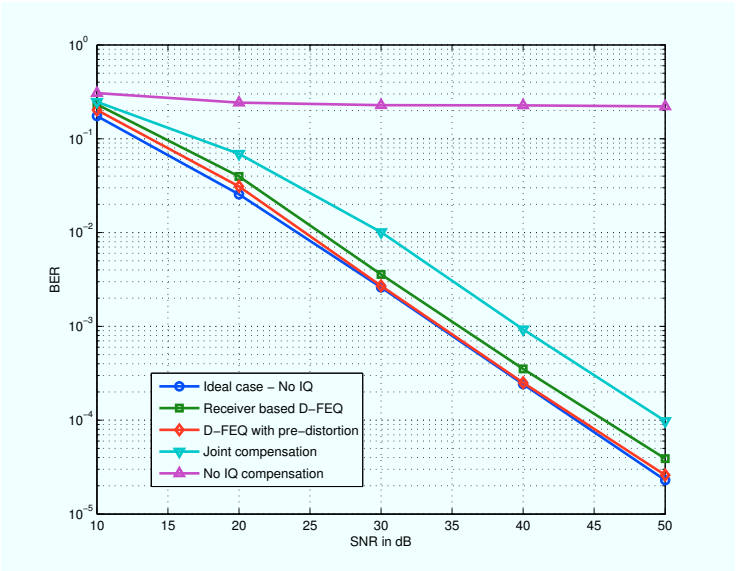

Figure 5.5: BER vs SNR with D-FEQ scheme for compensation of transmitter IQ imbalance

versus SNR performance curves depicted are obtained by averaging the BER curves over 10^4 independent channel realizations.

In the case of the D-FEQ compensation scheme, a transmission packet consists of a linearly independent LT symbol sequence followed by the data sequence for performance evaluation. We do not consider a ST symbol sequence, as these are not needed for the proposed compensation schemes. The length of the LT sequence is explained in the corresponding simulation setup.

In the case of the PR-(PTEQ)/FEQ scheme, a transmission packet consists of a 10 identical ST symbol sequence for CFO estimation (only for PR-PTEQ/FEQ), followed by a phase rotated LT symbol sequence for the estimation of compensation coefficients for receiver IQ imbalance and channel distortion, and finally the data sequence for performance evaluation. For all decoupled schemes, once the estimates of the IQ imbalance parameters are known, we then transmit only $M_l = 2$ linearly independent LT symbols for the estimation of the channel distortion, as this is also the minimal requirement for the joint compensation scheme (3.12).

- In the first setup, we consider the D-FEQ scheme for the compensation of only transmitter IQ imbalance. **Figure 5.5** shows the performance curves BER vs SNR obtained for an uncoded 16QAM OFDM system impaired with transmitter IQ imbalance. The transmitter filter impulse

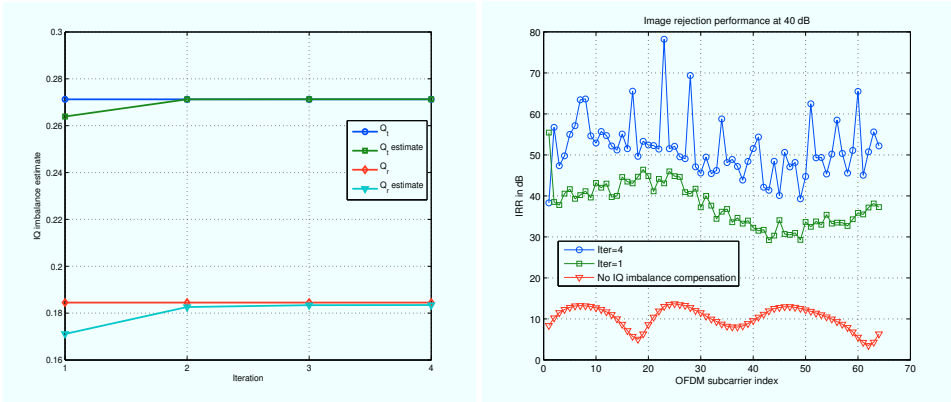

(a)Coefficient convergence (b) IRR improvement

Figure 5.6: Number of D-FEQ iterations required to perform adequate compensation for a system impaired with transmitter and receiver IQ imbalance

responses are $\mathbf{h}_{ti} = [0.01\ 0.5\ 0.06]$ and $\mathbf{h}_{tq} = [0.06\ 0.5\ 0.01]$ and the transmitter FI amplitude and phase imbalances are $g_t = 10\%$ and $\phi_t = 10^\circ$ respectively. During the estimation phase of the transmitter IQ imbalance gain parameters, we consider $M_l = 6$ LT symbols. Once the estimates of transmitter IQ imbalance parameters are known, we then employ $M_l = 2$ LT symbols to estimate the variation in channel characteristics. The figure compares the performance curves obtained for the entirely receiver based D-FEQ compensation scheme, pre-distortion based D-FEQ compensation scheme and the joint compensation scheme besides an ideal system with no IQ imbalance and a system with no IQ imbalance compensation algorithm included. It can be seen that the proposed D-FEQ compensation schemes provide a very good performance even with very low training symbols. The results obtained are very close to the ideal case in the case of pre-distortion based D-FEQ scheme. The difference between the pre-distortion scheme and the joint compensation scheme is almost 6 dB at BER of 10^{-3}. The joint compensation scheme provides poor performance as only $M_l = 2$ training symbols are not sufficient to give the performance close to the ideal case. The joint compensation scheme requires additional training symbols for better noise averaging. The figure shows that the proposed D-FEQ scheme provides an efficient compensation performance with very low training overhead.

- In the second setup, we consider the D-FEQ compensation scheme in the presence of both transmitter and receiver IQ imbalance in a 64QAM OFDM system. The transmitter and receiver filter impulse responses are $\mathbf{h}_{ti} = \mathbf{h}_{ri} = [0.01\ 0.5\ 0.06]$, and $\mathbf{h}_{tq} = \mathbf{h}_{rq} = [0.06\ 0.5\ 0.01]$. The transmitter

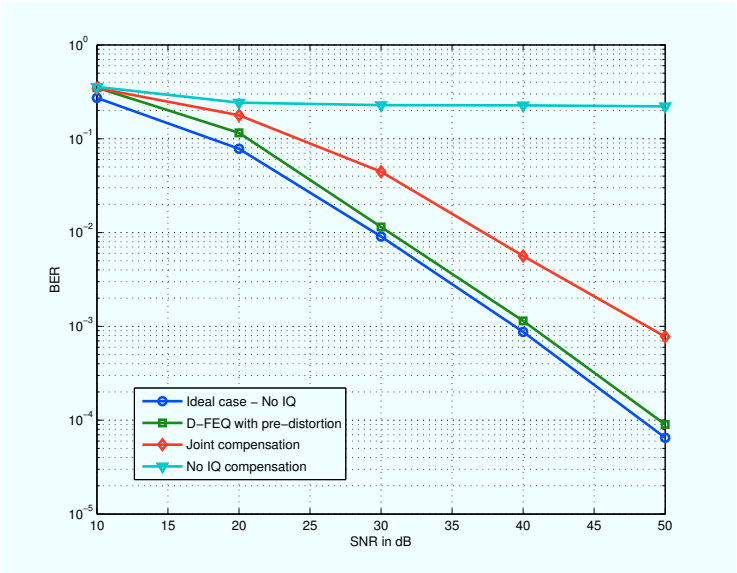

Figure 5.7: BER vs SNR with D-FEQ scheme for compensation of transmitter and receiver IQ imbalance

and receiver FI amplitude and phase imbalances are $g_t = g_r = 10\%$ and $\phi_t = 30°, \phi_r = 25°$ respectively. It should be noted that the imbalance levels are much higher than the level observed in a practical receiver. However we consider such an extreme case to evaluate the robustness/effectiveness of the proposed compensation schemes. Here we first consider $M_l = 8$ LT symbols during the estimation phase of transmitter and receiver IQ imbalance gain parameters and then $M_l = 2$ LT symbols to estimate the variation in channel characteristics.

Figure 5.6 illustrates the number of iterations required to perform adequate compensation for the given values of the IQ imbalance parameters. Both simulation results are obtained at SNR=40dB. Figure 5.6(a) shows the curves depicting the convergence of transmitter and receiver IQ imbalance gain estimates to their ideal IQ imbalance gain parameters. The curves measure the IQ imbalance gain estimates as the mean of the absolute values for all N subcarriers of an OFDM symbol taken together (i.e $\frac{1}{N}\sum_{l=1}^{N}\{|\widetilde{\mathbf{Q}}_t[l]|\}$ and $\frac{1}{N}\sum_{l=1}^{N}\{|\widetilde{\mathbf{Q}}_r[l]|\}$). It can be observed that 3-4 iterations can provide sufficiently accurate estimates.

Figure 5.6(b) shows the IRR observed for a system impaired with transmitter

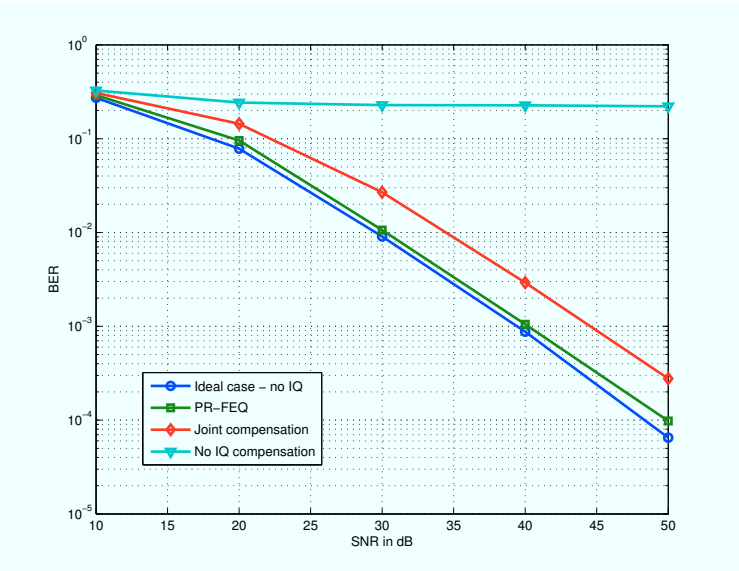

Figure 5.8: BER vs SNR with PR-FEQ scheme for compensation of receiver IQ imbalance

and receiver IQ imbalance. The figure shows that the IQ imbalance in our case is quite severe, in that with no compensation scheme in place the IRR is only 5-15 dB (3.9). The figure also shows the improvement in IRR in the presence of pre-distortion and a transmitter/receiver IQ imbalance compensation scheme (5.29). It can be observed that with only 1 iteration (Iter=1), an IRR improvement of around 30 dB is already obtained. Further improvement in IRR can be obtained by performing a few more iterations. This improvement is however limited as the IRR saturates after a certain number of iterations due to the noise. In our simulations, we obtained a further improvement of around 10 dB after performing 3 more iterations (Iter=4).

Figure 5.7 shows the BER vs SNR performance curve for this system setup. It can be seen that the proposed pre-distortion based D-FEQ compensation scheme is still very robust and the performance curves are very close to those of the ideal case even when only two LT symbols are used. The difference between the proposed scheme and the joint compensation scheme is now almost 9 dB at BER of 10^{-3}. Thus the proposed compensation scheme provides very efficient compensation results even with very low training overhead.

- In the third setup we consider the PR-FEQ scheme for the compensation of

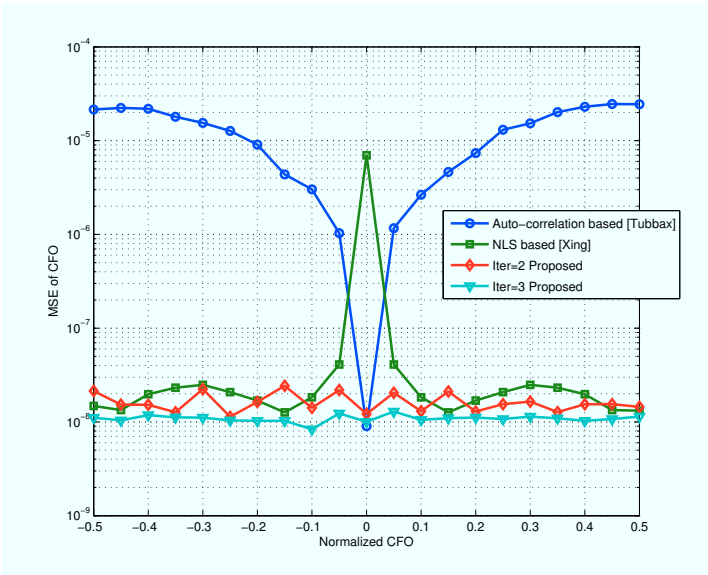

Figure 5.9: MSE of CFO estimation vs normalized CFO with iterative auto-correlation algorithm

receiver IQ imbalance in an uncoded 64QAM OFDM system. The receiver filter impulse responses are $\mathbf{h}_{ri} = [0.01\ 0.5\ 0.06]$ and $\mathbf{h}_{rq} = [0.06\ 0.5\ 0.01]$ and the receiver FI amplitude and phase imbalances are $g_r = 5\%$ and $\phi_r = 5^\circ$ respectively. During the estimation phase of the receiver IQ imbalance gain parameters, we consider $M_l = 4$ identically phase rotated LT symbols. The phase rotation of the symbols are $\Phi = 0, \pi/4, \pi/2, 3\pi/4$. Once again, we employ only $M_l = 2$ LT symbols to estimate the variation in channel characteristics. **Figure 5.8** shows the BER vs SNR performance curve for this system setup. As can be expected the proposed scheme provides an efficient compensation performance with a very small training overhead requirement.

- In the fourth setup, we consider the PR-PTEQ/FEQ compensation scheme for an uncoded 64QAM OFDM system. We consider the same simulation parameters as explained in the third setup. The CFO is now estimated by the auto-correlation algorithm (4.4) [109] based on a 10 identical ST symbol sequence. Since the non-iterative version of this algorithm may not yield the correct estimate for large CFOs, we therefore improve upon the CFO estimate by including the iterative scheme during the estimation phase, as explained in section 5.3.2. **Figure 5.9** illustrates the MSE performance of the CFO estimation vs normalized CFO ζ obtained for the auto-correlation

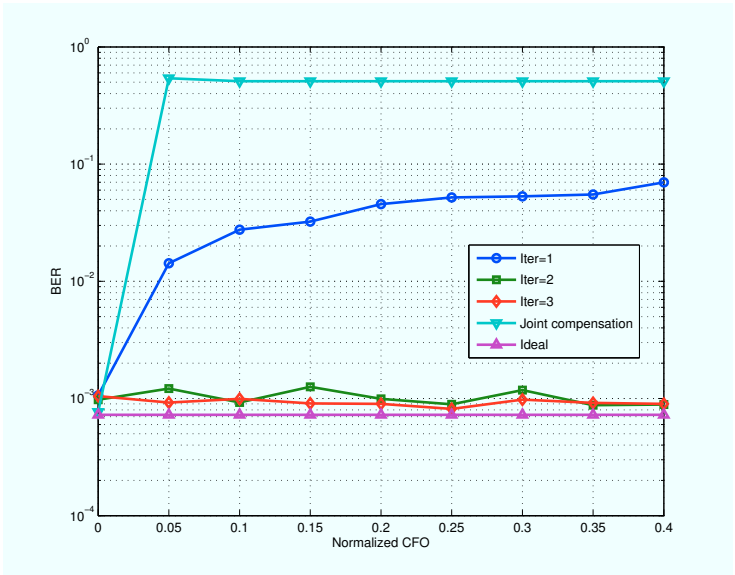

Figure 5.10: BER vs normalized CFO for PR-PTEQ/FEQ scheme in the presence of receiver IQ imbalance

based iterative CFO estimation algorithm. The MSE performance has been superimposed over the performance curves obtained for the two non-iterative CFO estimation schemes (Tubbax-[109] and Xing-[121]) explained in section 4.3. In the NLS scheme, we have used a step size of $\Delta\zeta = 0.0005$ for the exhaustive search. The performance curves are obtained at 40 dB SNR. The proposed iterative scheme shows that for the given IQ imbalance values, even 2 iterations are sufficient to obtain good estimates. The iterative scheme is robust and good estimates can be obtained for the entire range of CFO values. The iterative scheme (4.26) is also followed to finally obtain an optimal CFO value together with PTEQ coefficients.

Figure 5.10 compares the BER vs normalized CFO performance for the PR-PTEQ/FEQ scheme (5.40) and a simple two-tap FEQ scheme (3.12) that does not consider the presence of CFO. It can be observed that for $\zeta = 0$, the FEQ scheme and the PR-PTEQ/FEQ scheme provide a good compensation performance. As ζ is increased, the performance of the FEQ and the PR-PTEQ/FEQ with only 1 iteration deteriorates. The PR-PTEQ/FEQ scheme shows poor performance as the CFO estimate may not be accurate in the first iteration. As we perform more iterations, the CFO and receiver IQ imbalance estimates become more accurate resulting in improved BER performance. For the given IQ imbalance and CFO values, the proposed scheme requires only 3 iterations to obtain good performance.

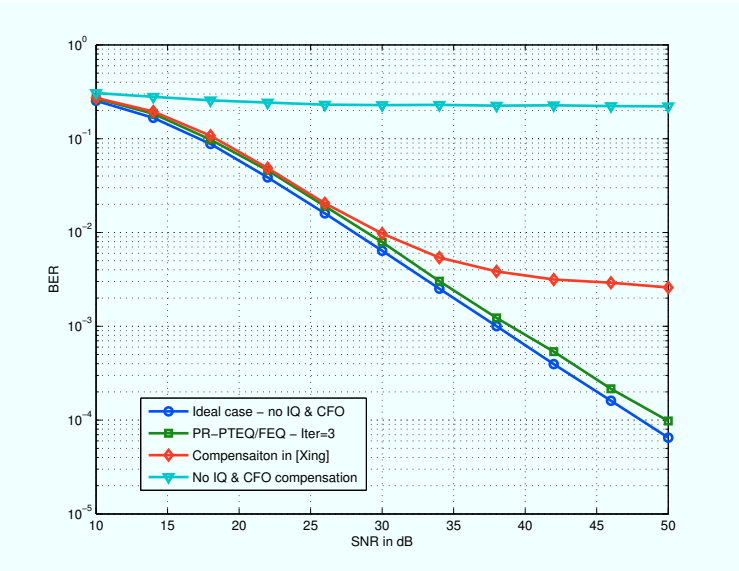

Figure 5.11: BER vs SNR with PR-PTEQ/FEQ scheme for compensation of receiver IQ imbalance and CFO

Figure 5.11 compares the BER vs SNR performance for the PR-PTEQ/FEQ scheme (5.40) and the proposed compensation scheme in Xing-[121]. Here, we consider a CFO $\zeta = 0.32$. The figure shows that the proposed scheme in [121] gives poor performance at higher SNR. This is because the compensation scheme depends only on one filter that measures the difference in impulse response of two-branch filters. A filter of this kind exhibits an infinite impulse response (IIR) and may also require the addition of cyclic postfix samples to the OFDM symbols [97]. The proposed compensation scheme estimates the complete impulse response of the two-branch filters $\mathbf{v}_c$ and $\mathbf{v}_d$ resulting in improved performance. The performance is further improved by performing multiple iterations over the CFO and IQ imbalance estimation.

Figure 5.12 once again shows the BER vs normalized CFO performance for the PR-PTEQ/FEQ scheme, but this time we also consider the presence of transmitter IQ imbalance. We now consider an identical LT symbol sequence without any additional phase rotation between them. We also modify the one-tap FEQ filter to a two-tap FEQ filter (3.12) in the PR-PTEQ/FEQ structure for the joint compensation of transmitter IQ imbalance and channel distortion. During the estimation phase of the receiver IQ imbalance gain parameters, we consider $M_l = 4$ identical LT symbols. Once the estimates of the receiver IQ imbalance parameters are known, we then transmit $M_l = 4$

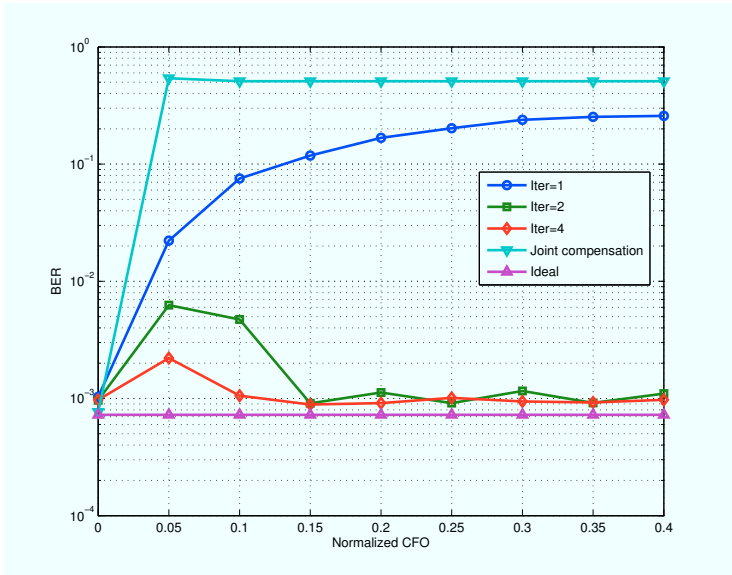

Figure 5.12: BER vs normalized CFO for PR-PTEQ/FEQ scheme in the presence of transmitter and receiver IQ imbalance

linearly independent LT symbols for the compensation of transmitter IQ imbalance and channel distortion by the two-tap FEQ.

The figure shows that as the CFO increases ($\zeta > 0.15$), there is a sufficient amount of natural phase rotation between adjacent LT symbols, thus leading to a good estimate of the TEQ filter coefficients and hence an improved BER performance. As small ζ leads to a poor estimate of the TEQ filter coefficients mainly due to ill-conditioning in matrices $\mathbf{X}^{(j,i)}$ and $\mathbf{Y}^{(j,i)}$ in (5.38), thus leading to a poor BER performance. The performance in the case of small ζ can be further improved, if additional iterations are performed, as this results in an improved estimate of both the CFO and the impulse response of the mismatched filters. At $\zeta = 0$, the matrices $\mathbf{X}^{(j,i)}$ and $\mathbf{Y}^{(j,i)}$ will be ill conditioned, as a result the TEQ filtering may result in additional receiver IQ imbalance in the system. However, when $\zeta = 0$, a two-tap FEQ is sufficient for the joint compensation of transmitter and receiver IQ imbalance. Thus the FEQ filters following the TEQ/PTEQ filter branches in the PR-PTEQ/FEQ structure now perform the entire joint compensation of transmitter/receiver IQ imbalance and channel distortion. The BER performance is once again close to the ideal case. The insertion of TEQ/PTEQ filters in the equalization structure does not deteriorate the performance.

5.5 Conclusion

In this chapter we have proposed training based schemes that can decouple the compensation of IQ imbalance and CFO from the compensation of channel distortion. We have proposed two decoupled schemes - firstly, the D-FEQ scheme, here the transmitter/receiver IQ imbalance and the channel parameters are estimated based on coefficients obtained from the joint estimation/compensation solution. Secondly, the PR-(PTEQ)/FEQ scheme, where the receiver IQ imbalance parameters are estimated directly from a sequence of phase rotated LT symbols. The PR-PTEQ/FEQ scheme can estimate receiver IQ imbalance parameters irrespective of the amount of CFO in the system model. It is shown that under certain conditions (for large CFOs), the PR-PTEQ scheme is also applicable in the presence of transmitter IQ imbalance.

Both schemes provide an efficient way to decouple the compensation of front-end non-idealities from the compensation of channel distortion. Once these parameters are available, then only one training symbol is needed to estimate the compensation coefficient for the channel distortion. The decoupled schemes result in an overall lower training overhead and a lower computational requirement, compared to the joint estimation/compensation scheme. Simulation results show that the proposed schemes provide a very efficient compensation with performance close to the ideal case without any IQ imbalance.

Part II

Multiple Antenna OFDM Systems

Chapter 6

Joint Compensation Schemes

6.1 Introduction

So far we have considered OFDM transmission for single-input single-output (SISO) antenna systems. But OFDM has also become a preferred modulation format in multiple antenna systems [81]. An OFDM based so-called multiple-input multiple-output (MIMO) transmission system takes advantage of the spatial diversity obtained by its multiple transmit and receive antennas to improve its performance in a dense multipath fading environment.

In this chapter we consider the joint effect of transmitter/receiver IQ imbalance and CFO in a multiple antenna scenario. The motivation for this extension is as follows: 1) The next generation of wireless systems will require even more simplified, low cost, flexible and reconfigurable radio front-ends, thus with the increase in the use of cheaper components, the effect of the front-end non-idealities will become more severe. All these problems are more pronounced when a device has to support multiple antennas at the transmitter and receiver front-ends, because in this case multiple parallel radios have to be implemented in a single device. 2) MIMO OFDM systems are designed to provide a higher effective SNR and, consequently, higher data throughput. One of the main methods to obtain an improved throughput is by using higher order constellations, but this may result in a higher sensitivity towards front-end non-idealities. 3) The current trend is also to utilize more bandwidth and higher carrier frequencies in MIMO transmission systems. The use of higher carrier frequencies and larger bandwidths leads to higher sensitivity to front-end non-idealities such as FS IQ imbalance due to filter

mismatch. Thus for all the above reasons, it is desirable to develop compensation schemes that help to eliminate the effect of front-end non-idealities in MIMO systems. In summary, many of the advantages for which MIMO systems have been designed may be rendered ineffective if the front-end non-idealities are not properly compensated.

The influence and compensation of IQ imbalance in MIMO OFDM system has been studied in [101],[77], [71] and [17]. In [101], the authors propose an adaptive compensation scheme for receiver caused IQ imbalance, while in [71] and [77] an adaptive compensation scheme for combined transmitter and receiver IQ imbalance is developed. In [17] a joint estimation of the FI receiver IQ imbalance and channel response based on exploiting the channel residual energy is proposed. MIMO compensation schemes generally tend to be more complex, leading to increased computational requirements of the receiver.

In this chapter we derive a PTEQ based joint compensation solution for transmitter/receiver IQ imbalance and CFO in different multiple antenna scenarios. The compensation schemes proposed earlier for SISO OFDM systems (chapter 3-4) provide a suitable framework for the development of MIMO compensation schemes. It is shown that for the case of single-user MIMO and space-time coded systems, the PTEQ based joint compensation solution can be scaled for any number of transmitter and receiver antennas. By exploiting the structure of orthogonal space-time codes, efficient and optimal receiver architectures that are robust to front-end non-idealities can be derived. The PTEQ scheme has also been extended to the multi-user scenario, where each individual user may have multiple antennas supported by the user's local oscillator. The local oscillators of the individual users may not be perfectly synchronized with the local oscillator of the base station and also with other user's local oscillator, leading to individual CFOs. In order to keep the compensation solutions simple, we always consider sufficiently long CP length in the system model, thus the influence of ISI between adjacent OFDM symbols is not considered. However the derived compensation solutions can be easily extended for insufficient CP length. The publications related to this chapter are: [91], [92] and [96].

This chapter is organized as follows: In **section 6.2** we derive an input-output system model governing a MIMO OFDM system impaired with IQ imbalance and CFO. In **section 6.3** a joint compensation scheme for single-user systems with only transmitter and receiver IQ imbalance is derived, which is then extended to include CFO in **section 6.4**. In **section 6.5**, the behavior of space-time block coded systems in the presence of transmitter/receiver IQ imbalances and CFO is studied. We propose joint compensation schemes for Alamouti coded OFDM systems. It is shown that the joint compensation solution can also be extended to higher order orthogonal space-time block codes. In **section 6.6**, we consider the multi-user up-link as well as the multi-user down-link scenario. Finally, the results of numerical performance evaluations are presented in **section 6.7** and

conclusions are given in **section 6.8**.

6.2 System Model

In this section we consider a point-to-point single-user (SU) MIMO OFDM system, the case of multi-user (MU) MIMO OFDM system is discussed in section 6.6. We will extend the system of notations considered in section 3.2.1 for SISO systems.

Let N_t and N_r denote the number of transmit and receive antennas. We will generally assume that $N_r \geq N_t$. Then $\mathbf{S}_{(K)}$ (for $K = 1 \dots N_t$) is the frequency domain OFDM symbol of size $(N \times 1)$, to be transmitted over the Kth transmit antenna where N is the number of subcarriers. The frequency domain symbol is transformed to the time domain by the IDFT operation. A CP of length ν is then added, resulting in a time domain baseband symbol $\mathbf{s}_{(K)}$ given as:

$$\mathbf{s}_{(K)} = \mathbf{P_{CI}} \mathbf{F}_N^{-1} \mathbf{S}_{(K)} \tag{6.1}$$

where $\mathbf{P_{CI}}$ is the CP insertion matrix as defined in equation (3.1).

The time domain symbol $\mathbf{s}_{(K)}$ is parallel-to-serial converted and then fed to the transmitter front-end. We consider a single local oscillator (LO) supporting all the transmit (receive) antennas at the transmitter (receiver) front-end. Due to design restrictions, the trace lengths between the LO and the individual antenna branches may not be exactly equal and this may result in a different FI IQ imbalance for each transmit antenna, given as $g_{t(K)}$ and $\phi_{t(K)}$ for the Kth transmit antenna. Similarly the frequency responses of the two mismatched filters at the I and Q branch of the Kth transmit antenna are given as $\mathbf{H}_{ti(K)} = \mathbf{F}_N \mathbf{h}_{ti(K)}$ and $\mathbf{H}_{tq(K)} = \mathbf{F}_N \mathbf{h}_{tq(K)}$ where $\mathbf{h}_{ti(K)}$ and $\mathbf{h}_{tq(K)}$ represent the impulse response of the mismatched filters respectively.

The equivalent baseband symbol $\mathbf{p}_{(K)}$ at the Kth transmit antenna is then given as:

$$\mathbf{p}_{(K)} = \mathbf{g}_{ta(K)} \star \mathbf{s}_{(K)} + \mathbf{g}_{tb(K)} \star \mathbf{s}^*_{(K)} \tag{6.2}$$

where

$$\mathbf{g}_{ta(K)} = \mathbf{F}_N^{-1} \mathbf{G}_{ta(K)} = \mathbf{F}_N^{-1} \left\{ \frac{\left[\mathbf{H}_{ti(K)} + g_{t(K)} e^{-\jmath \phi_{t(K)}} \mathbf{H}_{tq(K)} \right]}{2} \right\}$$

$$\mathbf{g}_{tb(K)} = \mathbf{F}_N^{-1} \mathbf{G}_{tb(K)} = \mathbf{F}_N^{-1} \left\{ \frac{\left[\mathbf{H}_{ti(K)} - g_{t(K)} e^{\jmath \phi_{t(K)}} \mathbf{H}_{tq(K)} \right]}{2} \right\}$$

Both $\mathbf{g}_{ta(K)}$ and $\mathbf{g}_{tb(K)}$ are truncated to length L_t (and then possibly padded with $N - L_t$ zero elements). They represent the combined FI and FS IQ imbalance for the Kth transmit antenna.

At the receiver, let $\mathbf{z}_{(J)}$ represent the down-converted baseband symbol for the Jth receive antenna. This symbol is distorted by combined FS and FI IQ imbalance modeled by filters $\mathbf{g}_{ra(J)}$ and $\mathbf{g}_{rb(J)}$ of length L_r, where $\mathbf{g}_{ra(J)}$ and $\mathbf{g}_{rb(J)}$ are defined similar to $\mathbf{g}_{ta(K)}$ and $\mathbf{g}_{tb(K)}$ in equation (6.2). The received symbol $\mathbf{z}_{(J)}$ can now be written as:

$$\mathbf{z}_{(J)} = \mathbf{g}_{ra(J)} \star \sum_{K=1}^{N_t} \Big(\mathbf{h}_{(J,K)} \star \mathbf{p}_{(K)} \Big) + \mathbf{g}_{rb(J)} \star \sum_{K=1}^{N_t} \Big(\mathbf{h}^*_{(J,K)} \star \mathbf{p}^*_{(K)} \Big) + \mathbf{n}_{c(J)} \quad (6.3)$$

where $\mathbf{n}_{c(J)} = \mathbf{g}_{ra(J)} \star \mathbf{n}_{(J)} + \mathbf{g}_{rb(J)} \star \mathbf{n}^*_{(J)}$ is an improper complex noise vector derived from a zero mean additive white Gaussian noise (AWGN) vector $\mathbf{n}_{(J)}$. $\mathbf{h}_{(J,K)}$ is the baseband equivalent of the multipath frequency selective quasi static channel of length L between the Kth transmit and J^{th} receive antenna. Substituting equation (6.2) in (6.3) leads to:

$$\begin{aligned} \mathbf{z}_{(J)} = \sum_{K=1}^{N_t} [& \underbrace{\big(\mathbf{g}_{ra(J)} \star \mathbf{h}_{(J,K)} \star \mathbf{g}_{ta(K)} + \mathbf{g}_{rb(J)} \star \mathbf{h}^*_{(J,K)} \star \mathbf{g}^*_{tb(K)} \big)}_{\mathbf{d}_{a(J,K)}} \star \mathbf{s}_{(K)} \\ & + \underbrace{\big(\mathbf{g}_{ra(J)} \star \mathbf{h}_{(J,K)} \star \mathbf{g}_{tb(K)} + \mathbf{g}_{rb(J)} \star \mathbf{h}^*_{(J,K)} \star \mathbf{g}^*_{ta(K)} \big)}_{\mathbf{d}_{b(J,K)}} \star \mathbf{s}^*_{(K)}] + \mathbf{n}_{c(J)} \end{aligned} \quad (6.4)$$

where $\mathbf{d}_{a(J,K)}$ and $\mathbf{d}_{b(J,K)}$ are the combined transmit IQ, channel and receive IQ impulse responses for the Kth transmit and J^{th} receive antenna. Both $\mathbf{d}_{a(J,K)}$ and $\mathbf{d}_{b(J,K)}$ are of length $L_t + L + L_r - 2$ and are assumed to be shorter than the CP length, i.e., $(L_t + L + L_r - 2 \leq \nu)$, thus no ISI appears between adjacent OFDM symbols.

The received symbol $\mathbf{z}_{(J)}$ is serial-to-parallel converted and the part corresponding to the CP is removed. The received symbol is then transformed to the frequency domain by the DFT operation. The frequency domain received symbol is now written as:

$$\begin{aligned} \mathbf{Z}_{(J)} = & \sum_{K=1}^{N_t} [\mathbf{D}_{a(J,K)}.\mathbf{S}_{(K)} + \mathbf{D}_{b(J,K)}.\mathbf{S}^*_{m(K)}] + \mathbf{G}_{ra(J)} \star \mathbf{N}_{(J)} + \mathbf{G}_{rb(J)} \star \mathbf{N}^*_{m(J)} \\ = & \sum_{K=1}^{N_t} [(\mathbf{G}_{ra(J)}.\mathbf{H}_{(J,K)}.\mathbf{G}_{ta(K)} + \mathbf{G}_{rb(J)}.\mathbf{H}^*_{m(J,K)}.\mathbf{G}^*_{tb_m(K)}).\mathbf{S}_{(K)} \\ & + (\mathbf{G}_{ra(J)}.\mathbf{H}_{(J,K)}.\mathbf{G}_{tb(K)} + \mathbf{G}_{rb(J)}.\mathbf{H}^*_{m(J,K)}.\mathbf{G}^*_{ta_m(K)}).\mathbf{S}^*_{m(K)}] + \mathbf{N}_{c(J)} \end{aligned} \quad (6.5)$$

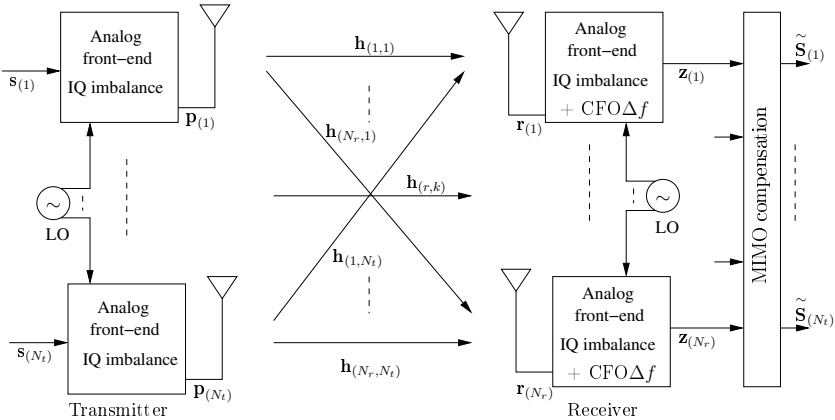

Figure 6.1: SU MIMO OFDM system impaired with transmitter/receiver IQ imbalance and CFO

where $\mathbf{Z}_{(J)}, \mathbf{D}_{a(J,K)}, \mathbf{D}_{b(J,K)}, \mathbf{H}_{(J,K)}, \mathbf{N}_{(J)}$ and $\mathbf{N}_{c(J)}$ are frequency domain representations of $\mathbf{z}_{(J)}, \mathbf{d}_{a(J,K)}, \mathbf{d}_{b(J,K)}, \mathbf{h}_{(J,K)}, \mathbf{n}_{(J)}$ and $\mathbf{n}_{c(J)}$.

Equation (6.5) shows that every received symbol $\mathbf{Z}_{(J)}$ (for $J = 1 \ldots N_r$) is a weighted sum of N_t transmitted OFDM symbols ($\mathbf{S}_{(K)}$) plus interference from the mirror symbols ($\mathbf{S}^*_{m(K)}$). This interference can severely deteriorate the performance of the system.

In the presence of a CFO Δf between the transmitter and receiver LOs, the received symbol $\mathbf{z}_{(J)}$ can be written as:

$$\mathbf{z}_{(J)} = \mathbf{g}_{ra(J)} \star (\mathbf{r}_{(J)}.e^{\jmath 2\pi \Delta f.\mathbf{t}}) + \mathbf{g}_{rb(J)} \star (\mathbf{r}^*_{(J)}.e^{-\jmath 2\pi \Delta f.\mathbf{t}}) \tag{6.6}$$

where $\mathbf{r}_{(J)} = \sum_{K=1}^{N_t} \mathbf{h}_{(J,K)} \star \mathbf{p}_{(K)} + \mathbf{n}_{(J)}$. A point-to-point SU MIMO OFDM system impaired with both transmitter/receiver IQ imbalance and CFO is illustrated in **Figure 6.1**. In the next sections, we develop joint compensation solutions based on equation (6.5) and (6.6).

6.3 Joint IQ Imbalance and Channel Compensation

We will first derive a joint compensation solution for transmitter/receiver IQ imbalance and channel distortion. Following the system model from section 6.2,

equation (6.5) can be written for the received symbol $\mathbf{Z}_{(J)}$ and the complex conjugate of its mirror symbol $\mathbf{Z}^*_{m(J)}$ (for $J = 1 \dots N_r$) as follows:

$$\underbrace{\begin{bmatrix} \begin{pmatrix} \mathbf{Z}_{(1)}[l] \\ \mathbf{Z}^*_{(1)}[l_m] \end{pmatrix} \\ \vdots \\ \begin{pmatrix} \mathbf{Z}_{(N_r)}[l] \\ \mathbf{Z}^*_{(N_r)}[l_m] \end{pmatrix} \end{bmatrix}}_{\mathbf{Z}_{tot}[l]} = \underbrace{\begin{bmatrix} \left(\mathbf{D}_{tot}(1,1)[l]\right) & \dots & \left(\mathbf{D}_{tot}(1,N_t)[l]\right) \\ \vdots & \ddots & \vdots \\ \left(\mathbf{D}_{tot}(N_r,1)[l]\right) & \dots & \left(\mathbf{D}_{tot}(N_r,N_t)[l]\right) \end{bmatrix}}_{\mathbf{D}_{tot}[l]} \underbrace{\begin{bmatrix} \begin{pmatrix} \mathbf{S}_{(1)}[l] \\ \mathbf{S}^*_{(1)}[l_m] \end{pmatrix} \\ \vdots \\ \begin{pmatrix} \mathbf{S}_{(N_t)}[l] \\ \mathbf{S}^*_{(N_t)}[l_m] \end{pmatrix} \end{bmatrix}}_{\mathbf{S}_{tot}[l]}$$

$$+ \underbrace{\begin{bmatrix} \begin{pmatrix} \mathbf{N}_{c(1)}[l] \\ \mathbf{N}^*_{c(1)}[l_m] \end{pmatrix} \\ \vdots \\ \begin{pmatrix} \mathbf{N}_{c(N_r)}[l] \\ \mathbf{N}^*_{c(N_r)}[l_m] \end{pmatrix} \end{bmatrix}}_{\mathbf{N}_{c_{tot}}[l]} \tag{6.7}$$

where the sub-matrix $\mathbf{D}_{tot}(J,K)[l] = \begin{pmatrix} \mathbf{D}_{a(J,K)}[l] & \mathbf{D}_{b(J,K)}[l] \\ \mathbf{D}^*_{b(J,K)}[l_m] & \mathbf{D}^*_{a(J,K)}[l_m] \end{pmatrix}$. The matrix $\mathbf{D}_{tot}[l]$ represents the joint transmitter/receiver IQ imbalance and channel distortion for the received symbol matrix $\mathbf{Z}_{tot}[l]$.

Based on equation (6.7), we can generate symbol estimates $\widetilde{\mathbf{S}}_{tot-}[l]$ as:

$$\underbrace{\begin{bmatrix} \widetilde{\mathbf{S}}_{(1)}[l] \\ \vdots \\ \widetilde{\mathbf{S}}_{(N_t)}[l] \end{bmatrix}}_{\widetilde{\mathbf{S}}_{tot-}[l]} = \mathbf{W}_{tot-}[l]\mathbf{Z}_{tot}[l] \tag{6.8}$$

where $\mathbf{W}_{tot-}[l] = \begin{bmatrix} (\mathbf{W}_{a(1,1)}[l] & \mathbf{W}_{b(1,1)}[l]) & \dots & (\mathbf{W}_{a(N_r,1)}[l] & \mathbf{W}_{b(N_r,1)}[l]) \\ & \vdots & \ddots & & \vdots \\ (\mathbf{W}_{a(1,N_t)}[l] & \mathbf{W}_{b(1,N_t)}[l]) & \dots & (\mathbf{W}_{a(N_r,N_t)}[l] & \mathbf{W}_{b(N_r,N_t)}[l]) \end{bmatrix}$

and $\mathbf{W}_{a(J,K)}[l]$ and $\mathbf{W}_{b(J,K)}[l]$ are the coefficients of a $2N_rN_t$-tap FEQ. Equation (6.8) show that a total of $2(N_t \times N_r)$ elements in $\mathbf{W}_{tot-}[l]$ will have to be known to finally obtain the estimate of transmitted symbols $\widetilde{\mathbf{S}}_{tot-}[l]$. The FEQ coefficients

are estimated based on an MSE minimization:

$$\underset{\mathbf{W}_{tot-}[l]}{min}\, \Xi \left\{ \left| \widetilde{\mathbf{S}}_{tot-}[l] - \mathbf{W}_{tot-}[l]\mathbf{Z}_{tot}[l] \right|^2 \right\} \tag{6.9}$$

To obtain an estimate of the $\mathbf{W}_{tot-}[l]$ coefficients, we consider the availability of an M_l long sequence of LT symbols that are also constructed based on equation (6.1). The LS estimate of $\mathbf{W}_{tot-}[l]$ is then given as:

$$\mathbf{W}_{tot-}[l] = \mathbf{S}^{Tr}_{tot-}[l]\mathbf{Z}^{Tr^{\dagger}}_{tot}[l] \tag{6.10}$$

where $\mathbf{Z}^{Tr}_{tot}[l] = \begin{bmatrix} \begin{pmatrix} \mathbf{Z}^{(1)}_{(1)}[l] \\ \mathbf{Z}^{*(1)}_{(1)}[l_m] \end{pmatrix} & \cdots & \begin{pmatrix} \mathbf{Z}^{(M_l)}_{(1)}[l] \\ \mathbf{Z}^{*(M_l)}_{(1)}[l_m] \end{pmatrix} \\ \vdots & \ddots & \vdots \\ \begin{pmatrix} \mathbf{Z}^{(1)}_{(N_r)}[l] \\ \mathbf{Z}^{*(1)}_{(N_r)}[l_m] \end{pmatrix} & \cdots & \begin{pmatrix} \mathbf{Z}^{(M_l)}_{(N_r)}[l] \\ \mathbf{Z}^{*(M_l)}_{(N_r)}[l_m] \end{pmatrix} \end{bmatrix}$

and $\mathbf{S}^{Tr}_{tot-}[l] = \begin{bmatrix} (\mathbf{S}^{(1)}_{(1)}[l]) & \cdots & (\mathbf{S}^{(M_l)}_{(1)}[l]) \\ \vdots & \ddots & \vdots \\ (\mathbf{S}^{(1)}_{(N_t)}[l]) & \cdots & (\mathbf{S}^{(M_l)}_{(N_t)}[l]) \end{bmatrix}$

Here superscript (i) represents the training symbol number. Equation (6.10) shows that there are M_l equations in $2N_r$ unknowns (for each row of $\mathbf{W}_{tot-}[l]$). Hence to estimate $\mathbf{W}_{tot-}[l]$, we need an LT sequence length $M_l \geq 2N_r$. A longer training sequence will provide improved estimates due to a better noise averaging. In the case where $M_l = 2N_r$, the training symbols at subcarrier $[l]$ and $[l_m]$ of every LT symbols are required to be linearly independent of each other and also independent of subcarrier $[l]$ and $[l_m]$ of the LT symbols transmitted from other transmit antennas. This is required so that the inversion operation on the $\mathbf{Z}^{Tr}_{tot}[l]$ matrix always generates a unique solution.

Any adaptive algorithm, e.g. RLS, can also be used for the estimation of FEQ coefficients $\mathbf{W}_{tot-}[l]$ based on (6.9). The $2N_rN_t$-tap FEQ scheme is illustrated in **Figure 6.2**. In the absence of any IQ imbalance, the coefficient $\mathbf{W}_{b(J,K)}[l] = 0$, and then we have to estimate only $(N_t \times N_r)$ elements in $\mathbf{W}_{tot-}[l]$. The LT symbol sequence requirement in this case is only $M_l \geq N_r$. This corresponds to a standard MIMO channel equalizer consisting of a N_rN_t-tap FEQ needed for the estimation of the transmitted symbol estimates $\widetilde{\mathbf{S}}_{tot-}[l]$.

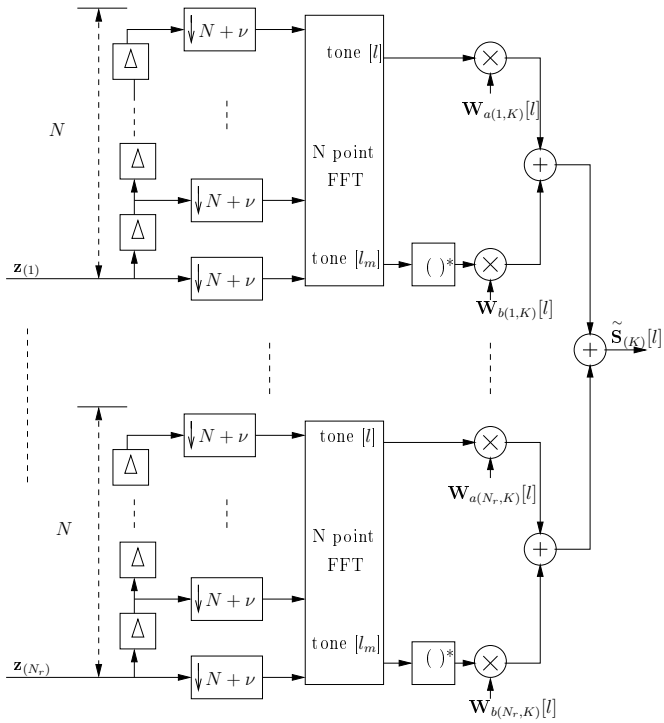

Figure 6.2: $2N_rN_t$-tap FEQ scheme for joint compensation of transmitter and receiver IQ imbalance

6.4 Joint IQ Imbalance, CFO and Channel Compensation

In the presence of CFO and transmitter/receiver IQ imbalance, we first develop a TEQ+FEQ based compensation scheme, similar to section 4.5, that compensates for receiver IQ imbalance and CFO in time domain and then a joint compensation of channel distortion and transmitter IQ imbalance in the frequency domain. In the second part, a PTEQ based compensation is derived, where we merge the entire equalization structure to form one unified equalizer in the frequency domain.

The estimation of CFO for a common LO at the front-end can be obtained by any suitable SISO CFO estimation algorithm which is robust under IQ imbalance distortion. Again, we consider the auto-correlation based scheme (for small CFOs) and the NLS based scheme (for large CFOs), as explained in section 4.3. The CFO estimation is obtained based on the transmission of M_s identical ST symbols of size $(N_s \times 1)$ from each of the Kth transmit antennas. A threshold can be considered

for the choice between the two CFO estimation schemes.

For both algorithms, a CFO $\Delta\widetilde{f}_{(J)}$ is initially estimated at each individual receive antenna and then the mean of all the obtained estimates $\Delta\widetilde{f} = \frac{1}{N_r}\sum_{J=1}^{N_r}\Delta\widetilde{f}_{(J)}$, provides an overall improved CFO estimate for the entire system. As in chapter 4, we also assume that the CFO estimate is quite accurate. Later on, an iterative scheme can be implemented to correct for any residual CFO in the system. Once the CFO is known, a TEQ+FEQ compensation scheme can be designed for the estimation of transmitted symbols $\widetilde{\mathbf{S}}_{tot-}[l]$.

TEQ + FEQ Based Compensation

In a MIMO system, every antenna branch experiences a different IQ imbalance distortion, hence, we design the TEQ filters for each receive antenna separately.

The TEQ has two filter branches $\mathbf{v}_{c(J)}$ and $\mathbf{v}_{d(J)}$ for every receive antenna ($J = 1 \ldots N_r$). Both $\mathbf{v}_{c(J)}$ and $\mathbf{v}_{d(J)}$ are L_r taps long. The filter $\mathbf{v}_{c(J)}$ is applied to $\mathbf{z}_{(J)}$ and the filter $\mathbf{v}_{d(J)}$ is applied to $\mathbf{z}^*_{(J)}$. This leads to:

$$\begin{aligned}\mathbf{z}_{q(J)} =& \mathbf{v}_{c(J)} \star \mathbf{z}_{(J)} + \mathbf{v}_{d(J)} \star \mathbf{z}^*_{(J)} \\ =& \underbrace{\left(\mathbf{v}_{c(J)} \star \mathbf{g}_{ra(J)} + \mathbf{v}_{d(J)} \star \mathbf{g}^*_{rb(J)}\right)}_{\mathbf{f}_{1(J)}} \star \left(\mathbf{r}_{(J)}.e^{\jmath 2\pi\Delta f.\mathbf{t}}\right) \\ &+ \underbrace{\left(\mathbf{v}_{c(J)} \star \mathbf{g}_{rb(J)} + \mathbf{v}_{d(J)} \star \mathbf{g}^*_{ra(J)}\right)}_{\mathbf{f}_{2(J)}} \star \left(\mathbf{r}^*_{(J)}.e^{-\jmath 2\pi\Delta f.\mathbf{t}}\right)\end{aligned} \tag{6.11}$$

Here, the filtered symbol $\mathbf{z}_{q(J)}$ is an $(N \times 1)$ vector and $\mathbf{z}_{(J)}$ is an $(N + L_r - 1 \times 1)$ received symbol vector. The received symbol $\mathbf{z}_{(J)}$ in equation (6.11) can be specified as:

$$\begin{aligned}\mathbf{z}_{(J)} =& \left(\sum_{K=1}^{N_t}[\mathbf{O}_1|\mathbf{T}_{da(J,K)}]\mathbf{P}_{\mathbf{CI}}\mathbf{F}^{-1}\mathbf{S}_{(K)}\right)e^{\jmath 2\pi\Delta f.\mathbf{t}} \\ &+ \left(\sum_{K=1}^{N_t}[\mathbf{O}_1|\mathbf{T}_{db(J,K)}]\mathbf{P}_{\mathbf{CI}}\mathbf{F}^{-1}\mathbf{S}^*_{m(K)}\right)e^{-\jmath 2\pi\Delta f.\mathbf{t}} + \mathbf{n}'_{c(J)}\end{aligned} \tag{6.12}$$

Here $\mathbf{O}_1 = \mathbf{0}_{(N+L_r-1\times\nu-L_t-L-2L_r+4)}, \mathbf{T}_{dk(J,K)}$ (for $k = a, b$) is a Toeplitz matrix of size $(N + L_r - 1 \times N + L_t + L + L_r + L_r - 4)$ with first column $[\mathbf{d}'_{k_{(J,K)}(L_t+L+L_r-3)}, \mathbf{0}_{(1\times N+L_r-1)}]^T$ and first row

$[\mathbf{d}'_{k_{(J,K)}(L_t+L+L_r-3)}, \ldots, \mathbf{d}'_{k_{(J,K)}(0)}, \mathbf{0}_{(1\times N+L_r-2)}]$. The vector $\mathbf{d}'_{k_{(J,K)}} = \mathbf{g}'_{rk(J)} \star \mathbf{h}_{(J,K)} \star \mathbf{g}_{ta(K)}$ where $\mathbf{g}'_{ra(J)} = \mathbf{g}_{ra(J)}.e^{-\jmath 2\pi \Delta \widetilde{f}.(0\ldots(L_r-1))^T}$ and $\mathbf{g}'_{rb(J)} = \mathbf{g}_{ra(J)}.e^{\jmath 2\pi \Delta \widetilde{f}.(0\ldots(L_r-1))^T}$. The noise term $\mathbf{n}'_{c(J)}$ is similarly modified by CFO.

The design target for the TEQ filters $\mathbf{v}_{c(J)}$ and $\mathbf{v}_{d(J)}$ is such that the term $\mathbf{f}_{2(J)}$ vanishes in equation (6.11). The solutions to this set of equations is $\mathbf{v}_{c(J)} = \mathbf{g}^*_{ra(J)}.\alpha$ and $\mathbf{v}_{d(J)} = -\mathbf{g}_{rb(J)}.\alpha$ where α is a non-zero scalar.

Once the receiver IQ imbalance has been compensated, we can then derotate the received symbol $\mathbf{z}_{q(J)}$ with $e^{-\jmath 2\pi \Delta \widetilde{f}.\mathbf{t}}$. This leads to:

$$\overset{\wedge}{\mathbf{z}}_{q(J)} = \mathbf{z}_{q(J)}.e^{-\jmath 2\pi \Delta \widetilde{f}.\mathbf{t}} = \overset{\wedge}{\mathbf{f}}_{1(J)} \star \mathbf{r}_{(J)} \tag{6.13}$$

where $\overset{\wedge}{\mathbf{f}}_{1(J)} = \mathbf{f}_{1(J)}.(e^{-\jmath 2\pi \Delta \widetilde{f}.(0\ldots(L_r-1))^T})$ is a modulated version of $\mathbf{f}_{1(J)}$. The resulting vector $\overset{\wedge}{\mathbf{z}}_{q(J)}$ is free from CFO and contains only transmitter IQ imbalance along with channel distortion. Each filtered sequence $\overset{\wedge}{\mathbf{z}}_{q(J)}$ (stacked into an N vector) is transformed into a frequency domain vector $\overset{\wedge}{\mathbf{Z}}_{q(J)}$ and then a $2N_rN_t$-tap FEQ is applied, similar to equation (6.8), to compensate for the remaining distortions and obtain an estimate of the transmitted symbol, given as:

$$\widetilde{\mathbf{S}}_{tot-}[l] = \mathbf{W}_{tot-}[l] \underbrace{\begin{bmatrix} \overset{\wedge}{\mathbf{Z}}_{q(1)}[l] \\ \overset{\wedge}{\mathbf{Z}}^*_{q(1)}[l_m] \\ \hline \vdots \\ \hline \overset{\wedge}{\mathbf{Z}}_{q(N_r)}[l] \\ \overset{\wedge}{\mathbf{Z}}^*_{q(N_r)}[l_m] \end{bmatrix}}_{\overset{\wedge}{\mathbf{z}}_{q_{tot}}[l]} \tag{6.14}$$

PTEQ Based Compensation

To transform the TEQ+FEQ scheme into a PTEQ scheme, we first swap the TEQ filtering operation (equation (6.11)) with the de-rotation $e^{-\jmath 2\pi \Delta \widetilde{f}.\mathbf{t}}$ (equation (6.13)). This results in a modified form (with modified equalizer coefficients $\mathbf{v}_{c(J)}$

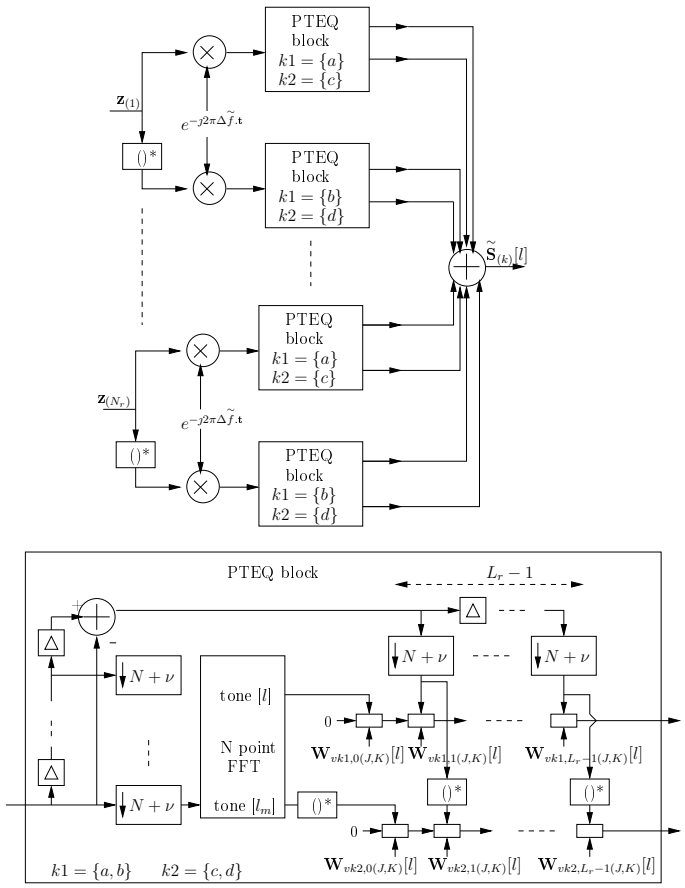

Figure 6.3: $4N_rN_t$-branch PTEQ scheme for joint compensation of transmitter/receiver IQ imbalance and CFO

and $\mathbf{v}_{d(J)}$) of equation (6.11) given as:

$$\begin{aligned}\overset{\wedge}{\mathbf{z}}_{q(J)} &= \mathbf{v}_{c(J)} \star \left(\mathbf{z}_{(J)}.e^{-\jmath 2\pi\Delta\widetilde{f}.\mathbf{t}}\right) + \mathbf{v}_{d(J)} \star \left(\mathbf{z}^*_{(J)}.e^{-\jmath 2\pi\Delta\widetilde{f}.\mathbf{t}}\right) \\ &= \underbrace{\left(\mathbf{v}_{c(J)} \star \overset{\wedge}{\mathbf{g}}_{ra(J)} + \mathbf{v}_{d(J)} \star \overset{\wedge}{\mathbf{g}}^*_{rb(J)}\right)}_{\mathbf{f}_{1(J)}} \star \mathbf{r}_{(J)} \\ &+ \underbrace{\left(\mathbf{v}_{c(J)} \star \overset{\wedge}{\mathbf{g}}_{rb(J)} + \mathbf{v}_{d(J)} \star \overset{\wedge}{\mathbf{g}}^*_{ra(J)}\right)}_{\mathbf{f}_{2(J)}} \star \left(\mathbf{r}^*_{(J)}.e^{-2\jmath 2\pi\Delta\widetilde{f}.\mathbf{t}}\right)\end{aligned} \tag{6.15}$$

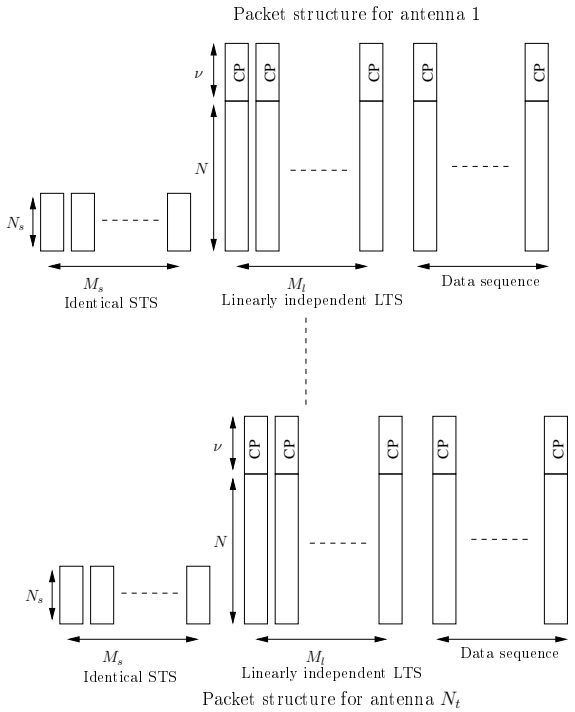

Figure 6.4: Packet structure for joint compensation scheme

Here $\hat{\mathbf{g}}_{ra(J)} = \mathbf{g}_{ra(J)}.(e^{-\jmath\tilde{\mathbf{w}}})$, $\hat{\mathbf{g}}_{rb(J)} = \mathbf{g}_{rb(J)}.(e^{\jmath\tilde{\mathbf{w}}})$ with $\tilde{\mathbf{w}} = 2\pi\Delta\tilde{f}.(0\ldots(L_r - 1))^T$. To suppress $\mathbf{r}^*_{(J)}$ in equation (6.15), we now require $\mathbf{v}_{c(J)} = \hat{\mathbf{g}}^*_{ra(J)}.\alpha$ and $\mathbf{v}_{d(J)} = -\hat{\mathbf{g}}_{rb(J)}.\alpha$.

The TEQ filtering is then transformed to the frequency domain resulting in a PTEQ employing two DFT operations and $L_r - 1$ difference terms [113]. Equation (6.15) can then be written as:

$$\hat{\mathbf{Z}}_{q(J)}[l] = \begin{bmatrix}\mathbf{V}_{c(J)}[l]\\ \mathbf{V}_{d(J)}[l]\end{bmatrix}^T \begin{bmatrix}\mathbf{F}_{ext}[l]\mathbf{z}_{(J)}.e^{-\jmath 2\pi\Delta\tilde{f}.\mathbf{t}}\\ (\mathbf{F}_{ext}[l]\mathbf{z}^*_{(J)}.e^{-\jmath 2\pi\Delta\tilde{f}.\mathbf{t}})\end{bmatrix} \tag{6.16}$$

where $\mathbf{V}_{c(J)}[l]$ and $\mathbf{V}_{d(J)}[l]$ are filter vectors of size $(L_r \times 1)$. Here $\mathbf{F}_{ext}[l]$ is defined as in equation (3.20). We can now compensate for the remaining channel distortion and transmitter IQ imbalance parameters by applying a $2N_rN_t$-tap FEQ, similar to equation (6.14), to the received symbols $\hat{\mathbf{Z}}_{q(J)}[l]$ and $\hat{\mathbf{Z}}^*_{q(J)}[l_m]$.

As a final step, we merge the PTEQ (6.16) and the FEQ (6.14), resulting in a $4N_rN_t$-branch PTEQ. The transmitted symbol estimate is then obtained as:

$$\widetilde{\mathbf{S}}_{(K)}[l] = \sum_{J=1}^{N_r} \begin{bmatrix} \mathbf{W}_{va(J,K)}[l] \\ \mathbf{W}_{vb(J,K)}[l] \\ \mathbf{W}_{vc(J,K)}[l] \\ \mathbf{W}_{vd(J,K)}[l] \end{bmatrix}^T \underbrace{\begin{bmatrix} \mathbf{F}_{ext}[l]\mathbf{z}_{(J)}.e^{-\jmath 2\pi \Delta \widetilde{f}.\mathbf{t}} \\ \mathbf{F}_{ext}[l]\mathbf{z}^*_{(J)}.e^{-\jmath 2\pi \Delta \widetilde{f}.\mathbf{t}} \\ (\mathbf{F}_{ext}[l_m]\mathbf{z}_{(J)}.e^{-\jmath 2\pi \Delta \widetilde{f}.\mathbf{t}})^* \\ (\mathbf{F}_{ext}[l_m]\mathbf{z}^*_{(J)}.e^{-\jmath 2\pi \Delta \widetilde{f}.\mathbf{t}})^* \end{bmatrix}}_{\mathbf{z}_{ext(J)}[l]} \tag{6.17}$$

where $\mathbf{W}_{va(J,K)}[l] \ldots \mathbf{W}_{vd(J,K)}[l]$ are filter vectors of size $(L_r \times 1)$. The PTEQ compensation scheme based on equation (6.17) is shown in **Figure 6.3**. We can now write an MMSE equation for (6.17), similar to equation (6.8), and then develop a training based LS or an adaptive RLS algorithm for the estimation of the PTEQ coefficients.

Equation (6.17) shows that in order to estimate the PTEQ coefficients an LT symbol sequence length $M_l \geq 4L_rNr$ is needed. The total number of PTEQ coefficients to be estimated is $4L_r(N_t \times N_r)$ per subcarrier. The transmission packet for the joint compensation scheme now consists of an identical ST symbol sequence for CFO estimation, followed by a linearly independent LT symbol sequence for the estimation of the PTEQ coefficients, and finally the data sequence. The ST symbol and LT symbol sequences can be obtained from any suitable alphabet. The packet structure for joint compensation scheme is shown in **Figure 6.4**.

Note:

- **Residual CFO error correction:** Following the section 4.5.2, the performance of the $4N_rN_t$-branch PTEQ (6.17) can be further improved by searching amongst various PTEQs and CFO values $\widetilde{\Delta f}$ such that the error in estimated symbol is minimized. As we assume to already have a good (initial) CFO estimate, the search amongst CFOs is now restricted to a narrow range of values. The PTEQ coefficients thus obtained are finally used for compensation.

- **Insufficient CP length:** Similar to the section 4.5.2, the derived $4N_rN_t$-branch PTEQ solution can also be applied in the case of insufficient CP length, i.e. $(\nu < L_t + L + 2L_r - 3)$. In this case, the PTEQ length is increased to $L'' = L' + L_r - 1$ taps, where L' taps are needed for the channel shortening operation and obtain sufficient improvement in performance. The total number of PTEQ coefficients to be estimated is $4L''(N_t \times N_r)$ per

subcarrier and we now need an LT symbol sequence length $M_l \geq 4L''Nr$ for the PTEQ initialization.

- **Generalized structure:** The proposed PTEQ solution is a generalized compensation structure that can be scaled for any number of transmitter and receiver antennas. The compensation structure can be further simplified for particular scenarios. For example, in the presence of only receiver IQ imbalance and CFO, the FEQ filters are applied only at the desired subcarriers $[l]$ and not at the mirror subcarriers $[l_m]$ in (6.14). Thus the final PTEQ structure has only half as many branches, i.e. $2N_rN_t$-branch PTEQ is now needed for compensation. Similarly the LT symbol sequence length $M_l \geq 2L_rNr$ is needed for the initialization of the PTEQ.

  In the case of transmitter and receiver IQ imbalance but no CFO, the transformation of the TEQ filters to the frequency domain is not needed. This is because the PTEQ will now jointly estimate and compensate the contribution of FS transmitter and receiver IQ imbalance in the frequency domain based on the suppression of interference from the mirror subcarrier. The PTEQ reduces to a $2N_rN_t$-tap FEQ as in (6.8). This PTEQ structure also corresponds to the case of only transmitter IQ imbalance or only receiver IQ imbalance with no CFO. In this case we need an LT sequence length $M_l \geq 2Nr$.

  In the presence of FI receiver IQ imbalance (i.e. no filter mismatch at the receiver front-end) together with FS transmitter IQ imbalance and CFO, the contribution of the TEQ is not needed any more in the PTEQ structure. The TEQ filters are set to unit coefficient filters with length $L_r = 1$ and the taps $\mathbf{v}_{c,0(J)} = \mathbf{v}_{d,0(J)} = 1$. Thus the PTEQ length is now reduced to $L_r = 1$. This finally results in a $4N_rN_t$-tap FEQ structure and we now need an LT sequence length $M_l \geq 4Nr$.

  Table 6.1 summarizes the different combination of FI/FS transmitter/receiver IQ imbalance, CFO and sufficient/insufficient CP length and their corresponding joint compensation solutions.

6.5 Space-Time Block Codes

Space-time block code (STBC) is a technique that transmits multiple copies of the data across a number of antennas so as to improve the reliability of data transfer. As the transmitted symbol has to traverse a multipath environment, some of the received copies will be less distorted compared to the others. STBC combines all the copies of the received data in an optimal way so as to extract as much information from each of them as possible. STBCs as originally introduced, and as usually studied, are orthogonal. This means that the STBC is designed such

Tx IQ	Rx IQ	CFO	CP length	#taps/ PTEQ branches	branch length	structure
no	no	no	sufficient	1	1	N_rN_t-tap FEQ
no	no	no	insufficient	1	L'	N_rN_t-branch PTEQ
FI	FI	no	sufficient	2	1	$2N_rN_t$-tap FEQ
FS	FS	no	sufficient	2	1	$2N_rN_t$-tap FEQ
no	FI	yes	sufficient	2	1	$2N_rN_t$-tap FEQ
FI	FI	no	insufficient	2	L'	$2N_rN_t$-branch PTEQ
FS	FS	no	insufficient	2	$L' + L_r - 1$	$2N_rN_t$-branch PTEQ
no	FS	yes	sufficient	2	L_r	$2N_rN_t$-branch PTEQ
no	FS	yes	insufficient	2	$L' + L_r - 1$	$2N_rN_t$-branch PTEQ
FI	FI	yes	sufficient	4	1	$4N_rN_t$-tap FEQ
FS	FI	yes	sufficient	4	1	$4N_rN_t$-tap FEQ
FI	FI	yes	insufficient	4	L'	$4N_rN_t$-branch PTEQ
FS	FI	yes	insufficient	4	L'	$4N_rN_t$-branch PTEQ
FS	FS	yes	sufficient	4	L_r	$4N_rN_t$-branch PTEQ
FS	FS	yes	insufficient	4	$L' + L_r - 1$	$4N_rN_t$-branch PTEQ

Table 6.1: Different combination of FI/FS transmitter/receiver IQ imbalance, CFO and sufficient/insufficient CP length and their corresponding joint compensation solutions

that the vectors representing any pair of columns taken from the coding matrix is orthogonal. The result of this is simple, linear, optimal decoding at the receiver.

In the presence transmitter/receiver IQ imbalance and CFO, the system of equations given by (6.4)-(6.6) can be reworked to exploit the structure of the STBC based single-user systems. In this section, we propose joint compensation schemes for Alamouti coded OFDM systems. It is later shown that the joint compensation solutions can also be extended for higher order orthogonal STBC systems.

6.5.1 Joint IQ Imbalance and Channel Compensation

The STBC systems can be considered as a special case of SU MIMO systems for the derivation of joint compensation solution. We consider the presence of transmitter and receiver IQ imbalance in a multiple-input single-output (MISO) based STBC systems. In this case the received symbol in equation (6.5) can be

rewritten as:

$$\mathbf{Z}^{(i_{stbc})} = \sum_{K=1}^{N_t} [\mathbf{D}_{a(K)}.\mathbf{S}_{(K)}^{(i_{stbc})} + \mathbf{D}_{b(K)}.\mathbf{S}_{m(K)}^{*(i_{stbc})}] + \mathbf{N}_c^{(i_{stbc})} \tag{6.18}$$

Here i_{stbc} corresponds to the time index of the STBC codeword $\mathbf{C}_w$. Notice that the receiver antenna subscript ($J = 1 \dots N_r$) has been removed here, as there is only one receiver antenna.

We first consider an (2x1) Alamouti coding based STBC OFDM system [2] i.e., the transmitter has 2 antennas ($N_t = 2$) and the receiver has 1 antenna ($N_r = 1$). The STBC codeword $\mathbf{C}_w$ can be given as:

$$\mathbf{C}_w = \begin{pmatrix} \mathbf{S}_1 & \mathbf{S}_2^* \\ \mathbf{S}_2 & -\mathbf{S}_1^* \end{pmatrix} \tag{6.19}$$

where the element of the pth row and the ith column of $\mathbf{C}_w$ denotes the OFDM symbol sent from the Kth transmit antenna at time i_{stbc} (i.e. $i_{stbc} = 1, 2$).

Equation (6.18) can now be rewritten in matrix form as:

$$\begin{pmatrix} \mathbf{Z}^{(1)}[l] \\ \mathbf{Z}^{(2)}[l] \end{pmatrix} = \begin{pmatrix} \mathbf{S}_1[l] & \mathbf{S}_1^*[l_m] & \mathbf{S}_2[l] & \mathbf{S}_2^*[l_m] \\ \mathbf{S}_2^*[l] & \mathbf{S}_2[l_m] & -\mathbf{S}_1^*[l] & -\mathbf{S}_1[l_m] \end{pmatrix} \begin{pmatrix} \mathbf{D}_{a(1)}[l] \\ \mathbf{D}_{b(1)}[l] \\ \mathbf{D}_{a(2)}[l] \\ \mathbf{D}_{b(2)}[l] \end{pmatrix} + \begin{pmatrix} \mathbf{N}_c^{(1)}[l] \\ \mathbf{N}_c^{(2)}[l] \end{pmatrix} \tag{6.20}$$

By also considering the complex conjugate of the mirror carrier and then exploiting the Alamouti code structure, equation (6.20) can be written as [101]:

$$\begin{pmatrix} \mathbf{Z}^{(1)}[l] \\ \mathbf{Z}^{*(2)}[l] \\ \mathbf{Z}^{*(1)}[l_m] \\ \mathbf{Z}^{(2)}[l_m] \end{pmatrix} = \begin{pmatrix} \Gamma_{1,1} & \Gamma_{1,2} \\ \Gamma_{2,1} & \Gamma_{2,2} \end{pmatrix} \begin{pmatrix} \mathbf{S}_1[l] \\ \mathbf{S}_2[l] \\ \mathbf{S}_1^*[l_m] \\ \mathbf{S}_2^*[l_m] \end{pmatrix} + \begin{pmatrix} \mathbf{N}_c^{(1)}[l] \\ \mathbf{N}_c^{*(2)}[l] \\ \mathbf{N}_c^{*(1)}[l_m] \\ \mathbf{N}_c^{(2)}[l_m] \end{pmatrix} \tag{6.21}$$

where the sub-matrices are given as:

$$\begin{aligned} \Gamma_{1,1} &= \begin{pmatrix} \mathbf{D}_{a(1)}[l] & \mathbf{D}_{a(2)}[l] \\ -\mathbf{D}_{a(2)}^*[l] & \mathbf{D}_{a(1)}^*[l] \end{pmatrix} \Gamma_{1,2} = \begin{pmatrix} \mathbf{D}_{b(1)}[l] & \mathbf{D}_{b(2)}[l] \\ -\mathbf{D}_{b(2)}^*[l] & \mathbf{D}_{b(1)}^*[l] \end{pmatrix} \\ \Gamma_{2,1} &= \begin{pmatrix} \mathbf{D}_{b(1)}^*[l_m] & \mathbf{D}_{b(2)}^*[l_m] \\ -\mathbf{D}_{b(2)}[l_m] & \mathbf{D}_{b(1)}[l_m] \end{pmatrix} \Gamma_{2,2} = \begin{pmatrix} \mathbf{D}_{a(1)}^*[l_m] & \mathbf{D}_{a(2)}^*[l_m] \\ -\mathbf{D}_{a(2)}[l_m] & \mathbf{D}_{a(1)}[l_m] \end{pmatrix} \end{aligned} \tag{6.22}$$

It should be noted that in the case of no transmitter and receiver IQ imbalance, the sub-matrices $\Gamma_{1,2}$ and $\Gamma_{2,1}$ will vanish, in which case equation (6.22) will reduce to two 2×2 decoupled systems as in standard Alamouti decoding [101]. A regular Alamouti decoder can then be used to recover the transmitted symbol. In the

present case, let $\overset{\sim}{\mathbf{S}}^{(1)}_{(K)}[l]$ be the estimate for the $[l]^{th}$ subcarrier of the OFDM symbol transmitted over K^{th} antenna at $i_{stbc} = 1$. This estimate is then obtained as:

$$\overset{\sim}{\mathbf{S}}^{(1)}_{(K)}[l] = \begin{pmatrix} \mathbf{W}_{1(K)}[l] \\ \mathbf{W}_{2(K)}[l] \\ \mathbf{W}_{3(K)}[l] \\ \mathbf{W}_{4(K)}[l] \end{pmatrix}^{T} \begin{pmatrix} \mathbf{Z}^{(1)}[l] \\ \mathbf{Z}^{*(2)}[l] \\ \mathbf{Z}^{*(1)}[l_m] \\ \mathbf{Z}^{(2)}[l_m] \end{pmatrix} \tag{6.23}$$

where $\mathbf{W}_{p(K)}[l]$ for $(p = \{1 \dots 4\})$ are the coefficients of a $(2N_rN_t=)$four-tap FEQ.

The compensation scheme can easily be extended for higher order STBC OFDM systems. It should be noted that the design of optimized STBC codes is beyond the scope of this thesis. As an example we consider a quasi orthogonal STBC (QOSTBC - 4x1) system where the STBC codeword $\mathbf{C}_w$ can be given as:

$$\mathbf{C}_w = \begin{pmatrix} \mathbf{S}_1 & -\mathbf{S}_2^* & -\mathbf{S}_3^* & \mathbf{S}_4 \\ \mathbf{S}_2 & \mathbf{S}_1^* & -\mathbf{S}_4^* & -\mathbf{S}_3 \\ \mathbf{S}_3 & -\mathbf{S}_4^* & \mathbf{S}_1^* & -\mathbf{S}_2 \\ \mathbf{S}_4 & \mathbf{S}_3^* & \mathbf{S}_2^* & \mathbf{S}_1 \end{pmatrix} \tag{6.24}$$

In this case, the estimate $\overset{\sim}{\mathbf{S}}^{(1)}_{(K)}[l]$ can be obtained as:

$$\overset{\sim}{\mathbf{S}}^{(1)}_{(K)}[l] = \begin{pmatrix} \mathbf{W}_{1(K)}[l] \\ \mathbf{W}_{2(K)}[l] \\ \mathbf{W}_{3(K)}[l] \\ \mathbf{W}_{4(K)}[l] \end{pmatrix}^{T} \begin{pmatrix} \mathbf{Z}^{(1)}[l] \\ \mathbf{Z}^{*(2)}[l] \\ \mathbf{Z}^{*(3)}[l] \\ \mathbf{Z}^{(4)}[l] \end{pmatrix} + \begin{pmatrix} \mathbf{W}_{5(K)}[l] \\ \mathbf{W}_{6(K)}[l] \\ \mathbf{W}_{7(K)}[l] \\ \mathbf{W}_{8(K)}[l] \end{pmatrix}^{T} \begin{pmatrix} \mathbf{Z}^{*(1)}[l_m] \\ \mathbf{Z}^{(2)}[l_m] \\ \mathbf{Z}^{(3)}[l_m] \\ \mathbf{Z}^{*(4)}[l_m] \end{pmatrix} \tag{6.25}$$

where $\mathbf{W}_{p(K)}[l]$ for $(p = \{1 \dots 8\})$ are the coefficients of a $(2N_rN_t=)$eight-tap FEQ.

Equations (6.23) and (6.25) show that we have to estimate $(2 \times N_t^2)$ coefficients and that the length of LT symbol sequence $M_l > 2N_t$ in order to estimate the transmitted symbols in Alamouti and QOSTBC OFDM systems.

6.5.2 Joint IQ Imbalance, CFO and Channel Compensation

In the presence of CFO, we follow the system of equations (6.11)-(6.14), because the compensation of receiver IQ imbalance and CFO in the time domain is not dependent on the STBC codeword. Thus the output of the TEQ filtered sequence $\overset{\wedge}{\mathbf{z}}_q[l]$ is transformed to the frequency domain symbol $\overset{\wedge}{\mathbf{Z}}_q[l]$, which is then applied to the STBC FEQ similar to equation (6.23) and (6.25) to recover the transmitted symbol $\overset{\sim}{\mathbf{S}}^{(1)}_{(K)}[l]$.

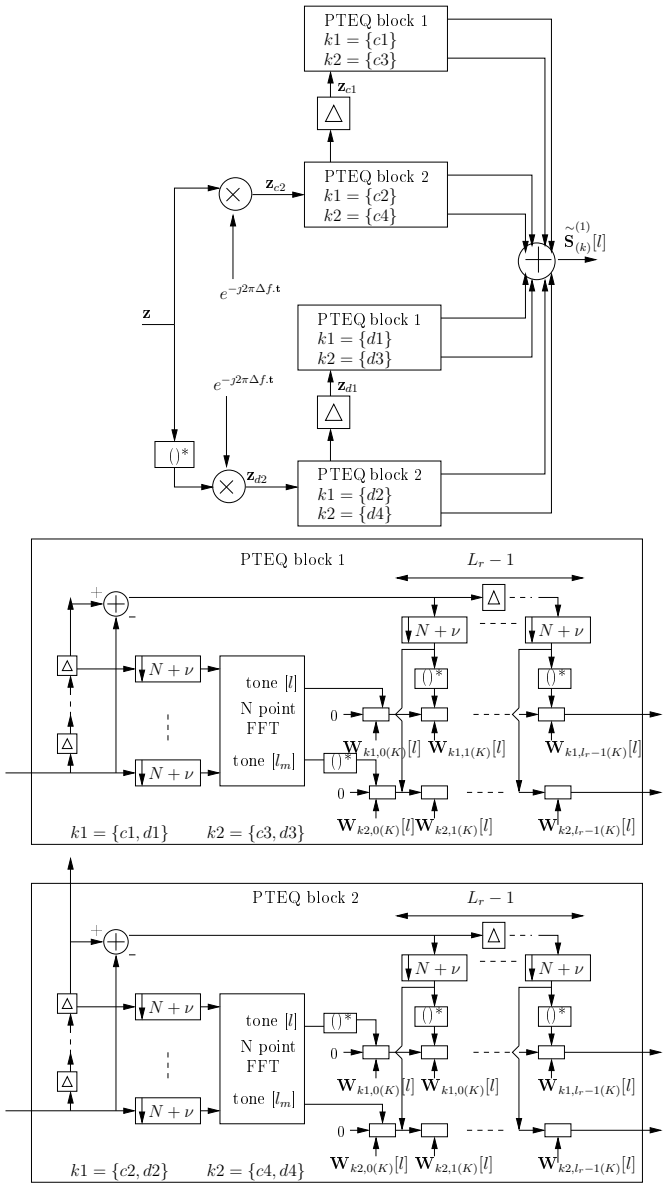

Figure 6.5: Eight-branch PTEQ compensation for Alamouti STBC transmission in the presence of transmitter/receiver IQ imbalance and CFO

In the case of Alamouti coding, the transmitted symbol is obtained as:

$$\overset{\sim}{\mathbf{S}}^{(1)}_{(K)}[l] = \begin{pmatrix} \mathbf{W}_{1(K)}[l] \\ \mathbf{W}_{2(K)}[l] \\ \mathbf{W}_{3(K)}[l] \\ \mathbf{W}_{4(K)}[l] \end{pmatrix}^{T} \begin{pmatrix} \overset{\wedge}{\mathbf{Z}}{}^{(1)}_{q}\ [l] \\ \overset{\wedge}{\mathbf{Z}}{}^{*(2)}_{q}\ [l] \\ \overset{\wedge}{\mathbf{Z}}{}^{*(1)}_{q}\ [l_m] \\ \overset{\wedge}{\mathbf{Z}}{}^{(2)}_{q}\ [l_m] \end{pmatrix} \tag{6.26}$$

The TEQ is then transformed to the frequency domain, resulting in a PTEQ employing two DFT operations and $L_r - 1$ difference terms. The PTEQ is now merged with the FEQ and this results into a $(4N_rN_t=)$eight-branch PTEQ, given as:

$$\overset{\sim}{\mathbf{S}}^{(1)}_{(K)}[l] = \begin{pmatrix} \mathbf{W}_{c1(K)}[l] \\ \mathbf{W}_{c2(K)}[l] \\ \mathbf{W}_{c3(K)}[l] \\ \mathbf{W}_{c4(K)}[l] \end{pmatrix}^{T} \begin{pmatrix} \mathbf{F}_{ext}[l]\mathbf{z}_{c1} \\ (\mathbf{F}_{ext}[l]\mathbf{z}_{c2})^{*} \\ (\mathbf{F}_{ext}[l_m]\mathbf{z}_{c1})^{*} \\ (\mathbf{F}_{ext}[l_m]\mathbf{z}_{c2}) \end{pmatrix} + \begin{pmatrix} \mathbf{W}_{d1(K)}[l] \\ \mathbf{W}_{d2(K)}[l] \\ \mathbf{W}_{d3(K)}[l] \\ \mathbf{W}_{d4(K)}[l] \end{pmatrix}^{T} \begin{pmatrix} \mathbf{F}_{ext}[l]\mathbf{z}_{d1} \\ (\mathbf{F}_{ext}[l]\mathbf{z}_{d2})^{*} \\ (\mathbf{F}_{ext}[l_m]\mathbf{z}_{d1})^{*} \\ (\mathbf{F}_{ext}[l_m]\mathbf{z}_{d2}) \end{pmatrix} \tag{6.27}$$

where $\mathbf{z}_{cx} = \mathbf{z}^{(x)}.e^{-\jmath 2\pi\Delta\widetilde{f}.\mathbf{t}}$ and $\mathbf{z}_{dx} = \mathbf{z}^{*(x)}.e^{-\jmath 2\pi\Delta\widetilde{f}.\mathbf{t}}$, and the filter coefficients $\mathbf{W}_{cp(K)}[l], \mathbf{W}_{dp(K)}[l]$ (for $p = \{1 \ldots 4\}$) are of size $(L_r \times 1)$.

Similarly we can also write equations for the QOSTBC case that correspond to (6.26) and (6.27). The final equalization structure in the QOSTBC consists of $(4N_rN_t=)$sixteen-branch PTEQ, given as:

$$\begin{aligned} \overset{\sim}{\mathbf{S}}^{(1)}_{(K)}[l] = {} & \begin{pmatrix} \mathbf{W}_{c1(K)}[l] \\ \mathbf{W}_{c2(K)}[l] \\ \mathbf{W}_{c3(K)}[l] \\ \mathbf{W}_{c4(K)}[l] \end{pmatrix}^{T} \begin{pmatrix} \mathbf{F}_{ext}[l]\mathbf{z}_{c1} \\ (\mathbf{F}_{ext}[l]\mathbf{z}_{c2})^{*} \\ (\mathbf{F}_{ext}[l]\mathbf{z}_{c3})^{*} \\ \mathbf{F}_{ext}[l]\mathbf{z}_{c4} \end{pmatrix} + \begin{pmatrix} \mathbf{W}_{c5(K)}[l] \\ \mathbf{W}_{c6(K)}[l] \\ \mathbf{W}_{c7(K)}[l] \\ \mathbf{W}_{c8(K)}[l] \end{pmatrix}^{T} \begin{pmatrix} (\mathbf{F}_{ext}[l_m]\mathbf{z}_{c1})^{*} \\ \mathbf{F}_{ext}[l_m]\mathbf{z}_{c2} \\ \mathbf{F}_{ext}[l_m]\mathbf{z}_{c3} \\ (\mathbf{F}_{ext}[l_m]\mathbf{z}_{c4})^{*} \end{pmatrix} + \\ & \begin{pmatrix} \mathbf{W}_{d1(K)}[l] \\ \mathbf{W}_{d2(K)}[l] \\ \mathbf{W}_{d3(K)}[l] \\ \mathbf{W}_{d4(K)}[l] \end{pmatrix}^{T} \begin{pmatrix} \mathbf{F}_{ext}[l]\mathbf{z}_{d1} \\ (\mathbf{F}_{ext}[l]\mathbf{z}_{d2})^{*} \\ (\mathbf{F}_{ext}[l]\mathbf{z}_{d3})^{*} \\ \mathbf{F}_{ext}[l]\mathbf{z}_{d4} \end{pmatrix} + \begin{pmatrix} \mathbf{W}_{d5(K)}[l] \\ \mathbf{W}_{d6(K)}[l] \\ \mathbf{W}_{d7(K)}[l] \\ \mathbf{W}_{d8(K)}[l] \end{pmatrix}^{T} \begin{pmatrix} (\mathbf{F}_{i}[l_m]\mathbf{z}_{d1})^{*} \\ \mathbf{F}_{i}[l_m]\mathbf{z}_{d2} \\ \mathbf{F}_{i}[l_m]\mathbf{z}_{d3} \\ (\mathbf{F}_{i}[l_m]\mathbf{z}_{d4})^{*} \end{pmatrix} \end{aligned} \tag{6.28}$$

where $\mathbf{z}_{cx}, \mathbf{z}_{dx}$, and the filter coefficients $\mathbf{W}_{cp(K)}[l], \mathbf{W}_{dp(K)}[l]$ (for $p = \{1 \ldots 8\}$) are defined similar to equation (6.27). Based on equations (6.27) and (6.28), a training

based LS or an adaptive RLS algorithm can be developed for the estimation of the PTEQ coefficients. The performance of the compensation schemes can be further improved by searching amongst various PTEQs and CFO values $\Delta\widetilde{f}$ such that the error in estimated symbol is minimized. The PTEQ coefficients thus obtained are finally used for compensation. Similar to the SU MIMO system, the derived PTEQ solutions can also be extended for the case of insufficient CP length by increasing the PTEQ length by $L' + L_r - 1$ taps, where L' taps are needed for the channel shortening operation. **Figure 6.5** illustrates the eight-branch PTEQ compensation scheme for the Alamouti case. A similar schematic for the QOSTBC case can also be drawn.

Equations (6.27) and (6.28) show that we need a LT symbol sequence length $M_l > 4N_t$ for the estimation of the PTEQ coefficients. The total number of coefficients to be estimated is $4L_rN_t^2$, and in the case of no filter mismatch, a total of $4N_t^2$ coefficients will have to be estimated. **Table 6.2** summarizes the computational complexity in terms of the number of coefficients to be estimated per subcarrier for the estimation of transmitted symbols in SU MIMO and Alamouti/QOSTBC based OFDM systems. The computational requirements are provided for different front-end non-idealities. The IQ imbalance is generally considered to be FS unless explicitly mentioned.

Non-ideality scenario	SU MIMO OFDM	STBC OFDM Alamouti/QOSTBC
Transmitter/Receiver IQ	$2(N_t \times N_r)$	$2N_t^2$
FI Receiver IQ + CFO	$2(N_t \times N_r)$	$2N_t^2$
Receiver IQ + CFO	$2L_r(N_t \times N_r)$	$2L_rN_t^2$
FI Transmitter/Receiver IQ + CFO	$4(N_t \times N_r)$	$2N_t^2$
Transmitter/Receiver IQ + CFO	$4L_r(N_t \times N_r)$	$4L_rN_t^2$

Table 6.2: Computational complexity in terms of number of coefficients to be estimated per subcarrier for different front-end non-ideality scenario

6.6 Multi-User MIMO

The joint compensation solutions proposed so far for MIMO and STBC systems address only the single-user scenario where a common LO serves at the transmitter (receiver) for all transmitter (receiver) antennas. In this section, we consider the multi-user (MU) scenario where every user has a front-end with multiple antennas supported by the user's individual LO.

We consider a base station (BS) equipped with N_b antennas supported by one LO, communicating with N_u users. Every user has N_y antennas supported by

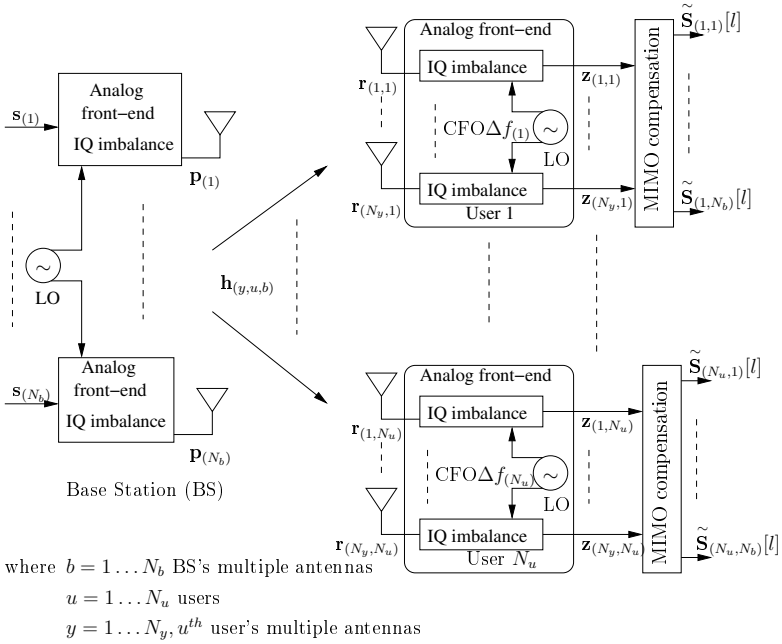

Figure 6.6: Down-link multi-user scenario

the user's individual LO. These LOs may not be perfectly synchronized with the LO of the BS and also with other users, leading to individual CFOs $\Delta f_{(U)}$ (for $U = 1 \ldots N_u$). In the following sections 6.6.1-6.6.2, we consider the down-link communication scenario (transmission from the BS to multiple users) and the up-link communication scenario (transmission from multiple users to the BS) respectively.

6.6.1 Down-Link Scenario

In the down-link scenario, the transmitter IQ imbalance is considered to be small or negligible as this occurs at the BS, whereas the receiver IQ imbalance can be severe due to the low-cost components used in the user's devices. **Figure 6.6** illustrates the down-link communication scenario between the BS and multiple users.

The expression of the received symbol (6.6) is now modified for the Yth antenna of the Uth user as:

$$\mathbf{z}_{(Y,U)} = \mathbf{g}_{ra(Y,U)} \star (\mathbf{r}_{(Y,U)}.e^{j2\pi\Delta f_{(U)}.\mathbf{t}}) + \mathbf{g}_{rb(Y,U)} \star (\mathbf{r}^*_{(Y,U)}.e^{-j2\pi\Delta f_{(U)}.\mathbf{t}}) \quad (6.29)$$

where $\mathbf{r}_{(Y,U)} = \sum_{b=1}^{N_b} \mathbf{h}_{(Y,U,B)} \star \mathbf{p}_{(B)} + \mathbf{n}_{(Y,U)}$. Here $\mathbf{h}_{(Y,U,B)}$ is the baseband equivalent of the multipath channel of length L between the Bth transmit (for $B = 1 \dots N_b$) and $(Y,U)^{th}$ (for $Y = 1 \dots N_y$ and $U = 1 \dots N_u$) receive antenna. Equation (6.29) is similar to equation (6.6), the only difference being that this time the CFO of the individual user is considered. Equation (6.29) shows that in the down-link scenario, the MU MIMO can be considered to be composed of N_u decoupled SU MIMO systems, i.e. the system model for each individual user is completely independent from other users. Thus, we can follow the estimation of the CFO and the joint compensation of IQ imbalance and CFO as explained earlier in section 6.4. The estimate of transmitted symbols is then given as:

$$\widetilde{\mathbf{S}}_{(U,B)}[l] = \sum_{Y=1}^{N_y} \begin{bmatrix} \mathbf{W}_{va(Y,U,B)}[l] \\ \mathbf{W}_{vb(Y,U,B)}[l] \\ \mathbf{W}_{vc(Y,U,B)}[l] \\ \mathbf{W}_{vd(Y,U,B)}[l] \end{bmatrix}^T \begin{bmatrix} \mathbf{F}_{ext}[l]\mathbf{z}_{(Y,U)}.e^{-\jmath 2\pi \Delta \widetilde{f}_{(U)}.\mathbf{t}} \\ (\mathbf{F}_{ext}[l_m]\mathbf{z}_{(Y,U)}.e^{-\jmath 2\pi \Delta \widetilde{f}_{(U)}.\mathbf{t}})^* \\ \mathbf{F}_{ext}[l]\mathbf{z}^*_{(Y,U)}.e^{-\jmath 2\pi \Delta \widetilde{f}_{(U)}.\mathbf{t}} \\ (\mathbf{F}_{ext}[l_m]\mathbf{z}^*_{(Y,U)}.e^{-\jmath 2\pi \Delta \widetilde{f}_{(U)}.\mathbf{t}})^* \end{bmatrix} \tag{6.30}$$

where $\mathbf{W}_{va(Y,U,B)}[l] \dots \mathbf{W}_{vd(Y,U,B)}[l]$ are filter coefficients of size $(L_r \times 1)$. A training based algorithm can be developed for the estimation of the compensation coefficients.

6.6.2 Up-Link Scenario

In the up-link scenario, the IQ imbalance at the transmitter front-end is considered to be severe due to the low cost components used in the user's devices, whereas the receiver IQ imbalance may be small or negligible as the BS front-end is considered to be close to ideal. **Figure 6.7** illustrates the up-link communication scenario between multiple users and the BS.

We assume the BS has a good estimate of the CFO's of the individual users. The estimate can be obtained either by using any one of the available CFO estimation algorithms for the MU MIMO case ([16], [120]), or by using the SU MIMO based CFO estimation algorithm during a period when only one user is operational (section 4.3).

We can now write the expression for the received symbol $\mathbf{z}_{(B)}$ at the Bth receive antenna as:

$$\mathbf{z}_{(B)} = \mathbf{g}_{ra(B)} \star \mathbf{r}_{(B)} + \mathbf{g}_{rb(B)} \star \mathbf{r}^*_{(B)} \tag{6.31}$$

where $\mathbf{r}_{(B)} = \sum_{U=1}^{N_u} \sum_{Y=1}^{N_y} \mathbf{h}_{(B,Y,U)} \star (\mathbf{p}_{(Y,U)}.e^{\jmath 2\pi \Delta f_{(U)}.\mathbf{t}}) + \mathbf{n}_{(B)}$ is the received symbol before being distorted by receiver IQ imbalance at the Bth receive antenna.

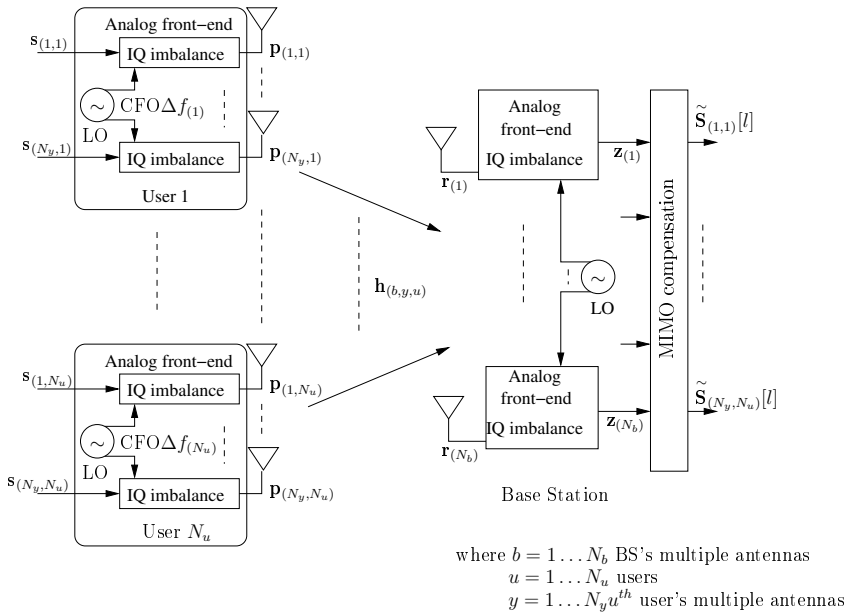

Figure 6.7: Up-link multi-user scenario

We apply two TEQ filters $\mathbf{v}_{c(B)}$ and $\mathbf{v}_{d(B)}$ of length L_r, similar to (6.11), at every B^{th} receive antenna. This results in the output symbol $\mathbf{z}_{q(B)}$ which is free of receiver IQ imbalance:

$$\begin{aligned}\mathbf{z}_{q(B)} =& \mathbf{v}_{c(B)} \star \mathbf{z}_{(B)} + \mathbf{v}_{d(B)} \star \mathbf{z}^*_{(B)} \\ =& \mathbf{f}_{1(B)} \star \left(\sum_{U=1}^{N_u} \sum_{Y=1}^{N_y} \mathbf{h}_{(B,Y,U)} \star \left(\mathbf{p}_{(Y,U)} . e^{\jmath 2\pi \Delta f_{(U)} . \mathbf{t}} \right) + \mathbf{n}_{(B)} \right)\end{aligned} \tag{6.32}$$

Here $\mathbf{f}_{1(B)} = (\mathbf{v}_{c(B)} \star \mathbf{g}_{ra(B)} + \mathbf{v}_{d(B)} \star \mathbf{g}^*_{rb(B)})$, $\mathbf{v}_{c(B)} = \mathbf{g}^*_{ra(B)}$ and $\mathbf{v}_{d(B)} = -\mathbf{g}_{rb(B)}$. The term $\mathbf{f}_{1(B)}$ can be considered as part of the channel $\mathbf{h}_{(B,Y,U)}$ as it does not result in any interference.

In order to eliminate the CFO, we have to suppress the entire contributing term from other users in the time domain. For this, an additional set of TEQ filters is needed, the design of which may vary depending on the number of antennas and users. We consider the case of a 2×2 MU MIMO system in detail. Here the system consists of two users where each user has one transmit antenna and a different CFO, and the BS has two receive antennas. Equation (6.32) is now

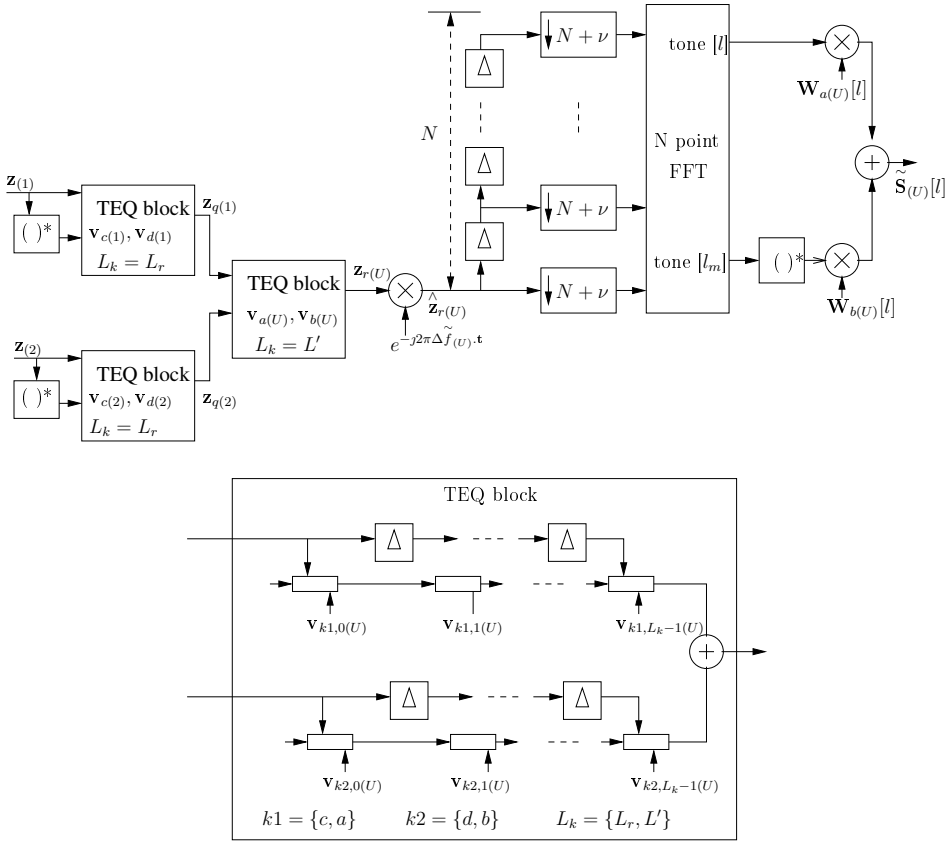

Figure 6.8: TEQ scheme for 2×2 MU MIMO up-link scenario in the presence of transmitter/receiver IQ imbalance and CFO

written in matrix form as:

$$\begin{bmatrix}\mathbf{z}_{q(1)}\\ \mathbf{z}_{q(2)}\end{bmatrix} = \begin{bmatrix}\mathbf{f}_{1(1)} \star \mathbf{h}_{(1,1,1)} & \mathbf{f}_{1(1)} \star \mathbf{h}_{(1,1,2)}\\ \mathbf{f}_{1(2)} \star \mathbf{h}_{(2,1,1)} & \mathbf{f}_{1(2)} \star \mathbf{h}_{(2,1,2)}\end{bmatrix} \star \begin{bmatrix}(\mathbf{p}_{(1,1)}.e^{\jmath 2\pi\Delta f_{(1)}.\mathbf{t}}) + \mathbf{n}_{(1)}\\ (\mathbf{p}_{(1,2)}.e^{\jmath 2\pi\Delta f_{(2)}.\mathbf{t}}) + \mathbf{n}_{(2)}\end{bmatrix} \quad (6.33)$$

To remove the term corresponding to the undesired user, we apply two additional TEQ filter branches given as $\mathbf{v}_{a(U)} = \mathbf{f}_{1(2)} \star \mathbf{h}_{(2,1,\tilde{\tilde{U}})}$ and $\mathbf{v}_{b(U)} = -\mathbf{f}_{1(1)} \star \mathbf{h}_{(1,1,\tilde{\tilde{U}})}$ to the symbols $\mathbf{z}_{q(1)}$ and $\mathbf{z}_{q(2)}$. Both filter are of length $L' = 2L_r + L - 2$. Here the subscript $\tilde{\tilde{U}}$ represents the undesired user that has to be suppressed. This results

in $\mathbf{z}_{s(U)}$ given as:

$$\begin{aligned}\mathbf{z}_{r(U)} =& \mathbf{v}_{a(U)} \star \mathbf{z}_{q(1)} + \mathbf{v}_{b(U)} \star \mathbf{z}_{q(2)} \\ =& \underbrace{\mathbf{v}_{a(U)} \star \mathbf{v}_{c(B)}}_{\mathbf{v}_{ac(U)}} \star \mathbf{z}_{(B)} + \underbrace{\mathbf{v}_{a(U)} \star \mathbf{v}_{d(B)}}_{\mathbf{v}_{ad(U)}} \star \mathbf{z}^*_{(B)} \\ &+ \underbrace{\mathbf{v}_{b(U)} \star \mathbf{v}_{c(B)}}_{\mathbf{v}_{bc(U)}} \star \mathbf{z}_{(B)} + \underbrace{\mathbf{v}_{b(U)} \star \mathbf{v}_{d(B)}}_{\mathbf{v}_{bd(U)}} \star \mathbf{z}^*_{(B)}\end{aligned} \tag{6.34}$$

where $\mathbf{v}_{xy(U)}$ are the unified TEQ filters formed by the linear combination of their respective filter constituents $\mathbf{v}_{x(U)}$ and $\mathbf{v}_{y(U)}$. If the estimate of the TEQ filter coefficients are accurate then the resulting symbol is given as:

$$\mathbf{z}_{r(1)} = \mathbf{f}_2 * (\mathbf{p}_{(1,1)}.e^{\jmath 2\pi \Delta f_{(1)}.\mathbf{t}} + \mathbf{n}_{(1)})$$

$$\mathbf{z}_{r(2)} = -\mathbf{f}_2 * (\mathbf{p}_{(1,2)}.e^{\jmath 2\pi \Delta f_{(2)}.\mathbf{t}} + \mathbf{n}_{(2)})$$

where $\mathbf{f}_2 = (\mathbf{f}_{1(1)} \star \mathbf{f}_{1(2)} \star \mathbf{h}_{(2,1,2)} \star \mathbf{h}_{(1,1,1)} - \mathbf{f}_{1(1)} \star \mathbf{f}_{1(2)} \star \mathbf{h}_{(1,1,2)} \star \mathbf{h}_{(2,1,1)})$. Thus the output of the TEQ consists of a scaled version of the desired user term rotated by the individual user's CFO. We can now derotate $\mathbf{z}_{r(U)}$ with $e^{-\jmath 2\pi \Delta \widetilde{f}_{(U)}.\mathbf{t}}$. The CFO free symbol is then transformed to the frequency domain by the DFT operation which is then followed by a two-tap FEQ, similar to (3.12), for the compensation of transmitter IQ imbalance and channel distortion of the individual user. The estimate of the transmitted symbol $\widetilde{\mathbf{S}}_{(U)}[l]$ is given as:

$$\widetilde{\mathbf{S}}_{(U)}[l] = \mathbf{W}_{a(U)}[l]\mathbf{F}[l](\mathbf{z}_{r(U)}e^{-\jmath 2\pi \Delta \widetilde{f}_{(U)}.\mathbf{t}}) + \mathbf{W}_{b(U)}[l](\mathbf{F}[l_m](\mathbf{z}_{r(U)}e^{-\jmath 2\pi \Delta \widetilde{f}_{(U)}.\mathbf{t}}))^* \tag{6.35}$$

This TEQ compensation scheme for a 2×2 MU MIMO up-link case is shown in **Figure 6.8**.

The entire compensation scheme is now simplified by first swapping the TEQ filters $\mathbf{v}_{ac(U)}, \mathbf{v}_{ad(U)}, \mathbf{v}_{bc(U)}$ and $\mathbf{v}_{bd(U)}$ with the de-rotation $e^{-\jmath 2\pi \Delta \widetilde{f}_{(U)}.\mathbf{t}}$. The swapped TEQ filters are then transferred to the frequency domain resulting in a eight-branch PTEQ, given as:

$$\widetilde{\mathbf{S}}_{(U)}[l] = \sum_{B=1}^{2} \begin{bmatrix} \mathbf{W}_{v1(U,B)}[l] \\ \mathbf{W}_{v2(U,B)}[l] \\ \mathbf{W}_{v3(U,B)}[l] \\ \mathbf{W}_{v4(U,B)}[l] \end{bmatrix}^T \begin{bmatrix} \mathbf{F}_{ext}[l]\mathbf{z}_{(B)}.e^{-\jmath 2\pi \Delta \widetilde{f}_{(U)}.\mathbf{t}} \\ (\mathbf{F}_{ext}[l_m]\mathbf{z}_{(B)}.e^{-\jmath 2\pi \Delta \widetilde{f}_{(U)}.\mathbf{t}})^* \\ \mathbf{F}_{ext}[l]\mathbf{z}^*_{(B)}.e^{-\jmath 2\pi \Delta \widetilde{f}_{(U)}.\mathbf{t}} \\ (\mathbf{F}_{ext}[l_m]\mathbf{z}^*_{(B)}.e^{-\jmath 2\pi \Delta \widetilde{f}_{(U)}.\mathbf{t}})^* \end{bmatrix} \tag{6.36}$$

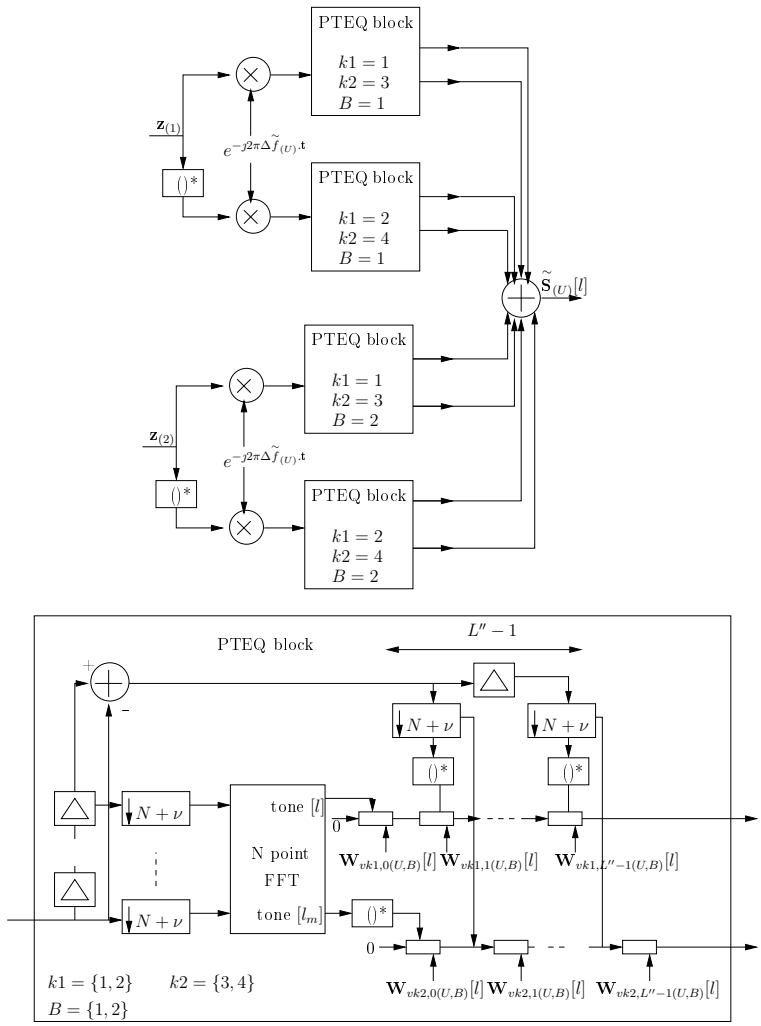

Figure 6.9: Eight-branch PTEQ scheme for 2×2 MU MIMO up-link scenario in the presence of transmitter/receiver IQ imbalance and CFO

The PTEQ filters $\mathbf{W}_{v1(U,B)}[l] \ldots \mathbf{W}_{v4(U,B)}[l]$ are of length $L'' = L_r + L' - 1$. Equation (6.36) shows that in order to estimate the PTEQ coefficients an LT symbol sequence length $M_l \geq 8L''$ is needed. The total number of PTEQ coefficients to be estimated is $16L''$ per subcarrier. The eight-branch PTEQ compensation scheme for 2×2 MU MIMO up-link scenario is shown in **Figure 6.9**.

Note:

- **Higher order MU system in up-link scenario:** It is possible to design compensation schemes for higher order MU systems in the up-link scenario, i.e. $(N_b \times N_c N_u) > (2 \times 2)$, but for every MU configuration, the TEQ design (6.34) may be different depending on the number of antennas and users. As a consequence, the PTEQ structure will also be different. For example, in the case of a 3×3 system, we perform TEQ filtering in three stages. In the first stage, the TEQ filters compensates only for receiver IQ imbalance. The remaining filter stages are then designed to suppress the terms from the two undesired users. Finally the TEQ filters are linearly combined to make one unified TEQ filter structure. This TEQ structure is then transformed to the frequency domain to realize one unified PTEQ structure for the respective 3×3 MU configuration. For even higher order systems, the solution will become very complex leading to higher implementation costs. The PTEQ solution is thus preferable for lower order systems.
- **Only transmitter/receiver IQ imbalance and no CFO:** In the absence of CFO, the MU MIMO system will be equivalent to a SU MIMO system. Thus, the compensation can be obtained by a simple FEQ scheme designed earlier for the SU MIMO system in section 6.3. This compensation scheme is applicable to both the up-link and the down-link scenario.

6.7 Simulations

We consider a transmission packet from every K^{th} transmit antenna consists of a 10 identical ST symbol sequence for CFO estimation, followed by a varying number of linearly independent LT symbol sequence for the estimation of the PTEQ coefficients, and finally the data sequence for performance evaluation. We consider the LT symbol sequence to be sufficiently long to achieve initialization and adequate noise averaging of the PTEQ coefficients. In general, we consider the LT sequence length to be atleast four to five times longer than the minimal required length for the initialization of the equalizer coefficients. The equalizers are initialized by an adaptive RLS algorithm.

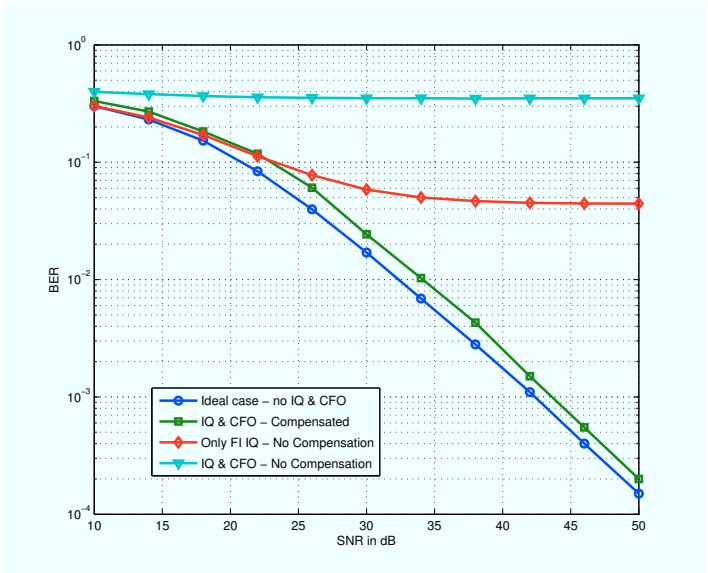

Figure 6.10: BER vs SNR for an Alamouti coded system with transmitter/receiver IQ imbalance and CFO

- In the first setup, we evaluate the performance of the joint compensation scheme for an Alamouti based STBC system (6.27). A similar compensation performance results will also be obtained with a SU MIMO 2×2 scenario. Hence, the performance results for the SU MIMO scenario are not given.

  The parameters used in the simulation are as follows: We consider an uncoded 64QAM OFDM transmission with symbol length $N = 64$, the CP length $\nu = 16$. The multipath channel has length $L = 4$ taps. The taps of the multipath channel are chosen independently with complex Gaussian distribution. The transmitter and receiver front-end mismatched filter impulse responses are $\mathbf{h}_{ti(K)} = \mathbf{h}_{ri} = [0.01\ 0.5\ 0.06]$ and $\mathbf{h}_{tq(K)} = \mathbf{h}_{rq} = [0.06\ 0.5\ 0.01]$, the FI amplitude imbalances are $g_{t(K)} = g_r = 5\%$ and the phase imbalances are $\phi_{t(K)} = \phi_r = 5^\circ$. The same IQ imbalance values have been kept for both transmit antennas so as to keep the simulation process simple. The CFO is uniformly varied between $\zeta = [-0.3 \longleftrightarrow +0.3]$. The threshold used to select between the two CFO estimation schemes is $\zeta = -0.02$ and $+0.02$, with the auto-correlation scheme used for small CFOs and the NLS scheme for large CFOs. We also implement the iterative scheme to further improve the estimate of the CFO and PTEQ coefficients.

  Figure 6.10 shows the BER vs SNR performance curves for this setup. The BER results depicted are obtained by averaging the BER curves over

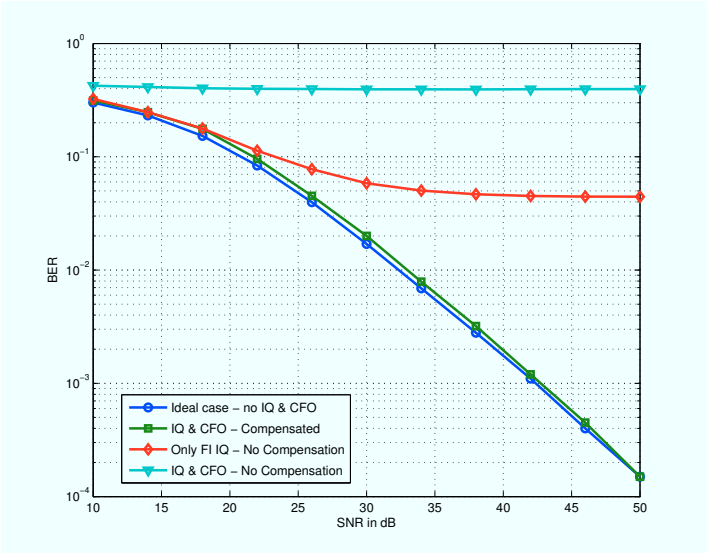

Figure 6.11: BER vs SNR for 2×2 MU MIMO OFDM (up-link scenario).

10^4 independent channel realizations. The performance comparison is made with an ideal system with no front-end distortion and with a system with no compensation algorithm included. The BER performance figure shows an efficient joint compensation performance. With the compensation scheme in place, the performance is very close to the ideal case. With no compensation scheme in place, even for the case when there is only frequency independent transmitter and receiver IQ imbalance, the system is unusable as the BER is very high. The compensation performance is seen to depend on how accurately the adaptive equalizer coefficients can converge to the ideal values.

- In the second setup, we evaluate the performance of the joint compensation solution for a 2×2 MU MIMO system in an up-link scenario (6.36). **Figure 6.11** shows the BER vs SNR performance curves for this setup. We consider the same simulation parameters as considered in setup 1, except that now the receiver IQ imbalance at the BS is considered to be FI, i.e. the I and Q branch filters are considered to be perfectly matched. Thus the resulting length of the PTEQ is now $L'' = 4$. We consider different CFOs for the two users, i.e. $\zeta_{(1)} = 0.32$ and $\zeta_{(2)} = 0.2$. We assume the receiver has the knowledge of the user's CFO. The figure shows that the MU MIMO compensation scheme performs effectively for the given IQ imbalance and CFO values.

6.8 Conclusion

In this chapter we have proposed efficient PTEQ based joint compensation solutions for transmitter/receiver IQ imbalance and CFO in different multiple antenna scenarios. It is shown that for single-user MIMO and STBC based systems, the PTEQ solution can be scaled for any number of transmitter and receiver antennas. By exploiting the structure of orthogonal space-time codes, efficient and optimal receiver architectures that are robust to front-end non-idealities can be derived.

The PTEQ scheme has also been extended for compensation of front-end non-idealities in multi-user scenarios, where each user may experience a different CFO. It is shown that the down-link communication scenario can be considered to be composed of N_u decoupled SU MIMO systems. Thus a PTEQ scheme for SU MIMO system can be extended directly in this case. In the up-link scenario, the PTEQ provides very efficient compensation solution for lower order 2×2 systems. The compensation scheme can be designed for higher order systems as well but the solution will lead to higher implementation costs.

Chapter 7

Decoupled Compensation Schemes

7.1 Introduction

In chapter 6, we derived joint estimation/compensation schemes for different multiple antenna scenarios. The joint compensation schemes can provide efficient performance results that are very close to the ideal conditions. However they tend to be heavy especially when transmitter/receiver IQ imbalance and CFO are considered together in a system model. The joint compensation schemes also require the entire compensation structure to be re-trained for every variation of channel characteristics.

In this chapter, the decoupled compensation schemes (D-FEQ and PR-(PTEQ) /FEQ) proposed earlier for SISO systems in chapter 5, are now extended for MIMO systems. The design and analysis of decoupled schemes in SISO was essential to provide a suitable framework for the development in the MIMO environment. It is shown that the MIMO decoupled schemes provide a large savings in the training overhead as well as the computational costs.

Once the front-end IQ imbalance and CFO parameters are known, the training symbols are then required to estimate only the variation in channel characteristics. In the decoupled MIMO schemes, a standard channel equalizer requires the initialization of only $N_t \times N_r$ coefficients per subcarrier for the compensation of channel distortion. In comparison, a joint estimation/compensation scheme for only IQ imbalance requires the initialization of $2(N_t \times N_r)$ coefficients per subcarrier (6.7). As less number of coefficients have to re-estimated in the

decoupled solutions, this also results in a reduced training overhead requirements. Besides the advantage of a reduced training overhead and a reduced coefficient re-initialization, the decoupled solutions also result in a significant reduction in the overall computational complexity when compared to the joint compensation scheme. The publications related to this chapter are: [96] and [99].

This chapter is organized as follows: In **section 7.2**, we derive decoupled FEQ (D-FEQ) based solutions for MIMO systems impaired with transmitter/receiver IQ imbalance and no CFO. In **section 7.3**, we derive phase rotation based compensation schemes (PR-(PTEQ)/FEQ) for the estimation of receiver IQ imbalance from a specially induced phase rotated LT symbol sequence. The similarities in the decoupled schemes for both SISO and MIMO systems will be kept to the minimum, with more focus provided on the modifications required for the MIMO case. Finally, the results of numerical performance evaluation are presented in **section 7.4** and conclusions are given in **section 7.5**.

Note: In this chapter we have considered only SU MIMO system, the extension to space-time coded system and MU MIMO system can be straightforwardly realized. We will follow the same system of equations as explained in section 6.2 for SU MIMO case.

7.2 Decoupled FEQ Schemes

In order to derive the decoupled FEQ (D-FEQ) scheme, we assume that the matrix $\mathbf{D}_{tot}[l]$ in (6.7) is accurately known. The coefficients in $\mathbf{D}_{tot}[l]$ can be estimated based on M_l long sequence of LT symbols, as follows:

$$\widetilde{\mathbf{D}}_{tot-}[l] = \mathbf{Z}^{Tr}_{tot-}[l]\mathbf{S}^{Tr^{\dagger}}_{tot}[l] \tag{7.1}$$

where $\widetilde{\mathbf{D}}_{tot-}[l]$ is the estimate of $\mathbf{D}_{tot-}[l] = \begin{bmatrix} \left(\mathbf{D}_{tot-}(1,1)[l]\right) & \dots & \left(\mathbf{D}_{tot-}(1,N_t)[l]\right) \\ \vdots & \ddots & \vdots \\ \left(\mathbf{D}_{tot-}(N_r,1)[l]\right) & \dots & \left(\mathbf{D}_{tot-}(N_r,N_t)[l]\right) \end{bmatrix}$,

$\mathbf{Z}^{Tr}_{tot-}[l] = \begin{bmatrix} \mathbf{Z}^{(1)}_{(1)}[l] & \dots & \mathbf{Z}^{(M_l)}_{(1)}[l] \\ \vdots & \ddots & \vdots \\ \mathbf{Z}^{(1)}_{(N_r)}[l] & \dots & \mathbf{Z}^{(M_l)}_{(N_r)}[l] \end{bmatrix}$, $\mathbf{S}^{Tr}_{tot}[l] = \begin{bmatrix} \begin{pmatrix} \mathbf{S}^{(1)}_{(1)}[l] \\ \mathbf{S}^{*(1)}_{(1)}[l_m] \end{pmatrix} & \dots & \begin{pmatrix} \mathbf{S}^{(M_l)}_{(1)}[l] \\ \mathbf{S}^{*(M_l)}_{(1)}[l_m] \end{pmatrix} \\ \vdots & \ddots & \vdots \\ \begin{pmatrix} \mathbf{S}^{(1)}_{(N_t)}[l] \\ \mathbf{S}^{*(1)}_{(N_t)}[l_m] \end{pmatrix} & \dots & \begin{pmatrix} \mathbf{S}^{(M_l)}_{(N_t)}[l] \\ \mathbf{S}^{*(M_l)}_{(N_t)}[l_m] \end{pmatrix} \end{bmatrix}$

and the sub-matrix $\mathbf{D}_{tot-}(J,K)[l] = \begin{pmatrix} \mathbf{D}_{a(J,K)}[l] & \mathbf{D}_{b(J,K)}[l] \end{pmatrix}$.

A total of $2(N_t \times N_r)$ elements in $\mathbf{D}_{tot-}[l]$ will have to be estimated. Equation (7.1) shows that there are M_l equations in $2N_t$ unknowns (for each row of $\mathbf{D}_{tot-}[l]$). Hence to estimate $\mathbf{D}_{tot-}[l]$, we need the LT symbol sequence length $M_l \geq 2N_t$.

Following the expression of $\mathbf{D}_{tot}[l]$ for the SISO case in (5.14), the matrix $\mathbf{D}_{tot}[l]$ for the MIMO case in (6.7) can be factorized as follows:

$$\mathbf{D}_{tot}[l] = \mathbf{Q}_{r_{tot}}[l]\mathbf{B}_{tot}[l]\mathbf{Q}_{t_{tot}}[l] \tag{7.2}$$

where $\mathbf{B}_{tot}[l] = \begin{bmatrix} \big(\mathbf{B}_{tot}(1,1)[l]\big) & \dots & \big(\mathbf{B}_{tot}(1,N_t)[l]\big) \\ \vdots & \ddots & \vdots \\ \big(\mathbf{B}_{tot}(N_r,1)[l]\big) & \dots & \big(\mathbf{B}_{tot}(N_r,N_t)[l]\big) \end{bmatrix}$,

$\mathbf{Q}_{r_{tot}}[l] = \begin{bmatrix} \big(\mathbf{Q}_{r_{tot}}(1)[l]\big) & & \\ & \ddots & \\ & & \big(\mathbf{Q}_{r_{tot}}(N_r)[l]\big) \end{bmatrix}$,

and $\mathbf{Q}_{t_{tot}}[l] = \begin{bmatrix} \big(\mathbf{Q}_{t_{tot}}(1)[l]\big) & & \\ & \ddots & \\ & & \big(\mathbf{Q}_{r_{tot}}(N_t)[l]\big) \end{bmatrix}$.

The sub-matrices in (7.2) are defined as $\mathbf{B}_{tot}(J,K)[l] = \begin{pmatrix} \mathbf{B}_{(J,K)}[l] & 0 \\ 0 & \mathbf{B}^*_{(J,K)}[l_m] \end{pmatrix}$,

$\mathbf{Q}_{r_{tot}}(J)[l] = \begin{pmatrix} 1 & \mathbf{Q}_{r(J)}[l] \\ \mathbf{Q}^*_{r(J)}[l_m] & 1 \end{pmatrix}$ and $\mathbf{Q}_{t_{tot}}(K)[l] = \begin{pmatrix} 1 & \mathbf{Q}_{t(K)}[l] \\ \mathbf{Q}^*_{t(K)}[l_m] & 1 \end{pmatrix}$.

Here $\mathbf{B}_{(J,K)}[l] = \mathbf{G}_{ra(J)}[l]\mathbf{G}_{ta(K)}[l]\mathbf{C}_{(J,K)}[l]$ is the composite channel between the Jth receive and K^{th} transmit antenna. $\mathbf{Q}_{t(K)}[l] = \frac{\mathbf{G}_{tb(K)}[l]}{\mathbf{G}_{ta(K)}[l]}$ is the transmitter IQ imbalance gain parameter for the Kth transmit antenna and $\mathbf{Q}_{r(J)}[l] = \frac{\mathbf{G}_{zb(J)}[l]}{\mathbf{G}^*_{za(J)}[l_m]}$ is the receiver IQ imbalance gain parameter for the Jth receive antenna. In (7.2) $\mathbf{Q}_{t_{tot}}[l]$ and $\mathbf{Q}_{r_{tot}}[l]$ are independent of the channel distortion. The channel distortion is contained entirely in the $\mathbf{B}_{tot}[l]$ matrix. Thus both transmitter and receiver IQ imbalance have been decoupled from the (composite) channel distortion.

If we assume that estimates $\widetilde{\mathbf{B}}_{tot}[l], \widetilde{\mathbf{Q}}_{t_{tot}}[l]$ and $\widetilde{\mathbf{Q}}_{r_{tot}}[l]$ of $\mathbf{B}_{tot}[l], \mathbf{Q}_{t_{tot}}[l]$ and $\mathbf{Q}_{r_{tot}}[l]$ are available, then we can perform the compensation of the channel distortion and transmitter/receiver IQ imbalance either entirely at the receiver, or compensate only the receiver IQ imbalance and channel distortion at the receiver, and compensate the transmitter IQ imbalance by pre-distortion of transmitted symbols. The entirely receiver based and the pre-distortion based compensation schemes are explained in section 7.2.1 and section 7.2.2., where it is assumed that $\widetilde{\mathbf{B}}_{tot}[l], \widetilde{\mathbf{Q}}_{t_{tot}}[l]$ and $\widetilde{\mathbf{Q}}_{r_{tot}}[l]$ are available. Sections 7.2.1.-7.2.2. also explain the

estimation method to track the variation in the channel matrix $\widetilde{\mathbf{B}}_{tot}[l]$, while the estimation of $\widetilde{\mathbf{Q}}_{t_{tot}}[l]$ and $\widetilde{\mathbf{Q}}_{r_{tot}}[l]$ is later explained in section 7.2.3.

7.2.1 Compensation Entirely at the Receiver

In this case, the estimate of $\mathbf{D}_{tot}[l]$ is computed as $\widetilde{\mathbf{D}}_{tot}[l] = \widetilde{\mathbf{Q}}_{r_{tot}}[l]\widetilde{\mathbf{B}}_{tot}[l]\widetilde{\mathbf{Q}}_{t_{tot}}[l]$, and then the estimate of the transmitted symbol $\widetilde{\mathbf{S}}_{tot}[l]$ is obtained based on MMSE criterion as:

$$\widetilde{\mathbf{S}}_{tot}[l] = \widetilde{\mathbf{D}}^{H}_{tot}[l](\widetilde{\mathbf{D}}_{tot}[l]\widetilde{\mathbf{D}}^{H}_{tot}[l] + \mathbf{R}_{Nc}[l])^{-1}\mathbf{Z}_{tot}[l] \tag{7.3}$$

where the noise covariance matrix $\mathbf{R}_{Nc}[l] = \Xi\{\mathbf{N}_{c_{tot}}[l]\mathbf{N}^{H}_{c_{tot}}[l]\}$. The total number of coefficients in $\widetilde{\mathbf{D}}_{tot}[l]$ is $4(N_t \times N_r)$, half of which are used to estimate the transmitted symbols at the desired subcarriers, i.e. $\mathbf{S}_{tot-}[l] = \begin{bmatrix} (\mathbf{S}_{(1)}[l]) \\ \vdots \\ (\mathbf{S}_{(N_t)}[l]) \end{bmatrix}$. Thus the total computational complexity is $2(N_t \times N_r)$ multiplications per subcarrier. Assuming $\widetilde{\mathbf{Q}}_{t_{tot}}[l]$ and $\widetilde{\mathbf{Q}}_{r_{tot}}[l]$ are available and fixed, based on the estimation obtained from section 7.2.3., then the variations in the channel can be tracked as:

$$\underbrace{\begin{bmatrix} \widetilde{\mathbf{B}}_{r(1,1)}[l] & \dots & \widetilde{\mathbf{B}}_{r(1,N_t)}[l] \\ \vdots & \ddots & \vdots \\ \widetilde{\mathbf{B}}_{r(N_r,1)}[l] & \dots & \widetilde{\mathbf{B}}_{r(N_r,N_t)}[l] \end{bmatrix}}_{\widetilde{\mathbf{B}}_{r_{tot-}}[l]} = (\widetilde{\mathbf{Q}}_{rv_{tot-}}[l]\mathbf{Z}^{Tr}_{tot}[l])(\widetilde{\mathbf{Q}}_{t_{tot-}}[l]\mathbf{S}^{Tr}_{tot}[l])^{\dagger} \tag{7.4}$$

Here $\widetilde{\mathbf{B}}_{r(J,K)}[l] = \widetilde{\mathbf{B}}_{(J,K)}[l](1 - \widetilde{\mathbf{Q}}_{r(J)}[l]\widetilde{\mathbf{Q}}^{*}_{r(J)}[l_m])$, the matrices $\mathbf{Z}^{Tr}_{tot}[l], \mathbf{S}^{Tr}_{tot}[l]$ are defined in equation (6.10) and (7.1) respectively, and

$$\widetilde{\mathbf{Q}}_{t_{tot-}}[l] = \begin{bmatrix} \begin{pmatrix} 1 & \widetilde{\mathbf{Q}}_{t(1)}[l] \end{pmatrix} & & \\ & \ddots & \\ & & \begin{pmatrix} 1 & \widetilde{\mathbf{Q}}_{t(N_t)}[l] \end{pmatrix} \end{bmatrix}$$

$$\widetilde{\mathbf{Q}}_{rv_{tot-}}[l] = \begin{bmatrix} \begin{pmatrix} 1 & -\widetilde{\mathbf{Q}}_{r(1)}[l] \end{pmatrix} & & \\ & \ddots & \\ & & \begin{pmatrix} 1 & -\widetilde{\mathbf{Q}}_{r(N_r)}[l] \end{pmatrix} \end{bmatrix}$$

Once $\widetilde{\mathbf{B}}_{r_{tot-}}[l]$ is known, we can then obtain the coefficients of the matrix $\widetilde{\mathbf{B}}_{tot}[l]$

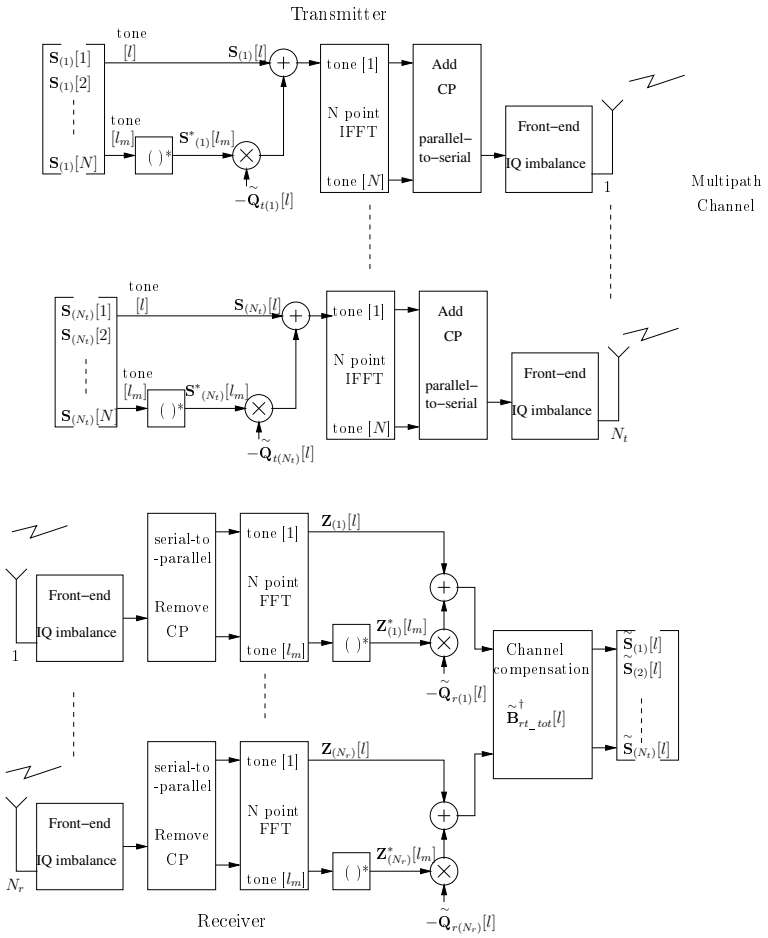

Figure 7.1: D-FEQ scheme with pre-distortion of transmitted symbols for the compensation of transmitter/receiver IQ imbalance and channel distortion

as $\widetilde{\mathbf{B}}_{(J,K)}[l] = \dfrac{\widetilde{\mathbf{B}}_{r(J,K)}[l]}{(1-\widetilde{\mathbf{Q}}_{r(J)}[l]\widetilde{\mathbf{Q}}^{*}_{r(J)}[l_m])}$.

Equation (7.4) shows that we have to estimate $(N_t \times N_r)$ coefficients per subcarrier in $\widetilde{\mathbf{B}}_{r_{tot-}}[l]$. Each row of $\widetilde{\mathbf{B}}_{r_{tot-}}[l]$ corresponds to M_l equations in N_t unknowns. Hence to obtain the estimate $\widetilde{\mathbf{B}}_{r_{tot-}}[l]$, we need an LT sequence length $M_l \geq N_t$.

7.2.2 Compensation with Pre-Distortion of Transmitted Symbols

In the pre-distortion scheme, the new OFDM symbol $\mathbf{S}_{\mathbf{n}(K)}$ is defined as $\mathbf{S}_{\mathbf{n}(K)} = \mathbf{S}_{(K)} - \widetilde{\mathbf{Q}}_{t(K)}.\mathbf{S}^*_{m(K)}$ where $\widetilde{\mathbf{Q}}_{t(K)}$ (obtained from section 7.2.3.) is the $\mathbf{Q}_{t(K)}$ estimate fed back from the receiver. In matrix form, $\mathbf{S}_{\mathbf{n}(K)}[l]$ and $\mathbf{S}^*_{\mathbf{n}(K)}[l_m]$ can be written as:

$$\underbrace{\begin{bmatrix} \begin{pmatrix} \mathbf{S}_{\mathbf{n}(1)}[l] \\ \mathbf{S}^*_{\mathbf{n}(1)}[l_m] \end{pmatrix} \\ \vdots \\ \begin{pmatrix} \mathbf{S}_{\mathbf{n}(N_r)}[l] \\ \mathbf{S}^*_{\mathbf{n}(N_t)}[l_m] \end{pmatrix} \end{bmatrix}}_{\mathbf{S}_{\mathbf{n}tot}[l]} = \underbrace{\begin{bmatrix} \left(\widetilde{\mathbf{Q}}_{tv_{tot}(1)}[l]\right) & & \\ & \ddots & \\ & & \left(\widetilde{\mathbf{Q}}_{tv_{tot}(N_t)}[l]\right) \end{bmatrix}}_{\widetilde{\mathbf{Q}}_{tv_{tot}}[l]} \underbrace{\begin{bmatrix} \begin{pmatrix} \mathbf{S}_{(1)}[l] \\ \mathbf{S}^*_{(1)}[l_m] \end{pmatrix} \\ \vdots \\ \begin{pmatrix} \mathbf{S}_{(N_r)}[l] \\ \mathbf{S}^*_{(N_t)}[l_m] \end{pmatrix} \end{bmatrix}}_{\mathbf{S}_{tot}[l]} \tag{7.5}$$

where $\widetilde{\mathbf{Q}}_{tv_{tot}(K)}[l] = \begin{pmatrix} 1 & -\widetilde{\mathbf{Q}}_{t(K)}[l] \\ -\widetilde{\mathbf{Q}}^*_{t(K)}[l_m] & 1 \end{pmatrix}$. Equation (6.7) is now modified as:

$$\begin{aligned} \mathbf{Z}_{tot}[l] &= \mathbf{D}_{tot}[l]\mathbf{S}_{\mathbf{n}tot}[l] + \mathbf{N}_{c_{tot}}[l] \\ &= \mathbf{Q}_{r_{tot}}[l]\mathbf{B}_{tot}[l] \underbrace{\begin{bmatrix} \left(\mathbf{Q}_{td_{tot}}(1)[l]\right) & & \\ & \ddots & \\ & & \left(\mathbf{Q}_{td_{tot}}(N_t)[l]\right) \end{bmatrix}}_{\mathbf{Q}_{td_{tot}}[l]} \mathbf{S}_{tot}[l] + \mathbf{N}_{c_{tot}}[l] \end{aligned} \tag{7.6}$$

where $\mathbf{Q}_{td_{tot}}(K)[l] = \begin{bmatrix} (1 - \mathbf{Q}_{t(K)}[l]\widetilde{\mathbf{Q}}^*_{t(K)}[l_m]) & (\mathbf{Q}_t[l] - \widetilde{\mathbf{Q}}_{t(K)}[l]) \\ (\mathbf{Q}^*_{t(K)}[l_m] - \widetilde{\mathbf{Q}}^*_{t(K)}[l_m]) & (1 - \mathbf{Q}^*_t[l_m]\widetilde{\mathbf{Q}}_{t(K)}[l]) \end{bmatrix}$. Under ideal conditions $\widetilde{\mathbf{Q}}_{t(K)}[l] = \mathbf{Q}_{t(K)}[l]$ and $\widetilde{\mathbf{Q}}_{t(K)}[l_m] = \mathbf{Q}_{t(K)}[l_m]$ and then $\mathbf{Q}_{td_{tot}}(K)[l]$ and $\widetilde{\mathbf{Q}}_{tv_{tot}}[l]$ are diagonalized and the remaining diagonalized elements $(1 - \mathbf{Q}_{t(K)}[l]\widetilde{\mathbf{Q}}^*_{t(K)}[l_m])$ can be merged with $\mathbf{B}_{tot}[l]$. The received symbol $\mathbf{Z}_{tot}[l]$ is then considered to be free from transmitter IQ imbalance. The estimate of the transmitted symbol $\widetilde{\mathbf{S}}_{tot}[l]$ is finally obtained as:

$$\widetilde{\mathbf{S}}_{tot}[l] = \widetilde{\mathbf{B}}^{\dagger}_{rt_{tot}}[l]\widetilde{\mathbf{Q}}_{rv_{tot}}[l]\mathbf{Z}_{tot}[l] \tag{7.7}$$

where the matrices $\widetilde{\mathbf{Q}}_{rv_{tot}}[l]$ and $\widetilde{\mathbf{B}}_{rt_{tot}}[l]$ are defined as:

$$\widetilde{\mathbf{Q}}_{rv_{tot}}[l] = \begin{bmatrix} \left(\widetilde{\mathbf{Q}}_{rv_{tot}}(1)[l]\right) & & \\ & \ddots & \\ & & \left(\widetilde{\mathbf{Q}}_{rv_{tot}}(N_r)[l]\right) \end{bmatrix},$$

$$\widetilde{\mathbf{B}}_{rt_{tot}}[l] = \begin{bmatrix} \left(\widetilde{\mathbf{B}}_{rt_{tot}}(1,1)[l]\right) & \cdots & \left(\widetilde{\mathbf{B}}_{rt_{tot}}(1,N_t)[l]\right) \\ \vdots & \ddots & \vdots \\ \left(\widetilde{\mathbf{B}}_{rt_{tot}}(N_r,1)[l]\right) & \cdots & \left(\widetilde{\mathbf{B}}_{rt_{tot}}(N_r,N_t)[l]\right) \end{bmatrix}$$

with $\widetilde{\mathbf{Q}}_{rv_{tot}}(J)[l] = \begin{pmatrix} 1 & -\widetilde{\mathbf{Q}}_{r(J)}[l] \\ -\widetilde{\mathbf{Q}}^{*}_{r(J)}[l_m] & 1 \end{pmatrix}$

and $\widetilde{\mathbf{B}}_{rt_{tot}}(J,K)[l] = \begin{pmatrix} \widetilde{\mathbf{B}}_{rt(J,K)}[l] & 0 \\ 0 & \widetilde{\mathbf{B}}^{*}_{rt(J,K)}[l_m] \end{pmatrix}$. Finally the term $\widetilde{\mathbf{B}}_{rt(J,K)}[l] = \widetilde{\mathbf{B}}_{(J,K)}[l](1 - \widetilde{\mathbf{Q}}_{r(J)}[l]\widetilde{\mathbf{Q}}^{*}_{r(J)}[l_m])(1 - \widetilde{\mathbf{Q}}_{t(K)}[l]\widetilde{\mathbf{Q}}^{*}_{t(K)}[l_m])$.

The D-FEQ scheme with pre-distortion of transmitted symbols is shown in **Figure 7.1**. The figure shows that the compensation of transmitter IQ imbalance takes place at every transmit antenna, and similarly the compensation of receiver IQ imbalance takes place at every receive antenna, before the inputs from all receive antenna branches are combined for the compensation of channel distortion.

The computational complexity to estimate the transmitted symbols $\widetilde{\mathbf{S}}_{tot-}[l]$ in (7.7) is now reduced to $N_t + N_r + (N_t \times N_r)$ coefficients per subcarrier, compared to $2(N_t \times N_r)$ coefficients in (6.8) and (7.3). It can be observed that the number of coefficients required for a lower order $(N_t \times N_r) = (2 \times 2)$ MIMO system is same for the joint compensation scheme and D-FEQ schemes, but when the system order is increased $(N_t \times N_r) > (2 \times 2)$, the decoupled scheme with pre-distortion provides a lower computational complexity.

Variations in the channel are now tracked as follows:

$$\underbrace{\begin{bmatrix} \widetilde{\mathbf{B}}_{rt(1,1)}[l] & \cdots & \widetilde{\mathbf{B}}_{rt(1,N_t)}[l] \\ \vdots & \ddots & \vdots \\ \widetilde{\mathbf{B}}_{rt(N_r,1)}[l] & \cdots & \widetilde{\mathbf{B}}_{rt(N_r,N_t)}[l] \end{bmatrix}}_{\widetilde{\mathbf{B}}_{rt_{tot-}}[l]} = (\widetilde{\mathbf{Q}}_{rv_{tot-}}[l]\mathbf{Z}^{Tr}_{tot}[l])(\mathbf{S}^{Tr}_{tot-}[l])^{\dagger} \tag{7.8}$$

where $\widetilde{\mathbf{Q}}_{rv_{tot-}}[l]$ is defined in equation (7.4) and $\mathbf{Z}^{Tr}_{tot}[l]$ and $\mathbf{S}^{Tr}_{tot-}[l]$ are defined in equation (6.10). We once again need an LT sequence length $M_l \geq N_t$.

Equations (7.7) and (7.8) are also valid in the presence of either only receiver IQ

imbalance ($\mathbf{Q}_{t(K)} = 0$) or only transmitter IQ imbalance ($\mathbf{Q}_{r(J)} = 0$). The total computational complexity per subcarrier for the estimation of transmitted symbols $\widetilde{\mathbf{S}}_{tot-}[l]$ is reduced to $N_t + (N_t \times N_r)$ coefficients in the case of only transmitter IQ imbalance, and $N_r + (N_t \times N_r)$ coefficients for only receiver IQ imbalance. In the absence of transmitter IQ imbalance, the entire compensation takes place at the receiver with a reduced computational complexity.

7.2.3 Estimation of Transmitter and Receiver IQ Imbalance Gain Parameters

We now develop an algorithm for the estimation of the transmitter and receiver IQ imbalance gain paramaters $\mathbf{Q}_{t(K)}[l]$ and $\mathbf{Q}_{r(J)}[l]$ based on the decoupled matrix $\mathbf{D}_{tot}[l]$ shown in equation (7.2). The $\mathbf{D}_{tot}[l]$ coefficients $\mathbf{D}_{a(J,K)}[l]$ and $\mathbf{D}_{b(J,K)}[l]$ can now be re-written as:

$$\begin{aligned}\mathbf{D}_{a(J,K)}[l] &= \mathbf{B}_{(J,K)}[l] + \mathbf{Q}_{r(J)}[l]\mathbf{Q}^{*}_{t(K)}[l_m]\mathbf{B}^{*}_{(J,K)}[l_m] \\ \mathbf{D}_{b(J,K)}[l] &= \mathbf{Q}_{t(K)}[l]\mathbf{B}_{(J,K)}[l] + \mathbf{Q}_{r(J)}[l]\mathbf{B}^{*}_{(J,K)}[l_m]\end{aligned} \tag{7.9}$$

In order to obtain the IQ imbalance gain parameter estimates, we first make an approximation, namely that the second order term $\mathbf{Q}_{r(J)}[l]\mathbf{Q}^{*}_{t(K)}[l_m] = 0$ in $\mathbf{D}_{a(J,K)}[l]$. This approximation is based on the fact that in practice $\mathbf{G}_{ta(K)}[l] >> \mathbf{G}_{tb(K)}[l]$ and $\mathbf{G}^{*}_{ra(J)}[l_m] >> \mathbf{G}_{rb(J)}[l]$. With this approximation the channel estimate $\widetilde{\mathbf{B}}_{(J,K)}[l] \backsimeq \widetilde{\mathbf{D}}_{a(J,K)}[l]$. Equation (7.9) can then be written for $\widetilde{\mathbf{D}}_{b(J,K)}[l]$ as follows:

$$\widetilde{\mathbf{D}}_{b(J,K)}[l] = \widetilde{\mathbf{Q}}_{t(K)}[l]\widetilde{\mathbf{D}}_{a(J,K)}[l] + \widetilde{\mathbf{Q}}_{r(J)}[l]\widetilde{\mathbf{D}}^{*}_{a(J,K)}[l_m] \tag{7.10}$$

Based on equation (7.10), we can now estimate the transmitter/receiver IQ imbalance gain parameters for the FS and FI cases as follows.

FI transmitter and receiver IQ imbalance

In this case the IQ imbalance gain parameter estimates for each antenna pair (J, K), are straightforwardly obtained from (7.10) as:

$$\begin{bmatrix} \widetilde{Q}_{t(K)} \\ \widetilde{Q}_{r(J)} \end{bmatrix} = \begin{bmatrix} \widetilde{\mathbf{D}}_{a(J,K)}[2] & \widetilde{\mathbf{D}}^{*}_{a(J,K)}[N] \\ \vdots & \vdots \\ \widetilde{\mathbf{D}}_{a(J,K)}[l] & \widetilde{\mathbf{D}}^{*}_{a(J,K)}[l_m] \\ \vdots & \vdots \\ \widetilde{\mathbf{D}}_{a(J,K)}[N] & \widetilde{\mathbf{D}}^{*}_{a(J,K)}[2] \end{bmatrix}^{\dagger} \begin{bmatrix} \widetilde{\mathbf{D}}_{b(J,K)}[2] \\ \vdots \\ \widetilde{\mathbf{D}}_{b(J,K)}[l] \\ \vdots \\ \widetilde{\mathbf{D}}_{b(J,K)}[N] \end{bmatrix} \tag{7.11}$$

Here the multipath diversity of the channel $\mathbf{B}_{(J,K)}[l]$, and hence $\widetilde{\mathbf{D}}_{a(J,K)}[l]$, allows us to estimate $\widetilde{Q}_{t(K)}$ and $\widetilde{Q}_{r(J)}$ respectively. It should be noted that we can also obtain $\widetilde{Q}_{t(K)}$ and $\widetilde{Q}_{r(J)}$ estimates from other antenna pairs, i.e. $(\overline{\overline{J}}, K)$ and $(J, \overline{\overline{K}})$ in equation (7.11). Finally $\widetilde{Q}_{t(K)}$ and $\widetilde{Q}_{r(J)}$ obtained from different antenna pairs can be averaged to obtain improved estimates.

FS transmitter and receiver IQ imbalance

In this case the estimate of the IQ imbalance gain parameters is to be performed for each subcarrier individually. To obtain these estimates we need at least two independent channel realizations for each antenna pair (J, K), i.e. $\mathbf{B}^{(1)}_{(J,K)}[l]$ and $\mathbf{B}^{(2)}_{(J,K)}[l]$, and hence $\widetilde{\mathbf{D}}^{(1)}_{a(J,K)}[l]$,$\widetilde{\mathbf{D}}^{(2)}_{a(J,K)}[l]$ and $\widetilde{\mathbf{D}}^{(1)}_{b(J,K)}[l]$ $\widetilde{\mathbf{D}}^{(2)}_{b(J,K)}[l]$ respectively. Here the superscript (i) in $\mathbf{X}^{(i)}_{(J,K)}[l]$ indicates a different realization of $\mathbf{X}_{(J,K)}[l]$. The estimates $\widetilde{\mathbf{Q}}_{t(K)}[l]$ and $\widetilde{\mathbf{Q}}_{r(J)}[l]$ for the (J, K) antenna pair can then be obtained as follows:

$$\begin{bmatrix} \widetilde{\mathbf{Q}}_{t(K)}[l] \\ \widetilde{\mathbf{Q}}_{r(J)}[l] \end{bmatrix} = \begin{bmatrix} \widetilde{\mathbf{D}}^{(1)}_{a(J,K)}[l] & \widetilde{\mathbf{D}}^{*(1)}_{a(J,K)}[l_m] \\ \widetilde{\mathbf{D}}^{(2)}_{a(J,K)}[l] & \widetilde{\mathbf{D}}^{*(2)}_{a(J,K)}[l_m] \end{bmatrix}^{-1} \begin{bmatrix} \widetilde{\mathbf{D}}^{(1)}_{b(J,K)}[l] \\ \widetilde{\mathbf{D}}^{(2)}_{b(J,K)}[l] \end{bmatrix} \tag{7.12}$$

For guaranteed invertibility we should have $\widetilde{\mathbf{D}}^{(2)}_{a(J,K)}[l] \neq \widetilde{\mathbf{D}}^{(1)}_{a(J,K)}[l]$ and/or $\widetilde{\mathbf{D}}^{*(2)}_{a(J,K)}[l_m] \neq \widetilde{\mathbf{D}}^{*(1)}_{a(J,K)}[l_m]$. If the channel does not vary for a particular subcarrier and its mirror subcarrier for any combination of (J, K), then the joint compensation scheme is performed on these subcarrier pairs as in (6.8).

The transmitter/receiver IQ imbalance gain estimates $\widetilde{\mathbf{Q}}_{t(\bar{\bar{K}})}[l]$ and $\widetilde{\mathbf{Q}}_{r(\bar{\bar{J}})}[l]$ for a different antenna pair $(\bar{\bar{J}}, \bar{\bar{K}})$, can be obtained from the estimates of $\widetilde{\mathbf{Q}}_{r(J)}[l]$ and $\widetilde{\mathbf{Q}}_{t(K)}[l]$ as follows:

$$\begin{aligned}\widetilde{\mathbf{Q}}_{t(\bar{\bar{K}})}[l] &= \frac{\widetilde{\mathbf{D}}_{b(J,\bar{\bar{K}})}[l] - \widetilde{\mathbf{Q}}_{r(J)}[l]\widetilde{\mathbf{D}}^{*}_{a(J,\bar{\bar{K}})}[l_m]}{\widetilde{\mathbf{D}}_{a(J,\bar{\bar{K}})}[l]} \\ \widetilde{\mathbf{Q}}_{r(\bar{\bar{J}})}[l] &= \frac{\widetilde{\mathbf{D}}_{b(\bar{\bar{J}},K)}[l] - \widetilde{\mathbf{Q}}_{t(K)}[l]\widetilde{\mathbf{D}}_{a(\bar{\bar{J}},K)}[l]}{\widetilde{\mathbf{D}}^{*}_{a(\bar{\bar{J}},K)}[l_m]}\end{aligned} \tag{7.13}$$

If more than one antenna pair (J, K) has at least two independent channel realizations, then $\widetilde{\mathbf{Q}}_{t(\bar{\bar{K}})}$ and $\widetilde{\mathbf{Q}}_{r(\bar{\bar{J}})}$ estimates obtained from different antenna pairs can be averaged to obtain improved estimates.

Equations (7.12) and (7.13) provides good estimates as long as $\mathbf{Q}_{r(J)}[l]\mathbf{Q}^{*}_{t(K)}[l_m] \backsimeq 0$ i.e as long as the transmitter and receiver IQ imbalance gain parameters are relatively small. The estimates are optimal if either $\mathbf{Q}_{r(J)}[l] = 0$ or $\mathbf{Q}_{t(K)}[l] = 0$, as in this case $\mathbf{B}^{(1)}_{(J,K)}[l] = \mathbf{D}^{(1)}_{a(J,K)}[l]$ and $\mathbf{B}^{(2)}_{(J,K)}[l] = \mathbf{D}^{(2)}_{a(J,K)}[l]$. We will treat this simplified case of only transmitter or only receiver IQ imbalance at the end. However, for large transmitter and receiver IQ imbalance values, the estimates obtained from (7.12) and (7.13) may not be sufficiently accurate, resulting in only a partial compensation of the transmitter and receiver IQ imbalance. The same holds true for the estimates of the FI transmitter and receiver IQ imbalance gain parameters obtained from equation (7.11). From now on we will not further consider the FI case as the description of the FS case will also apply to the FI case.

To further improve the estimates for large IQ imbalance values, we apply an iterative procedure as follows. The $\mathbf{D}_{tot}[l]$ matrix (ignoring the superscripts corresponding to different channel realizations) is first compensated by the raw estimates of the receiver IQ imbalance gain parameters $\widetilde{\mathbf{Q}}_{rv_{tot}}[l]$ (defined in (7.7)), leading to a matrix $\mathbf{D}_{1_{tot}}[l]$, given as:

$$\mathbf{D}_{1_{tot}}[l] = \widetilde{\mathbf{Q}}_{rv_{tot}}[l]\mathbf{D}_{tot}[l] = \widetilde{\mathbf{Q}}_{rv_{tot}}[l]\mathbf{Q}_{r_{tot}}[l]\mathbf{B}_{tot}[l]\mathbf{Q}_{t_{tot}}[l] \tag{7.14}$$

where

$$\widetilde{\mathbf{Q}}_{rv_{tot}}[l]\mathbf{Q}_{r_{tot}}[l] = \begin{bmatrix} \left(\mathbf{Q}_{rvr_{tot}}(1)[l]\right) & & \\ & \ddots & \\ & & \left(\mathbf{Q}_{rvr_{tot}}(N_r)[l]\right) \end{bmatrix}$$

and $\mathbf{D}_{1_{tot}}[l] = \begin{bmatrix} \left(\mathbf{D}_{1_{tot}}(1,1)[l]\right) & \dots & \left(\mathbf{D}_{1_{tot}}(1,N_t)[l]\right) \\ \vdots & \ddots & \vdots \\ \left(\mathbf{D}_{1_{tot}}(N_r,1)[l]\right) & \dots & \left(\mathbf{D}_{1_{tot}}(N_r,N_t t)[l]\right) \end{bmatrix}$

The sub-matrices are defined as:

$$\mathbf{Q}_{rvr_{tot}}(J)[l] = \begin{pmatrix} (1 - \widetilde{\mathbf{Q}}_{r(J)}[l]\mathbf{Q}^*_{r(J)}[l_m]) & (\mathbf{Q}_{r(J)}[l] - \widetilde{\mathbf{Q}}_{r(J)}[l]) \\ (\mathbf{Q}^*_{r(J)}[l_m] - \widetilde{\mathbf{Q}}^*_{r(J)}[l_m]) & (1 - \widetilde{\mathbf{Q}}^*_{r(J)}[l_m]\mathbf{Q}_{r(J)}[l]) \end{pmatrix}$$

and $\mathbf{D}_{1_{tot}}(J,K)[l] = \begin{pmatrix} \mathbf{D}_{a1(J,K)}[l] & \mathbf{D}_{b1(J,K)}[l] \\ \mathbf{D}^*_{b1(J,K)}[l_m] & \mathbf{D}^*_{a1(J,K)}[l_m] \end{pmatrix}$

In equation (7.14), where '1' is the iteration index, the definition of $\mathbf{D}_{1_{tot}}[l]$ is in line with $\mathbf{D}_{tot}[l]$ in equation (6.7). Thus the matrix $\mathbf{D}_{1_{tot}}[l]$ can once again be decoupled, similar to (7.2) as follows:

$$\mathbf{D}_{1_{tot}}[l] = \mathbf{Q}_{r1_{tot}}[l]\mathbf{B}_{1_{tot}}[l]\mathbf{Q}_{t1_{tot}}[l] \tag{7.15}$$

where $\mathbf{Q}_{r1_{tot}}[l] = \begin{bmatrix} \left(\mathbf{Q}_{r1_{tot}}(1)[l]\right) & & \\ & \ddots & \\ & & \left(\mathbf{Q}_{r1_{tot}}(N_r)[l]\right) \end{bmatrix}$,

$\mathbf{B}_{1_{tot}}[l] = \begin{bmatrix} \left(\mathbf{B}_{1_{tot}}(1,1)[l]\right) & \dots & \left(\mathbf{B}_{1_{tot}}(1,N_t)[l]\right) \\ \vdots & \ddots & \vdots \\ \left(\mathbf{B}_{1_{tot}}(N_r,1)[l]\right) & \dots & \left(\mathbf{B}_{1_{tot}}(N_r,N_t)[l]\right) \end{bmatrix}$,

$\mathbf{Q}_{t1_{tot}}[l] = \begin{bmatrix} \left(\mathbf{Q}_{t1_{tot}}(1)[l]\right) & & \\ & \ddots & \\ & & \left(\mathbf{Q}_{t1_{tot}}(N_t)[l]\right) \end{bmatrix}$

and where $\mathbf{Q}_{r1_{tot}}(J)[l] = \begin{pmatrix} 1 & \mathbf{Q}_{r1(J)}[l] \\ \mathbf{Q}^*_{r1(J)}[l_m] & 1 \end{pmatrix}$,
$\mathbf{B}_{1_{tot}}(J,K)[l] = \begin{pmatrix} \mathbf{B}_{1(J,K)}[l] & 0 \\ 0 & \mathbf{B}^*_{1(J,K)}[l_m] \end{pmatrix}$ and $\mathbf{Q}_{t1_{tot}}(K)[l] = \begin{pmatrix} 1 & \mathbf{Q}_{t1(K)}[l] \\ \mathbf{Q}^*_{t1(K)}[l_m] & 1 \end{pmatrix}$
with $\mathbf{Q}_{t1(K)}[l] = \mathbf{Q}_{t(K)}[l]$, $\mathbf{B}_{1(J,K)}[l] = \mathbf{B}_{(J,K)}[l](1 - \widetilde{\mathbf{Q}}^*_{r(J)}[l_m]\mathbf{Q}_r[l])$ and $\mathbf{Q}_{r1(J)}[l] = \frac{\mathbf{Q}_r[l] - \widetilde{\mathbf{Q}}_{r(J)}[l]}{1 - \widetilde{\mathbf{Q}}^*_{r(J)}[l_m]\mathbf{Q}_r[l]}$. The receiver IQ imbalance gain parameter $\mathbf{Q}_{r1(J)}[l]$ is now much smaller than $\mathbf{Q}_r[l]$ in (7.2).

Based on definition of $\mathbf{D}_{1_{tot}}[l]$ in (7.15), the coefficients $\mathbf{D}_{a1(J,K)}[l]$ and $\mathbf{D}_{b1(J,K)}[l]$ can be written as:

$$\begin{aligned}\mathbf{D}_{a1(J,K)}[l] &= \mathbf{B}_{1(J,K)}[l] + \mathbf{Q}_{r1(J)}[l]\mathbf{Q}^{*}_{t(K)}[l_m]\mathbf{B}^{*}_{1(J,K)}[l_m] \\ \mathbf{D}_{b1(J,K)}[l] &= \mathbf{Q}_{t(K)}[l]\mathbf{B}_{1(J,K)}[l] + \mathbf{Q}_{r1(J)}[l]\mathbf{B}^{*}_{1(J,K)}[l_m]\end{aligned} \tag{7.16}$$

which is similar to (7.9).

The estimates $\widetilde{\mathbf{D}}_{a1(J,K)}[l]$ and $\widetilde{\mathbf{D}}_{b1(J,K)}[l]$ of $\mathbf{D}_{a1(J,K)}[l]$ and $\mathbf{D}_{b1(J,K)}[l]$ can be obtained by replacing $\mathbf{D}_{tot}[l]$ with the estimate $\widetilde{\mathbf{D}}_{tot}[l]$ in (7.14), as follows:

$$\widetilde{\mathbf{D}}_{1_{tot}}[l] = \widetilde{\mathbf{Q}}_{rv_{tot}}[l]\widetilde{\mathbf{D}}_{tot}[l] = \begin{bmatrix} \left(\widetilde{\mathbf{D}}_{1_{tot}}(1,1)[l]\right) & \cdots & \left(\widetilde{\mathbf{D}}_{1_{tot}}(1,N_t)[l]\right) \\ \vdots & \ddots & \vdots \\ \left(\widetilde{\mathbf{D}}_{1_{tot}}(N_r,1)[l]\right) & \cdots & \left(\widetilde{\mathbf{D}}_{1_{tot}}(N_r,N_t)[l]\right) \end{bmatrix} \tag{7.17}$$

where $\widetilde{\mathbf{D}}_{1_{tot}}(J,K)[l] = \begin{pmatrix} \widetilde{\mathbf{D}}_{a1(J,K)}[l] & \widetilde{\mathbf{D}}_{b1(J,K)}[l] \\ \widetilde{\mathbf{D}}^{*}_{b1(J,K)}[l_m] & \widetilde{\mathbf{D}}^{*}_{a1(J,K)}[l_m] \end{pmatrix}$

If two or more independent channel realizations are available only for some antenna pairs, then the estimate of the sub-matrix $\mathbf{D}_{1_{tot}}(J,K)[l]$, given as $\widetilde{\mathbf{D}}_{1_{tot}}(J,K)[l]$, is derived by multiplying the sub-matrix $\widetilde{\mathbf{D}}_{tot}(J,K)[l]$ with sub-matrix $\widetilde{\mathbf{Q}}_{rv_{tot}}(J)[l]$ (defined in (7.7)). The multiplication results in the compensation of receiver IQ imbalance only on the sub-matrix $\widetilde{\mathbf{D}}_{tot}(J,K)[l]$.

Finally $\widetilde{\mathbf{Q}}_{r1(J)}[l]$ and the improved estimate $\widetilde{\mathbf{Q}}_{t1(K)}[l]$ of $\mathbf{Q}_{t(K)}[l]$ are obtained based on an expression similar to equation (7.12), with $\widetilde{\mathbf{D}}^{(1)}_{a(J,K)}[l]$, $\widetilde{\mathbf{D}}^{(2)}_{a(J,K)}[l]$ and $\widetilde{\mathbf{D}}^{(1)}_{b(J,K)}[l], \widetilde{\mathbf{D}}^{(2)}_{b(J,K)}[l]$ replaced by $\widetilde{\mathbf{D}}^{(1)}_{a1(J,K)}[l], \widetilde{\mathbf{D}}^{(2)}_{a1(J,K)}[l]$ and $\widetilde{\mathbf{D}}^{(1)}_{b1(J,K)}[l]$, $\widetilde{\mathbf{D}}^{(2)}_{b1(J,K)}[l]$. Equations (7.12) and (7.17) may be repeated a number of times until $\widetilde{\mathbf{Q}}_{ri(J)}[l] \simeq 0$, which corresponds to $\widetilde{\mathbf{D}}_{ai(J,K)}[l] \simeq \widetilde{\mathbf{B}}_{i(J,K)}[l]$, where i is the iteration index. It should be noted that the number of iterations required may vary for different antenna pairs, depending on the amount of transmitter and receiver IQ imbalance at the different antennas. Thus after performing a sufficient number of iterations, the fine estimate of the receiver IQ imbalance gain parameter $\widetilde{\mathbf{Q}}_{rf(J)}[l]$ can be derived from $\widetilde{\mathbf{Q}}_{ri(J)}[l]$ as:

$$\widetilde{\mathbf{Q}}_{rf(J)}[l] = \frac{\mathbf{Q}_{r1(J)}[l] + \widetilde{\mathbf{Q}}_{r(J)}[l]}{1 + \mathbf{Q}_{r1(J)}[l]\widetilde{\mathbf{Q}}^{*}_{r(J)}[l_m]} \tag{7.18}$$

where $\mathbf{Q}_{r1(J)}[l] = \frac{\mathbf{Q}_{r2(J)}[l]+\widetilde{\mathbf{Q}}_{r1(J)}[l]}{1+\mathbf{Q}_{r2(J)}[l]\widetilde{\mathbf{Q}}^{*}_{r1(J)}[l_m]}$ and so on. The fine estimate of transmitter IQ imbalance gain parameter $\widetilde{\mathbf{Q}}_{tf(K)}[l]$ is the $\widetilde{\mathbf{Q}}_{ti(K)}[l]$ obtained from the last iteration.

To obtain estimates of IQ imbalance gain parameters for other antenna pairs $(\bar{\bar{J}}, \bar{\bar{K}})$ (lacking independent channel realizations), we multiply the sub-matrix $\widetilde{\mathbf{D}}_{tot}(J, \bar{\bar{K}})[l]$ with the sub-matrix containing the fine receiver IQ imbalance estimate $\widetilde{\mathbf{Q}}_{rvf_{tot}}(J)[l] = \begin{pmatrix} 1 & -\widetilde{\mathbf{Q}}_{rf(J)}[l] \\ -\widetilde{\mathbf{Q}}^{*}_{rf(J)}[l_m] & 1 \end{pmatrix}$ in (7.17). The resulting estimates $\widetilde{\mathbf{D}}_{a1(J,\bar{\bar{K}})}[l]$ and $\widetilde{\mathbf{D}}_{b1(J,\bar{\bar{K}})}[l]$ are then considered to be completely free of receiver IQ imbalance. Both $\widetilde{\mathbf{D}}_{a1(J,\bar{\bar{K}})}[l]$ and $\widetilde{\mathbf{D}}_{b1(J,\bar{\bar{K}})}[l]$ are then substituted in (7.13), to obtain the fine estimate of **transmitter** IQ imbalance gain parameter $\widetilde{\mathbf{Q}}_{tf(\bar{\bar{K}})}[l]$.

The estimate of **receiver** IQ imbalance gain parameter $\widetilde{\mathbf{Q}}_{rf(\bar{\bar{J}})}[l]$ is obtained by first multiplying the sub-matrix $\widetilde{\mathbf{D}}_{tot}(\bar{\bar{J}}, K)[l]$ with $\widetilde{\mathbf{Q}}_{rv_{tot}}(\bar{\bar{J}})[l]$ in (7.17). The estimates $\widetilde{\mathbf{D}}_{a1(\bar{\bar{J}},K)}[l]$ and $\widetilde{\mathbf{D}}_{b1(\bar{\bar{J}},K)}[l]$ along with the fine estimate of transmitter IQ imbalance $\widetilde{\mathbf{Q}}_{tf(K)}[l]$ are then substituted in equation (7.13) to obtain a further improved estimate of receiver IQ imbalance gain parameter, now given as $\widetilde{\mathbf{Q}}_{r1(\bar{\bar{J}})}[l]$. Equation (7.17) and (7.13) are repeated a number of times until $\widetilde{\mathbf{Q}}_{ri(\bar{\bar{J}})}[l] = 0$. At this point the fine estimate of $\widetilde{\mathbf{Q}}_{rf(\bar{\bar{J}})}[l]$ can be obtained with (7.18).

Finally the fine estimates of all the transmitter and receiver IQ imbalance gain parameters can be substituted in equations (7.3) and (7.7) to obtain estimates of transmitted symbols $\widetilde{\mathbf{S}}_{tot}[l]$. A complete algorithm description for the estimation of transmitter and receiver IQ imbalance gain parameters is provided in **Table 7.1**.

In the presence of only transmitter ($\mathbf{Q}_{r(J)}[l] = 0$) or only receiver IQ imbalance ($\mathbf{Q}_{t(K)}[l] = 0$), the IQ imbalance gain parameter estimates are obtained directly from the coefficients $\widetilde{\mathbf{D}}_{a(J,K)}[l]$ and $\widetilde{\mathbf{D}}_{b(J,K)}[l]$, i.e. without the need for an iterative scheme. The channel estimate can then be written as $\mathbf{B}_{(J,K)}[l] = \mathbf{D}_{a(J,K)}[l]$ in equation (7.9). Thus for the case of only transmitter IQ imbalance, the estimate

1. Consider the term $\mathbf{Q}_{r(J)}[l]\mathbf{Q}^{*}_{t(K)}[l_m] = 0$ in (7.9).
2. For **FI transmitter/receiver IQ imbalance**, the raw estimates $\widetilde{Q}_{r(J)}$, $\widetilde{Q}_{t(K)}$ are computed with (7.11). Also obtain $\widetilde{Q}_{t(K)}$ and $\widetilde{Q}_{r(J)}$ estimates from other antenna pairs, i.e. $(\overline{\overline{J}}, K)$ and $(J, \overline{\overline{K}})$ based on (7.11). Average all the estimates to obtain improved estimates of $\widetilde{Q}_{r(J)}$ and $\widetilde{Q}_{t(K)}$.

   For **FS transmitter/receiver IQ imbalance**, the raw estimates $\widetilde{Q}_{r(J)}$ and $\widetilde{Q}_{t(K)}$ are computed from at least two independent realizations of $\widetilde{\mathbf{D}}^{(1)}_{a(J,K)}[l]$, $\widetilde{\mathbf{D}}^{(2)}_{a(J,K)}[l]$ and $\widetilde{\mathbf{D}}^{(1)}_{b(J,K)}[l]$, $\widetilde{\mathbf{D}}^{(2)}_{b(J,K)}[l]$ by (7.12).
3. In the case of FS IQ imbalance, compute the raw estimates for other antenna pairs (lacking independent channel realizations) $\widetilde{\mathbf{Q}}_{t(\overline{\overline{K}})}[l]$ and $\widetilde{\mathbf{Q}}_{r(\overline{\overline{J}})}[l]$ from $\widetilde{\mathbf{Q}}_{r(J)}[l]$ and $\widetilde{\mathbf{Q}}_{t(K)}[l]$ based on (7.13).
4. Compensate $\widetilde{\mathbf{D}}_{tot}[l]$ with the raw estimates of receiver IQ imbalance parameters $\widetilde{\mathbf{Q}}_{rv_{tot}}[l]$ in (7.17) to obtain the matrix $\widetilde{\mathbf{D}}_{i_{tot}}[l]$ with coefficients $\widetilde{\mathbf{D}}_{ai(J,K)}[l]$ and $\widetilde{\mathbf{D}}_{bi(J,K)}[l]$, where i is the iteration number. If two or more channel realizations are available only for some (J, K) antenna pairs, then derive the sub-matrix estimate $\widetilde{\mathbf{D}}_{1_{tot}}(J, K)[l]$ by multiplying the sub-matrix $\widetilde{\mathbf{Q}}_{rv_{tot}}(J)[l]$ with the sub-matrix $\widetilde{\mathbf{D}}_{tot}(J, K)[l]$.
5. Obtain $\widetilde{\mathbf{Q}}_{ri(J)}[l]$ and $\widetilde{\mathbf{Q}}_{ti(K)}[l]$ by substituting the coefficients $\widetilde{\mathbf{D}}_{ai(J,K)}[l]$ and $\widetilde{\mathbf{D}}_{bi(J,K)}[l]$ in step 2.
6. Repeat steps 2,4 and 5, until $\widetilde{\mathbf{Q}}_{ri(J)}[l] = 0$.
7. Obtain $\widetilde{\mathbf{Q}}_{rf(J)}[l]$ with (7.18), and $\widetilde{\mathbf{Q}}_{tf(K)}[l]$ from the last iteration of $\widetilde{\mathbf{Q}}_{ti(K)}[l]$.
8. Obtain $\widetilde{\mathbf{Q}}_{tf(\overline{\overline{K}})}[l]$ for other transmit antenna branches by first multiplying $\widetilde{\mathbf{D}}_{tot}(J, \overline{\overline{K}})[l]$ with $\widetilde{\mathbf{Q}}_{rf(J)}[l]$, and then substituting $\widetilde{\mathbf{D}}_{a1(J,\overline{\overline{K}})}[l]$ and $\widetilde{\mathbf{D}}_{b1(J,\overline{\overline{K}})}[l]$ in (7.13).
9. Obtain $\widetilde{\mathbf{Q}}_{rf(\overline{\overline{J}})}[l]$ for other receive antenna branches by first multiplying the $\widetilde{\mathbf{D}}_{tot}(\overline{\overline{J}}, K)[l]$ with $\widetilde{\mathbf{Q}}_{rv_{tot}}(\overline{\overline{J}})[l]$, and then substituting $\widetilde{\mathbf{D}}_{a1(\overline{\overline{J}},K)}[l]$, $\widetilde{\mathbf{D}}_{b1(\overline{\overline{J}},K)}[l]$ and $\widetilde{\mathbf{Q}}_{tf(K)}[l]$ in (7.13) to obtain an improved estimate $\widetilde{\mathbf{Q}}_{r1(\overline{\overline{J}})}[l]$. Repeat (7.17) and (7.13) until $\widetilde{\mathbf{Q}}_{ri(\overline{\overline{J}})}[l] = 0$. Obtain $\widetilde{\mathbf{Q}}_{rf(\overline{\overline{J}})}[l]$ with (7.18).

Table 7.1: D-FEQ algorithm for the estimation of transmitter and receiver IQ imbalance parameters

$\widetilde{\mathbf{Q}}_{t(K)}[l]$ is obtained as:

$$\widetilde{\mathbf{Q}}_{t(K)}[l] = \frac{1}{N_r}\sum_{J=1}^{N_r}\frac{\widetilde{\mathbf{D}}_{b(J,K)}[l]}{\widetilde{\mathbf{D}}_{a(J,K)}[l]} \tag{7.19}$$

and for the case of only receiver IQ imbalance, the estimate $\widetilde{\mathbf{Q}}_{r(J)}[l]$ is obtained as:

$$\widetilde{\mathbf{Q}}_{r(J)}[l] = \frac{1}{N_t}\sum_{k=1}^{N_t}\frac{\widetilde{\mathbf{D}}_{b(J,K)}[l]}{\widetilde{\mathbf{D}}^{*}_{a(J,K)}[l_m]} \tag{7.20}$$

7.3 Phase Rotation Based Schemes

In the presence of receiver IQ imbalance and CFO, it is possible to extend the PR-(PTEQ)/FEQ schemes, section 5.3, also for MIMO scenarios. The extension from SISO to MIMO is straightforward, as the estimation of receiver IQ imbalance for individual receive antenna takes place separately irrespective of the MIMO structure. Below we provide a brief description of the two phase rotation PR-FEQ and PR-PTEQ/FEQ schemes:

- **Decoupled receiver IQ imbalance and channel compensation (PR-FEQ):** In the case of only receiver IQ imbalance, we estimate the IQ imbalance gain parameter $\mathbf{V}_{d(J)}[l] = -\widetilde{\mathbf{Q}}_{r(J)}[l]$ (equation 5.34), now for every J^{th} receive antenna by an M_{la} long phase rotated LT symbol sequence. The compensation coefficients are then applied on the respective received symbol $\mathbf{Z}_{(J)}[l]$ and the mirror of its complex conjugate $\mathbf{Z}^{*}_{(J)}[l_m]$, resulting in symbol $\mathbf{Z}_{q(J)}[l]$, given as:

$$\mathbf{Z}_{q(J)}[l] = \begin{bmatrix}1 & \mathbf{V}_{d(J)}[l]\end{bmatrix}\begin{bmatrix}\mathbf{Z}_{(J)}[l] \\ \mathbf{Z}^{*}_{(J)}[l_m]\end{bmatrix} \tag{7.21}$$

  Assuming that the receiver IQ imbalance has been properly compensated, a standard MIMO equalizer is then applied to estimate the transmitted symbol, given as:

$$\begin{bmatrix}\widetilde{\mathbf{S}}_{(1)}[l] \\ \vdots \\ \widetilde{\mathbf{S}}_{(N_t)}[l]\end{bmatrix} = \begin{bmatrix}\mathbf{W}_{a(1,1)}[l] & \cdots & \mathbf{W}_{a(N_r,1)}[l] \\ \vdots & \vdots & \vdots \\ \mathbf{W}_{a(1,N_t)}[l] & \cdots & \mathbf{W}_{a(N_r,N_t)}[l]\end{bmatrix}\begin{bmatrix}\mathbf{Z}_{q(1)}[l] \\ \vdots \\ \mathbf{Z}_{q(N_r)}[l]\end{bmatrix} \tag{7.22}$$

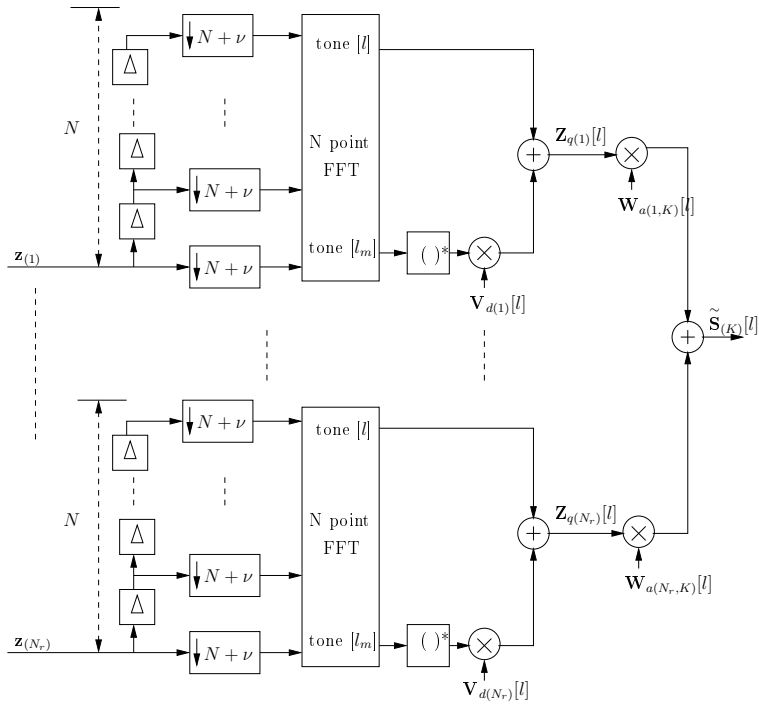

Figure 7.2: PR-FEQ compensation scheme for MIMO system

where $\mathbf{W}_{a(J,K)}[l]$ are the coefficients of the N_tN_r-tap FEQ. The coefficients of the FEQ can be initialized based on an LS or an adaptive RLS training algorithm.

Equation (7.22) is a reduced form of equation (6.7) with only half as many FEQ coefficients to be estimated. The number of coefficients to be estimated for the FEQ is now $N_t \times N_r$ per subcarrier and hence the required LT symbol sequence length is $M_{lb} \geq Nr$. As the N_tN_r-tap FEQ filters are not required to compensate for any mirror image interference, the training symbols transmitted on subcarrier $[l]$ should only be linearly independent of training symbols transmitted from other transmit antennas on subcarrier $[l]$. The transmission packet for PR-FEQ consists of M_{la} long phase rotated identical LT symbol sequence for receiver IQ imbalance compensation, followed by M_{lb} long linearly independent LT symbol sequence for the estimation of FEQ coefficients, and finally the data sequence. In terms of computational complexity, the total number of equalizer coefficients to be estimated is $N_r + (N_r \times N_t)$ per subcarrier. The PR-FEQ compensation scheme for MIMO systems is shown in **Figure 7.2**

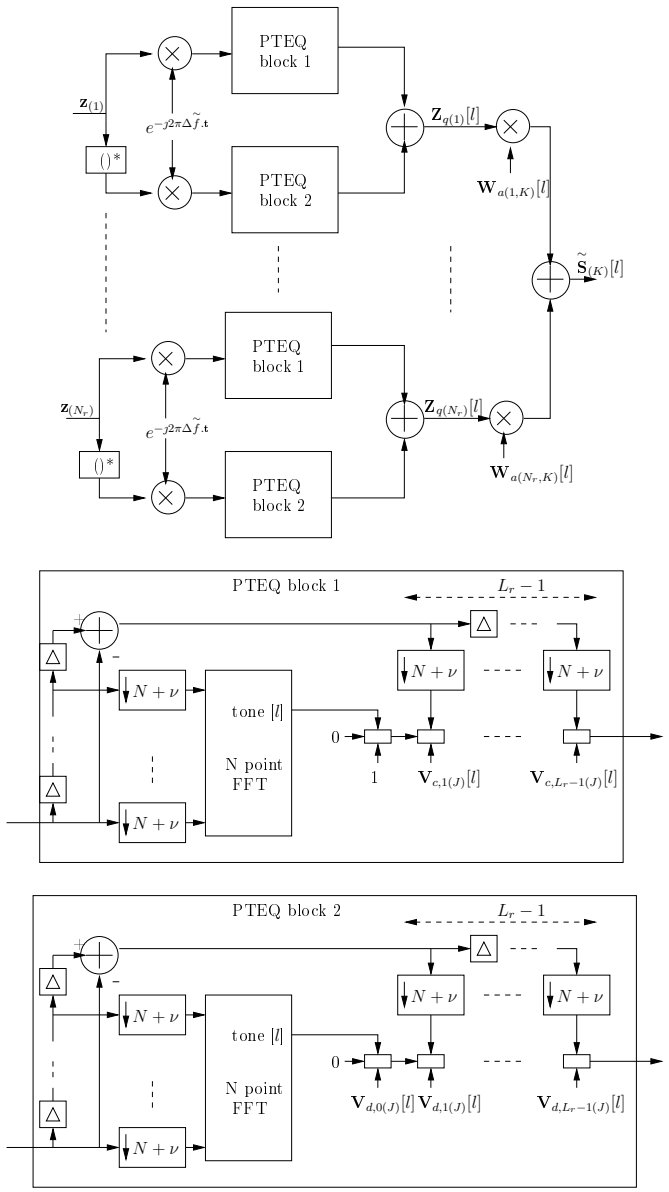

Figure 7.3: PR-PTEQ/FEQ compensation scheme for MIMO system

- **Decoupled receiver IQ imbalance and CFO compensation (PR-PTEQ/FEQ):** In the presence of CFO, the receiver IQ imbalance estimation is carried out in the time domain. We consider two filters branches $\mathbf{v}_{c(J)}$ and $\mathbf{v}_{d(J)}$, each L_r taps long (6.11), applied to the received symbol $\mathbf{z}_{(J)}$ and its complex conjugate $\mathbf{z}^*_{(J)}$. The design target for these filters are: $\mathbf{v}_{c(J)} = \frac{\mathbf{g}^*_{ra(J)}}{\mathbf{g}^*_{ra,0(J)}}$ and $\mathbf{v}_{d(J)} = \frac{\mathbf{g}_{rb(J)}}{\mathbf{g}^*_{ra,0(J)}}$. The estimation for the filter coefficients is then obtained based on M_{la} long phase rotated identical LT symbol sequence as shown in equation (5.39). In the MIMO, we perform the estimation of filter coefficients for every receive antenna separately.

  The TEQ thus obtained is swapped by the de-rotation operation for the compensation of CFO. Finally the TEQ is transformed to two-branch PTEQ for every receive antenna. The output of the PTEQ is given as:

$$\mathbf{Z}_{q(J)}[l] = \left(\begin{bmatrix} \mathbf{V}_{c(J)}[l] & \mathbf{V}_{d(J)}[l] \end{bmatrix} \begin{bmatrix} \mathbf{F}_{ext}[l]\mathbf{z}_{(J)}.e^{-\jmath 2\pi \Delta \widetilde{f}.\mathbf{t}} \\ \mathbf{F}_{ext}[l]\mathbf{z}^*_{(J)}.e^{-\jmath 2\pi \Delta \widetilde{f}.\mathbf{t}} \end{bmatrix} \right) \tag{7.23}$$

  where $\mathbf{V}_{c(J)}[l], \mathbf{V}_{d(J)}[l]$ are PTEQ filter vectors of length $L'' = L_r$ obtained from the TEQ filters $\mathbf{v}_{c(J)}$ and $\mathbf{v}_{d(J)}$. The PTEQ is then followed by a standard MIMO channel equalizer (7.22) for the estimation of the transmitted symbol. **Figure 7.3** illustrates the PR-PTEQ/FEQ scheme for a SU MIMO system.

  The transmission packet now consists of M_s long identical ST symbol sequence for CFO estimation, followed by M_{la} long phase rotated identical LT symbol sequence for receiver IQ imbalance compensation, M_{lb} long linearly independent LT symbol sequence for the estimation of FEQ coefficients, and finally the data sequence. The packet structure for the PR-PTEQ/FEQ scheme is shown in **Figure 7.4**. The computational complexity in terms of the number of equalizer coefficients to be estimated is now $(2L_r - 1)N_r + (N_r \times N_t)$.

Computational Complexity

Table 7.2 shows the overall computational requirements for the joint compensation schemes (FEQ(6.8), PTEQ (6.17)) and the decoupled schemes (D-FEQ (7.7), PR-(PTEQ)/FEQ (7.21/7.23)) for SU MIMO systems. In the second column of the table we consider the D-FEQ scheme when there is only IQ imbalance and the PR-PTEQ/FEQ when receiver IQ imbalance is present together with CFO. The IQ imbalance is generally considered to be frequency selective unless explicitly mentioned for FI IQ imbalance case.

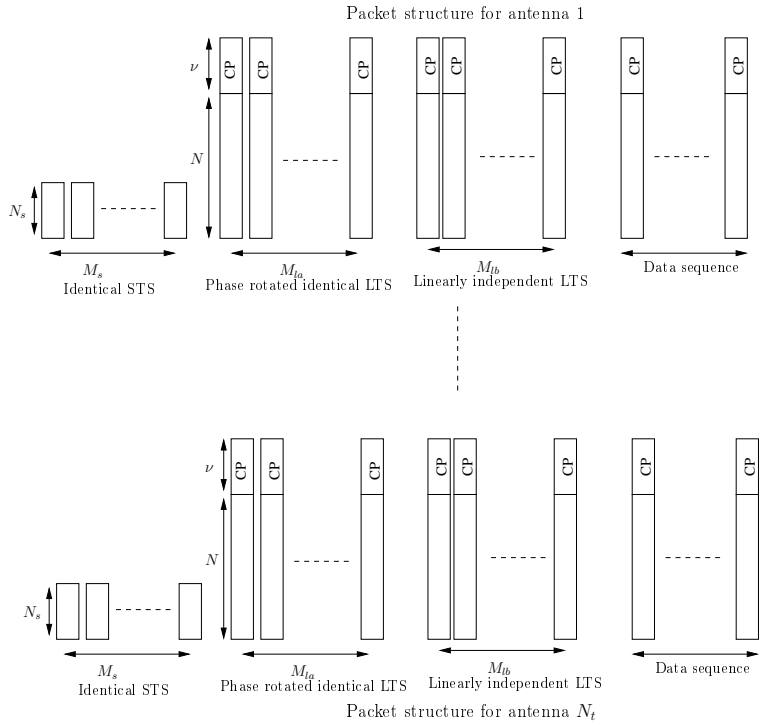

Figure 7.4: Packet structure for PR-PTEQ/FEQ compensation scheme

It can be observed from the table that the decoupled schemes provides a significant reduction in computational complexity compared to the joint compensation schemes. Besides the saving in computational complexity, the decoupled schemes also result in lower training overhead. The joint compensation schemes on the other hand provides solution that can always be straightforwardly trained for all combinations of front-end non-idealities.

7.4 Simulation Results

We have simulated an uncoded 16QAM 2×2 SU MIMO OFDM transmission to evaluate the proposed decoupled schemes. We consider OFDM symbol length $N = 64$ and CP length $\nu = 16$. We consider a quasi static multipath channel that is $L = 4$ taps long. The taps of the multipath channel are chosen independently with complex Gaussian distribution and their realization may vary from one packet

Non-ideality scenario	Decoupled schemes D-FEQ, PR-(PTEQ)/FEQ	Joint schemes
Receiver IQ	$(N_r + (N_t \times N_r))$	$2(N_t \times N_r)$
Transmitter/receiver IQ	$N_t + N_r + (N_t \times N_r)$	$2(N_t \times N_r)$
FI Receiver IQ + CFO	$N_r + (N_t \times N_r)$	$2(N_t \times N_r)$
Receiver IQ + CFO	$(2L_r - 1)N_r + (N_t \times N_r)$	$2L_r(N_t \times N_r)$
FI transmitter/receiver IQ + CFO	-	$4(N_t \times N_r)$
FS transmitter/receiver IQ + CFO	-	$4L_r(N_t \times N_r)$

Table 7.2: Computational complexity in terms of the number of coefficients to be estimated per subcarrier for different front-end non-ideality scenarios

to another. All BER versus SNR performance curves depicted are obtained by averaging the BER curves over 10^4 independent channel realizations.

In the case of D-FEQ compensation scheme, a transmission packet consists of a M_l long linearly independent LT symbol sequence followed by a data sequence. We do not consider ST symbol sequence, as they are not needed for the proposed compensation schemes. The length of the LT sequence is explained in the corresponding simulation setup.

In the case of PR-PTEQ/FEQ scheme, a transmission packet consists of $M_s = 10$ identical ST symbol sequence for CFO estimation, followed by $M_{la} = 4$ phase rotated LT symbol sequence for the compensation of receiver IQ imbalance, $M_{lb} = 4$ linearly independent LT symbol sequence for the compensation of channel distortion, and finally the data sequence for performance evaluation.

- In the first setup, we evaluate the BER vs SNR performance of the D-FEQ compensation scheme in the presence of transmitter and receiver IQ imbalance. The transmitter and receiver filter impulse responses are $\mathbf{h}_{ti(K)} = \mathbf{h}_{ri(J)} = [0.01\ 0.5\ 0.06]$, and $\mathbf{h}_{tq(K)} = \mathbf{h}_{rq(J)} = [0.06\ 0.5\ 0.01]$. The FI amplitude and phase imbalances are $g_{t(K)} = g_{r(J)} = 10\%$ and $\phi_{t(K)} = \phi_{r(J)} = 20^\circ$ respectively. We consider $M_l = 10$ LT symbol sequence during the estimation phase of IQ imbalance gain parameters and then $M_l = 4$ LT symbol sequence for the estimation of variation in channel characteristics.

  For the estimation phase of the transmitter and receiver IQ imbalance gain parameters, we consider two independent channel realizations for the antenna pair $(J, K) = (1, 1)$, while the remaining antenna pairs are considered to have a static channel characteristics. Thus the estimates of the transmitter and receiver IQ imbalance gain parameters for the remaining antenna pairs are obtained based on the estimates obtained for the $(1, 1)$ antenna pair. We follow the algorithm explained in Table 7.1 for the estimation of the IQ

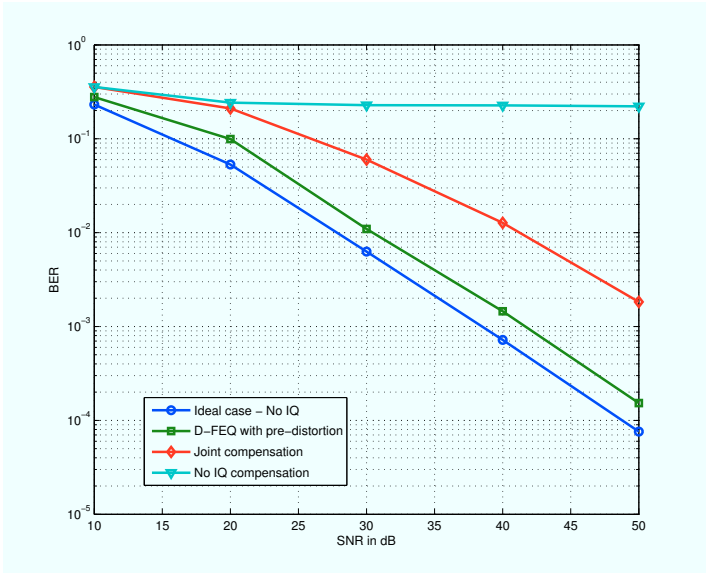

Figure 7.5: BER vs SNR for D-FEQ scheme in the presence of transmitter and receiver IQ imbalance

imbalance gain parameters. We consider about three iterations to obtain the fine estimates of transmitter and receiver IQ imbalance gain parameters for all antenna pairs.

Figure 7.5 illustrates the BER vs SNR curve for the D-FEQ scheme with pre-distortion based transmitter IQ imbalance compensation. The performance comparison is made with the joint compensation scheme as shown in equation (6.8). The initialization of the $2N_rN_t$-tap FEQ for joint compensation is obtained by $M_l = 4$ long LT symbol sequence. The figure shows that the proposed D-FEQ compensation scheme provides a very robust compensation performance for only $M_l = 4$ LT symbol sequence. The difference between the proposed scheme and the joint compensation scheme is almost 12 dB at BER of 10^{-2}. Thus the proposed compensation scheme provides very efficient compensation results even with very low training overhead.

- In the second setup, we evaluate the compensation performance of PR-PTEQ/FEQ scheme. The receiver filter impulse responses are $\mathbf{h}_{ri} = [0.01\ 0.5\ 0.06]$ and $\mathbf{h}_{rq} = [0.06\ 0.5\ 0.01]$ and the receiver FI amplitude and phase imbalances are now $g_r = 5\%$ and $\phi_r = 5^\circ$ respectively. During the estimation phase of receiver IQ imbalance gain parameters, we consider $M_{la} = 4$ identically phase rotated LTS. The phase rotation of the symbols are

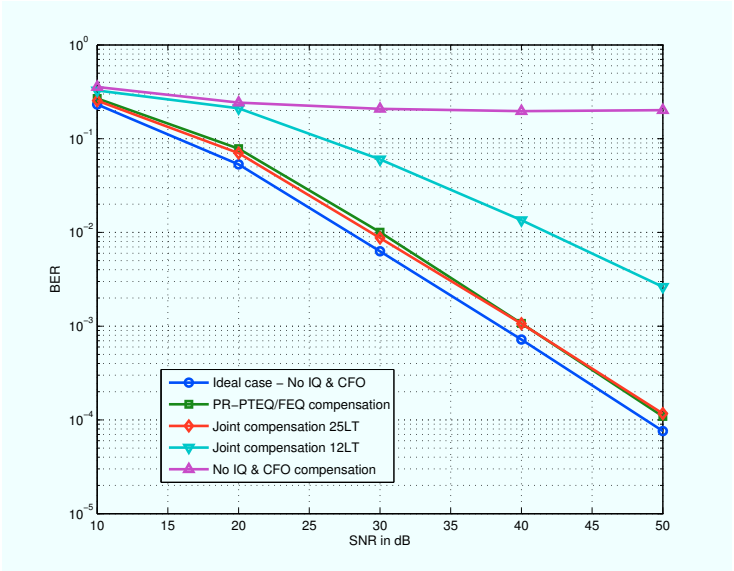

Figure 7.6: BER vs SNR for PR-PTEQ/FEQ scheme in the presence of receiver IQ imbalance and CFO

$\Phi = 0, \pi/4, \pi/2, 3\pi/4$. Once again, for the estimation of channel variation, we employ $M_{lb} = 4$ long LT symbol sequence. The CFO is uniformly varied between $\zeta = [-0.3 \longleftrightarrow +0.3]$. We estimate the CFO by the auto-correlation algorithm (4.4) [109] based on a 10 identical ST symbol sequence. Since the non-iterative version of this algorithm may not yield the correct estimate for large CFOs, we therefore improve upon the CFO estimate by including the iterative scheme during the estimation phase, as explained in section 5.3.2. We consider 3 iterations to obtain the fine estimates of receiver IQ imbalance and the CFO.

The performance comparison is made with the PTEQ (6.17) for the joint compensation of receiver IQ imbalance with CFO. As the transmitter IQ imbalance is not considered in the system model, we employ PTEQ filter branches only to the desired subcarriers $[l]$ from the DFT outputs, resulting in $2N_rN_t$-branch PTEQ. The threshold used to select between the two CFO estimation schemes is $\zeta = -0.02$ and $+0.02$ (auto-correlation [109] and NLS [121]), with the auto-correlation scheme used for small CFOs and the NLS scheme for large CFOs. In the NLS scheme, we have used a step size of $\Delta\zeta = 0.0005$ for the exhaustive search. We also implement the iterative scheme to further improve the estimate of the CFO and PTEQ coefficients, as explained in (4.26). In order to initialize the PTEQ, we now need $M_l = 2L_rNr = 12$ long LT symbol sequence. The performance comparison is drawn for both

$M_l = 12$ and $M_l = 25$ LT symbols.

Figure 7.6 shows the BER vs SNR performance curve for this system setup. As can be expected the proposed PR-PTEQ/FEQ scheme provides efficient compensation with a very low training overhead when compared to the joint compensation scheme. For $M_l = 12$, the joint compensation scheme provides poor performance. The $2N_rN_t$-branch PTEQ scheme requires about $M_l = 25$ LT symbols for the same compensation performance as the PR-PTEQ/FEQ scheme.

7.5 Conclusion

In this chapter, the decoupled compensation schemes (D-FEQ and PR-(PTEQ) /FEQ) have been extended for MIMO systems. It is shown that in the presence of transmitter and receiver IQ imbalance, the D-FEQ scheme requires only two independent channel realizations between any one transmit and receive antenna pair in order to estimate IQ imbalance parameters for the remaining transmit and receive antennas. In the case of PR-(PTEQ)/FEQ scheme, the extension from SISO to MIMO is straightforward, as the estimation of receiver IQ imbalance for individual receive antenna takes place separately irrespective of the MIMO structure.

Once the front-end IQ imbalance and CFO parameters are known, the training symbols are then required to estimate only the variation in channel characteristics. In the decoupled MIMO schemes, a standard channel equalizer requires the initialization of only $N_t \times N_r$ coefficients per subcarrier for the compensation of channel distortion. As less number of equalizer coefficients have to re-estimated, this also results in a lower training overhead requirements. Besides the advantage of a reduced training overhead and a reduced coefficient re-initialization, the decoupled solutions also result in a significant reduction in the overall computational complexity when compared to the joint compensation scheme.

Chapter 8

Conclusions and Future Work

In this chapter we highlight the main conclusions in **section 8.1** and list some suggestions for further research in **section 8.2**.

8.1 Conclusions

The overall objective of this dissertation was to provide digital solutions that can enable low cost, small and highly reconfigurable radios in broadband communication systems. An attractive front-end design for such systems is a direct conversion architecture as it utilizes minimal analog electronics and is small in size. However the direct conversion architecture is sensitive to various analog front-end non-idealities that can result in a severe performance degradation. This dissertation was focused on the investigation of the two most essential front-end non-idealities and their impact in the context of modern communications systems using direct conversion front-ends. In particular, we investigated the mirror frequency interference due to IQ imbalance and the CFO for OFDM systems. The proposed solutions effectively compensate for these non-idealities and thus allow the utilization of low cost, small and highly reconfigurable direct conversion front-ends for OFDM based systems.

In particular the proposed solutions meet the following requirements:

- The proposed solutions took into account the practical problems inherent to real-life communication systems. The IQ imbalance was considered

to be present at the transmitter as well as the receiver front-end. The dissertation considered the IQ imbalance to be frequency selective in nature with variation over different carriers. The time variation in the channel was due to the CFO between the transmitter and receiver local oscillators.

The dissertation also considered the case of insufficient CP length, i.e., the case where the CP used in the OFDM transmission is unable to completely accommodate the combined transmitter/receiver IQ imbalance and channel impulse response.

In addition, the dissertation also considered different multiple antenna scenarios: from single-user MIMO systems and space time coded systems to multi-user MIMO systems. The problem of front-end non-idealities is more pronounced in a MIMO system, as in this case multiple parallel radios are implemented in a single device. Thus due to increased size restrictions, the front-end radios may be designed with minimal electronics and as a result the front-end may exhibit severe non-idealities. The MIMO solutions proposed in this dissertation allowed to effectively compensate for IQ imbalance, CFO and channel distortion in such systems.

- The proposed solutions are flexible and their efficient implementation allowed to minimize the computational costs and power consumption requirements of the system. It was shown that the proposed solutions could be reduced to a smaller form factor in the presence of only few non-idealities. For example in the case of joint compensation schemes, the 4-branch PTEQ in SISO or $4N_tN_r$-branch PTEQ in MIMO solution required to compensate for all the non-idealities need not be implemented when only some of the non-idealities are present. Thus the efficient implementation of the proposed algorithms allow only a nominal increase in computational costs when compared to a simplified and the standard case of 1-tap FEQ in SISO or N_tN_r-tap FEQ in MIMO systems.

  The decoupled schemes allowed for additional savings in computational costs and training overhead requirements as in this case the compensation of IQ imbalance and CFO was performed independently of the channel equalization. The feedback of the transmitter IQ imbalance parameters to the transmitter in the pre-distortion based D-FEQ transmitter IQ imbalance compensation scheme allowed to split the burden of IQ imbalance compensation between the transmitter and receiver respectively. This resulted in a simplified receiver compensation scheme.

  A similar feedback approach can also be extended for other parameters in order to further reduce the computational costs and as a result the power consumption requirements of the receiver. For example it is possible to compensate for CFO by pre-distortion at the transmitter when there is no transmitter IQ imbalance. In this case the joint compensation scheme will be reduced to a simple two-tap FEQ in SISO and $2N_tN_r$-tap FEQ in MIMO.

Also the complexity in the PR-PTEQ/FEQ scheme for the MIMO systems will be reduced to $N_r + N_t N_r$ from $(2L_r - 1)N_r + N_t N_r$ coefficients per subcarrier.

Similarly, the receiver IQ imbalance and channel compensation parameters can also be fedback to the transmitter, so as to perform their compensation by pre-distortion of the transmitted symbol. Recent OFDM standards such as mobile broadband wireless access schemes [32], [44] allow for the transmission of variable CP length. Thus if the required CP length can be fedback, then the channel shortening requirements can be completely eliminated at the receiver. The feedback measures are especially attractive when the transmitter is a base station, as this relieves the receiver (user terminal) from performing additional compensation and save on power consumption and computational cost requirements of the user terminal.

A typical implementation of direct conversion architecture results in a 15-20% direct savings in terms of cost and power consumption requirements when compared to a traditional superheterodyne architecture [23], [103]. Efficient implementation of digital solutions will allow the utilization of direct conversion architectures and thus significantly save the overall costs and power consumption requirements. In general, the digital solutions have the advantage of flexibility, and the power consumption and computational costs can be limited by a number of low-power methodologies - from highly efficient and low complexity algorithms (some proposed in this dissertation), to low-power high-level programming, and finally the hardware implementation with various low-power techniques, etc. As the digital technology is considered to scale faster than its analog counterpart, the digital strategies developed to relax the analog specifications will continue to become more attractive with the development of next generation wireless systems.

- The proposed solutions adequately compensated for non-ideality levels much higher than those observed in today's transceiver designs. This is to guarantee the robustness/effectiveness of the proposed schemes for next generation systems where the effects of non-idealities are expected to be much more severe. The proposed solutions were shown to perform equally well for higher order modulated wideband communication waveforms. The various compensation schemes were demonstrated to provide a performance that were close to the ideal case without any front-end non-idealities.

- The proposed solutions required minor adjustments so as to be accommodated in the existing standards. The performance of the proposed algorithms were assessed based on an OFDM system similar to the WLAN IEEE 802.11a standard. However, the proposed solutions are generic enough to be extended in a straightforward manner to other systems operating under similar conditions.

This dissertation was broadly divided into two parts, **part 1** derived the estimation and compensation solutions for single antenna OFDM systems. The derivation and analysis of the single antenna systems was essential in order to extend the compensation schemes for multiple antenna systems. In **part 2**, we explored the proposed compensation solutions under various multiple antenna scenarios.

In **chapter 2** an overview study of an end-to-end system model in a modern wireless communication scenario was provided. The most important digital, analog blocks, together with OFDM system and multipath channel model were introduced. The system model comprised of all important building blocks in a broadband wireless communication link: the most important digital, analog blocks, together with the OFDM transmission system and the multipath channel model were introduced. A discussion on different front-end radio architectures along with some of the most common non-idealities were discussed. It was shown that a direct conversion front-end is an attractive radio architecture for a modern communication system. A discussion on the underlying wireless channel parameters were provided in detail. Finally the basic building blocks and the parameters associated with OFDM transmission scheme along with WLAN IEEE 802.11a case study were presented.

In **chapter 3** we derived the input-output system model for an OFDM system impaired with transmitter and receiver IQ imbalance. The impact of IQ imbalance in an OFDM system were discussed in detail. It was shown that IQ imbalance can result in a severe ICI and may even render the system useless. We proposed joint compensation solutions that consider transmitter/receiver IQ imbalance and channel distortion. In the case of sufficiently long CP length, a simple two-tap FEQ scheme was presented. In the case of insufficient CP length, we proposed a two-branch PTEQ solution which can shorten the combined channel and transmitter/receiver IQ imbalance impulse response to fit within the CP length, and at the same time compensate for the imperfection of the analog front-end. The performance curves demonstrated that an OFDM system impaired with IQ imbalance results in a very poor throughput. The proposed algorithms provided an efficient, post FFT adaptive equalization which led to a near ideal compensation.

In **chapter 4** we presented a study of the joint impact of transmitter/receiver IQ imbalance and CFO for an OFDM system. We discussed some of the suitable CFO estimation schemes available in the literature that can be used in the presence of IQ imbalance. Digital joint compensation solutions that incorporate CFO in addition to transmitter and receiver IQ imbalance were proposed. In the case of FI transmitter and receiver IQ imbalance, a straightforward method to jointly compensate for transmitter/receiver IQ imbalance, CFO and channel distortion by a four-tap FEQ was proposed. In the case of FS transmitter and receiver IQ imbalance, a four-branch PTEQ solution was obtained by combining the TEQ structure into the FEQ structure. It was shown that the four-branch PTEQ

solution is the most generalized form of a joint compensation solution as the equalizer can compensate for different combination of non-idealities and also for ISI distortion due to insufficient CP length.

In **chapter 5** we derived the so-called decoupled schemes for single-antenna systems. Training based compensation schemes that could decouple the compensation of transmitter and receiver IQ imbalance from the compensation of the channel distortion were proposed. We proposed two decoupled schemes - firstly, the D-FEQ scheme, where the transmitter/receiver IQ imbalance and the channel parameters were estimated based on coefficients obtained from the joint estimation/compensation solution. Secondly, the PR-PTEQ/FEQ scheme, where the receiver IQ imbalance parameters were estimated directly from a sequence of specially induced phase rotated LT symbols. It was shown that the PR-PTEQ/FEQ scheme could estimate the receiver IQ imbalance parameter irrespective of the amount of CFO in the system model. Both schemes provided an efficient way to decouple front-end non-idealities from channel distortion.

In **chapter 6** we proposed efficient PTEQ based joint compensation solutions for transmitter/receiver IQ imbalance and CFO in different multiple antenna scenarios. It was shown that for SU MIMO systems, a PTEQ solution could be scaled for any number of transmitter and receiver antennas. For STBC systems, the inherent structure of the orthogonal codes were exploited to obtain an efficient and optimal receiver architecture that were robust to front-end non-idealities. The joint compensation schemes were also extended for MU scenarios, where the individual users could experience a different CFO. It was shown that the down-link communication scenario could be considered to be composed of N_u number of decoupled SU MIMO system models. Thus a PTEQ scheme for SU MIMO system was directly implementable in the down-link scenario. In the case of up-link communication scenario, the PTEQ provided efficient compensation solutions for lower order 2×2 systems. The implementation for higher order systems can lead to complex solutions with high implementation costs.

In **chapter 7** the decoupled compensation schemes were extended for MIMO systems. It was shown that in the presence of transmitter and receiver IQ imbalance, the D-FEQ scheme required only two independent channel realizations between any one transmit and receive antenna pair, so as to estimate the IQ imbalance parameters for the remaining transmit and receive antenna branches. In case of phase rotated based schemes, the extension from SISO to MIMO was rather straightforward, as the estimation of receiver IQ imbalance for individual receive antenna could be obtained by the phase rotated scheme irrespective of the MIMO structure. Once the front-end distortions parameters were accurately known, the training symbols were then required to track only the variation in channel characteristics. A standard MIMO channel equalizer was then employed and this required the re-estimation of only $N_t \times N_r$ coefficients for every variation of the channel. As less number of equalizer coefficients had to re-estimated, this

also resulted in a lower training overhead requirements. Besides the advantage of a reduced training overhead and a reduced coefficient re-initialization, the decoupled solutions also resulted in an overall reduced computational complexity when compared to the joint compensation scheme.

8.2 Further Research

The following are some of the interesting directions for further research:

1. **IQ imbalance and CFO compensation in time and frequency selective channels**
   In this dissertation we focused only on time-invariant multipath channels i.e. the channel propagation was always assumed to be stationary. This is a valid assumption for the indoor environment where the broadband wireless channel indeed varies very slowly. However in a mobile environment, the channel can be selective in both time and frequency, resulting in a so-called doubly selective channel. The time selectivity of the channel arises due to the user mobility (Doppler shift) and CFO between the transmitter and the receiver. So far we considered only CFO as the source of time selectivity, it will be interesting to extend the compensation solutions to also include user mobility. It has been shown in the literature that the problem of ICI due to user mobility and CFO can be efficiently approximated and equalized by a TEQ based on basis expansion model (BEM) [9]. A TEQ obtained from the BEM can be transformed to the frequency domain and then combined with the FEQ designed for the compensation of IQ imbalance, CFO and channel selectivity. Based on BEM approximation, the presented joint compensation solution in this dissertation can also be extended for doubly selective channel.

2. **Joint compensation of phase noise, IQ imbalance and CFO**
   In an ideal receiver, the local oscillator in the front-end produces a central carrier frequency to down-convert the received signal to baseband. But in practice this generated signal may have power not only at the central carrier but also in a band around it. This phenomenon is called phase noise. OFDM based systems are not only sensitive to carrier frequency offset, but also to phase noise, resulting in a severe ICI. There have been studies on the joint effects of phase noise, CFO and IQ imbalance [107], but a comprehensive investigation that considers frequency selective transmitter and receiver IQ imbalance together with phase noise, CFO and insufficient CP length is still an open issue. Later on the compensation scheme may also include the effects of a doubly-selective channel. Similarly joint compensation solutions can be developed that also consider the effects of other front-end non-idealities such as DC-offset, non-linearities, etc. This way a generic compensation solution

can be developed. Extending the compensation solution in the presence of transmitter and receiver IQ imbalance with other non-idealities will not be straightforward and may require extensive investigation.

3. **Multi-user MIMO systems**
   In this dissertation we proposed a joint compensation solution for IQ imbalance and CFO in a multi-user down-link as well as up-link communication scenario. It was shown that the PTEQ based joint compensation scheme was able to solve the problem for a limited number of users (2-3 users at most) in the up-link scenario. The solution leads to increased complexity when a higher order system is considered. Thus there is a need to develop tractable solutions for multi-user systems that can effectively compensate transmitter and receiver IQ imbalance together with individual user's CFO. One interesting solution can be the approximation of the leakage due to CFO from multiple users by a BEM model and then combine it with the frequency domain equalizer designed for compensating IQ imbalance, and channel selectivity.

4. **OFDM related systems**
   In this dissertation we considered the effects of IQ imbalance and CFO for OFDM systems, but extension of the work towards other related system designs is also of interest. Lately, the single carrier frequency division multiple access (SC FDMA) scheme has drawn lot of attention as an attractive transmission scheme for future wireless systems [63] and [29]. SC FDMA is currently a working assumption for uplink multiple access scheme in 3GPP LTE, or E-UTRA. The SC FDMA has a significant advantage over OFDM scheme in terms of lower peak to average power ratio (PAPR). They are especially attractive in the uplink communication scenario where the mobile terminal can benefit in terms of transmit power efficiency. The SC FDMA is also considered to be less sensitive to CFO, but it will be interesting to study the effects of transmitter and receiver IQ imbalance together with doubly selective channel for such systems. Similarly, the increased interest in multicarrier code division multiple access (MC-CDMA) justifies a careful study of the impact of impairments in other OFDM related systems [41].

5. **Semi-blind approach**
   All the estimation/compensation schemes proposed in this dissertation are based on training symbols. Authors in [4], [110] and [111] have proposed blind approaches where the compensation of IQ imbalance is obtained based on statistical signal properties. However these methods generally result in a very long convergence time. It will indeed be interesting to develop semi-blind approaches where a good trade off between some of the blind methods and training based methods can be explored.

6. **Analog-Digital tradeoff**
   This work was focussed on digital compensation solutions for front-end

non-idealities. However the non-idealities can also be compensated either by purely analog or hybrid analog/digital solutions [12], [80]. The digital solutions are generally more flexible, and the power consumption and computational costs can be limited by a number of low-power methodologies - from highly efficient and low complexity algorithms, to low-power high-level programming, and finally the hardware implementation with various low-power techniques, etc. Similarly analog solutions can also be designed and implemented with different methodologies in order to limit the power consumption requirements. Thus obtaining the power consumption values and computational cost requirements in terms of gate and cycle count, etc in absolute terms for the analog as well as digital solutions with various implementation methodologies will require extensive investigation. It will indeed be interesting to explore the best trade-off between the various compensation solutions in terms of overall power consumption and computational costs.

Bibliography

[1] A.A. Abidi. Direct-conversion radio transceivers for digital communications. *IEEE Journal on Solid-State Circuits*, 30:1399–1410, December 1995.

[2] S.M. Alamouti. A simple transmit diversity technique for wireless communications. *IEEE Journal on Selected Areas in Communications*, 16:1451–1458, 1998.

[3] J.B. Andersen, T.S. Rappaport, and S. Yoshida. Propagation measurements and models for wireless communications channels. *IEEE Communications Magazine*, pages 42–49, January 1995.

[4] L. Anttila, M. Valkama, and M. Renfors. Circularity-based i/q imbalance compensation in wideband direct-conversion receivers. *IEEE Transactions on Vehicular Technology*, 57:2099–2113, July 2008.

[5] L. Anttila, M. Valkama, and M. Renfors. Efficient mitigation of frequency-selective i/q imbalances in ofdm receivers. In *IEEE 68th VTC conference*, Calgary, Canada, September 2008.

[6] J. Armstrong. Analysis of new and existing methods of reducing intercarrier interference due to carrier frequency offset in ofdm. *IEEE Transactions on Communications*, 47(3):365–369, March 1999.

[7] S. Barbarossa and A. Scaglione. Theoretical bounds on the estimation and prediction of multipath time-varying channels. In *IEEE International Conference on Acoustics, Speech, and Signal Processing (ICASSP)*, pages 2545–2548, June 2000.

[8] I. Barhumi and M. Moonen. Frequency-domain iq-imbalance and carrier frequency offset for ofdm over doubly selective channels. In *European Signal Processing Conference*, Florence, Italy, September 2006.

[9] I. Barhumi and M. Moonen. Iq-imbalance compensation for ofdm in the presence of ibi and carrier-frequency offset. *IEEE Transactions on Signal Processing*, 55(1):256–266, 2007.

[10] J. Bingham. Multi-carrier modulation for data transmission: An idea whose time has come. *IEEE Communications Magazine*, pages 5–14, May 1990.

[11] H. Bolcskei. Mimo-ofdm wireless systems: Basics, perspectives, and channelnges. *IEEE Wirless Communcications*, pages 31–37, August 2006.

[12] I. Bouras, S. Bouras, T. Georgantas, N. Haralabidis, G. Kamoulakos, C. Kapnistis, and et al. A digitally calibrated 5.15-5.825 ghz transceiver for 802.11a wireless lans in 0.18 micro meter cmos. In *IEEE International Solid-State Circuits Conference*, pages 352–353, February 2003.

[13] M. Brandolini and et al. Toward multi-standard mobile terminals- fully integrated receivers requirements and architectures. *IEEE Trans. on Microwave Theory and techniques*, 53:1026–1038, March 2005.

[14] X. Cai and G.B. Giannakis. Bounding performance and suppressing inter-carrier interference in wireless mobile ofdm. *IEEE Transactions on Communicaitons*, 51(12):2047–2056, December 2003.

[15] E. Cetin, I. Kale, and R.C.S. Morling. Living and dealing with rf impairments in communication transceivers. In *Proc IEEE International Symposium on Circuits and systems (ISCAS)*, pages 21–24, New Orleans, LA, may 2007.

[16] J. Chen, Y. Wu, and T.S. Ng. Optimal joint cfo and channel estimation for multi-user mimo ofdm systems. In *IEEE International Conference on Communications (ICC)*, pages 563–567, Beijing, China, May 2008.

[17] Y.H. Chung and S.M. Phoong. Joint estimation of i/q imbalance and channel response for mimo ofdm system. In *European Signal Processing Conference*, pages 906–910, 2007.

[18] Y.H. Chung and S.M. Phoong. Ofdm channel estimation in the presence of transmitter and receiver i/q imbalance. In *European Signal Processing Conference*, 2008.

[19] Y.H. Chung, K.D. Wu, and S.M. Phoong. Joint estimation of i/q imbalance, cfo and channel response for ofdm systems. In *IEEE International Conference on Acoustics, Speech and Signal Processing*, April 2009.

[20] Jr. L. Cimini. Analysis and simulation of a digital mobile channel using orthogonal frequency division multiplexing. *IEEE Transactions on Communications*, 33(7):665–675, July 1985.

[21] J. Crols and M.S.J. Steyaert. *CMOS Wireless Transceiver Design*. Kluwer, Dordrecht , The Netherlands, 1997.

[22] J. Crols and M.S.J. Steyaert. Low-if topologies for high-performance analog front ends of fully integrated receivers. *IEEE Transactions on Circuits Syst. II*, 45:269–282, March 1998.

[23] P. Cusinato. Configurable direct-conversion/superheterodyne baseband down-link channel for w-cdma applications. In *International Symposium on Circuits and Systems*, pages 741–745, May 2004.

[24] A. Dutta-Roy. Networks for homes. *IEEE Spectrum*, 36(12):26–33, December 1999.

[25] ECMA. Homepage: www.ieee802.org/15 and www.wimedia.org.

[26] ETSI. Homepage. http://www.etsi.org/bran.

[27] ETSI. *ETSI digital video broadcasting; framing structure, channel coding & modulation for digital TV*, 2004.

[28] C. Evans-Pughe. Bzzz zzz [zigbee wireless standard]. *IEE Review*, 49(2):28–31, March 2003.

[29] D. Falconera, S.L. Ariyavisitakul, A. Benyamin-Seeyar, and B. Eidson. Frequency domain equalization for single-carrier broadband wireless systems. *IEEE Communications Magazine*, 40(4):58–66, April 2002.

[30] G. Fettweis and et al. Dirty rf: A new paradign. In *Proc. IEEE Personal, Indoor and Mobile Radio Communications (PIMRC)*, Berlin, Germany, September 2005.

[31] S. Fouladifard and H. Shafiee. Frequency offset estimation in ofdm systems in presence of iq imbalance. In *Proceedings International Conference on Communications (ICC)*, pages 2071–2075, Anchorage, AK, May 2003.

[32] A. Greenspan, M. Klerer, R. Canchi, and J. Wilson. Ieee802.20: Mobile broadband wireless access for the twenty-first century. *IEEE communication Magazine*, 46:56–63, July 2008.

[33] J.C. Haartsen. The bluetooth radio system. *IEEE Communications Magazine*, 38(2):28–36, February 2000.

[34] L. Hanzo. Bandwidth-efficient wireless multimedia communications. *IEE*, 86(7):1342–1382, July 1998.

[35] H. Hashemi. Impulse response modeling of indoor radio propagation channels. *IEEE Journal on Selected Areas in Communications*, 11(7):967–977, September 1993.

[36] S. Haykin. *Adaptive Filter Theory*. Prentice Hall, 2002.

[37] J. Heiskala and J. Terry. *OFDM Wireless LANs: a theoretical and practical guide*. Sams Publishing, IndianaPolis, USA, 2002.

[38] W. Honcharenko, J.P. Kruys, D.Y. Lee, and N.J. Shah. Broadband wireless access. *IEEE Communications Magazine*, 35(1):20–26, January 1997.

[39] F. Horlin and A. Bourdoux. *Digital Compensation for Analog Front-Ends: A New Approach to Wireless Transceiver Design*. Wiley, Chichester, England, 2008.

[40] F. Horlin, A. Bourdoux, and L. Van der Perre. Low-complexity em-based joint acquistion of the carrier frequence offset and iq imbalance. *IEEE Transactions on Wireless Communications*, 2008.

[41] F. Horlin, S. De Rore, E. Lopez-Estraviz, F. Naessens, and L. Van der Perre. Impact of frequency offset and iq imbalance on mc-cdma reception based on channel tracking. *IEEE Journal on Selected Areas of Communications*, 24(6), June 2006.

[42] IEEE. Homepage. http://www.ieee.org.

[43] IEEE. *IEEE standard 802.11a-1999: wireless LAN medium access control (MAC) & physical layer (PHY) specifications, high-speed physical layer in the 5 GHz band*, 1999.

[44] IEEE. *IEEE standard for Local and metropolitan area networks: Air Interface for Mobile Broadband Wireless Access Systems Supporting Vehicular Mobility- Physical and Media Access Control Layer Specification*, 2008.

[45] IEEE. *IEEE 802.11n-2009-Amendment 5: Enhancements for Higher Throughput*, October 2009.

[46] ITU. Homepage. http://www.itu.org.

[47] ITU. Measuring the information society: The ict development index. Technical report, International Telecommunication Union, 2009.

[48] G.J. Janssen, P.A. Stigter, and R. Prasad. Wideband indoor channel measurements and ber analysis of frequency selective multipath channel at 2.4, 4.75 and 11.5 ghz. *IEEE Transactions on Communications*, 44(10):1272–1281, October 1996.

[49] Y.K. Kim and R. Prasad. *4G Roadmap and Emerging Communication Technologies*. Artech House, 2006.

[50] I. Koffman and V. Roman. Broadband wireless access solutions based on ofdm access in ieee 802.16. *IEEE Communications Magazine*, 40(4):96–103, April 2002.

[51] E.A. Lee and D.G. Messerschmitt. *Digital Communication*. Kluwer Academic Publishers, Boston, MA, 1988.

[52] W.C.Y Lee. *Mobile communications engineering:Theory and Applications*. McGraw-Hill, 2nd ed. edition, March 1997.

[53] J. Lin and E. Tsui. Adaptive iq imbalance correction for ofdm systems with frequency and timing offsets. In *IEEE Globecom*, Dallas, TX, November 2004.

[54] C.L. Liu. Impact of i/q imbalance on qpsk-ofdm-qam detection. *IEEE Transactions on Consumer Electronics*, 44(8):984–989, August 1998.

[55] E. Lopez-Estraviz, S. De Rore, F. Horlin, and L. Van der Perre. Pilot design for joint channel and frequency-dependent transmit/receive iq imbalance estimation and compensation in ofdm-based transceivers. In *IEEE International Conference on Communications (ICC)*, pages 4861–4866, 2007.

[56] J. Medbo, H. Hallenberg, and J.E. Berg. Propagation characteristics at 5 ghz in typical radio-lan scenarios. In *IEEE Vehicular Technology Conference (VTC) Spring*, volume 1, pages 185–189, May 1999.

[57] S. Mirabbasi and K. Martin. Classical and modern receiver architectures. *IEEE Communications Magazine*, 38:132–139, November 2000.

[58] J. Mitola-III and G.Q. Maguire-Jr. Cognitive radio: making software radios more personal. *IEEE Personal Communications Magazine*, 6(4):13–18, August 1999.

[59] W. Mohr and W. Konhauser. Access network evolution beyond third generation mobile communications. *IEEE Communications Magazine*, 38(12):122–133, December 2000.

[60] P.H. Moose. A technique for orthogonal frequency division multiplpexing frequence offset correction. *IEEE Transactions on Communications*, 42(10):2908–2914, 1994.

[61] R.J. Muirhead. *Aspects of Multivariate Statistical Theory*. John Wiley, May 1982.

[62] C. Muschallik. Influence of rf oscillators on an ofdm signal. *IEEE Transactions on Consumer Electronics*, 41(3):592–603, August 1995.

[63] H.G. Myung, Junsung Lim, , and David J. Goodman. Single carrier fdma for uplink wireless transmission. *IEEE Vehicular Technology Magazine*, 1(3):30–38, September 2006.

[64] B. Narasimhan, D. Wang, S. Narayanan, H. Minn, and N. Al-Dhahir. Digital compensation of frequency-dependent joint tx/rx i/q imbalance in ofdm systems under high mobility. *IEEE J. Sel. Topics on Signal Processing*, 3(3):405–417, June 2009.

[65] F.D. Neeser and J.L. Massey. Proper complex random processes with applications to information theory. *IEEE Transactions on Information Theory*, 39(4):1293–1302, July 1993.

[66] B.C. Ng, M. Cedervall, and A. Paulraj. A structured channel estimator for maximum-likelihood sequence estimation. *IEEE Communications Letters*, 1(2):52–55, March 1997.

[67] A. Papoulis. *Probability, Random Variables and Stochastic Processes*. McGraw-Hill, March 1984.

[68] T. Pollet, M. Van Bladel, and M. Moeneclaey. Ber sensitivity of ofdm systems to carrier frequency offset and wiener phase noise. *IEEE Transactions on Communications*, 43(2/3/4):191–193, 1995.

[69] T. Pollet, H. Steendam, and M. Moeneclaey. Performance degradation of multi-carrier systems caused by an insufficient guard interval duration. In *Proc. Int. Workshop on Copper Wire Access Systems 'Bridging the Last Copper Drop' (CWAS'97)*, pages 265–270, 1997.

[70] J.G. Proakis. *Digital Communications*. McGraw-Hill, 2nd ed. edition, 2001.

[71] R.M. Rao and B. Daneshrad. I/q mismatch cancellation for mimo-ofdm systems. In *Proc. IEEE Int. Symp. on Personal, Indoor, Mobile Radio Communications (PIMRC)*, volume 5, pages 2710–2714, September.

[72] T.S. Rappaport. *Wireless Communications: Principles and practice*. Prentice Hall, January 1996.

[73] B. Razavi. Design consideration for direct-conversion receivers. *IEEE Transactions on Circuit Systems II, Analog Digital Signal Processing*, 44(6):428–435, June 1997.

[74] U. Reimers. Dvb-t: the cofdm-based system for terrestrial television. *IEE Electronics and Communication Engineering Journal*, 9(1):28–32, February 1997.

[75] S. De Rore, E. Lopez-Estraviz, F. Horlin, and L. Van der Perre. Joint estimation of carrier frequency offset and iq imbalance for 4g mobile wireless systems. In *IEEE International Conference on Communications (ICC)*, pages 2066–2071, 2006.

[76] B. Salzberg. Performance of an efficient parallel data transmission system. *IEEE Transactions on Communications*, 15(805-811), 1967.

[77] T. Schenck, P. Smulders, and E. Fledderus. Estimation and compensation of frequency selective transmitter/receiver iq imbalance in mimo ofdm systems. In *Proc. IEEE Internatinal Conference on Communications (ICC)*, Istanbul, Turkey, June 2006.

[78] A. Schuchert, R. Hasholzner, and P. Antoine. A novel iq imbalance compensation scheme for the reception of ofdm signals. *IEEE Trans. Consumer Electronics*, 47(8):313–318, August 2001.

[79] P. Shelswell. The cofdm modulation system: the heart of digital audio broadcasting. *IEE Electronics and Communication Engineering Journal*, 7(3):127–136, June 1995.

[80] S. Simoens, M.de Courville, F. Bourzeix, and P. de Champs. New i/q imbalance modeling and compensation in ofdm systems with frequency offset. In *Personal, Indoor and Mobile Radio Communications*, volume 2, pages 561–566, September 2002.

[81] G. Stuber, J. Barry, S. Mclaughlin, M. Ingram Y. Li, and T. Pratt. Broadband mimo-ofdm wireless communications. *Proceedings of the IEEE*, 92(2):271–294, February 2004.

[82] K. Tachikawa. A perspective on the evolution of mobile communications. *IEEE Communications Magazine*, 41(10):66–73, October 2003.

[83] R. Tafazolli. *Technologies for the wireless future: wireless world research forum.* UK:Wiley, Chichester, 2004.

[84] D. Tandur and M. Moonen. Adaptive compensation of ofdm frequency selective transmitter and receiver iq imbalance. In *IAP-motion 2nd workshop on Mobile Multimedia Communication Systems and Networks (IAP)*, Liege, Belgium, November 2006.

[85] D. Tandur and M. Moonen. Adaptive compensation of frequency selective iq imbalance and carrier frequency offset for ofdm based receivers. In *Proc. of 8th IEEE workshop on Signal Processing Advances in Wireless Communications (SPAWC)*, Helsinki, Finland, June 2007.

[86] D. Tandur and M. Moonen. Digital compensation of rf impairments for broadband wireless systems. In *Proc. of 14th IEEE Symposium on Communications and Vehicular Technology (SCVT)*, Delft, The Netherlands, November 2007.

[87] D. Tandur and M. Moonen. Joint adaptive compensation of transmitter and receiver iq imbalance under carrier frequency offset in ofdm based systems. *IEEE Transactions on Signal Processing (IEEE TSP)*, 2007.

[88] D. Tandur and M. Moonen. Joint compensation of carrier frequency offset and frequency selective iq imbalance for ofdm based receivers. In *Proc. of 3rd IEEE BENELUX/DSP Valley Signal Processing Symposium (SPS-DARTS)*, number 13-16, Antwerp, Belgium, March 2007.

[89] D. Tandur and M. Moonen. Joint compensation of ofdm frequency selective transmitter and receiver iq imbalance. In *IEEE International Conference on Acoustics, Speech and Signal Processing (ICASSP)*, Honolulu, Hi, April 2007.

[90] D. Tandur and M. Moonen. Joint compensation of ofdm frequency selective transmitter/receiver iq imbalance. *Eurasip Journal on Wireless Communications and Networking (JWCN)*, (68563):10, 2007.

[91] D. Tandur and M. Moonen. Compensation of rf impairments in mimo ofdm systems. In *Proc. of IEEE International Conference on Acoustics, Speech and Signal Processing (ICASSP)*, pages 3097–3100, Las Vegas, NV, April 2008.

[92] D. Tandur and M. Moonen. Stbc mimo ofdm systems with implementation impairments. In *IEEE Vehicular Technology Conference (VTC2008-fall)*, Calgary, Canada, September 2008.

[93] D. Tandur and M. Moonen. Efficient compensation of frequency selective tx and rx iq imbalances in ofdm systems. In *Proc. of IEEE 7th International Workshop on Multi-Carrier Systems & Solutions (MC-SS)*, Herrsching, Germany, May 2009.

[94] D. Tandur and M. Moonen. Joint compensation of ofdm transmitter and receiver iq imbalance in the presence of carrier frequency offset. In *Proc. of 14th European Signal Processing Conference (EUSIPCO)*, Florence, Italy, September 2009.

[95] D. Tandur and M. Moonen. *Springer Lecture Notes on Electrical Engineering, Multi-Carrier Systems & Solutions*, chapter Efficient compensation of frequency selective Tx and Rx IQ imbalances in OFDM systems. Springer, 2009.

[96] D. Tandur and M. Moonen. Mimo ofdm systems with digital rf impairment compensation. *Signal Processing*, Accepted with minor revision, Jan. 2010.

[97] D. Tandur and M. Moonen. Efficient compensation of rf impairments for ofdm systems. In *Proc. of IEEE Wireless Communications and Networking Conference (WCNC)*, Budapest, Hungary, April 2009.

[98] D. Tandur and M. Moonen. Efficient compensation of transmitter and receiver iq imbalance in ofdm systems. *Eurasip Journal on Advances in Signal Processing (JASP)*, submitted in Dec. 2009.

[99] D. Tandur and M. Moonen. Decoupled compensation of iq imbalance in mimo ofdm systems. *Signal Processing*, submitted in Feb. 2010.

[100] A. Tarighat, R. Bagheri, and A.H. Sayed. Compensation schemes and performance analysis of iq imbalances in ofdm receivers. *IEEE Transactions on Signal Processing*, 53(8):1293–1302, August 2005.

[101] A. Tarighat and A.H. Sayed. Mimo ofdm receivers for systems with iq imbalances. *IEEE Transactions on Signal Processing*, 53(9):3583–3596, September 2005.

[102] A. Tarighat and A.H. Sayed. Ofdm systems with both transmitter and receiver iq imbalances. In *IEEE International Workshop on Signal Processing Advances in Wireless Communications (SPAWC)*, pages 735–739, New York, NY, June 2005.

[103] EE Times. Resonext says wlan chipset cuts power, space and costs. Technical report, Resonext, October 2001. http://www.eetimes.com/story/OEG20011030S0006, October 2001.

[104] T. Tjela, A. Nordbotten, M. Annoni, E. Scarrone, S. Bizzari, L. Tokarchuk, and et al. Future broadband radio access systems for integrated services with flexible resource management. *IEEE Communications Magazine*, 39(8):56–63, August 2001.

[105] J. Tsui. *Digital Techniques for Wideband Receivers*. Artech House, 1995.

[106] J. Tubbax, B. Come, L. Van der Perre, L. Deneire, S. Donnay, and M. Engels. Iq imbalance compensation for ofdm. In *IEEE International Conference on Communication*, volume 5, pages 3403–3407, May 2003.

[107] J. Tubbax, B. Come, L. Van der Perre, S. Donnay, and M. Engels. Joint compensation of iq imbalance and phase noise. In *IEEE Proceedings of VTC Spring*, pages 1605–1609, April 2003.

[108] J. Tubbax, B. Come, L. Van der Perre, S. Donnay, H. De Man, and M. Moonen. Compensation of transmitter iq imbalance for ofdm systems. In *IEEE Procc International Conference on Acoustics, Speech and Signal Processing (ICASSP)*, May 2004.

[109] J. Tubbax, B. Come, L. Van der Perre, M. Engels, M. Moonen, and H. De Man. Joint compensation of iq imbalance and carrier frequency offset in ofdm systems. In *Proc. Radio and Wireless Conference*, pages 39–42, Boston, MA, August 2003.

[110] M. Valkama, M. Renfors, and V. Koivunen. Blind source separation based i/q imbalance compensation. In *IEEE Adaptive Systems for Signal Processing, Communications and Control Symposium*, pages 310–314, October 2000.

[111] M. Valkama, M. Renfors, and V. Koivunen. Advanced methods for i/q imbalance compensation in communication receivers. *IEEE Transactions on Signal Processing*, 49(10):2335–2344, October 2001.

[112] M. Valkama, M. Renfors, and V. Koivunen. Compensation of frequency-selective iq imbalances in wideband receivers: models and algorithms. In *Proceedings IEEE 3rd Workshop on Signap Processing Advances in Wireless Communications (SPAWC)*, pages 42–45, Taoyuan, Taiwan, March 2001.

[113] K. van Acker, G. Leus, and M. Moonen. Per-tone equalization for dmt based systems. *IEEE Transactions on Communications*, 49(1), January 2001.

[114] J.J. van de Beek, O. Edfors, M. Sandell, S.K. Wilson, and P.O. Borjesson. On channel estimation in ofdm systems. In *Vehicular Technology Conference*, pages 815–819, Chicago, IL, September 1995.

[115] R.D.J. van Nee, G.A. Awater, M. Morikura, H. Takanashi, M. Webster, and K. Helford. New high rate wireless lan standards. *IEEE Communications Magazine*, 37(12):82–88, 1999.

[116] R.D.J. van Nee and R.Prasad. *OFDM for Wireless Multimedia Communications*. Artech House Publishers, 2000.

[117] U. Wahlberg. Mobile broadband technology evolution. In *Keynote presenation at IEEE VTC2006-Spring*. Melbourne, Australia, May 2006.

[118] Z. Wang and G. B. Giannakis. Wireless multicarrier communications, where fourier meets shannon. *IEEE Signal Processing Magazine*, 17(3):29–48, May 2000.

[119] S. Weinstein and P. Elbert. Data transmission by frequency division multiplpexing using the discrete fourier transform. *IEEE Transactions on Communications*, 19:628–634, October 1971.

[120] Y. Wu, S. Attallah, and J.W.M Bergmans. Carrier frequency offset estimation for multi-user mimo ofdm uplink using cazac sequences. In *IEEE Wireless Communications and Networking Conference (WCNC)*, Budapest, Hungary, April 2009.

[121] G. Xing, M. Shen, and H. Liu. Frequency offset and i/q imbalance compensation for direct-conversion receivers. *IEEE Transactions on Wireless Communications*, 4(2):673–680, March 2005.

[122] F. Yan, W.P. Zhu, and M.O. Ahmad. Carrier frequency offset estimation for ofdm systems with i/q imbalance. In *IEEE Midwest Symposium on Circuits and Systems (MWSCAS)*, volume 2, pages 633–636, July 2004.

[123] L. Yu and W.M. Snelgrove. A novel adaptive mismatch cancellation system for quadrature if radio receivers. *IEEE Transactions on Circuits Syst. II*, 46(10):789–801, June 1999.

Publication List

Journals

- **D.Tandur** and M.Moonen, "Joint compensation of OFDM frequency selective transmitter and receiver IQ imbalance", *Eurasip Journal on Wireless Communications and Networking (JWCN)*, Volume 2007 (2007), Article ID 68563, 10 pages.
- **D.Tandur** and M.Moonen, "Joint adaptive compensation of transmitter and receiver IQ imbalance under carrier frequency offset in OFDM based systems", *IEEE Transactions on Signal Processing (IEEE TSP)*, vol. 55, no. 11, pp. 5246-5252, Nov. 2007.
- **D.Tandur** and M.Moonen, "MIMO OFDM systems with digital RF impairment compensation", *Signal Processing*, Accepted with minor revision, Jan. 2010.
- **D.Tandur** and M.Moonen, "Efficient compensation of transmitter and receiver IQ imbalance in OFDM systems", *Eurasip Journal on Advances in Signal Processing (JASP)*, submitted in Dec. 2009.
- **D.Tandur** and M.Moonen, "Decoupled compensation of IQ imbalance in MIMO OFDM systems", *Signal Processing*, submitted in Feb. 2010.

Article in books

- **D.Tandur** and M.Moonen, "Efficient compensation of frequency selective Tx and Rx IQ imbalances in OFDM systems", *Springer Lecture Notes on Electrical Engineering, Multi-Carrier Systems & Solutions*, pp. 343-351, Springer, 2009.

Conferences

- **D.Tandur** and M.Moonen, "Efficient compensation of frequency selective Tx and Rx IQ imbalances in OFDM systems", in Proc. of IEEE 7th International Workshop on Multi-Carrier Systems & Solutions (MC-SS), Herrsching, Germany, May 2009.
- **D.Tandur**, Chong-you Lee and M.Moonen, "Efficient compensation of RF impairments for OFDM systems", in Proc. of IEEE Wireless Communications and Networking Conference (WCNC), Budapest, Hungary, April 2009.
- **D.Tandur** and M.Moonen, "STBC MIMO OFDM systems with implementation impairments", in Proc. of IEEE Vehicular Technology Conference (VTC2008-fall), Calgary, Canada, Sept. 2008, pp. 1-5.
- **D.Tandur** and M.Moonen, "Compensation of RF impairments in MIMO OFDM systems", in Proc. of IEEE International Conference on Acoustics, Speech and Signal Processing (ICASSP), Las Vegas, Nevada, April 2008, pp. 3097-3100.
- **D.Tandur** and M.Moonen, "Digital compensation of RF impairments for Broadband wireless systems", in Proc. of 14th IEEE Symposium on Communications and Vehicular Technology (SCVT), Delft, The Netherlands, Nov 2007.
- **D.Tandur** and M.Moonen, "Adaptive compensation of frequency selective IQ imbalance and carrier frequency offset for OFDM based receivers", in Proc. of 8th IEEE workshop on Signal Processing Advances in Wireless Communications (SPAWC), Helsinki, Finland, June 2007.
- **D.Tandur** and M.Moonen, "Joint compensation of OFDM frequency selective transmitter and receiver IQ imbalance", in Proc. of IEEE International Conference on Acoustics, Speech and Signal Processing (ICASSP), Honolulu, Hi, April 2007, pp. III-81.
- **D.Tandur** and M.Moonen, "Joint compensation of carrier frequency offset and frequency selective IQ imbalance for OFDM based receivers", in Proc. of 3rd IEEE BENELUX/DSP Valley Signal Processing Symposium (SPS-DARTS), Antwerp, Belgium, March 2007, pp. 13-16.
- **D.Tandur** and M.Moonen, "Adaptive compensation of OFDM frequency selective transmitter and receiver IQ imbalance", Poster at IAP-motion 2nd workshop on Mobile Multimedia Communication Systems and Networks (IAP), Liege, Belgium, Nov. 2006.
- **D.Tandur** and M.Moonen, "Joint compensation of OFDM transmitter and receiver IQ imbalance in the presence of carrier frequency offset", in Proc.

of 14th European Signal Processing Conference (EUSIPCO), Florence, Italy, Sept. 2006.

Curriculum Vitae



Deepaknath Tandur was born in Bangalore, India in 1979. He received a B.Sc. degree in electronics and communications engineering (first class with distinction) from RV College of Engineering, Bangalore University, Bangalore, India, in 2001 and a M.S. degree in embedded systems design engineering from University of Lugano, ALaRI, Lugano, Switzerland, in 2004. Since Nov. 2004 he has been pursuing a Ph.D. degree in electrical engineering under the supervision of Prof. Marc Moonen at the Katholieke Universiteit Leuven, Belgium. His research interests are in the area of digital signal processing techniques for telecommunications, specifically, front-end non-idealities estimation and compensation, channel identification and equalization for wireless communication systems.

He was selected for a student exchange program between India and Italy for an advanced diploma in software engineering with specialization in wireless communications (2002-2003). During the course of this program he did an internship with the Tetra Mobile Testing and Integration Department of Marconi Mobile, Florence, Italy. During his PhD he was partially funded by the Katholieke Universiteit grant for advanced doctoral students from non-EEA countries (db).

Arenberg Doctoral School of Science, Engineering & Technology
Faculty of Engineering
Department of Electrical Engineering
Research group ESAT/SISTA
Address: Kasteelpark Arenberg 10, Leuven 3001

KATHOLIEKE UNIVERSITEIT LEUVEN

ASSOCIATIE K.U.LEUVEN